Journal of Analytical Methods in Chemistry

Chemistry of Medicinal Plants, Foods, and Natural Products

Guest Editors: Shixin Deng, Shao-Nong Chen, and Jian Yang

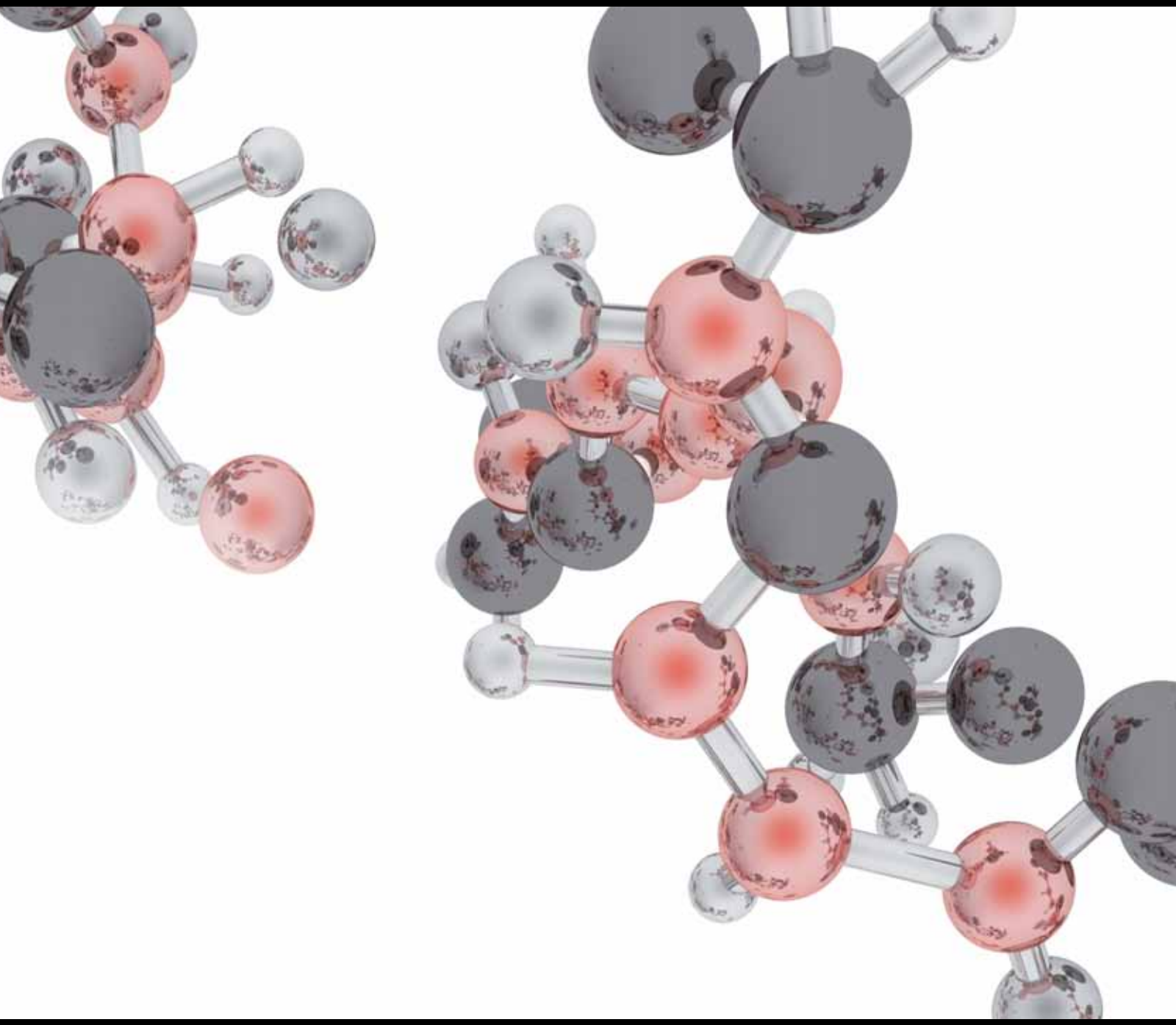

Chemistry of Medicinal Plants, Foods, and Natural Products

Journal of Analytical Methods in Chemistry

Chemistry of Medicinal Plants, Foods, and Natural Products

Guest Editors: Shixin Deng, Shao-Nong Chen, and Jian Yang

Editorial Board

Contents

Hindawi Publishing Corporation
Journal of Analytical Methods in Chemistry
Volume 2014, Article ID 252516, 2 pages
http://dx.doi.org/10.1155/2014/252516

Editorial

Chemistry of Medicinal Plants, Foods, and Natural Products

Shixin Deng,[1] Shao-Nong Chen,[2] and Jian Yang[3]

[1] *Research and Development Department, Morinda Inc., American Fork, UT 84003, USA*
[2] *UIC/NIH Center for Botanical Dietary Supplements Research, Department of Medicinal Chemistry and Pharmacognosy, College of Pharmacy, University of Illinois, Chicago, IL 60612, USA*
[3] *Western Pacific Tropical Research Center, College of Natural and Applied Sciences, University of Guam, Mangilao, GU 96923, USA*

Correspondence should be addressed to Shixin Deng; shixin_deng@morinda.com

Received 18 May 2014; Accepted 18 May 2014; Published 4 June 2014

Medicinal foods and plants have been widely used as foods, dietary supplements, or medicines worldwide and demonstrated a diversified health benefits with a long history. The raw materials and finished products of botanicals are becoming increasingly popular to public and scientific communities, highlighting the need for analytical methodology to ensure the quality. The safety and efficacy of these medicinal natural products are closely associated to their identify, authenticity and quality, which in turn relate to many factors, such as geographical conditions (soil, sunlight, precipitation, and air) and post-growth factors (harvesting, storage, transportation, manufacturing processes, etc.). As such, it is always a challenge for scientific researchers to evaluate safety and efficacy of the complicated plant matrix. In this special, we have invited 15 original research articles addressing the novel analytical method development and validation, methodology and instrumentation improvement, chemical characterization, biological activities of plant materials, extracts, and pure phytochemicals.

The first paper of this special issue investigates the feasibility of electronic tongue and multivariate analysis for discriminating the specific geographical origins of a Chinese green tea with protected designation of origin, and the authors concludes that electronic tongue and chemometrics can provide a rapid and reliable tool for discriminating the specific producing areas of Longjing. The second paper describes a quantitative method of flavonoids and chlorogenic acid in the leaves of *Arbutus unedo* L. by using HPTLC and their antioxidant activities by DPPH. The third paper reports a reliable HPLC method for the determination of aflatoxin M1 in eggs. The forth paper explores the characteristics of the anthocyanin and flavonol composition and content in grapes from plants resulting from intraspecific crosses of *Vitis vinifera* varieties Monastrell × Cabernet Sauvignon, Monastrell × Syrah, and Monastrell × Barbera. The fifth paper presents a rapid and sensitive method for determining aesculin of *Cortex fraxini* in rat by using HPLC-MS/MS with QTOF as a detector.

The sixth paper reports antioxidant activity and free radical scavenging capacity of the essential oil and three different extracts of wildly grown *Mentha longifolia*. Meanwhile, the study also establishes volatile and phenolic profiles of essential oil and different extracts of wild mint (*Mentha longifolia*) from the Pakistani Flora by using GC-MS method. The seventh paper establishes a phytochemical profile of *Cornus mas* by identifying the biological constituents in the fruits with the advanced UPLC-MS-TOF technology. Additionally, it reports DNA protective and antigenotoxic activities of the main phytochemicals. The eighth paper proposes a GC-MS fingerprint method for comparison of volatile components in the different plant parts (leaves and roots) of *Agrimonia eupatoria*. The ninth paper describes the isolation of α- and β-carotene from crude palm oil and evaluates their antioxidant potential in an in vitro model. The tenth paper focuses on the development of a sensitive and specific gas chromatographic-mass spectrometry with selected ion monitoring (GC-MS/SIM) method for simultaneous identification and quantification of α-asarone,

β-asarone, and methyl eugenol of *Acorus tatarinowii* Schott in rat plasma.

The eleventh paper addresses in vivo evaluation of the antioxidant activity of deacetylasperulosidic acid (DAA), a major iridoid in *Morinda citrifolia* (noni) fruit, and the study concludes that DAA contributes to the antioxidant activity of noni juice by increasing superoxide dismutase activity. The twelfth paper demonstrates that 1H NMR spectroscopy is a suitable detection technique in the analysis of various phytosterol forms in natural extracts. The thirteenth paper investigates the effects of varying temperatures with constant pressure of solvent on extraction efficiency of two chemically different alkaloids, camptothecin (CPT) from stem of *Nothapodytes nimmoniana* (Grah.) Mabb. and piperine from the fruits of *Piper nigrum* L., and determines a compound specific extraction for the two target alkaloids. The fourteenth paper isolates and purifies a protein called agathi leaf protein (ALP) from *Sesbania grandiflora* Linn. (agathi) leaves and evaluates its antioxidant, antibacterial, and cytoprotective activity. The fifteenth paper describes the characterization of nine polyphenols in Korean Prostrate Spurge (*Euphorbia supina*) by using HPLC-MS/MS, and the dose-dependent antioxidant activities of flavonoids were also observed.

Shixin Deng
Shao-Nong Chen
Jian Yang

Hindawi Publishing Corporation
Journal of Analytical Methods in Chemistry
Volume 2014, Article ID 418690, 8 pages
http://dx.doi.org/10.1155/2014/418690

Research Article

Determination of Polyphenol Components of Korean Prostrate Spurge (*Euphorbia supina*) by Using Liquid Chromatography—Tandem Mass Spectrometry: Overall Contribution to Antioxidant Activity

Yi Song,[1] Sung Woo Jeong,[1] Won Sup Lee,[2] Semin Park,[1] Yun-Hi Kim,[1] Gon-Sup Kim,[3] Soo Jung Lee,[4] Jong Sung Jin,[5] Chi-Yeon Kim,[6] Ji Eun Lee,[1] Se Yun Ok,[1] Ki-Min Bark,[7] and Sung Chul Shin[1]

[1] *Department of Chemistry and Research Institute of Life Science, Gyeongsang National University, Jinju 660-701, Republic of Korea*
[2] *Department of Internal Medicine, Institute of Health Sciences and Gyeongnam Regional Cancer Center, Gyeongsang National University, Jinju 660-702, Republic of Korea*
[3] *Research Institute of Life Science and College of Veterinary Medicine, Gyeongsang National University, Jinju 660-701, Republic of Korea*
[4] *Department of Food and Nutrition, Institute of Agriculture and Life Science, Gyeongsang National University, Jinju 660-701, Republic of Korea*
[5] *Division of High Technology Materials Research, Busan Center, Korea Basic Science Institute (KBSI), Busan 618-230, Republic of Korea*
[6] *Department of Dermatology Institute of Health Science, Gyeongsang National University Hospital, Jinju 660-702, Republic of Korea*
[7] *Department of Chemical Education and Research Institute of Life Science, Gyeongsang National University, Jinju 660-701, Republic of Korea*

Correspondence should be addressed to Gon-Sup Kim; gonskim@gnu.ac.kr and Sung Chul Shin; sshin@gnu.ac.kr

Received 11 September 2013; Accepted 2 January 2014; Published 3 March 2014

Academic Editor: Shixin Deng

The Korean prostrate spurge *Euphorbia supina* is a weed that has been used in folk medicine in Korea against a variety of diseases. Nine polyphenols were characterized for this plant by using high-performance liquid chromatography-tandem mass spectrometry (HPLC-MS/MS) and the results were compared with the literature data. The individual components were validated using the calibration curves of structurally related external standards and quantified for the first time by using the validated method. Correlation coefficients (r^2) were >0.9907. The limit of detection and limit of quantification of the method were >0.028 mg/L and 0.094 mg/L, respectively. Recoveries measured at 50 mg/L and 100 mg/L were 76.1–102.8% and 85.2–98.6%, respectively. The total amount of the identified polyphenols was 3352.9 ± 2.8 mg/kg fresh plant. Quercetin and kaempferol derivatives formed 84.8% of the total polyphenols. The antioxidant activities of the flavonoids were evaluated in terms of 1,1-diphenyl-2-picrylhydrazyl and 2,2′-azinobis(3-ethylbenzothiazoline-6-sulfonic acid) radical cation-scavenging activity, and the reducing power showed a dose-dependent increase. Cell viability was effectively suppressed at polyphenol mixture concentrations >250 mg/L.

1. Introduction

The Korean prostrate spurge *Euphorbia supina* is a weed that belongs to the Euphorbiaceae family and is native to North America. It is found in poor, drought-stressed turf and grows well during hot, dry weather in thin soils. It sprouts purple-spotted, up to 0.60-in oval leaves, and blooms very small, inconspicuous flowers in the summer [1].

The plant has been used in folk medicine in Korea against a variety of conditions such as diarrhea and suppurated swelling and as a styptic [2]. It was reported that the plant contains a number of biologically interesting organic substances, including terpenoids [3, 4], tannins, and polyphenols [5–7].

Of all bioactive natural constituents, polyphenols have attracted a great deal of interest, because they have beneficial effects to human health. Epidemiological studies have shown that polyphenols render many biological benefits, including a reduced risk of chronic diseases [8, 9] and antioxidant, antiaging, and antimicrobial properties [10]. In the plants, polyphenols function as physiologically active substances, such as attractants, feeding deterrents, materials used to communicate with the surrounding environment, and materials used as defense against biotic and abiotic stresses [11, 12]. Although the pharmaceutical efficacy of *E. supina* could be ascribed, at least partly, to the polyphenols, few studies have been conducted to validate this [3, 13].

The objective of the present study was to comprehensively characterize the polyphenol metabolomes of Korean *E. supina* by using high-performance liquid chromatography-tandem mass spectrometry (HPLC–MS/MS) and to investigate their biological benefits, including antioxidant and hepatoprotective effects. HPLC–MS/MS is a useful technique for analyzing plant polyphenols, because it provides online structural information and characterizes unknown substances even when no reference standards are available [14].

2. Materials and Methods

2.1. Materials and Chemicals. E. supina was purchased in mid-April 2012 from a market in Jinju, South Korea. The plant was authenticated by Professor Moo Ryong Huh, a plant taxonomist with the Research Institute of Agricultural Life Science, Gyeongsang National University. A voucher plant was deposited in the herbarium at this institute. The plant was washed with water, lyophilized, and stored in dark containers at −70°C until needed. All chemicals were purchased from Sigma-Aldrich Co., LLC (St. Louis, MO, USA). Gallic acid, protocatechuic acid, 7-hydroxycoumarin, quercetin 3-*O*-glucoside, and kaempferol, which were purchased from Sigma-Aldrich Co., LLC (St. Louis, MO, USA), were used as external standards after recrystallization in ethanol. The purity of all standards was confirmed to be >99% by using HPLC. All solvents and water were obtained from Duksan Pure Chemicals Co., Ltd. (Ansan, Republic of Korea).

2.2. Extraction and Purification. The lyophilized *E. supina* tissue (10 g) was ground into powder and extracted in ethyl acetate (300 mL) at 80°C for 20 h. The extract was filtered through a Büchner funnel and concentrated at reduced pressure under 40°C by using a rotator evaporator. The concentrated solution was washed with *n*-hexane (100 mL × 3), extracted with ethyl acetate (100 mL × 3), and dried over anhydrous sodium sulfate (Na_2SO_4). The solvent was removed under reduced pressure. The sticky residue was placed on top of a silica gel sorbent (3 × 1.7 cm i.d.) and eluted using a mixture of methanol:dichloromethane (1 : 5, 25 mL). The solvent was removed to give a mixture of polyphenols (0.9% of the dried plant). The mixtures were reconstituted in ethyl acetate (0.03 g/mL), filtered through 0.45 μm cellulose membranes, transferred into silanized vials, and stored at −20°C until analysis.

2.3. HPLC–MS/MS. HPLC–MS/MS experiments were conducted according to a previously reported method [15], except for the use of a solvent system consisting of 0.5% aqueous formic acid (A) and methanol (B). The gradient conditions of the mobile phase were from 10 to 30% B over 10 min, increased to 90% B over 40 min, and increased again to 98% B over 5 min.

2.4. Quantification and Validation. All components were quantified using chromatograms obtained at 254 nm. The quantification was validated in terms of linearity, limit of detection (LOD), limit of quantification (LOQ), accuracy, and precision.

The individual components for which standards were not available, except for gallic acid (**1**) and protocatechuic acid (**2**), were quantified using the calibration curves of structurally related external standards. Thus, nodakenin (**3**) was quantified as 7-hydroxycoumarin, quercetin derivatives (**4**, **5**, **8**) as quercetin 3-*O*-glucoside, and kaempferol derivatives (**6**, **7**, **9**) as kaempferol. Plant polyphenols can be quantified using a standard curve of structurally related compounds [16]. A stock solution of each standard (10 mg/L) was prepared by dissolving the appropriate amounts in methanol and storing at −20°C. Linearity was assessed using six different concentrations, (1, 10, 50, 100, 1000, and 2000 mg/L) of each standard and by plotting the concentration of the standard against the peak area. LOD and LOQ were determined by injecting each standard solution into the HPLC until the signal-to-noise ratio for the standards reached 3 : 1 and 10 : 1, respectively. The accuracy of the methods was estimated as recovery = A/IS-C/B/IS-C, where A is the peak area obtained for the analyte spiked preextraction, B is the area obtained for the analyte spiked after extraction, and C is the area of the blank extraction. The precision of the method was represented as a relative standard deviation (RSD).

2.5. Antioxidant Activity Measurement. A series of methanol solutions of the *E. supina* polyphenol mixture (25, 50, 100, 200, and 500 mg/L) were prepared and used for the antioxidant assay. Antioxidant activities were measured in terms of 1,1-diphenyl-2-picrylhydrazyl radical ($DPPH^{\bullet}$) and 2,2′-azinobis(3-ethylbenzothiazoline-6-sulfonic acid) ($ABTS^{\bullet+}$) radical cation-scavenging activity and reducing power (RP) assay according to a method reported in our previous studies [16].

2.6. Effects of the Polyphenol Mixture of E. supina on Hep3B Cell Viability

2.6.1. Cell Viability Assay. Hepatic cancer cells (1×10^4 cells per well) were plated onto 12-well plates and treated

Table 1: Mass spectral data of the *Euphorbia supina* polyphenol mixture.

Compounds	$[M-H]^-/[M+H]^+$	MS/MS	References
Gallic acid (**1**)	169	169, 125, 97	[17]
Protocatechuic acid (**2**)	153	153, 109, 108	[17]
Nodakenin (**3**)	/409	409, 391, 353, 389, 247, 229, 203, 185	[18]
Quercetin 3-*O*-hexoside (**4**)	463	463, 301, 300, 283, 271, 255, 151	[16, 19]
Quercetin 3-*O*-pentoside (**5**)	433	433, 300, 273, 271, 255, 179, 151	[20]
Kaempferol 3-*O*-hexoside (**6**)	447	447, 285, 255	[16, 21]
Kaempferol 3-*O*-pentoside (**7**)	/419	419, 309, 287, 155	[22, 23]
Quercetin (**8**)	/301	301, 273, 179, 153	[24, 25]
Kaempferol (**9**)	/287	287, 258, 165, 153, 121	[26, 27]

Table 2: Regression data, limit of detection (LOD), and limit of quantification (LOQ) for the five external standards.

Standard	Calibration curve	r^2	LOD (mg/L)	LOQ (mg/L)	Recovery (%) ± RSD	
					50 mg/L	100 mg/L
Gallic acid	$y = 25.171x + 335.04$	0.9993	0.032	0.107	79.6 ± 6.1	85.2 ± 0.5
Protocatechuic acid	$y = 37.614x + 1137.3$	0.9982	0.030	0.102	88.5 ± 0.2	87.8 ± 0.5
7-Hydroxycoumarin	$y = 10.873x - 28.39$	0.9955	0.142	0.473	102.8 ± 0.7	98.6 ± 11.6
Quercetin 3-*O*-glucoside	$y = 30.166x + 267.56$	0.9949	0.037	0.125	76.1 ± 0.1	90.9 ± 14.0
Kaempferol	$y = 39.493x + 1475.4$	0.9907	0.028	0.094	100.0 ± 3.0	97.4 ± 1.4

y: peak area of standard; *x*: concentration of standard (mg/L).

with the polyphenol mixture of *E. supina* at concentrations of 31.25, 62.5, 125, 250, and 500 mg/L or vehicle (dimethyl sulfoxide, DMSO) alone for 24 h. Cell viability was estimated by measuring the 3-(4,5-dimethylthiazol-2-yl)-2,5-diphenyltetrazolium bromide (MTT) metabolism. Thus, 100 μL of MTT solution (5 mg/L) was added to each well of a 12-well plate, and the cells were maintained for 3 h at 37°C. After the supernatant was removed, the remaining violet residue was dissolved in DMSO (1 mL). The absorbance values were measured using a microplate reader at 540 nm. Cell viability was expressed as a percentage of proliferation versus controls, which was set at 100%.

2.6.2. Cell Morphology Observation. Hep3B cells (5×10^4 cells per well) were plated onto 6-well plates and treated with the polyphenol mixture of *E. supina* at concentrations of 31.25, 62.5, 125, 250, and 500 mg/L or vehicle alone for 24 h. Cell morphological change was observed under an optical microscope (Olympus CKX 41, Japan).

2.7. Statistical Analysis. All statistical analyses were performed according to a method described previously [16].

3. Results and Discussion

3.1. Separation and Characterization. A mixture of polyphenols was isolated from *E. supina* by methanol extraction at 80°C, followed by elution in ethyl acetate over a silica gel cartridge. The polyphenols were characterized through HPLC by using a C_{18} column, MS/MS in negative- and positive-ion modes, and comparison with the previous literature data. The HPLC chromatograms of the plant are shown in Figure 1.

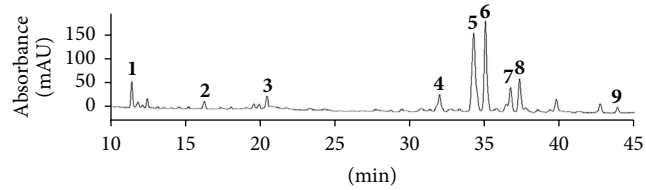

Figure 1: Chromatograms of the *Euphorbia supina* polyphenol mixture obtained using high-performance liquid chromatography:**1**, gallic acid; **2**, protocatechuic acid; **3**, nodakenin; **4**, quercetin 3-*O*-hexoside; **5**, quercetin 3-*O*-pentoside; **6**, kaempferol 3-*O*-hexoside; **7**, kaempferol 3-*O*-pentoside; **8**, quercetin; **9**, kaempferol. Detection wavelength: 254 nm.

Nine polyphenols were labeled in the 10 to 45 min retention time segments of the chromatograms. The structures and HPLC–MS/MS data of the nine polyphenols are shown in Figure 2 and Table 1, respectively.

Polyphenol **1** was identified as gallic acid. Its MS/MS spectrum produced a $[M-H]^-$ of *m/z* 169, which fragmented to yield 125 $[M-H-CO_2]^-$ and 97 $[M-H-CO_2-CO]^-$ [17]. Polyphenol **2** was identified as protocatechuic acid. Its MS/MS consisted of $[M-H]^-$ at *m/z* 153 and 109 $[M-H-CO_2]^-$ [17]. Component **3** was identified as nodakenin. Its MS/MS spectrum produced a $[M+H]^+$ of *m/z* 409, which fragmented to 247 $[M+H-\text{glucosyl}]^+$, 229 $[M+H-\text{glucosyl}-H_2O]^+$, and 203 $[M+H-\text{glucosyl}-CO_2]^+$ [18]. Polyphenol **4** yielded $[M-H]^-$ of *m/z* 463, which fragmented to 301 $[M-H-\text{hexosyl}]^-$, 283 $[M-H-\text{hexosyl}-H_2O]^-$, and 255 $[M-H-\text{hexosyl}-H_2O-CO]^-$. Polyphenol **4** was quercetin 3-*O*-hexoside [16, 19]. The MS/MS spectrum of polyphenol **5** consisted of $[M-H]^-$ at *m/z* 433, 301 $[M-2H-\text{pentosyl}]^-$, and

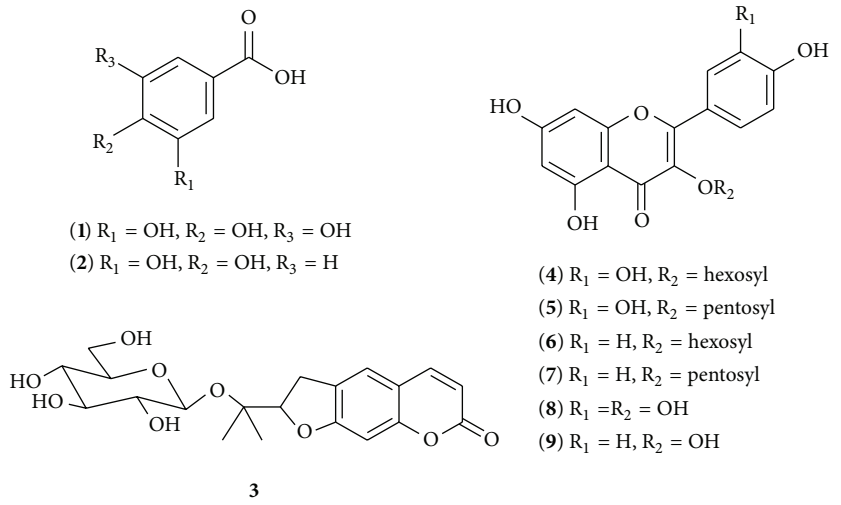

Figure 2: Structures of the eight polyphenols and one nodakenin in *Euphorbia supina*.

Table 3: Concentration of polyphenols in *Euphorbia supina* (mg/kg fresh plant).

Compounds	Mean ± SD
Gallic acid (**1**)	264.4 ± 0.7
Protocatechuic acid (**2**)	124.3 ± 0.3
Nodakenin (**3**)	120.0 ± 4.7
Quercetin 3-*O*-hexoside (**4**)	458.3 ± 4.9
Quercetin 3-*O*-pentoside (**5**)	1648.2 ± 20.2
Kaempferol 3-*O*-hexoside (**6**)	553.8 ± 4.2
Kaempferol 3-*O*-pentoside (**7**)	126.9 ± 1.5
Quercetin (**8**)	118.7 ± 1.0
Kaempferol (**9**)	21.0 ± 4.6
Total	3352.9 ± 2.8

273 $[M–2H–pentosyl–CO]^-$; polyphenol **5** was identified as quercetin 3-*O*-pentoside [20]. Polyphenol **6** gave $[M–H]^-$ at *m/z* 447, which produced 285 ($[M–H]^-$–hexosyl) and 255 ($[M–H]^-$–hexosyl–H_2). It was identified as kaempferol 3-*O*-hexoside [16, 21]. Polyphenol **7** was identified as kaempferol 3-*O*-pentoside. Its MS/MS consisted of $[M+H]^+$ at *m/z* 419 and 287 $[M+H–pentosyl]^+$ [22, 23]. Polyphenol **8** yielded $[M+H]^+$ at *m/z* 302, which was fragmented to typical fragment ions 273 $[M+H–CO]^+$, 179 $[M–CC_6H_5O_2]^+$, and 153 [$C_7H_5O_4$, retro-Diels-Alder fragment]. Polyphenol **8** was quercetin [24, 25]. Polyphenol **9** was identified as kaempferol and gave $[M+H]^+$ at *m/z* 287, which produced 257 $[M+H–CO]^+$ and 153 [$C_7H_5O_4$, retro-Diels-Alder fragment] [26, 27].

3.2. Quantification. The nine polyphenols identified in the Korean *E. supina* were quantified for the first time from peak areas of the LC-UV chromatogram obtained at 254 nm. Quantification was validated based on representative external standards from the same group. The validation data are listed in Table 2. Regression equations were prepared in the form of $y = ax + b$, where y and x were the peak area and the concentration of each standard, respectively. The regression analysis showed correlation coefficients (r^2) > 0.9907 for all five standards ($n = 5$), indicating good linearity. The LODs of the method were 0.028–0.142 mg/L and LOQs were 0.094–0.473 mg/L, indicating good performance limits. Recoveries measured at 50 mg/L and 100 mg/L were 76.1–102.8% and 85.2–98.6%, respectively. Precisions of the method at 50 mg/L and 100 mg/L were 0.1–6.1% and 0.5–14.0%, respectively. Both the accuracy and precision values were acceptable.

The contents of individual components are listed in Table 3. The total amount of the identified polyphenols was 3352.9 ± 2.8 mg/kg fresh plant. Quercetin and kaempferol derivatives formed 84.8% of the total polyphenols. The plant comprised quercetin 3-*O*-pentoside (**5**) as the most dominant component, followed by kaempferol 3-*O*-hexoside (**6**). Quercetin, kaempferol, and their sugar-bound derivatives are major representatives of the polyphenol subclass that display the antioxidant activity to scavenge reactive oxygen species. As a result, *E. supina*, which is rich in such components, could be effective for reducing the risk of various chronic diseases resulting from oxidative damage, such as cancer, atherosclerosis, and inflammation [27, 28].

3.3. Antioxidant Activity. The polyphenol mixture isolated from Korean *E. supina* was evaluated for its antioxidant effects. Contemporary interest in polyphenols focuses on the epidemiological association between their potent antioxidant properties and a low incidence of chronic diseases. Epidemiological studies have shown that oxidative stress plays an important role in the pathogenesis of various chronic diseases, including cancer, cardiovascular disease, atherosclerosis, hypertension, diabetes, neurodegenerative disorders, rheumatoid arthritis, and aging [29–31]. Polyphenols can reduce oxidative stress and thus might protect and/or retard disease development [32, 33]; therefore, it is necessary to evaluate the antioxidant properties of the polyphenols in medicinal herbs.

Table 4: Antioxidant activity (%).

	Concentration, mg/L					Scavenging activity
	25	50	100	200	500	
DPPH	29.85 ± 0.86[a]	31.75 ± 1.41[a]	40.88 ± 1.15[b]	47.63 ± 1.93[c]	71.44 ± 1.04[d]	229.19 ± 22.34[A]
ABTS	12.25 ± 0.67[a]	19.76 ± 0.63[b]	32.38 ± 0.46[c]	53.83 ± 0.27[d]	88.13 ± 0.73[e]	180.94 ± 3.48[A]
RP	0.091 ± 0.001[a]	0.108 ± 0.002[b]	0.132 ± 0.002[c]	0.178 ± 0.001[d]	0.328 ± 0.001[e]	443.60 ± 4.01[B]

Assay wavelength: 1,1-diphenyl-2-picrylhydrazyl (DPPH) = 517 nm and 2,2′-azinobis(3-ethylbenzothiazoline-6-sulfonic acid) (ABTS) = 414 nm, and reducing power (RP) = 700 nm.

Butylated hydroxytoluene (BHT) EC_{50}; DPPH: 121.85 ± 0.39 mg/L; ABTS: 93.85 ± 0.43 mg/L; RP: 26.71 ± 0.69 mg/L.

Each value represents mean ± standard deviation (SD), $n = 5$.

[a–e]Means with different superscripts in the row are significantly different at $P < 0.05$.

[A]EC_{50} (mg/L) values were calculated from the calibration curves using five different concentrations (25–500 mg/L) in quintuplicate and their data were presented as 50% scavenging activity.

[B]RP value ($EC_{0.3}$) was reducing activity calculated from the calibration curves using five different concentrations (25–500 mg/L) in quintuplicate.

Antioxidant capacity can be evaluated by using a number of *in vitro* methods. Because the assay results are method dependent, a combined assay involving several methods is often used [34]. In this study, the antioxidant activity of the polyphenol mixture isolated from *E. supina* was determined by $DPPH^{\bullet}$ and $ABTS^{\bullet+}$ scavenging and RP assay at a concentration ranging from 25 to 500 mg/L. In $DPPH^{\bullet}$ scavenging tests, antioxidant activity is monitored by measuring the disappearance of purple $DPPH^{\bullet}$, which can be detected spectrophotometrically at 517 nm [16]. In the $ABTS^{\bullet+}$ scavenging assay, the added antioxidants reduce the deep blue $ABTS^{\bullet+}$ to ABTS, and the decrease in absorbance of $ABTS^{\bullet+}$ at 414 nm is monitored [16]. The RP assay can also serve as an indicator of antioxidant activity. The added antioxidants convert the iron ion (Fe^{3+}) to Fe^{2+}. The increase in absorbance of the deep-green Fe^{2+} solution at ~700 nm is monitored [16]. The assay results are provided in Table 4. The antioxidant capacity assayed using three methods showed a similar tendency. Thus, the antioxidant capacity of the *E. supina* polyphenol mixture showed a dose-dependent increase. $DPPH^{\bullet}$ or $ABTS^{\bullet+}$ scavenging activity can be represented as an EC_{50} value, which is the antioxidant concentration required to bring about a 50% loss in absorbance at 517 nm for $DPPH^{\bullet}$ and 414 nm for $ABTS^{\bullet+}$ as determined by linear regression analysis [16]. RP can be represented as $EC_{0.3}$, which is the reducing activity presented by the sample concentration at 0.3 of the absorbance value at 700 nm. Low EC_{50} and RP values signify high antioxidant activity [33]. The $DPPH^{\bullet}$ and $ABTS^{\bullet+}$ scavenging activity of butylated hydroxytoluene (BHT) as the control were 121.85 ± 0.39 mg/L and 93.85 ± 0.43 mg/L, respectively. The $EC_{0.3}$ value of BHT was 26.71 ± 0.69 mg/L. The antioxidant capacity values represented in terms of the $DPPH^{\bullet}$ and $ABTS^{\bullet+}$ scavenging activity and RP value were lower than those of BHT ($P < 0.05$).

3.4. Growth Inhibitory and Morphological Effects of Polyphenol Mixture of Korean E. supina. The anticancer activity of the polyphenol mixture of Korean *E. supina* was evaluated for human hepatocellular carcinoma Hep3B cells by MTT assay. The assay is a colorimetric method that measures cancer cell viability, quantifying the activity of the mitochondrial enzyme that reduces the yellow MTT molecule to purple formazan [34]. The cell line was incubated with serial concentrations of the polyphenol mixture ranging from 31.25 to 500 mg/L for 24 h and then subjected to MTT assays. The results are shown in Figure 3. The cell viability was decreased at polyphenol mixtures >250 mg/L, and the IC_{50} value was 500 mg/L. After treatment with the polyphenol mixtures for 24 h, the morphological changes such as loss of cell adhesion and floating cell debris were also observed, as shown in Figure 4. The MTT assay results and morphological changes show that the polyphenol mixtures effectively suppressed cell viability.

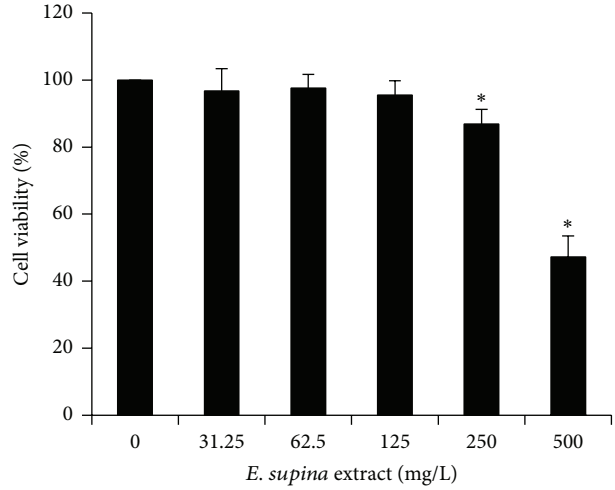

Figure 3: Antiproliferation effect on Hep3B cells by the *Euphorbia supina* polyphenol mixture. Hep3B cells were treated with the indicated concentrations of the *E. supina* polyphenol mixture for 24 h and viability was determined using 3-(4,5-dimethylthiazol-2-yl)-2,5-diphenyltetrazolium bromide (MTT) assay. Data represent the mean ± standard deviation (SD) of three replicates of independent experiments. The asterisk (∗) indicates a significant difference from the control group ($P < 0.05$).

4. Conclusion

Nine polyphenols from the Korean *E. supina* were profiled using a single HPLC–MS/MS run. The antioxidant activities of the flavonoids were evaluated in terms of $DPPH^{\bullet}$

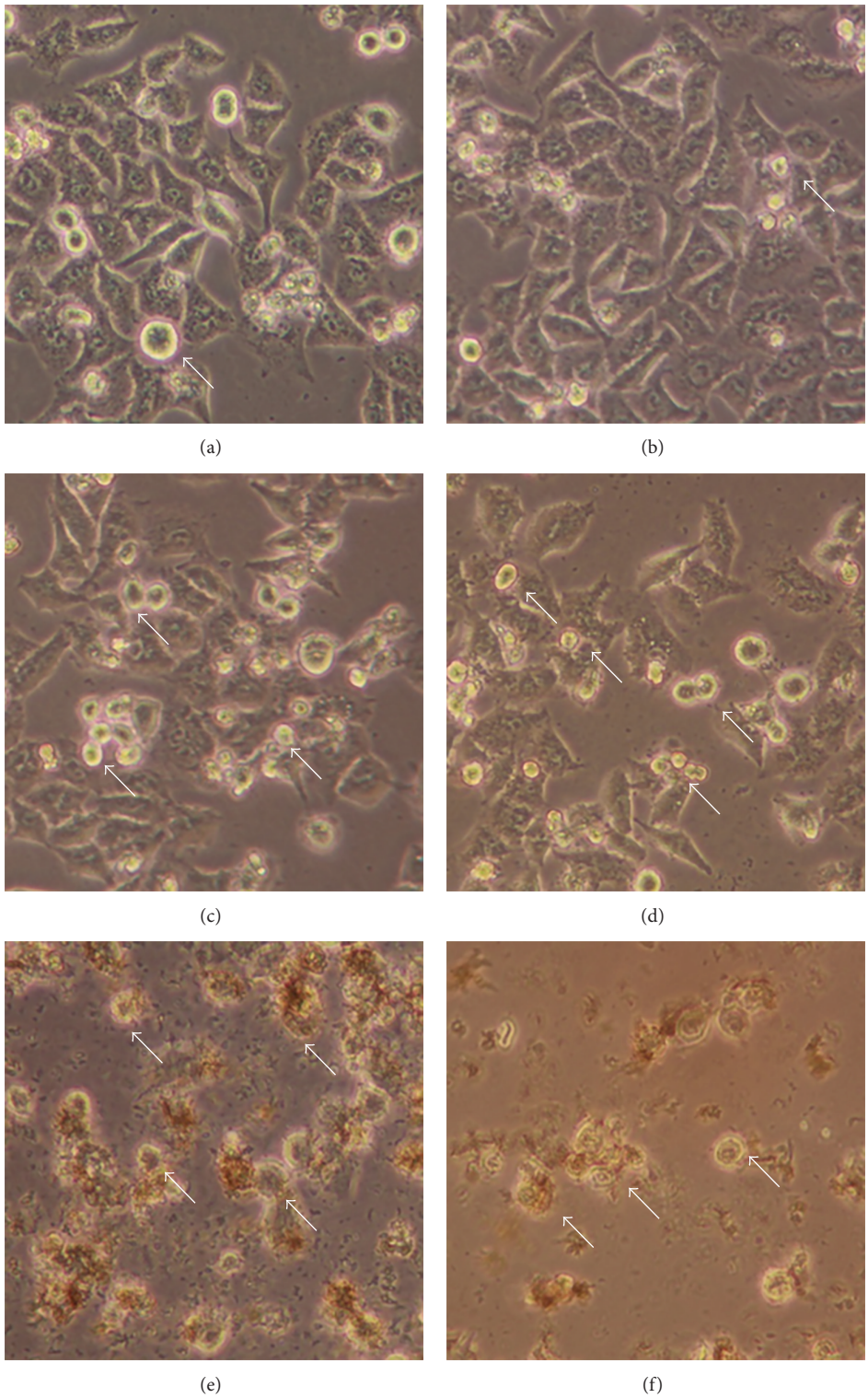

Figure 4: Morphological changes in Hep3B cells. Morphology of Hep3B cells visualized by optical microscopy (×100). The cells were treated with various concentrations of the *Euphorbia supina* polyphenol mixture for 24 h. (a) Control, (b) 31.25 mg/L, (c) 62.5 mg/L, (d) 125 mg/L, (e) 250 mg/L, and (f) 500 mg/L. White arrows indicate suspended cells.

and $ABTS^{\bullet+}$ scavenging activities, and the reducing power showed a dose-dependent increase. Suppression of cell viability was observed at polyphenol mixture concentrations >250 mg/L.

Conflict of Interests

The authors declare that there is no conflict of interests regarding the publication of this paper.

Authors' Contribution

Yi Song, Sung Woo Jeong, and Won Sup Lee contributed equally to this study.

Acknowledgments

This study was supported by the National R&D Program for Cancer Control, Ministry of Health & Welfare, Republic of Korea (no. 0820050), and the National Research Foundation (NRF) of Korea Grant funded by the Korean government (MEST) (no. 2012R1A2A2A06045015).

References

[1] Prostrate Spurge Description, http://www.turf.uiuc.edu/weed_web/descriptions/prostratespurge.htm.

[2] R. Tanaka, M. Kurimoto, M. Yoneda, and S. Matsunaga, "17β,21β-Epoxyhopan-3β-ol and β-alnincanol from *Euphorbia supina*," *Phytochemistry*, vol. 29, no. 7, pp. 2253–2256, 1990.

[3] R.-B. An, J.-W. Kwon, T.-O. Kwon, W.-T. Chung, H.-S. Lee, and Y.-C. Kim, "Chemical constituents from the whole plants of *Euphorbia supina* Rafin," *Korean Journal of Pharmacognosy*, vol. 38, no. 3, pp. 291–295, 2007.

[4] R. Tanaka and S. Matsunaga, "Loliolide and olean-12-en-3β,9α,11α-triol from *Euphorbia supina*," *Phytochemistry*, vol. 28, no. 6, pp. 1699–1702, 1989.

[5] I. Agata, T. Hatano, Y. Nakaya et al., "Tannins and related polyphenols of euphorbiaceous plants. VIII. Eumaculin A and eusupinin A, and accompanying polyphenols from *Euphorbia maculata* L. and *E. supina* Rafin," *Chemical and Pharmaceutical Bulletin*, vol. 39, no. 4, pp. 881–883, 1991.

[6] S.-H. Lee, T. Tanaka, G. Nonaka, and I. Nishioka, "Tannins and related compounds. CV. Monomeric and dimeric hydrolyzable tannins having a dehydrohexahydroxydiphenoyl group, supinanin, euphorscopin, euphorhelin and jolkianin, from *Euphorbia* species," *Chemical and Pharmaceutical Bulletin*, vol. 39, no. 3, pp. 630–638, 1991.

[7] Z. Fang, X. Zeng, Y. Zhang, and G. Zhou, "Chemical constituents of spotted leaf euphorbia (*Euphorbia supina*)," *Zhongcaoyao*, vol. 24, pp. 230–233, 1993.

[8] I. Erlund, "Review of the flavonoids quercetin, hesperetin, and naringenin. Dietary sources, bioactivities, bioavailability, and epidemiology," *Nutrition Research*, vol. 24, no. 10, pp. 851–874, 2004.

[9] L. Le Marchand, "Cancer preventive effects of flavonoids—a review," *Biomedicine and Pharmacotherapy*, vol. 56, no. 6, pp. 296–301, 2002.

[10] Y. C. Xu, S. W. S. Leung, D. K. Y. Yeung et al., "Structure-activity relationships of flavonoids for vascular relaxation in porcine coronary artery," *Phytochemistry*, vol. 68, no. 8, pp. 1179–1188, 2007.

[11] D. Treutter, "Significance of flavonoids in plant resistance: a review," *Environmental Chemistry Letters*, vol. 4, no. 3, pp. 147–157, 2006.

[12] H. Nierheilig and Y. Piché, "Signalling in arbuscular mycorrhiza: facts and hypotheses," *Flavonoids in Cell Function*, vol. 505, pp. 23–39, 2002.

[13] H. K. Hong, J. H. Kwak, S. C. Kang et al., "Antioxidative constituents from the whole plants of *Euphorbia supina*," *Korean Journal of Pharmacognosy*, vol. 39, no. 3, pp. 260–264, 2008.

[14] E. de Rijke, P. Out, W. M. A. Niessen, F. Ariese, C. Gooijer, and U. A. T. Brinkman, "Analytical separation and detection methods for flavonoids," *Journal of Chromatography A*, vol. 1112, no. 1-2, pp. 31–63, 2006.

[15] H. G. Kim, G.-S. Kim, S. Park et al., "Flavonoid profiling in three citrus varieties native to the Republic of Korea using liquid chromatography coupled with tandem mass spectrometry: contribution to overall antioxidant activity," *Biomedical Chromatography*, vol. 26, no. 4, pp. 464–470, 2012.

[16] O. N. Seo, G.-S. Kim, S. Park et al., "Determination of polyphenol components of *Lonicera japonica* Thunb. Using liquid chromatography-tandem mass spectrometry: contribution to the overall antioxidant activity," *Food Chemistry*, vol. 134, no. 1, pp. 572–577, 2012.

[17] L. Chen, J. Qi, Y.-X. Chang, D. Zhu, and B. Yu, "Identification and determination of the major constituents in Traditional Chinese Medicinal formula Danggui-Shaoyao-San by HPLC-DAD-ESI-MS/MS," *Journal of Pharmaceutical and Biomedical Analysis*, vol. 50, no. 2, pp. 127–137, 2009.

[18] X. Liu, S. Jiang, K. Xu et al., "Quantitative analysis of chemical constituents in different commercial parts of Notopterygium incisum by HPLC-DAD-MS," *Journal of Ethnopharmacology*, vol. 126, no. 3, pp. 474–479, 2009.

[19] S. Ek, H. Kartimo, S. Mattila, and A. Tolonen, "Characterization of phenolic compounds from lingonberry (*Vaccinium vitis-idaea*)," *Journal of Agricultural and Food Chemistry*, vol. 54, no. 26, pp. 9834–9842, 2006.

[20] A. Lhuillier, N. Fabre, F. Moyano et al., "Comparison of flavonoid profiles of *Agauria salicifolia* (Ericaceae) by liquid chromatography-UV diode array detection-electrospray ionisation mass spectrometry," *Journal of Chromatography A*, vol. 1160, no. 1-2, pp. 13–20, 2007.

[21] N. Kumar, P. Bhandari, B. Singh, and S. S. Bari, "Antioxidant activity and ultra-performance LC-electrospray ionization-quadrupole time-of-flight mass spectrometry for phenolics-based fingerprinting of Rose species: *Rosa damascena*, *Rosa bourboniana* and *Rosa brunonii*," *Food and Chemical Toxicology*, vol. 47, no. 2, pp. 361–367, 2009.

[22] M. Olszewska, "Quantitative HPLC analysis of flavonoids and chlorogenic acid in the leaves and inflorescences of *Prunus serotina* Ehrh," *Acta Chromatographica*, no. 19, pp. 253–269, 2007.

[23] H. K. Hong, J. H. Kwak, S. C. Kang et al., "Antioxidative constituents from the whole plants of *Euphorbia supina*," *Korean Journal of Pharmacognosy*, vol. 39, no. 3, pp. 260–264, 2008.

[24] Y.-J. Hong and A. E. Mitchell, "Metabolic profiling of flavonol metabolites in human urine by liquid chromatography and tandem mass spectrometry," *Journal of Agricultural and Food Chemistry*, vol. 52, no. 22, pp. 6794–6801, 2004.

[25] X. Meng, P. Maliakal, H. Lu, M.-J. Lee, and C. S. Yang, "Urinary and plasma levels of resveratrol and quercetin in humans, mice,

and rats after ingestion of pure compounds and grape juice," *Journal of Agricultural and Food Chemistry*, vol. 52, no. 4, pp. 935–942, 2004.

[26] M. Dehkharghanian, H. Adenier, and M. A. Vijayalakshmi, "Study of flavonoids in aqueous spinach extract using positive electrospray ionisation tandem quadrupole mass spectrometry," *Food Chemistry*, vol. 121, no. 3, pp. 863–870, 2010.

[27] K. Murota and J. Terao, "Antioxidative flavonoid quercetin: implication of its intestinal absorption and metabolism," *Archives of Biochemistry and Biophysics*, vol. 417, no. 1, pp. 12–17, 2003.

[28] J. M. Calderón-Montaño, E. Burgos-Morón, C. Pérez-Guerrero, and M. López-Lázaro, "A review on the dietary flavonoid kaempferol," *Mini-Reviews in Medicinal Chemistry*, vol. 11, no. 4, pp. 298–344, 2011.

[29] Oxidative stress, http://en.wikipedia.org/wiki/Oxidative_stress.

[30] E. Hopps, D. Noto, G. Caimi, and M. R. Averna, "A novel component of the metabolic syndrome: the oxidative stress," *Nutrition, Metabolism and Cardiovascular Diseases*, vol. 20, no. 1, pp. 72–77, 2010.

[31] T. Finkel, "Radical medicine: treating ageing to cure disease," *Nature Reviews Molecular Cell Biology*, vol. 6, no. 12, pp. 971–976, 2005.

[32] M. Valko, D. Leibfritz, J. Moncol, M. T. D. Cronin, M. Mazur, and J. Telser, "Free radicals and antioxidants in normal physiological functions and human disease," *International Journal of Biochemistry and Cell Biology*, vol. 39, no. 1, pp. 44–84, 2007.

[33] J. H. Lee, S. J. Lee, S. Park et al., "Characterisation of flavonoids in *Orostachys japonicus* A. Berger using HPLC-MS/MS: contribution to the overall antioxidant effect," *Food Chemistry*, vol. 124, no. 4, pp. 1627–1633, 2011.

[34] T. Mosmann, "Rapid colorimetric assay for cellular growth and survival: application to proliferation and cytotoxicity assays," *Journal of Immunological Methods*, vol. 65, no. 1-2, pp. 55–63, 1983.

Hindawi Publishing Corporation
Journal of Analytical Methods in Chemistry
Volume 2014, Article ID 989543, 8 pages
http://dx.doi.org/10.1155/2014/989543

Research Article

Antioxidant, Antibacterial, and Cytoprotective Activity of Agathi Leaf Protein

A. S. Zarena, Shubha Gopal, and R. Vineeth

Department of Studies in Microbiology, University of Mysore, Mysore 570006, India

Correspondence should be addressed to Shubha Gopal; shubhagopal_mysore@yahoo.com

Received 30 May 2013; Revised 23 October 2013; Accepted 5 November 2013; Published 28 January 2014

Academic Editor: Jian Yang

In the present study a protein termed agathi leaf protein (ALP) from *Sesbania grandiflora Linn*. (agathi) leaves was isolated after successive precipitation with 65% ammonium sulphate followed by purification on Sephadex G 75. The column chromatography of the crude protein resulted in four peaks of which Peak I (P I) showed maximum inhibition activity against hydroxyl radical. SDS-PAGE analysis of P I indicated that the molecular weight of the protein is ≈29 kDa. The purity of the protein was 98.4% as determined by RP-HPLC and showed a single peak with a retention time of 19.9 min. ALP was able to reduce oxidative damage by scavenging lipid peroxidation against erythrocyte ghost (85.50 ± 6.25%), linolenic acid (87.67 ± 3.14%) at 4.33 μM, ABTS anion (88 ± 3.22%), and DNA damage (83 ± 4.20%) at 3.44 μM in a dose-dependent manner. The purified protein offered significant protection to lymphocyte (72% at 30 min) induced damage by t-BOOH. In addition, ALP showed strong antibacterial activity against *Pseudomonas aeruginosa* (20 ± 3.64 mm) and *Staphylococcus aureus* (19 ± 1.53 mm) at 200 μg/mL. The safety assessment showed that ALP does not induce cytotoxicity towards human lymphocyte at the tested concentration of 0.8 mg/mL.

1. Introduction

Plants contain a huge range of active compounds with the most abundant being polyphenols, carotenoids, vitamin, and metals like zinc and selenium which form an integral part of antioxidant systems and reduce cellular damages. In addition fruits and vegetables are often low in fat and therefore dietary sources have been recognized as safe and effective antioxidants. In recent years considerable effort has been directed towards the search for safe antioxidants from natural sources in context to their efficiency and nontoxicity.

Sesbania grandiflora also known as agathi belongs to the family Fabaceae. It is a fast growing tree and is widely distributed in India, Indonesia, Myanmar, Philippines, and Thailand. The tree grows 5–15 m tall and the leaves and flowers of this tree are eaten as nutrition source. The leaves are bitter in taste and are rich in vitamin C, calcium, sterols, saponin, quercetin, myricetin, and kaempferol [1]. The leaves of the agathi are well known for their antiurolithiatic activity against calcium oxalate-type stones [2]. In a recent study, China et al. [3] have reported antimicrobial property of polyphenolic extract of *S. grandiflora* on pathogenic bacteria and growth promoting effect on *Lactobacillus acidophilus*. Boonmee et al. [4] have isolated two unique proteins (SGF60 and SGF90) from the flower extract of agathi showing α-glucosidase inhibiting property. Laladhas et al. [5] have isolated a protein fraction (*Sesbania* fraction 2) from the flower of *S. grandiflora* which possesses anticancer efficacy. We herein report the details of our study leading to the isolation and purification of a novel ≈29 kDa protein from *S. grandiflora* leaves. The newly isolated protein hereafter called agathi leaf protein (ALP) was tested *in vitro* for antioxidant, cytoprotective, and antibacterial activity.

2. Experimental

2.1. Materials. BHA (butylated hydroxyanisole), N,N,N′,N′-tetramethylethylenediamine (TEMED) bisacrylamide, 2,2-azinobis(3-ethylbenzothiazoline-6-sulfonic acid) diammonium salt (ABTS), and 5,5′-dithiobis-(2-nitrobenzoic acid) (DTNB) were from Sigma Chemicals (St. Louis, MO, USA). t-BOOH (tertiary butylated hydroperoxide) and Sephadex G 75 were purchased from Pharmacia, Sweden. Ferric chloride, hydrogen peroxide (H_2O_2), ferrous sulphate, ascorbic

acid, potassium persulfate, ethylenediaminetetraacetic acid (EDTA), thiobarbituric acid (TBA), polyvinyl pyrrolidone, and 2-deoxyribose were purchased from Merck (Mumbai, India). Calf thymus DNA was from Himedia Private Ltd. (Mumbai, India). All other reagents used were of analytical grade.

The plant sample of *Sesbania grandiflora* (Family: Fabaceae) was collected from Mysore (Karnataka), India. The fresh uninfected leaves were washed in autoclaved water to remove extraneous material, air-dried in an open space at aseptic condition for about 10–15 days, ground to fine powder, and stored at 4°C overnight until further use.

2.2. Bacterial Strains. Bacterial strains used in the study were *Staphylococcus aureus* ATCC 12600 (Gram-positive bacteria), *Salmonella typhimurium* ATCC 13311, *Escherichia coli* ATCC *11775*, *Vibrio parahaemolyticus* ATCC 17802, *Klebsiella pneumoniae* ATCC 10031, and *Pseudomonas aeruginosa* ATCC 10145 (Gram-negative bacteria).

2.3. Preparation of the Agathi Leaf Protein Extract. Five grams of agathi leaf powder was added to 50 mL of hot double-distilled water; to this 100 mg of polyvinyl pyrrolidone was added to remove polyphenols. The resultant solution was homogenized and incubated overnight at 4°C. The supernatant was centrifuged at 10,000 rpm for 15 min at 4°C (refrigerated centrifugation) and was filtered through Whatman number 1 filter paper. The above crude extract was precipitated with 0–80% ammonium sulphate and dialyzed against double-distilled water for 3 days with four changes. The precipitates were pooled by centrifugation at 10,000 rpm for 15 min and resuspended in double-distilled water and dialysed to desalt $(NH_4)_2SO_4$. The solution was concentrated and fractionated on Sephadex G 75 using Tris-HCl buffer (25 mM, pH 7.4) as eluent (1 g crude protein, V_o 35.4 mL, V_t 114 mL, and flow rate 1.5 mL/5 min). Each fraction was monitored at 280 nm and the protein content was estimated by Bradford's method [6]. The peak fractions (Peak I) which had maximum antioxidant activity were pooled, lyophilized, and rechromatographed on Sephadex G 75 column for further analysis.

2.4. Proximate Analysis

2.4.1. Estimation of Protein Content. The total protein content of the crude extract was determined by Bradford's [6] method. Various concentrations of bovine albumin (0–100 μg/mL) or agathi leaves extract at the concentration ranging from 0 to 20 μL were added to series of tubes and the volume was made up to 100 μL with 0.15 M NaCl. 1 mL Bradford's reagent was added to all the tubes and mixed well. The absorbance was measured at 595 nm. The concentration of the protein in the samples was determined from the calibration curve.

2.4.2. Estimation of Total Sugar. The total sugar was estimated by the phenol-sulphuric acid method [7]. Different aliquots of the extract (0–25 μL) were made up to 1 mL with distilled water. To this 1 mL of 5% phenol and 5 mL of concentrated sulphuric acid were added. Orange color developed was read at 520 nm immediately. The sugar concentration of the extract was calculated according to the standard glucose calibration curve.

2.4.3. Determination of SH Groups. Sulphydryl group was estimated by Ellman's method [8]. 5-6 mg of agathi leaf protein extract was taken in 2 mL of phosphate buffer (0.1 M, pH 8.0), to this 0.4% 5,5′-dithiobis-(2-nitrobenzoic acid) (DTNB) of aqueous solution was added and mixed well. Absorbance was measured at 412 nm after 1 min. The concentration of the sample was determined using the formula

$$C_o = \frac{A}{ED}, \tag{1}$$

where C_o is the concentration of the sample, A is the absorbance at 412 nm, E is the molar extinction coefficient of 13,600 M^{-1} cm^{-1}, and D is the dilution factor.

2.4.4. Determination of Total Phenol Content. The total phenolic content was determined according to the method of Folin-Ciocalteu reaction [9] with minor modifications, using gallic acid as standard. An aliquot of the samples (10–40 μL) was mixed with 50% Folin-Ciocalteu reagent; the volume was made up to 1 mL with methanol: water mixture (50 : 50 v/v). The mixture was then allowed to stand for 10 min followed by the addition of 20% Na_2CO_3. After 10 min incubation at ambient temperature, absorbance was measured at 725 nm. Results were expressed as milligrams of gallic acid equivalents (GAE) per gram.

2.4.5. Estimation of Total Chlorophyll. The total chlorophyll content was determined according to the method of Sadasivam and Manickam [10] with minor modifications. 1 g of agathi leaves was ground in a clean mortar and pestle with 15–20 mL of 80% acetone and centrifuged at 5000 rpm for 10 min and supernatant was collected. This procedure was repeated several times till a clear supernatant was obtained and the volume was made up to 100 mL with 80% acetone. The absorbance of the solution was read at 645 nm and 663 nm against solvent (80% acetone) blank. The amount of total chlorophyll present in the extract was calculated using the following equation:

$$\text{mg chlorophyll/g extract} = 20.2\ (A_{645}) + 8.02\ (A_{663}) \times \frac{V}{100 \times V}, \tag{2}$$

where A is the absorbance at specific wavelengths, V is the final volume of chlorophyll extract in 80% acetone, and W is the dry weight of extract.

2.4.6. Test for Protein. Agathi leaf protein was spotted on chromatography paper, sprayed with 0.2% solution of ninhydrin (indane-1,2,-3-trione hydrate), and dried. The appearance of purple/violet color spot indicated the presence of protein.

2.5. Determination of Molecular Weight and Purity Check. Polyacrylamide slab gel (12% acrylamide in separating gel and with 4% in stacking gel) was prepared and electrophoresis was performed as described by Laemmli [11]. The samples were mixed with sample buffer containing glycerol, sodium dodecyl sulfate (SDS) in Tris buffer (pH 8.3), and bromophenol blue as tracking dye. Prior to electrophoresis, the samples were incubated at 95°C for 5 min. Gel was run at 50 V for stacking and 100 V for separating gel. The bands were stained with coomassie brilliant blue-250 and destained in methanol/acetic acid/water (5/1/5; v/v/v).

A reversed-phase high-performance liquid chromatographic was performed for evaluation of purity of the isolated protein. Separation of the peak was accomplished on a Phenomenex C-18 column 250 mm × 4.60 mm i.d.; particle size, 5 mm at ambient temperature using 0.1% formic acid in acetonitrile : methanol (75 : 25) as mobile phase in an isocratic elution mode. A photodiode array detector set at 280 nm was used for detection.

2.6. Hydroxyl Radical Scavenging Activity. Deoxyribose assay was used to determine the hydroxyl radical scavenging activity according to the method of Chung et al. [12] with some modification. The reaction mixture contained $FeCl_3$ and ascorbate (100 μM), H_2O_2 (1 mM), EDTA (100 μM), 2-deoxy-D-ribose (2.8 mM), and 1 mL of 0.1 mM potassium phosphate buffer (pH 7.4) mixed in various concentrations of ALP extract (50–400 μg/mL). The reaction mixture was incubated for 1 hour at 37°C. The reaction was terminated by adding 1 mL each of TCA (2.8%) and TBA (0.5%); this mixture was placed in boiling water bath for 15 min. After cooling, the reaction mixture was centrifuged for 5 min at 5000 rpm. The control was without any test compound and the readings were taken at 535 nm. The percentage hydroxyl radical scavenging activity was determined by comparing with control. Decreased absorbance of the reaction mixture indicated decreased oxidation. Consider the following:

$$\% \ \text{Inhibition} = \frac{\text{Absorbance}_{\text{Control}} - \text{Abosorbance}_{\text{Test}}}{\text{Absorbance}_{\text{Control}}} \times 100. \quad (3)$$

2.7. Determination of Antioxidant Activity Using Erythrocyte Ghost and Linolenic Acid Micelles. Erythrocyte membranes (ghosts) preparation was carried out according to the method of Dodge et al. [13] with modifications. Fresh heparinised human blood samples were drawn with anticoagulant (acid citrate dextrose) and centrifuged at 2500 rpm for 10 min at 4°C; the supernatant was discarded and the pellet was washed 3–5 times with isotonic phosphate buffer (PBS 5 mM, pH 7.4, and 150 mM NaCl). The RBC cell pellet was suspended in hypotonic phosphate buffer (PBS 5 mM, pH 7.4 at 4°C) for hemolysis to take place. Contents were centrifuged at 12,000 rpm at 4°C for 20 min. Erythrocytes were separated from plasma and buffy coat and buffy cat was washed with fresh hypotonic phosphate buffer centrifuged at 1500 rpm for 10 min to remove unlysed RBC cells. Finally, the membranes were resuspended in isotonic 5 mM phosphate buffer, pH 7.4, to yield a dispersed pale yellowish pink "ghost." The protein content of ghost was estimated by Bradford's method [6]. Ghost suspension (200 μg) and linolenic acid (1.8 μmole) were subjected to peroxidation by ferrous sulphate and ascorbic acid (10 : 100 μmole) in a final volume of 0.5 mL Tris buffered saline (TBS 100 mM, pH 7.4, and 0.15 M NaCl) with increasing concentration of ALP extracts (0.86–4.33 μM); the contents were incubated at 37°C for 1 h; to this 1% TBA was added; and the contents were kept in a boiling water bath for 15 min and then cooled, centrifuged to remove precipitate if any. The color developed was measured at 535 nm (see ((3)))

$$\% \ \text{Inhibition} = \frac{\text{Absorbance}_{\text{Control}} - \text{Abosorbance}_{\text{Test}}}{\text{Absorbance}_{\text{Control}}} \times 100. \quad (4)$$

2.8. DNA Sugar Damage by Spectrophotometric Method. Oxidative DNA sugar damage was induced with Fenton's reactants and was determined according to the method of Cao et al. [14]. The reaction mixture in a total volume of 1 mL containing 1 mg calf thymus DNA was treated with Fe^{3+} (10 mM), EDTA (10 mM), and H_2O_2 (2 mM) without or with various concentrations of the extract (0.68–3.44 μM) in potassium phosphate buffer (20 mM, pH 7.4). Ascorbic acid (10 mM) was added to the reaction mixture and was incubated at 37°C for 1 h in water bath with shaker. To 1 mL of the above mixture 1 mL, of TCA and 1 mL of 1% TBA were added and boiled for 20 min. The contents were cooled and the pink color absorbance was read at 523 nm (see ((3)))

$$\% \ \text{Inhibition} = \frac{\text{Absorbance}_{\text{Control}} - \text{Abosorbance}_{\text{Test}}}{\text{Absorbance}_{\text{Control}}} \times 100. \quad (5)$$

2.9. Scavenging of $ABTS^{\bullet+}$ Radical. ABTS radical cation decoloration assay was performed according to Re et al. [15] with some modifications. ABTS stock solution was prepared by reacting 7 mM ABTS with an oxidant 2.45 mM potassium persulfate in dark, at room temperature, for 12–16 h before use. Prior to the assay, the solution was diluted in water and equilibrated at room temperature to give an absorbance of 0.70 ± 0.02 at 734 nm. Different volumes of the sample (0.68–3.44 μM) were mixed with 3 mL of $ABTS^{\bullet+}$ solution and absorbance at 734 nm was measured. BHT was used as positive control. The scavenging activity was calculated using the following equation:

$$\% \ \text{Inhibition} = \frac{\text{Absorbance}_{\text{Control}} - \text{Abosorbance}_{\text{Test}}}{\text{Absorbance}_{\text{Control}}} \times 100. \quad (6)$$

2.10. Lymphocyte Isolation and Protection Study. Human peripheral lymphocytes were isolated according to the method of Smitha et al. [16]. To 10 mL of venous blood, four volumes of hemolysing buffer (150 mM NH_4Cl in 10 mM tris buffer, pH 7.4) were added and mixed well; the contents were

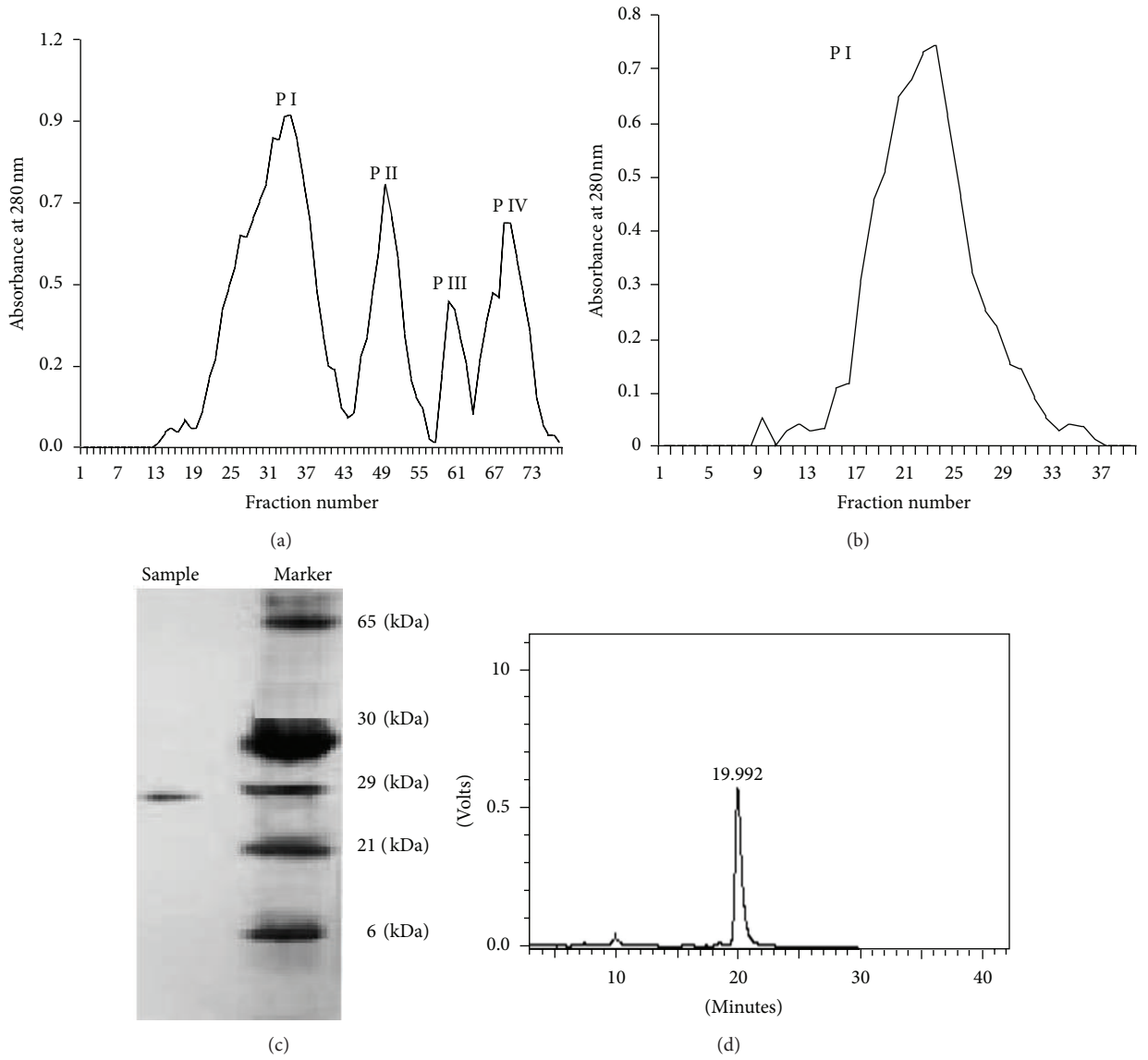

Figure 1: (a) Agathi leaf protein fractionated on Sephadex G-75 column and the fractions monitored at 280 nm. (b) Rechromatography of Peak I on Sephadex G-75 and the fractions monitored at 280 nm. Fractions were obtained at a flow rate of mL/min using Tris-HCl buffer. (c) SDS-PAGE analysis of Peak I yielding a single band of ≈29 kDa. (d) RP-HPLC of Peak I on Phenomenex C-18 column 250 mm × 4.60 mm i.d.; particle size, 5 mm.

incubated at 4°C for 30 min and centrifuged at 1200 rpm for 12 min, the supernatant was discarded, and pellet was washed thrice with 10 mL of 250 mM m-inositiol in 10 mM phosphate buffer, pH 7.4, and resuspended in the same solution. The cell viability was determined by trypan dye blue exclusion method. Percentage viability was calculated as

$$\% \ \text{Viability} = \frac{\text{Number of viable cells}}{\text{Total number of cells}} \times 100. \quad (7)$$

The isolated lymphocyte was subjected to lipid peroxidation by t-BOOH (1 mM) in the presence of ALP (6.8 μM) and BHA (400 μM) in a reaction mixture of 1 mL buffered with Hanks' buffer saline solution (HBSS), pH 7.4, and incubated at 37°C. To 10 μL of lymphocyte sample, 100 μL of tryphan blue (1%) was added and the viable cells (unstained) were counted using Neuber's chamber. (The dead cells being permeable to tryphan blue appear blue against white color of the viable cells.) The survival rate of lymphocyte was determined at time intervals 15, 30, 60, 180, and 300 min of incubation.

2.11. Cytotoxicity Study. Cell suspensions were incubated with different concentrations of ALP (0–0.8 mg/mL) for 30 min at 37°C in dark together with untreated control samples. Samples were then centrifuged at 2700 rpm, the lymphocytes were suspended in 0.9% saline and 1% trypan blue, and viable and dead cells were observed.

2.12. Antibacterial Activity of ALP. Antibacterial activity of the extract was determined by the disc diffusion method.

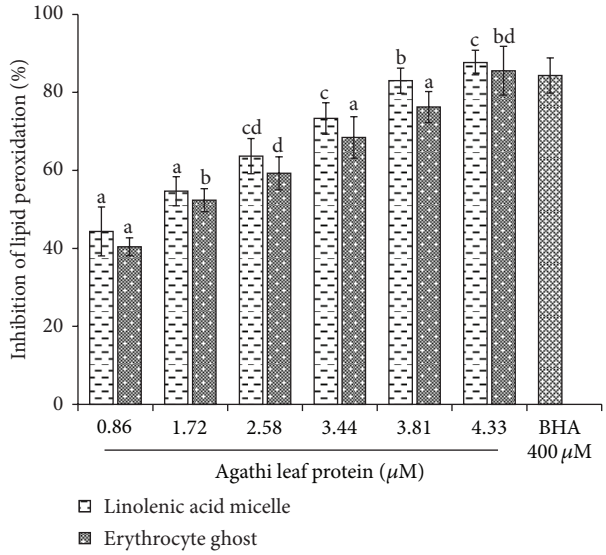

Figure 2: Inhibition of lipid peroxidation in linolenic acid micelle and erythrocyte ghost. Data are expressed as the mean ± standard deviation ($n = 3$). Means with different letters (a–d) are significantly different ($P < 0.05$).

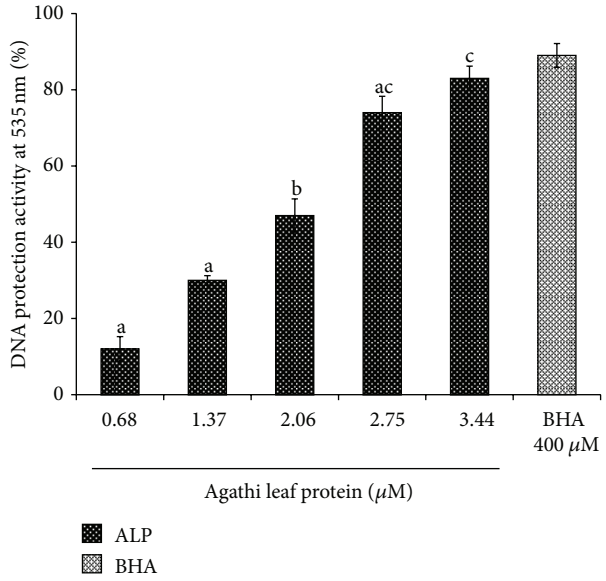

Figure 3: Inhibition of hydroxyl radical-mediated DNA degradation by ALP. Data are expressed as the mean ± standard deviation ($n = 3$). Means with different letters (a–c) are significantly different ($P < 0.05$).

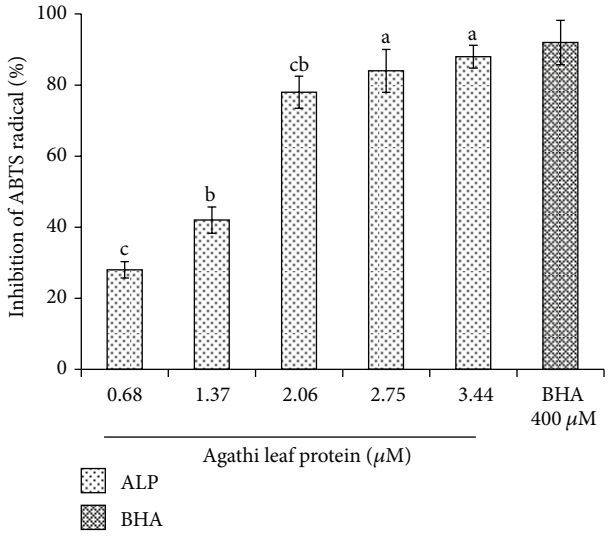

Figure 4: Scavenging effect of ALP on ABTS radical. Mean values ± standard deviations ($n = 3$) with the same letter are not significantly different ($P < 0.05$).

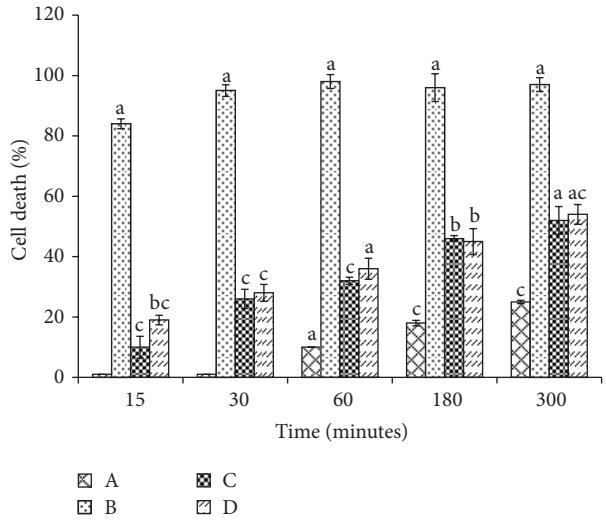

Figure 5: Prevention of t-BOOH induced cell death in lymphocytes by ALP and BHA. A: lymphocytes; B: lymphocytes + t-BOOH (1 mM); C: lymphocytes + t-BOOH (1 mM) + BHA (400 μM); D: lymphocytes + t-BOOH (1 mM) + ALP (6.88 μM). Data are expressed as the mean ± standard deviation ($n = 3$). Means with different letters (a–c) are significantly different ($P < 0.05$).

100 μL of overnight bacterial culture in Tryptic soy broth, adjusted to 0.4-0.5 Mc Farland turbidity (10^4 CFU/mL), was used as inoculum. The suspension was homogenously swabbed on Muller-Hinton agar media (MHA) using sterile cotton swab. The extract (100–200 μg/mL) was loaded on sterile disc (6 mm), placed on MHA medium containing the culture, and allowed to diffuse for 15 min. The plates were kept for incubation at 37°C for 24 hrs and the inhibition zones formed around the disc were measured in mm. Gentamicin (10 μg) disc was used as positive control and negative control was 20 mM Tris buffer saline.

2.13. Experimental Design and Statistical Analysis. Our present study was classified into two stages. The first stage was to isolate and purify the protein from agathi leaf extract. The second stage was to fix the effective concentration of ALP to carry out antioxidant, antimicrobial, and cytotoxicity study. Statistical analysis was carried out using Statistical Package for Social Science (SPSS, version 20.0). The experimental

results were expressed as the mean ± standard deviation ($n = 3$). Group comparisons were performed using one-way ANOVA followed by Tukey's post hoc test. A P value of 0.05 was considered statistically significant.

3. Results and Discussion

In the present study, 65% ammonium sulphate precipitation of the crude agathi leaf protein on their subsequent fractionation through sephadex G 75 column yielded four peaks that were designated as P I, II, III, and IV (Figure 1(a)). P I showed a maximum hydroxyl scavenging activity up to 83% at 100 μg followed by P III 54% at 250 μg, whereas P II and P I showed 38% and 32% activity at 400 μg, respectively. P I fraction that showed maximum antioxidant activity was pooled separately, lyophylised, and rechromatographed through Sephadex G 75, yielding a single peak (Figure 1(b)). Further the homogeneity and the purity of P I were confirmed by SDS-PAGE that resulted in a single band with approximate molecular weight of ≈29 kDa (Figure 1(c)). The molecular mass of the purified protein was estimated by comparison with the molecular mass of the marker protein. The HPLC chromatogram showed a single peak with a retention time of 19.9 min in isocratic mode and purity was 98.4% (Figure 1(d)). P I was designated as agathi leaf protein (ALP). The proximate analysis of the ALP extract proved to be positive for ninhydrin. There was no presence of polyphenols and chlorophyll. The total sugar was found to be 0.188 mmol. The test for sulphydryl group was positive with 6 μmol of sulfhydryl groups/g being detected.

The *in vitro* peroxidation of human erythrocyte ghosts and linolenic acid micelles was used as a model system to study the free radical induced damage of biological membranes and the protective effect of ALP. Membrane lipids being rich in unsaturated fatty acids especially linoleic, linolenic, and arachidonic acids when attacked by free radicals form lipid peroxide. In the present study the antioxidant activity of the ALP was studied in comparison with known antioxidant like BHA. It was observed that the inhibitory effect of ALP in erythrocyte ghost and linolenic acid micelles was found to be 85.50 ± 6.25% and 87.67 ± 3.14% at 4.33 μM dose dependently compared to BHA which showed an activity of 84.33 ± 4.50 at 400 μM (Figure 2). Erythrocyte ghost and linolenic acid micelles are simple suitable model system commonly used in the study of LOP as the protein composition of the former is well known and they lack organelles [17]. On the other hand, linolenic acids are present in food and organisms and their oxidation results in the formation of hydroperoxides.

The effect of ALP on hydroxyl radicals generated by Fe^{3+}/H_2O_2 ions was measured by determining the degree of DNA degradation by test tube assay (Figure 3). While a marginal inhibition was evident at the lower concentration, nearly 83 ± 4.20% inhibition was observed at higher concentration at 3.44 μM. The scavenging effect increased with increasing ALP concentration up to a certain extent (3.44 μM) and then leveled off with further increase. Further $ABTS^{\bullet+}$ method showed an activity of 88 ± 3.22% at 3.44 μM when compared to synthetic antioxidant BHA which showed an activity of 92 ± 4.03% at 400 μM (Figure 4) and leveled off thereafter. It was observed that the inhibition value of ALP increased with increase in concentration.

Table 1: Cytotoxicity of ALP extract toward human blood lymphocytes.

Concentration (mg/mL)	Viability (%)
0	98.0 ± 3.42^{c}
0.2	98.0 ± 1.34^{c}
0.4	96.0 ± 1.77^{a}
0.6	98.0 ± 1.86^{c}
0.8	97.0 ± 0.91^{b}

Data are expressed as the mean ± standard deviation ($n = 3$). Means with different letters (a–c) are significantly different ($P < 0.05$).

We also investigated the lipid peroxidation induced cell death by t-BOOH (Figure 5). Treatment with t-BOOH on lymphocyte cells significantly showed cell toxicity. The maximum cell death was induced by t-BOOH at 30 min, while the cells incubated with BHA (400 μM) or ALP (6.88 μM) showed an increase in cell viability. The protection offered by ALP was 72% and BHA was 74% at 30 min. As the time of incubation period increased, the percentage of cell death increased. The differences in antioxidant activity in the above assays could probably be due to the different mechanisms occurring in the assay, varying sensitivity of the assay system, and their concentration-dependent activities.

The protective effect of ALP toward human lymphocytes is shown in Table 1. The cell viability was greater than 95% at the concentrations tested (0–0.8 mg/mL). The high percentage of viable cell clearly indicates that ALP is a nontoxic protein with no cytotoxicity toward human lymphocytes. Table 2 shows the antimicrobial screening of ALP against Gram-positive and Gram-negative bacteria. ALP extract showed maximum antibacterial activity against *S. aureus, K. pneumonia*,and *P. aeruginosa* with zone of inhibition ranging from 15 to 20 mm at 200 μg/mL and no activity against *S. typhimurium* at the same concentrations. The most susceptible bacterium was *P. aeruginosa* ATCC 10031 (20 ± 3.64 mm diameter). The extract showed lower sensitivity in comparison to the positive control gentamicin. The antioxidant and antimicrobial activity of ALP could be attributed to the presence of cysteine/cystine and the occurrence of disulphide bridge [18] as determined by Ellman's test. In the present study, Ellman's test for "S–S" group proved to be positive indicating the presence of cysteine/cystine residues. SH group acts as free radical scavenger in plants and animals and facilitates the antioxidant activity of glutathione [19].

4. Conclusions

The results obtained in the present study demonstrate ALP obtained from water extract of agathi leaf can effectively scavenge various ROS *in vitro* conditions at low dose. ALP showed strong inhibitory activity toward lipid peroxidation

Table 2: Antimicrobial activity of ALP (zone size, mm).

Test bacteria	ALP (100 μg/mL)	ALP (200 μg/mL)	Gentamicin (10 μg)
Staphylococcus aureus ATCC 12600	—	19 ± 1.53^{a}	26 ± 0.25^{a}
Salmonella typhimurium ATCC 13311	—	—	15 ± 0.97^{c}
Escherichia coli ATCC 11775	13 ± 1.31^{c}	15 ± 1.24^{a}	17 ± 0.48^{a}
Vibrio parahemolyticus ATCC 17802	—	15 ± 2.20^{b}	18 ± 0.49
Klebsiella pneumoniae ATCC 10031	11 ± 0.40	18 ± 1.61^{b}	22 ± 0.83^{d}
Pseudomonas aeruginosa ATCC 10145	18 ± 0.86^{d}	20 ± 3.64^{c}	21 ± 0.62^{a}

(—): no inhibition.
Data are expressed as the mean ± standard deviation ($n = 3$). Means with different letters (a–d) within the same column are significantly different ($P < 0.05$).

on RBC ghost and linolenic acid micelle system. Furthermore, ALP exhibited a strong concentration-dependent inhibition against deoxyribose oxidation and DNA damage. ALP is not only interesting source for antioxidant but also potential source of antimicrobial agent and nontoxic in nature. The present study showed that the investigated proteins are promising ingredients for the development of functional foods with a beneficial impact on human health and an important source for the production of bioactive proteins.

Conflict of Interests

The authors declare that there is no conflict of interests regarding the publication of this paper.

Acknowledgment

A. S. Zarena acknowledges UGC—Dr. D. S. Kothari Fellowship (India).

References

[1] R. A. Mustafa, A. A. Hamid, S. Mohamed, and F. A. Bakar, "Total phenolic compounds, flavonoids, and radical scavenging activity of 21 selected tropical plants," *Journal of Food Science*, vol. 75, no. 1, pp. C28–C35, 2010.

[2] S. Doddola, H. Pasupulati, B. Koganti, and K. V. S. R. G. Prasad, "Evaluation of *Sesbania grandiflora* for antiurolithiatic and antioxidant properties," *Journal of Natural Medicines*, vol. 62, no. 3, pp. 300–307, 2008.

[3] R. China, S. Mukherjee, S. Sen et al., "Antimicrobial activity of *Sesbania grandiflora* flower polyphenol extracts on some pathogenic bacteria and growth stimulatory effect on the probiotic organism *Lactobacillus acidophilus*," *Microbiological Research*, vol. 167, no. 8, pp. 500–506, 2012.

[4] A. Boonmee, C. D. Reynolds, and P. Sangvanich, "α-glucosidase inhibitor proteins from *Sesbania grandiflora* flowers," *Planta Medica*, vol. 73, no. 11, pp. 1197–1201, 2007.

[5] K. P. Laladhas, V. T. Cheriyan, V. T. Puliappadamba et al., "A novel protein fraction from *Sesbania grandiflora* shows potential anticancer and chemopreventive efficacy, in vitro and in vivo," *Journal of Cellular and Molecular Medicine*, vol. 14, no. 3, pp. 636–646, 2010.

[6] M. M. Bradford, "A rapid and sensitive method for the quantitation of microgram quantities of protein utilizing the principle of protein dye binding," *Analytical Biochemistry*, vol. 72, no. 1-2, pp. 248–254, 1976.

[7] M. Dubois, K. A. Gilles, J. K. Hamilton, P. A. Rebers, and F. Smith, "Colorimetric method for determination of sugars and related substances," *Analytical Chemistry*, vol. 28, no. 3, pp. 350–356, 1956.

[8] G. L. Ellman, "Tissue sulfhydryl groups," *Archives of Biochemistry and Biophysics*, vol. 82, no. 1, pp. 70–77, 1959.

[9] P. Siddhuraju, P. S. Mohan, and K. Becker, "Studies on the antioxidant activity of Indian Laburnum (*Cassia fistula* L.): a preliminary assessment of crude extracts from stem bark, leaves, flowers and fruit pulp," *Food Chemistry*, vol. 79, no. 1, pp. 61–67, 2002.

[10] S. Sadasivam and A. Manickam, *Biochemical methods*, A New Age International, New Delhi, India, 1996.

[11] U. K. Laemmli, "Cleavage of structural proteins during the assembly of the head of bacteriophage T4," *Nature*, vol. 227, no. 5259, pp. 680–685, 1970.

[12] S.-K. Chung, T. Osawa, and S. Kawakishi, "Hydroxyl radical-scavenging effects of spices and scavengers from brown mustard (*Brassica nigra*)," *Bioscience, Biotechnology and Biochemistry*, vol. 61, no. 1, pp. 118–123, 1997.

[13] J. T. Dodge, C. Mitchell, and D. J. Hanahan, "The preparation and chemical characteristics of hemoglobin-free ghosts of human erythrocytes," *Archives of Biochemistry and Biophysics*, vol. 100, no. 1, pp. 119–130, 1963.

[14] W. Cao, W. J. Chen, X. H. Zheng, and J. B. Zheng, "Modified method to evaluate the protection of the antioxidants against hydroxyl radical-mediated DNA damage," *Acta Nutrimenta Sinica*, vol. 30, pp. 74–77, 2008.

[15] R. Re, N. Pellegrini, A. Proteggente, A. Pannala, M. Yang, and C. Rice-Evans, "Antioxidant activity applying an improved ABTS radical cation decolorization assay," *Free Radical Biology and Medicine*, vol. 26, no. 9-10, pp. 1231–1237, 1999.

[16] S. Smitha, B. L. Dhananjaya, R. Dinesha, and L. Srinivas, "Purification and characterization of a ~34 kDa antioxidant protein (β-turmerin) from turmeric (*Curcuma longa*) waste grits," *Biochimie*, vol. 91, no. 9, pp. 1156–1162, 2009.

[17] C. G. Fraga, M. K. Shigenaga, J.-W. Park, P. Degan, and B. N. Ames, "Oxidative damage to DNA during aging: 8-Hydroxy-2'-deoxyguanosine in rat organ DNA and urine," *Proceedings of the National Academy of Sciences of the United States of America*, vol. 87, no. 12, pp. 4533–4537, 1990.

[18] Z. Wang and G. Wang, "APD: the antimicrobial peptide database," *Nucleic Acids Research*, vol. 32, pp. D590–D592, 2004.

[19] H. Rennenberg, "Glutathione metabolism and possible biological roles in higher plants," *Phytochemistry*, vol. 21, no. 12, pp. 2771–2781, 1982.

Hindawi Publishing Corporation
Journal of Analytical Methods in Chemistry
Volume 2014, Article ID 932036, 6 pages
http://dx.doi.org/10.1155/2014/932036

Research Article

Compound Specific Extraction of Camptothecin from *Nothapodytes nimmoniana* and Piperine from *Piper nigrum* Using Accelerated Solvent Extractor

Vinayak Upadhya,[1] Sandeep R. Pai,[1] Ajay K. Sharma,[1,2] Harsha V. Hegde,[1] Sanjiva D. Kholkute,[1] and Rajesh K. Joshi[1]

[1] *Regional Medical Research Centre, Indian Council of Medical Research (ICMR), Nehru Nagar, Belgaum, Karnataka 590 010, India*
[2] *Department of Pharmacy, G.S.V.M. Medical College Kanpur, Uttar Pradesh 208002, India*

Correspondence should be addressed to Sandeep R. Pai; sandeeprpai@rediffmail.com
and Rajesh K. Joshi; joshirk_natprod@yahoo.com

Received 27 May 2013; Accepted 15 October 2013; Published 2 January 2014

Academic Editor: Shixin Deng

Effects of varying temperatures with constant pressure of solvent on extraction efficiency of two chemically different alkaloids were studied. Camptothecin (CPT) from stem of *Nothapodytes nimmoniana* (Grah.) Mabb. and piperine from the fruits of *Piper nigrum* L. were extracted using Accelerated Solvent Extractor (ASE). Three cycles of extraction for a particular sample cell at a given temperature assured complete extraction. CPT and piperine were determined and quantified by using a simple and efficient UFLC-PDA (245 and 343 nm) method. Temperature increased efficiency of extraction to yield higher amount of CPT, whereas temperature had diminutive effect on yield of piperine. Maximum yield for CPT was achieved at 80°C and for piperine at 40°C. Thus, the study determines compound specific extraction of CPT from *N. nimmoniana* and piperine from *P. nigrum* using ASE method. The present study indicates the use of this method for simple, fast, and accurate extraction of the compound of interest.

1. Introduction

Camptothecin (CPT) a known potent anticancer active compound and piperine an economically important high valued alkaloid were used as the marker compounds (Figure 1(a)). Camptothecin was originally isolated from a Chinese tree *Camptotheca acuminata* (Nyssaceae) [1]. It is also reported in *Nothapodytes nimmoniana* and few other species belonging to unrelated orders of angiosperm classification [2–4]. *Nothapodytes nimmoniana* occupies important position in plant-based anticancer drugs because of CPT. Enormous demand for this alkaloid worldwide in the recent years has been subject to haphazard exploitation of the populations from wild. More than 20% decline in the population of *N. nimmoniana* from Western Ghats region has led to classify it in "*vulnerable*" category [5].

Piperine, an important alkaloid, has been reported from the fruits of many wild species and domesticated cultivars of *Piper nigrum* L. (Figure 1(b)) [6–8]. *Piper nigrum* also known as "King of Spices" (black pepper) is considered an important commodity of commerce in agriculture [9].

Identification and quantification of metabolites by any analytical technique depend upon its extraction. Extraction may refer to separation of analytes from a complex matrix. The extraction efficiency is greatly influenced by factors such as: solvent composition, solvent to solid ratio, temperature, time, and method of extraction [10–12]. Till date the number of extraction methods has been implied for extraction of CPT [13, 14] and piperine [15–17] by using Soxhlet, continuous shaking, ultrasonication, microwave assisted extractions, and many more. However, most of the methods consume both time and solvents and very few are effective in complete extraction of analytes or compounds of interests.

A thorough learning and understanding of the experimental optimization is essential for validation and commercial application of the process. Accelerated Solvent Extractor (ASE) is a new technique applied to extract organic

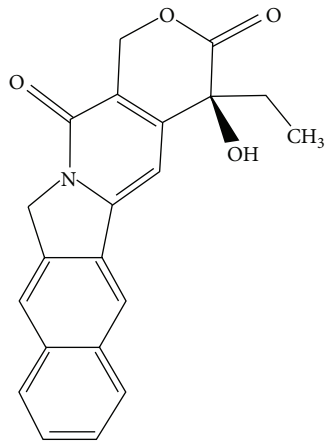

(a) Camptothecin (CPT) mol. formula: $C_{20}H_{16}N_2O_6$ mol. wt.: 348.40

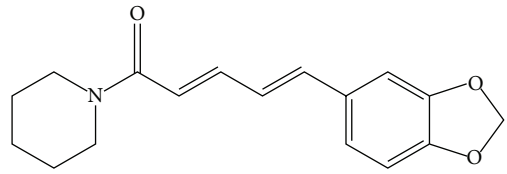

(b) Piperine mol. formula: $C_{20}H_{16}N_2O_6$ mol. wt.: 285.34

Figure 1: Chemical structures of camptothecin and piperine.

compounds from a variety of samples to optimize solvent condition and to reduce extraction time. It accelerates the extraction process by elevating temperature at high pressure of the solvents. Therefore, important plant metabolites and their optimization of extraction method are the need of today. Thus the present work implies optimization of extraction method using ASE and studies the effect of temperature on extraction efficiency of CPT and piperine from *N. nimmoniana* and *P. nigrum*, respectively.

2. Materials and Methods

2.1. Chemical Reagents and Standards. Standards camptothecin and piperine (HPLC grade) were obtained from Sigma-Aldrich (India). HPLC grade acetonitrile, methanol, ethanol, glacial acetic acid, and water were used for analysis.

2.2. Collection and Preparation of Plant Material. Stem parts of *N. nimmoniana* and fruits of *P. nigrum* were collected from Belgaum (N 15.6383° E 074.2784°) and North Canara (N 14.4721°, E 074.5131°), region of Western Ghats of Karnataka, India. Herbaria of plant twigs were authenticated and deposited at Regional Medical Research Centre (RMRC), Indian Council of Medical Research (ICMR), Belgaum, Karnataka, India, for future reference (Voucher Numbers-*N. nimmoniana*: RMRC 1313 and *P. nigrum*: RMRC 1213). The plant materials were dried at room temperature and grounded to powder. The powdered material was sieved through a 20 μm stainless sieve and taken for further analysis.

2.3. Accelerated Solvent Extractor (ASE) Sample Preparation. Extraction was carried out in Accelerated Solvent Extraction system ASE 350 (Dionex Corporation, Sunnyvale, CA, USA) equipped with a solvent controller unit. The cells of 5 mL capacity were employed for the study. Two cellulose filters were placed at the bottom of the sample cells before filling. The sample cells were filled with 1 g dried stem powder of *N. nimmoniana* and 0.1 g dry fruit powder of *P. nigrum* was utilized for extraction separately. Three scoops (~2.5 g) of ASE prep diatomaceous earth (Dinoex Corporation, Sunnyvale, California) were mixed with plant powder and loaded on the cell tray. Methanol and ethanol were used for extraction of CPT and piperine, respectively. The selection of the solvents for extraction was based on earlier reports [13–15]. To assure complete extraction, a particular sample cell at a given temperature was extracted in 3 cycles.

2.4. Quantification of Camptothecin and Piperine Using Reversed Phase-Ultraflow Liquid Chromatographic (RP-UFLC) Analysis

2.4.1. Instrumentation. The reversed phase-ultraflow liquid chromatographic (RP-UFLC) analysis was performed on Shimadzu chromatographic system (Model number LC-20AD) consisting of a quaternary pump, manual injector, degasser (DGU-20A5), and dual λ UV absorbance diode array detector SPD-M20A. The built-in LC-Solution software system was used for data processing. Chromatographic separation was achieved on a Hibar RP-select B column (LiChrospher 60, 5 μm, 4.6 × 250 mm) for CPT and RP-18e (LiChrospher 100, 5 μm, 4.6 × 250 mm) for piperine.

2.4.2. Chromatographic Conditions. Mobile phase consisting of acetonitrile : water (40 : 60) for CPT and methanol : water (70 : 30) for piperine was used for separation with an injection volume of 20 μL. A chromatographic condition of 1.0 and 1.4 mL min^{-1} flow rate at 254 and 343 nm was set for CPT and piperine, respectively. The retention time was observed 8 min for CPT and 10 min for piperine.

2.4.3. Calculations, Calibration Curves, and Linearity. Camptothecin was accurately weighed and dissolved in few drops (50 μL) of DMSO by warming and the volume was

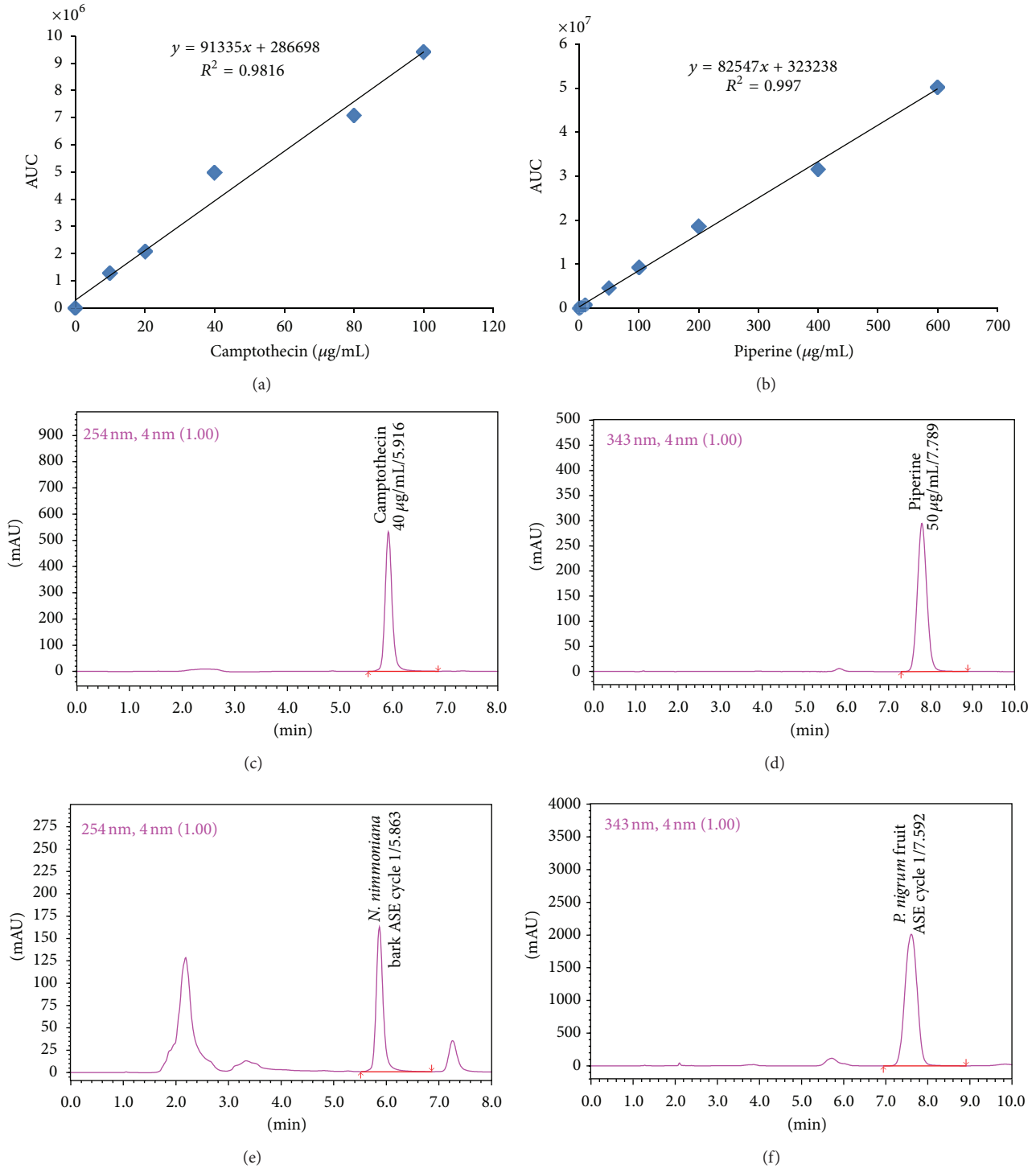

Figure 2: (a) Calibration curve of camptothecin; (b) calibration curve of piperine; (c) standard camptothecin (40 μg mL^{-1}); (d) standard piperine (50 μg mL^{-1}); (e) camptothecin from stem of *N. nimmoniana* extracted by ASE (Cycle 1); (f) piperine from fruits of *P. nigrum* extracted by ASE (Cycle 1).

made with methanol to produce a standard stock solution (0.5 mg mL^{-1}). Similarly, 1 mg mL^{-1} stock solution of piperine in methanol was prepared. The stock solutions of CPT and piperine were prepared and serially diluted with respective solvents to obtain working concentrations for plotting calibration curves. Seven different concentration levels of CPT (0.001, 0.01, 10, 20, 40, 80, and 100 μg mL^{-1}) and nine of piperine (0.01, 1, 3, 10, 50, 100, 200, 400, and

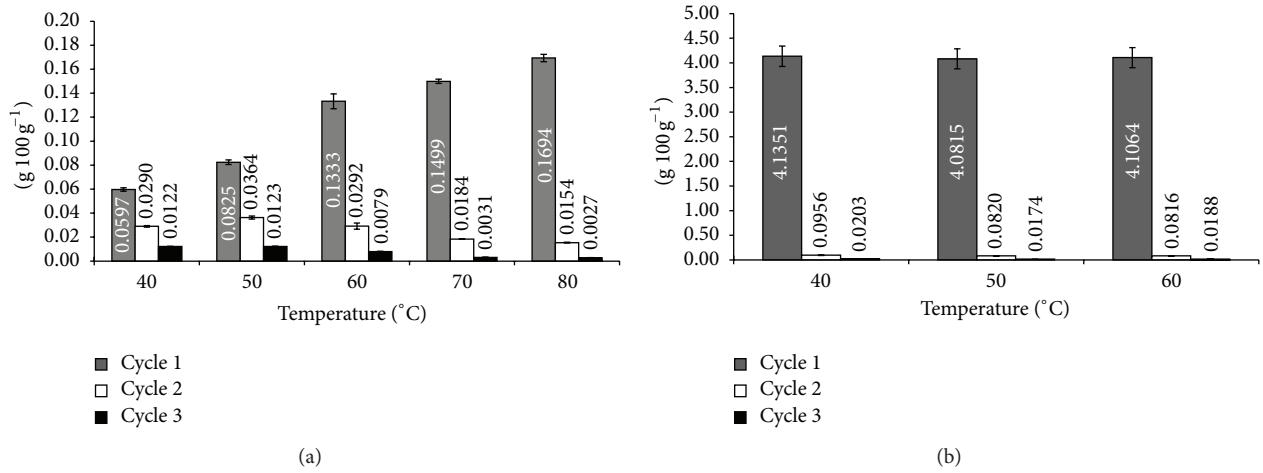

FIGURE 3: Content yield of Accelerated Solvent Extractor (ASE): (a) camptothecin (g 100 g^{-1}) in stem extracts of *N. nimmoniana*; (b) piperine (g 100 g^{-1}) in fruit extracts of *P. nigrum*.

600 μg mL^{-1}) were used for the study. All the solutions and analytes were stored in microfuge tubes at 4°C until further use.

2.4.4. System Suitability, LOD, and LOQ. The system suitability test was assessed by three replicates of standard CPT and piperine at a particular concentration 40 and 50 μg mL^{-1}, respectively. The peak areas were used to evaluate repeatability of the method and analyzed for resolution and tailing factors. The limit of detection (LOD) and limit of quantification (LOQ) were determined with the signal : noise method. Signal : noise ratios of 3.3 and 10 were used for estimating the LOD and LOQ, respectively.

3. Results and Discussions

The present study signifies use of improved, simple, fast, and accurate method of extraction by using ASE. The work was carried out to study the effect of varying temperatures at a constant pressure for determination of two chemically different but pharmacologically and commercially important compounds (CPT and piperine). Both the compounds were analyzed on reverse phase columns under isocratic system as described in experimental section.

Quantitative determination of CPT and piperine were achieved using RP-UFLC method and the results were expressed as g 100 g^{-1} on dry weight basis. Calibration curves were constructed against their area under curve to obtain a regression equation with coefficients of determination (R^2) above 0.980 (Figures 2(a) and 2(b)). This was used to estimate CPT and piperine content from both species. To reduce the impurity matrix and for quantification within the range of standard concentrations, a 1 : 9 dilution for extracts of *N. nimmoniana* was made. Table 1 represents conditions for ASE method and details of UFLC analysis. The lowest concentrations were 0.001 (CPT) and 0.01 μg mL^{-1} (piperine) for calibration. The relative standard deviation (RSD) values for both analytes that were found less than 2% indicate that the methods used in this study were précised and reproducible. Validation of the method was carried out by spiking known amount of CPT and piperine standards to equal volume of sample extracts to obtain recovery within the range of 95–100% for both.

Profiles with retention time of 5.9326 ± 0.051 min for CPT and 7.7694 ± 0.0900 min for piperine in standards and samples were obtained as final output (Figures 2(c)–2(f)). Clear, sharp peaks of standard compounds ensured purity (98%) and also reduced compatibility issues between extractive solvents and mobile phase in the analysis. The autoscaled chromatograms were generated for 3 cycles each for *N. nimmoniana* and *P. nigrum* extracts at varying temperatures (Figures 2(e), 2(f), 3(a), and 3(b)). All samples were detected above LOD and quantifications above LOQ (Table 1) for CPT and piperine.

A constant increase in the content of CPT after step wise (10°C) increase in temperature up to 80°C was observed at cycle 1, whereas successive cycles 2 and 3 showed decline in CPT content (Figure 3(a)). Highest content of CPT in *N. nimmoniana* stem extract was observed in cycle 1 at maximum temperature elevation of 80°C (Figures 2(e) and 3(a)). It is well understood that temperature is a significant factor influencing the rate of extraction. Thus, the relationship between rate of extraction and temperature is important in designing extraction methods of plant-based materials [13]. The total CPT content taken as a sum of cycle 1, 2, and 3 was 0.1875 g 100 g^{-1} dry weight. The yield of CPT in this study was found comparatively higher than the earlier reports [3, 18]. On contrary, minute variation was observed in piperine content from fruits of *P. nigrum* in all the cycles studied using ASE (Figure 3(b)). Cycle 1 at each step of temperature (40, 50 and 60°C) yielded a mean highest amount of piperine (4.1077 ± 0.0268 g 100 g^{-1} dry weight) compared to cycle 2 (0.0864 ± 0.0079 g 100 g^{-1} dry weight) and cycle 3 (0.0188 ± 0.0014 g 100 g^{-1} dry weight), indicating diminutive effect of temperature and pressure on extraction yield of piperine. The

Table 1: Accelerated Solvent Extraction (ASE) conditions for extraction and UFLC attributes during determination of CPT and piperine from *N. nimmoniana* and *P. nigrum*, respectively.

Plant name	*N. nimmoniana*	*P. nigrum*
Compound	Camptothecin	Piperine
Sample size (g)	1.0	0.1
Extraction solvents	Methanol	Ethanol
Temperature range (°C)	40–80	40–60
Temperature elevation (°C)	10	10
Heat (min)	5	5
Max pressure range (psi)	1525–1675	1520–1570
Static time (min)	1.0	1.0
Static cycles	1.0	1.0
Flush (%)	10	10
Purge time (min)	0.5	0.5
Total extraction time/cycle (min)	6.5	6.5
Linearity equation	$y = 81036x + 41525$	$y = 91335x + 28669$
R^2	0.992	0.981
LOD ($\mu g\,mL^{-1}$)	0.2020	0.1173
LOQ ($\mu g\,mL^{-1}$)	0.6121	0.3554

total piperine content (cycle 1 + 2 + 3) in our finding was found in the range of earlier reports [19, 20].

The time required for completion of each extraction stage was 6.5 min including purge, heat, and static time. ASE proves to be the better option in studying temperature-dependent extractions of compounds from plant based matrices. The temperature-based extractions not only reduced time but also are simple, fast, and accurate. The extraction method was found efficient with small amount of plant material (0.1 g dried fruit powder of *P. nigrum*), signifying, its utility in standardization and quality control of herbal medicines. Besides, use of parameters such as pressure, time, and choice of solvents makes more appropriate extraction of plant materials. This study also proposes compound specific extraction by using ASE and its suitability for obtaining optimum yield of compound of interest with less solvent consumption and time.

4. Conclusions

Results of the study conclusively affirm that compound-based extraction by using ASE from complex plant matrices is a suitable tool for standardization or quality control of the herbal products. The study indicated simple, fast, and accurate extraction methods for extraction of the compounds from different plant materials. Significant variation in the method of extraction for both the compounds was noticed. Therefore, these new improved and automated extraction methods would complement for extraction-based experiments.

Conflict of Interests

The authors declare that there is no conflict of interests regarding the publication of this paper.

Acknowledgments

The authors are indebted to Indian Council of Medical Research (ICMR), New Delhi, India, for support. SRP and VU are thankful to ICMR for providing grants during the study.

References

[1] M. E. Wall, M. C. Wani, C. E. Cook, K. H. Palmer, A. T. McPhail, and G. A. Sim, "Plant antitumor agents. I. The isolation and structure of camptothecin, a novel alkaloidal leukemia and tumor inhibitor from *Camptotheca acuminata*," *Journal of the American Chemical Society*, vol. 88, no. 16, pp. 3888–3890, 1966.

[2] B. T. Ramesha, T. Amna, G. Ravikanth et al., "Prospecting for camptothecines from *Nothapodytes nimmoniana* in the Western Ghats, south India: identification of high-yielding sources of camptothecin and new families of camptothecines," *Journal of Chromatographic Science*, vol. 46, no. 4, pp. 362–368, 2008.

[3] B. V. Padmanabha, M. Chandrashekar, B. T. Ramesha et al., "Patterns of accumulation of camptothecin, an anti-cancer alkaloid in *Nothapodytes nimmoniana* Graham., in the Western Ghats, India: implications for identifying high-yielding sources of the alkaloid," *Current Science*, vol. 90, no. 1, pp. 95–100, 2006.

[4] B. T. Ramesha, H. K. Suma, U. Senthilkumar et al., "New plant sources of the anti-cancer alkaloid, camptothecine from the Icacinaceae taxa, India," *Phytomedicine*, vol. 20, no. 6, pp. 521–527, 2013.

[5] R. Kumar and D. K. Ved, *100 Red Listed Medicinal Plants of Conservation Concern in Southern India*, Foundation for Revitalization of Local Health and Traditions, Bangalore, India, 2000.

[6] I. M. Scott, E. Puniani, H. Jensen et al., "Analysis of piperaceae germplasrn by HPLC and LCMS: a method for isolating and identifying unsaturated amides from *Piper* spp extracts," *Journal of Agricultural and Food Chemistry*, vol. 53, no. 6, pp. 1907–1913, 2005.

[7] V. S. Parmar, S. C. Jain, K. S. Bisht et al., "Phytochemistry of the genus *Piper*," *Phytochemistry*, vol. 46, no. 4, pp. 597–673, 1997.

[8] M. Verzele and S. Qureshi, "HPLC determination of piperine in pepper and in pepper extracts," *Chromatographia*, vol. 13, no. 4, pp. 241–243, 1980.

[9] P. N. Ravindran, K. Nirmal Babu, B. Sasikumar, and K. S. Krishnamurthy, "Botany and crop improvement of black pepper," in *Black Pepper: Piper Nigrum*, P. N. Ravindran, Ed., pp. 25–146, Overseas Publishers Association, Amsterdam, The Netherlands, 2000.

[10] M. Wettasinghe and F. Shahidi, "Evening primrose meal: a source of natural antioxidants and scavenger of hydrogen peroxide and oxygen-derived free radicals," *Journal of Agricultural and Food Chemistry*, vol. 47, no. 5, pp. 1801–1812, 1999.

[11] J. E. Cacace and G. Mazza, "Extraction of anthocyanins and other phenolics from black currants with sulfured water," *Journal of Agricultural and Food Chemistry*, vol. 50, no. 21, pp. 5939–5946, 2002.

[12] J. E. Cacace and G. Mazza, "Optimization of extraction of anthocyanins from black currants with aqueous ethanol," *Journal of Food Science*, vol. 68, no. 1, pp. 240–248, 2003.

[13] D. P. Fulzele and R. K. Satdive, "Comparison of techniques for the extraction of the anti-cancer drug camptothecin from *Nothapodytes foetida*," *Journal of Chromatography A*, vol. 1063, no. 1-2, pp. 9–13, 2005.

[14] S. R. Pai, N. V. Pawar, M. S. Nimbalkar, P. R. Kshirsagar, F. K. Kolar, and G. B. Dixit, "Seasonal variation in content of camptothecin from the bark of *Nothapodytes nimmoniana* (Grah.) Mabb., using HPLC analysis," *Pharmacognosy Research*, vol. 5, no. 3, pp. 219–223, 2013.

[15] Z. Zarai, E. Boujelbene, N. B. Salem, Y. Gargouri, and A. Sayari, "Antioxidant and antimicrobial activities of various solvent extracts, piperine and piperic acid from *Piper nigrum*," *LWT—Food Science and Technology*, vol. 50, no. 2, pp. 634–641, 2013.

[16] B. B. Madhavi, A. Nath, D. Banji, M. Madhu, R. Ramalingam, and D. Swetha, "Extraction, identification, formulation and evaluation of piperine in alginate beads," *International Journal of Pharmacy and Pharmaceutical Sciences*, vol. 1, no. 2, pp. 156–161, 2009.

[17] W. W. Epstein, D. F. Netz, and J. L. Seidel, "Isolation of piperine from black pepper," *Journal of Chemical Education*, vol. 70, no. 7, pp. 598–599, 1993.

[18] G. Roja, "Comparative studies on the camptothecin content from *Nothapodytes foetida* and *Ophiorrhiza* species," *Natural Product Research*, vol. 20, no. 1, pp. 85–88, 2006.

[19] P. D. Hamrapurkar, K. Jadhav, and S. Zine, "Quantitative estimation of piperine in *Piper nigrum* and *Piper longum* using high performance thin layer chromatography," *Journal of Applied Pharmaceutical Science*, vol. 1, no. 3, pp. 117–120, 2011.

[20] A. B. Wood, M. L. Barrow, and D. J. James, "Piperine determination in pepper (*Piper nigrum* L.) and its oleoresins—a reversed-phase high-performance liquid chromatographic method," *Falvour and Fragrance Journal*, vol. 3, no. 2, pp. 55–64, 1988.

Hindawi Publishing Corporation
Journal of Analytical Methods in Chemistry
Volume 2013, Article ID 526818, 7 pages
http://dx.doi.org/10.1155/2013/526818

Research Article

LC-NMR Technique in the Analysis of Phytosterols in Natural Extracts

Štěpán Horník,[1] Marie Sajfrtová,[1] Jindřich Karban,[1] Jan Sýkora,[1] Anna Březinová,[2] and Zdeněk Wimmer[3,4]

[1] *Institute of Chemical Process Fundamentals of the ASCR, v.v.i., Rozvojová 2/135, 16502 Prague 6, Czech Republic*
[2] *Institute of Organic Chemistry and Biochemistry of the ASCR, v.v.i., Flemingovo Náměstí 2, 16610 Prague 6, Czech Republic*
[3] *Institute of Experimental Botany of the ASCR, v.v.i., Isotope Laboratory, Vídeňská 1083, 14220 Prague 4, Czech Republic*
[4] *Institute of Chemical Technology Prague, Faculty of Food and Biochemical Technology, Department of Chemistry of Natural Compounds, Technická 5, 16628 Prague 6, Czech Republic*

Correspondence should be addressed to Jan Sýkora; sykora@icpf.cas.cz

Received 12 September 2013; Revised 24 November 2013; Accepted 25 November 2013

Academic Editor: Shao-Nong Chen

The ability of LC-NMR to detect simultaneously free and conjugated phytosterols in natural extracts was tested. The advantages and disadvantages of a gradient HPLC-NMR method were compared to the fast composition screening using SEC-NMR method. Fractions of free and conjugated phytosterols were isolated and analyzed by isocratic HPLC-NMR methods. The results of qualitative and quantitative analyses were in a good agreement with the literature data.

1. Introduction

Phytosterols are compounds naturally occurring in plants. They are structural analogues of cholesterol which is predominant in animals (although cholesterol has been found in very small amounts in plants as well). Phytosterols occur either in a free form or in the form of the so-called conjugates. The conjugated form is composed of a sterol having at position C-3 either a fatty acid (esters), or a hexose (glycosides), or a hexose with a fatty acid bonded to 6-OH of the hexose skeleton (acylated glycosides) [1, 2]. Regarding human nutrition, phytosterols are most abundant in vegetable oils and margarines, followed by vegetables, seeds, or pods [1]. They have become a subject of interest due to their biological properties. They are able to lower the cholesterol level in blood, especially low-density lipoprotein (LDL) cholesterol, thereby reducing the risk of cardiovascular diseases [3]. Phytosterols also have been proven to have antioxidant [4], anti-inflammatory [5], and antitumor effects [6, 7].

All the applications of phytosterols as dietary supplements are preceded by sophisticated analytical procedures which usually begin with the analysis of crude plant extracts. Gas and/or liquid chromatography techniques with various detectors play the pivotal role in the analysis of phytosterols. Currently, GC-FID technique prevails [8–12], followed by GC-MS [8, 9, 13, 14]. Liquid chromatography mostly uses coupled mass spectrometers [14–17] as an alternative to UV detection [18]. A comprehensive review of analytical and detection techniques utilized in the phytosterol analysis of dietary products was published by Abidi [19] and later extended by Lagarda et al. [20]. A particular analysis is usually preceded by saponification of oil or extract [16, 17, 21]. Saponification provides a concentrated sterol fraction which facilitates analysis. On the other hand, the information regarding conjugated sterols is lost as they are converted into their free form. Therefore, the usual result is the information on overall sterol composition. To the best of our knowledge, any method for simultaneous evaluation of free and conjugated sterol contents has not yet been published despite extensive research being conducted on biological properties of conjugated phytosterols [22].

Generally, GC and HPLC techniques require compound verification by an authentic sample, which might be difficult to obtain in the case of conjugated sterols. The lack of

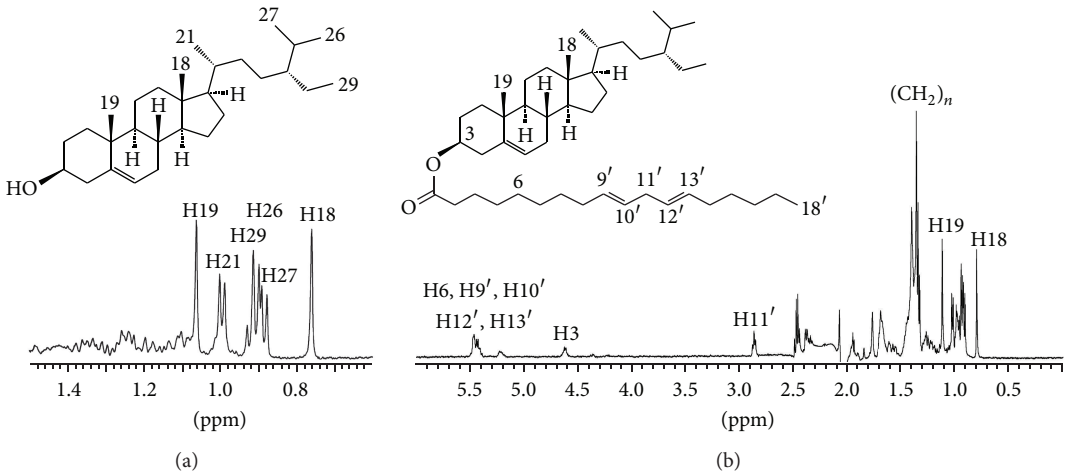

Figure 1: ^{1}H NMR spectra of free (a) and conjugated (b) β-sitosterols. Spectra were collected in a stop-flow LC-NMR experiment.

authentic samples can be compensated for by means of structure-sensitive detection techniques, for example, ^{1}H NMR [23]. Most of the free phytosterols have similar signal fingerprints in ^{1}H NMR spectra [24]. The same fingerprint is also preserved in the spectra of their conjugated forms but these spectra show additional signals due to substituents at position C-3 [25]. Besides giving structural/qualitative information, ^{1}H NMR detection is also a quantitative method [22]. Therefore, HPLC-NMR hyphenation can also provide information about quantitative composition of a given sample.

For the purpose of simultaneous analysis of free and conjugated sterols in natural extracts, we have extended previously published LC-NMR method originally developed for the analysis of free fatty acids in natural oils [26]. We have also developed fast composition screening method using SEC-NMR technique. The advantages and disadvantages of both methods are discussed in this paper.

2. Results and Discussion

Generally, LC-NMR is limited by the availability of solvents in "LC-NMR" purity grade [27]. Combination of D_2O-acetonitrile and acetonitrile-$CDCl_3$ is usually used in reverse phase chromatography for the analysis of polar or nonpolar samples, respectively. The latter combination was also utilized in our method for the analysis of nonpolar phytosterols and their fatty acid conjugates. The samples were obtained by supercritical carbon dioxide extraction and therefore consisted mostly of nonpolar compounds. A mild gradient of $CDCl_3$ in acetonitrile was applied to achieve sufficient separation of individual components. The separation started at 10% and ended at 90% of $CDCl_3$ in 100 minutes. Other chromatographic parameters were adjusted to the requirements of the quantitative LC-NMR analysis [26], for example, flow rate 0.5 mL/min (for details see the Supplementary Material available online at http://dx.doi.org/10.1155/2013/526818).

The stinging nettle (*Urtica dioica*) has many therapeutic effects [28] and it is also known for its relatively high content of phytosterols (namely, β-sitosterol) [29]. The root extract of the stinging nettle was chosen as a testing sample for our chromatographic method. Under given chromatographic conditions the free phytosterols eluted at retention time between 30 and 40 minutes followed by conjugated phytosterols whose signals were detected around 60 minutes of the separation. The predominant free phytosterol was identified as β-sitosterol (confirmed by off-line GC-MS). The detected conjugated phytosterol was recognized as β-sitosterol linoleate. The structure was deduced from ^{1}H NMR data and confirmed by off-line HR-MS ($[M\text{-}Na]^+$ peak, m/z = 699.6047; calculated m/z = 699.6051; see Supplementary Material). The separation was solely monitored by on-flow ^{1}H NMR detection. Because the signals of the methyl groups in phytosterols occupy specific region in the ^{1}H NMR spectrum (0.6–1.1 ppm), they can be easily recognized even at low concentrations and/or in the mixtures (Figure 1).

It is noteworthy that the extract was used without any derivatization or treatment; it was just dissolved in $CDCl_3$ and subjected to HPLC. The on-flow arrangement of the NMR experiment provided one spectrum every 5 seconds; one spectrum is the result of accumulation of four scans. The quantitative analysis can be performed just by simple integration of a given signal across all NMR spectra. In our particular case the most upfield signal (usually H18) was chosen for integration. Estimated integration revealed that the free: conjugated phytosterol ratio was 6 : 1 in the stinging nettle extract sample. To estimate overall phytosterol content a precise calibration had to be performed.

The calibration was performed with a $CDCl_3$ solution of β-sitosterol standard (~97%, SigmaAldrich). The calibration plot obtained from measurements at seven concentration levels showed a linear response of ^{1}H NMR detection covering two orders of magnitude (Figure 2). The residual $CHCl_3$ signal served as an internal reference.

Although the calibration was performed only with the β-sitosterol standard, we presumed that the calibration line can be applied also to other phytosterols. Because the integrated signal (usually H18) originates from the methyl group at

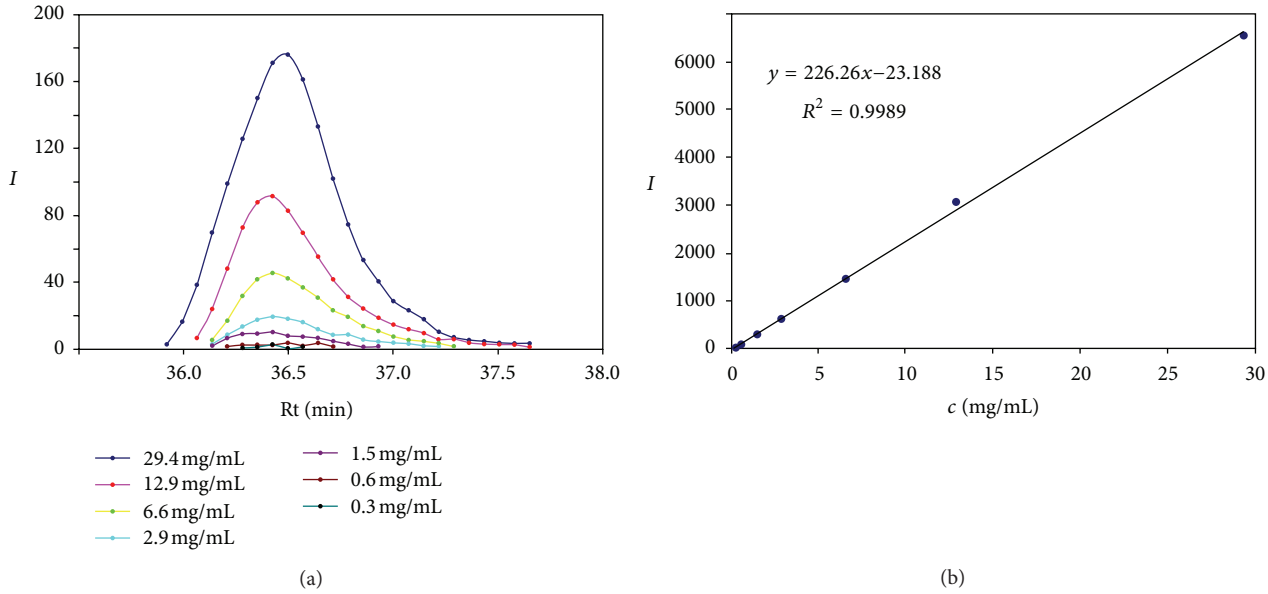

FIGURE 2: Calibration of the on-flow HPLC-NMR experiment. "I" on the y-axis stands for integral in the individual ^{1}H NMR spectra (a) or overall integral obtained by numerical integration (b).

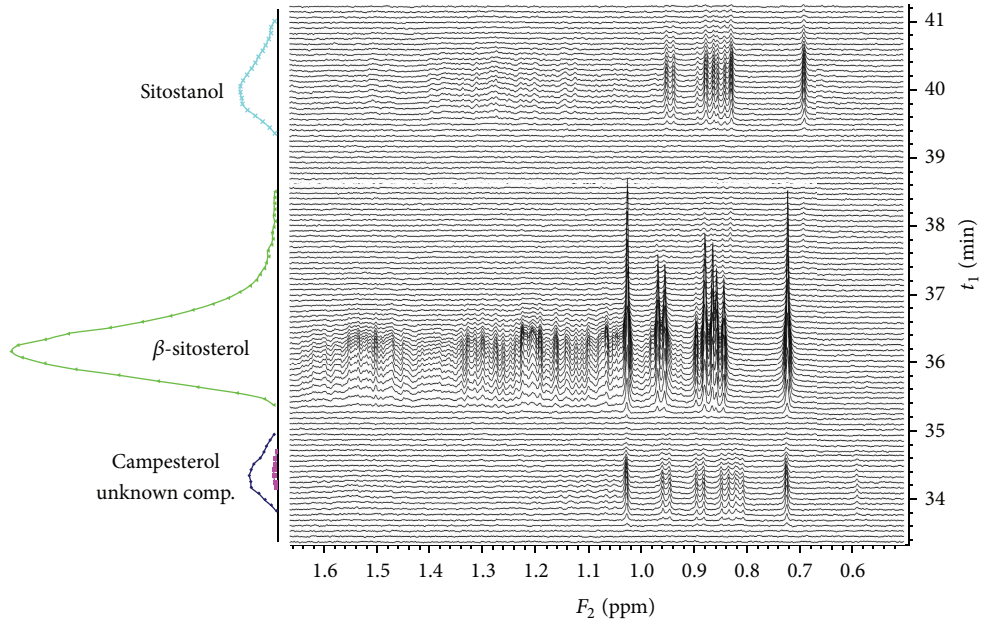

FIGURE 3: On-flow HPLC-NMR measurement of technical β-sitosterol and its quantitative analysis.

the centre of the sterol molecule its nature and the chemical environment are very similar in all phytosterols. Therefore, the relaxation properties and consequently the response for quantitation remain similar even in other types of phytosterol molecules, for example in conjugated phytosterols. The quantification limit of the method was estimated to 0.3 mg/mL.

Technical β-sitosterol (~60%, SigmaAldrich) was chosen as a reference mixture as it contains two other phytosterols (campesterol and sitostanol) which can be used for further authentication of chromatographic peaks in natural samples. The separation is shown in Figure 3. The separation revealed the following composition and elution order: 6% of campesterol (34 min), 81% of β-sitosterol (36 min), and 12% of sitostanol (40 min). Campesterol coeluted with an unknown compound (1%) which could not be identified due to its low concentration and strong signal overlap.

The major disadvantage of the method described above is its time requirement. 90 minutes including column reconditioning is unsatisfactory time frame in the era of UPLC and/or UHPLC. Another option providing separation of free and conjugated molecules is the size exclusion chromatography (SEC). Components are separated by their different

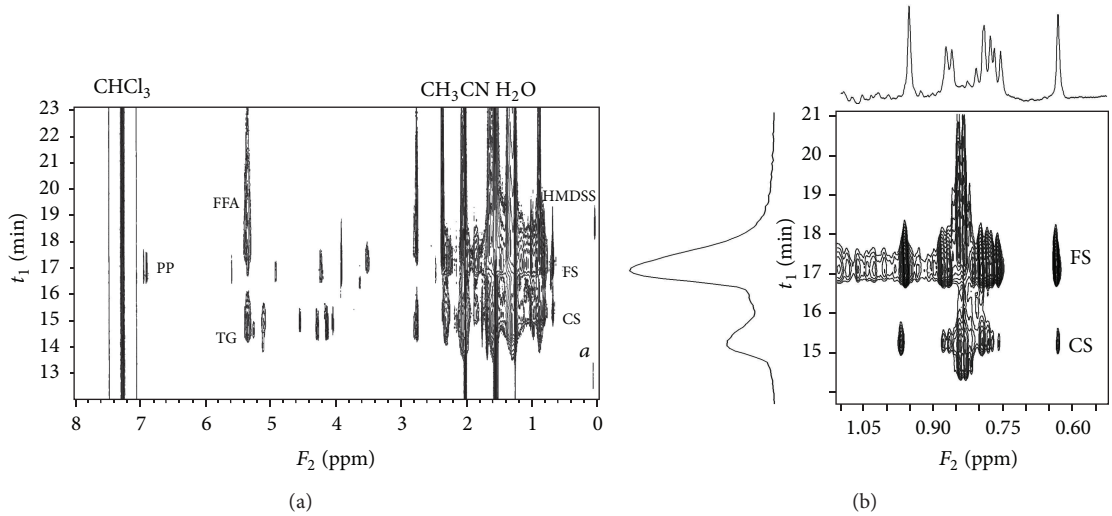

Figure 4: On-flow SEC-NMR measurement of the stinging nettle extract, whole spectrum (a) and a detail of the upfield region (b). FFA: free fatty acid, TG: triglycerides, PP: polyphenolic compounds, HMDSS: hexamethyldisilane, FS: free phytosterols, CS: conjugated phytosterols, and *a*: silicone grease.

molecular size in SEC. It can also be coupled to the ^{1}H NMR for structure-sensitive detection. SEC-NMR had to be run in 100% $CDCl_3$ (due to the solvent purity requirements) with the flow rate 0.5 mL/min. Under these conditions the signals of conjugated phytosterols occurred at 15 minutes and the free phytosterols were detected at 17 minutes in the stinging nettle sample (Figure 4).

The SEC-NMR method seems to be reasonably fast (30 minutes) and also sensitive as we detect accumulated signals of all phytosterols present in the sample in the same region of the chemical shift. In the resulting pseudo-2D spectrum we can also recognize signals of other present molecules such as free fatty acids, triglycerides, and some polyphenolic compounds. On the other hand, we cannot identify individual components within each group of compounds due to a strong signal overlap. The calibration was performed for the purpose of quantitative analysis. It showed again linear response of ^{1}H NMR detection and surprisingly a slightly higher quantification limit (~1.0 mg/mL) which is caused mainly by significant tailing of the chromatographic peaks; the chromatographic peak elutes for 2 minute in SEC-NMR (see Figure S1 in Supplementary Material) compared to 1 minute in HPLC-NMR method (Figure 2).

However, the SEC-NMR method seems to be a suitable method for fast screening of the phytosterol content, for example, in different extracts from the same plant. Thus, samples of leaves, seed oil, and seed coat of sea buckthorn (*Hippophae rhamnoides*), whose medicinal and therapeutic potential has been recently reviewed [30], were extracted by supercritical CO_2 and the extracts were analyzed by SEC-NMR method for their phytosterol content. The results are given in Figure 5.

The leave extract showed the highest content of conjugated phytosterols of the three extracts; it was even higher than the content of free phytosterol in this sample. The seed oil extract contained more free phytosterols than conjugated ones. Triglycerides were the predominant compounds in this sample as expected. The seed coat extract contained triglycerides and fatty acids in large amounts and only traces of phytosterols, mostly in a conjugated form (Figure 6).

Additionally, the results of SEC-NMR analyses facilitate choice of an appropriate method for detailed qualitative analysis. Both groups of phytosterols can be easily isolated from the leave extract by means of preparative SEC. There is no significant coelution with other compounds in this sample. The seed oil extract is also rich in phytosterol; however, phytosterol isolation by means of SEC would be impractical due to the high content of triglycerides which would prevail in the fraction of conjugated phytosterols. The seed oil extract was therefore saponified [31] and analyzed for its overall phytosterol composition. The seed coat extract was excluded from further investigation as its phytosterol content was negligible.

Saponified seed oil extract was dissolved in $CDCl_3$ and subjected to HPLC-NMR. The isocratic conditions provided sufficient separation of phytosterol content ($CDCl_3$: acetonitrile, 25 : 75). Nine major compounds were found, seven of them were fully identified, one was assigned to a compound family, and one compound remained unidentified. The assignment was based mainly on ^{1}H NMR spectral patterns and was confirmed by an off-line GC-MS measurement. ^{1}H NMR spectra of identified phytosterols are shown in Figure S2 in Supplementary Material. β-sitosterol was identified as a main phytosterol in the seed oil. The found composition, listed in Table 1, is in good agreement with the published data [32].

The fraction of free phytosterols isolated by preparative SEC from the leave extract showed completely different composition. Signals of seven phytosterols were observed, three polar phytosterols (erythrodiol, uvaol, and oleanolic aldehyde), one unidentified, and three common phytosterols (α- and β-amyrin and β-sitosterol). ^{1}H NMR spectra of identified phytosterols are shown in Figure S2 in Supplementary Material. The most abundant phytosterol in this fraction was β-amyrin. The comparative composition is listed in Table 2.

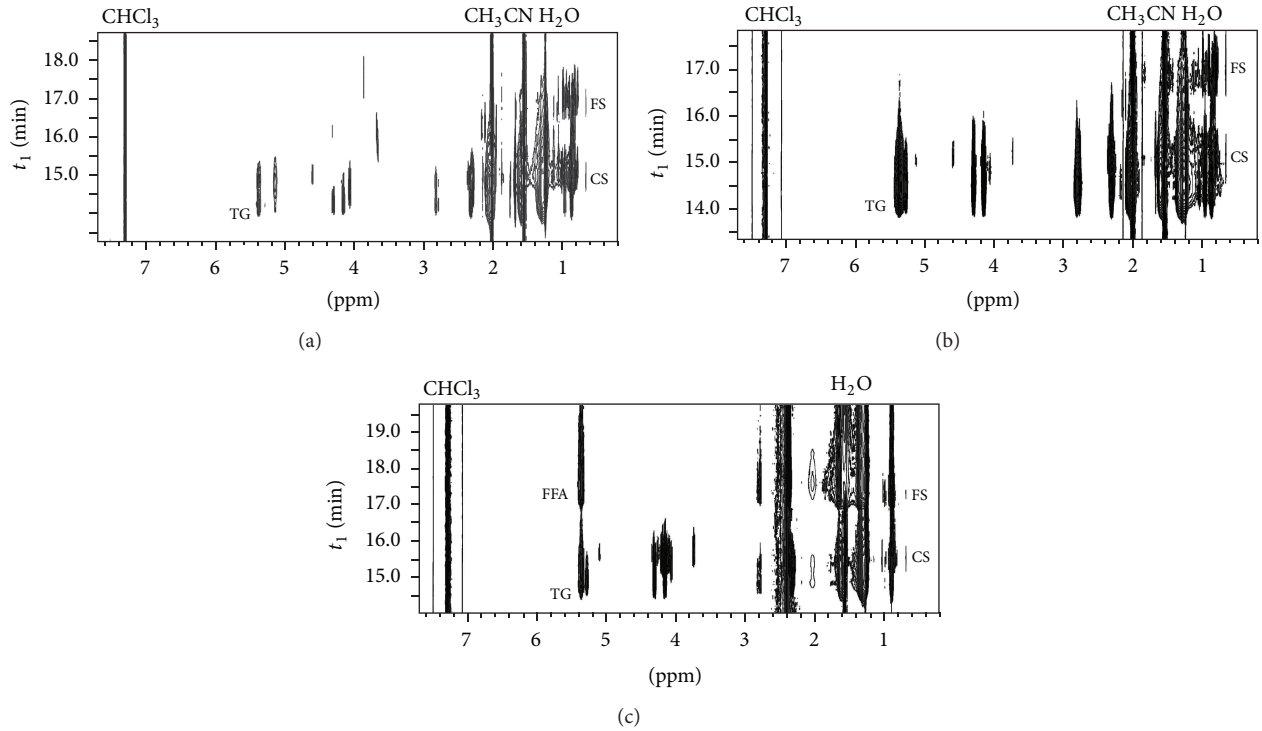

Figure 5: SEC-NMR measurement of the sea buckthorn extract samples, leaves (a), seed oil (b), and seed coat (c). FFA: free fatty acid, TG: triglycerides, FS: free phytosterols, and CS: conjugated phytosterols.

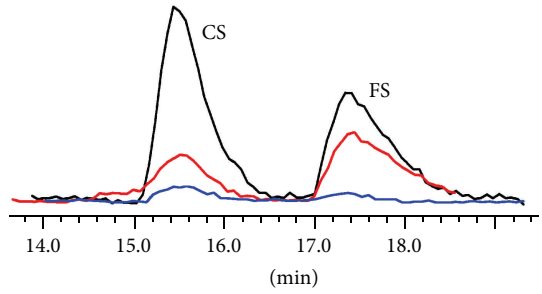

Figure 6: Projection of the phytosterol content in the sea buckthorn extracts (SEC-NMR measurement in 100% $CDCl_3$), leaves (black), seed oil (red), and seed coat (blue). CS: conjugated phytosterols and FS: free phytosterols.

The fraction of conjugated phytosterols isolated by preparative SEC from the leave extract was analyzed under different isocratic conditions ($CDCl_3$: acetonitrile, 50 : 50). Five predominant conjugates were identified in the pseudo-2D spectrum (Figure 7). According to the elution order, the first compound can be attributed to conjugated α-amyrin, the second and third to conjugates of β-sitosterol, and the last two to conjugates of β-amyrin. The comparative composition is listed in Table 3. It is apparent that the conjugate with unsaturated fatty acid elutes before that with saturated fatty acid. According to the integration of ^{1}H NMR signals these fatty acids are probably linoleic and palmitic acids. This has to be confirmed by HR-MS. The overall composition of isolated conjugates is in good correlation with the composition found in free phytosterols confirming β-amyrin as the most populated phytosterol in the sea buckthorn leaves.

Table 1: Composition of the saponified sea buckthorn seed oil determined by HPLC-NMR.

Compound	Comparative content[a]	Overall content in the seed oil[b]	Retention time (min)[c]
Δ^5-avenasterol	13%	0.3%	24
Unknown I	2%	<0.1%	25
Unknown II (Δ^7-sterol)	1%	<0.1%	25
Cykloeukalenol	4%	0.1%	26
α-amyrin	4%	0.1%	27
Campesterol	2%	<0.1%	27
β-amyrin	3%	<0.1%	28
β-sitosterol	69%	1.7%	29
Sitostanol	2%	<0.1%	32

[a]Molar ratio in the phytosterol fraction, [b]weight ratio in the extract sample, and [c]isocratic method ($CDCl_3$: acetonitrile, 25 : 75).

3. Conclusion

^{1}H NMR spectroscopy was shown to be a suitable detection technique in the analysis of various phytosterol forms in natural extracts. The HPLC-NMR method can be utilized in the qualitative analysis of phytosterols when the structural information is necessary, whereas the SEC-NMR method

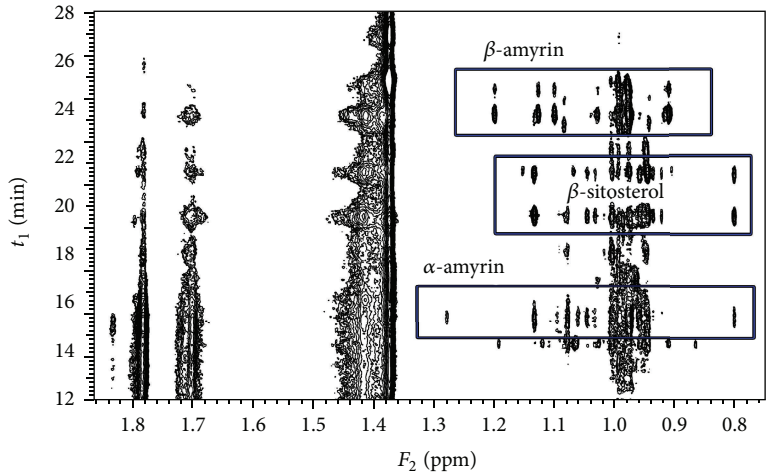

Figure 7: HPLC-NMR measurement of the conjugated phytosterol fraction extracted from the sea buckthorn leaves; isocratic method ($CDCl_3$: acetonitrile, 50 : 50).

Table 2: Composition of the fraction of free phytosterols in the sea buckthorn leaves determined by HPLC-NMR.

Compound	Comparative content[a]	Overall content in the leave extract[b]	Retention time (min)[c]
Erythrodiol	3%	<0.1%	13
Uvaol	14%	0.3%	14
Oleanolic aldehyde	4%	<0.1%	16
Unknown	3%	<0.1%	24
α-amyrin	12%	0.3%	27
β-amyrin	47%	1.0%	28
β-sitosterol	17%	0.4%	29

[a]Molar ratio in the phytosterol fraction, [b]weight ratio in the extract sample, and [c]isocratic method ($CDCl_3$: acetonitrile, 25 : 75).

Table 3: Composition of the fraction of conjugated phytosterols in the sea buckthorn leaves determined by HPLC-NMR.

Compound	Comparative content[a]	Overall content in the leave extract[b]	Retention time (min)[c]
α-amyrin + FA	11%	0.6%	15
β-sitosterol + unsat. FA	18%	1.0%	20
β-sitosterol + sat. FA	12%	0.6%	22
β-smyrin + unsat. FA	39%	2.1%	25
β-amyrin + sat. FA	20%	1.1%	26

[a]Molar ratio in the phytosterol fraction, [b]weight ratio in the extract sample, and [c]isocratic method ($CDCl_3$: acetonitrile, 50 : 50).

can be used for the fast composition screening. The main disadvantage of ^{1}H NMR as a detection technique is its low sensitivity.

Conflict of Interests

The authors declare no conflict of interests.

Acknowledgments

This research was supported by Technology Agency of the Czech Republic (Grant no. TA01010578) and by the Czech Science Foundation (Grant no. P503/11/0616).

References

[1] R. A. Moreau, B. D. Whitaker, and K. B. Hicks, "Phytosterols, phytostanols, and their conjugates in foods: structural diversity, quantitative analysis, and health-promoting uses," *Progress in Lipid Research*, vol. 41, no. 6, pp. 457–500, 2002.

[2] N. V. Kovganko and Z. N. Kashkan, "Sterol glycosides and acyl-glycosides," *Chemistry of Natural Compounds*, vol. 35, no. 5, pp. 479–497, 1999.

[3] S. Rochfort and J. Panozzo, "Phytochemicals for health, the role of pulses," *Journal of Agricultural and Food Chemistry*, vol. 55, no. 20, pp. 7981–7994, 2007.

[4] S. J. van Rensburg, W. M. U. Daniels, J. M. van Zyl, and J. J. F. Taljaard, "A comparative study of the effects of cholesterol,

beta-sitosterol, beta-sitosterol glucoside, dehydroepiandrosterone sulphate and melatonin on in vitro lipid peroxidation," *Metabolic Brain Disease*, vol. 15, no. 4, pp. 257–265, 2000.

[5] P. J. D. Bouic, "Sterols and sterolins: new drugs for the immune system?" *Drug Discovery Today*, vol. 7, no. 14, pp. 775–778, 2002.

[6] A. B. Awad and C. S. Fink, "Phytosterols as anticancer dietary components: evidence and mechanism of action," *Journal of Nutrition*, vol. 130, no. 9, pp. 2127–2130, 2000.

[7] P. G. Bradford and A. B. Awad, "Phytosterols as anticancer compounds," *Molecular Nutrition and Food Research*, vol. 51, no. 2, pp. 161–170, 2007.

[8] N. Nasri, B. Fady, and S. Triki, "Quantification of sterols and aliphatic alcohols in Mediterranean stone pine (Pinus pinea L.) populations," *Journal of Agricultural and Food Chemistry*, vol. 55, no. 6, pp. 2251–2255, 2007.

[9] W.-H. Liu, B. Ding, X.-M. Ruan, H.-T. Xu, J. Yang, and S.-M. Liu, "Analysis of free and conjugated phytosterols in tobacco by an improved method using gas chromatography-flame ionization detection," *Journal of Chromatography A*, vol. 1163, no. 1-2, pp. 304–311, 2007.

[10] M. Vosoughkia, M. Ghavamib, M. Gharachorloo, M. Sharrifmoghaddasi, and A. H. Omidi, "Lipid composition and oxidative stability of oils in safflower (Carthamus tinctorius L.) seed varieties grown in Iran," *Advances in Environmental Biology*, vol. 5, no. 5, pp. 897–902, 2011.

[11] N. Tlili, N. Nasri, E. Saadaoui, A. Khaldi, and S. Triki, "Sterol composition of caper (Capparis spinosa) seeds," *African Journal of Biotechnology*, vol. 9, no. 22, pp. 3328–3333, 2010.

[12] P. A. D. Costa, C. A. Ballus, J. Teixeira-Filho, and H. T. Godoy, "Phytosterols and tocopherols content of pulps and nuts of Brazilian fruits," *Food Research International*, vol. 43, no. 6, pp. 1603–1606, 2010.

[13] M. Orozco-Solano, J. Ruiz-Jiménez, and M. D. Luque de Castro, "Ultrasound-assisted extraction and derivatization of sterols and fatty alcohols from olive leaves and drupes prior to determination by gas chromatography-tandem mass spectrometry," *Journal of Chromatography A*, vol. 1217, no. 8, pp. 1227–1235, 2010.

[14] M. F. Caboni, G. Iafelice, M. Pelillo, and E. Marconi, "Analysis of fatty acid steryl esters in tetraploid and hexaploid wheats: Identification and comparison between chromatographic methods," *Journal of Agricultural and Food Chemistry*, vol. 53, no. 19, pp. 7465–7472, 2005.

[15] B. Lu, Y. Zhang, X. Wu, and J. Shi, "Separation and determination of diversiform phytosterols in food materials using supercritical carbon dioxide extraction and ultraperformance liquid chromatography-atmospheric pressure chemical ionization-mass spectrometry," *Analytica Chimica Acta*, vol. 588, no. 1, pp. 50–63, 2007.

[16] W. Zarrouk, A. Carrasco-Pancorbo, M. Zarrouk, A. Segura-Carretero, and A. Fernández-Gutiérrez, "Multi-component analysis (sterols, tocopherols and triterpenic dialcohols) of the unsaponifiable fraction of vegetable oils by liquid chromatography-atmospheric pressure chemical ionization-ion trap mass spectrometry," *Talanta*, vol. 80, no. 2, pp. 924–934, 2009.

[17] A. S. Carretero, A. Carrasco-Pancorbo, S. Cortacero, A. Gori, L. Cerretani, and A. Fernández-Gutiérrez, "A simplified method for HPLC-MS analysis of sterols in vegetable oil," *European Journal of Lipid Science and Technology*, vol. 110, no. 12, pp. 1142–1149, 2008.

[18] X. Zhang, A. Cambrai, M. Miesch et al., "Separation of Δ5- and Δ7-phytosterols by adsorption chromatography and semipreparative reversed phase high-performance liquid chromatography for quantitative analysis of phytosterols in foods," *Journal of Agricultural and Food Chemistry*, vol. 54, no. 4, pp. 1196–1202, 2006.

[19] S. L. Abidi, "Chromatographic analysis of plant sterols in foods and vegetable oils," *Journal of Chromatography A*, vol. 935, no. 1-2, pp. 173–201, 2001.

[20] M. J. Lagarda, G. García-Llatas, and R. Farré, "Analysis of phytosterols in foods," *Journal of Pharmaceutical and Biomedical Analysis*, vol. 41, no. 5, pp. 1486–1496, 2006.

[21] A. Rocco and S. Fanali, "Analysis of phytosterols in extra-virgin olive oil by nano-liquid chromatography," *Journal of Chromatography A*, vol. 1216, no. 43, pp. 7173–7178, 2009.

[22] M. A. Micallef and M. L. Garg, "Beyond blood lipids: phytosterols, statins and omega-3 polyunsaturated fatty acid therapy for hyperlipidemia," *Journal of Nutritional Biochemistry*, vol. 20, no. 12, pp. 927–939, 2009.

[23] *High Resolution Nuclear Magnetic Resonance Spectroscopy*, Pergamon Press, Oxford, UK, 1966, edited by J. W. Emsley, J. Feeney and L. H. Sutcliffe.

[24] I. Rubinstein, L. J. Goad, A. D. H. Clague, and L. J. Mulheirn, "The 220 MHz NMR spectra of phytosterols," *Phytochemistry*, vol. 15, no. 1, pp. 195–200, 1976.

[25] S. R. P. Madawala, R. E. Andersson, J. A. Jastrebova, M. Almeida, and P. C. Dutta, "Phytosterol and α-lipoic acid conjugates: synthesis, free radical scavenging capacity and RP-LC-MS-APCI analysis," *Polish Journal Of Food And Nutrition Sciences*, vol. 62, pp. 159–169, 2012.

[26] J. Sýkora, P. Bernášek, M. Zarevúcka, M. Kurfürst, H. Sovová, and J. Schraml, "High-performance liquid chromatography with nuclear magnetic resonance detection—a method for quantification of alpha- and gamma-linolenic acids in their mixtures with free fatty acids," *Journal of Chromatography A*, vol. 1139, pp. 152–155, 2007.

[27] *On-Line LC-NMR and Related Techniques*, John Wiley & Sons, Chichester, UK, 2002, edited by K. Albert.

[28] S. Vogl, P. Picker, J. Mihaly-Bison et al., "Ethnopharmacological in vitro studies on Austria's folk medicine—an unexplored lore in vitro anti-inflammatory activities of 71 Austrian traditional herbaldrugs," *Journal of Ethnopharmacology*, vol. 149, pp. 750–771, 2013.

[29] N. Chaurasia and M. Wichtl, "Sterols and steryl glycosides from Urtica dioica," *Journal of Natural Products*, vol. 50, no. 5, pp. 881–885, 1987.

[30] G. Suryakumar and A. Gupta, "Medicinal and therapeutic potential of Sea buckthorn (*Hippophae rhamnoides* L.)," *Journal of Ethnopharmacology*, vol. 138, no. 2, pp. 268–278, 2011.

[31] A. S. Carretero, A. Carrasco-Pancorbo, S. Cortacero, A. Gori, L. Cerretani, and A. Fernández-Gutiérrez, "A simplified method for HPLC-MS analysis of sterols in vegetable oil," *European Journal of Lipid Science and Technology*, vol. 110, no. 12, pp. 1142–1149, 2008.

[32] T. S. C. Li, T. H. J. Beveridge, and J. C. G. Drover, "Phytosterol content of sea buckthorn (Hippophae rhamnoides L.) seed oil: extraction and identification," *Food Chemistry*, vol. 101, no. 4, pp. 1633–1639, 2007.

Hindawi Publishing Corporation
Journal of Analytical Methods in Chemistry
Volume 2013, Article ID 804504, 5 pages
http://dx.doi.org/10.1155/2013/804504

Research Article

In Vivo Antioxidant Activity of Deacetylasperulosidic Acid in Noni

De-Lu Ma,[1] Mai Chen,[2] Chen X. Su,[3] and Brett J. West[3]

[1] *Division of Pharmacology, Tianjin Medical University, Tianjin 300070, China*
[2] *Quality Control, Tahitian Noni Beverages Company Ltd., Room A 12F, No. 789, Zhaojiabang Road, Shanghai 200032, China*
[3] *Research and Development, Morinda Inc., 737 East 1180 South, American Fork, UT 84003, USA*

Correspondence should be addressed to Brett J. West; brett_west@tni.com

Received 10 September 2013; Accepted 15 October 2013

Academic Editor: Jian Yang

Deacetylasperulosidic acid (DAA) is a major phytochemical constituent of *Morinda citrifolia* (noni) fruit. Noni juice has demonstrated antioxidant activity *in vivo* and in human trials. To evaluate the role of DAA in this antioxidant activity, Wistar rats were fed 0 (control group), 15, 30, or 60 mg/kg body weight per day for 7 days. Afterwards, serum malondialdehyde concentration and superoxide dismutase and glutathione peroxidase activities were measured and compared among groups. A dose-dependent reduction in malondialdehyde was evident as well as a dose-dependent increase in superoxide dismutase activity. DAA ingestion did not influence serum glutathione peroxidase activity. These results suggest that DAA contributes to the antioxidant activity of noni juice by increasing superoxide dismutase activity. The fact that malondialdehyde concentrations declined with increased DAA dose, despite the lack of glutathione peroxidase-inducing activity, suggests that DAA may also increase catalase activity. It has been previously reported that noni juice increases catalase activity *in vivo* but additional research is required to confirm the effect of DAA on catalase. Even so, the current findings do explain a possible mechanism of action for the antioxidant properties of noni juice that have been observed in human clinical trials.

1. Introduction

Morinda citrifolia, commonly known as noni, is a small tree that has been used as a traditional source of food and medicine throughout the tropics [1, 2]. A variety of potential health benefits have been reported for noni fruit juice [3]. These include immunomodulation [4, 5] and antioxidant activities *in vitro* and *in vivo* [6–8]. The antioxidant activity of noni juice was found to be associated with increased endurance in athletes [9]. In a human clinical trial involving heavy cigarette smokers, consumption of noni juice resulted in lowered plasma concentrations of superoxide anion radicals (SAR) and lipid hydroperoxides [10]. Further, consumption of noni juice also decreased the level of lipid peroxidation-derived DNA adducts in the lymphocytes of heavy smokers [11].

In vivo research has demonstrated that noni juice increases superoxide dismutase (SOD) and glutathione peroxidase (GPx) enzyme activities [12]. The superoxide anion radical (SAR) is a major cellular reactive oxygen species and may be generated via enzymatic and nonenzymatic process or may come from exogenous sources, including cigarette smoke [13]. SOD catalyzes the dismutation of SAR to hydrogen peroxide and oxygen [14]. GPx is capable of reducing free hydrogen peroxide to water [15]. GPx also reduces lipid hydroperoxides, as well as prevents free radical attack on polyunsaturated fatty acids in cellular membranes [16]. As such, the effect of noni juice on these two enzymes may be at least two of the major antioxidant mechanisms of action through which it protects lymphocyte DNA and lowers plasma concentration of tobacco smoke-induced free radicals and peroxides.

Chemical studies of noni fruit have revealed that iridoids are the main phytochemical constituents, with deacetylasperulosidic acid (DAA) comprising the majority of the iridoid content [17]. DAA has anticlastogenic activity, suppressing the induction of chromosome aberrations in Chinese hamster ovary cells and in mice [18]. DAA is reported to inhibit the

release of tumor necrosis factor-alpha from cultured mouse peritoneal macrophages and inhibits low-density lipoprotein oxidation [19, 20]. DAA also prevented 4-nitroquinoline 1-oxide (4NQO) induced DNA damage *in vitro* [21]. 4NQO exposure leads to the formation of superoxide, hydrogen peroxide, and hydroxyl radicals, resulting in the production of a substantial amount of 8-hydroxydeoxyguanosine, a product of DNA oxidation in mammalian and bacterial cells [22, 23]. Treatment with DAA reduced 4NQO genotoxicity by 98.96%, suggesting that iridoids are responsible for the DNA protective effects of noni juice in cigarette smokers.

With demonstrated antioxidant activity of noni juice and the potential bioactivities of its major phytochemical constituent, the current study was conducted to investigate the role of DAA on SOD and GPx activities *in vivo*.

2. Materials and Methods

2.1. Test Material. Deacetylasperulosidic acid (DAA) was obtained from Chengdu Biopurify Phytochemicals Ltd. (Chengdu, China). The purity of DAA was 98%, and the identity was confirmed by high performance liquid chromatography [24]. DAA was dissolved in MeOH-H_2O (1 : 1) at a concentration of 0.2 mg/mL. Separation of the standard was performed with a HC-C18 column (25 cm × 4.6 mm; 5 μm, Agilent Technologies, Santa Clara, CA, USA) in a Waters 2690 separations module (Waters Corporation, Milford, MA, USA) and detected with a Waters 2489 UV/Vis detector at 235 nm. DAA was eluted at a flow rate of 0.8 mL/min with two mobile phases: (A) MeCN and (B) 0.1% formic acid in H_2O (v/v). The elution gradient was 5 min with 100% B, 35 min with 30% A and 70% B, 12 min 95% A and 5% B, and then 8 minutes with 100% B. The retention time and absorbance spectrum were compared against those of a DAA standard.

2.2. Animals and Treatment. For this study, 40 Wistar rats (male and female, 180–200 g) were obtained from the Experimental Animal Center, Academy of Military Medical Sciences (Beijing), Approval no. SCXK-Army-2009-003. The care of animals and experimental procedures were compliant with ethical and institutional animal welfare guidelines of Tianjin Medical University. Following acclimation, rats were randomly divided into 4 groups of 10 each (5 male and 5 female). Each group was provided feed and water *ad libitum*. DAA was dissolved in saline and each animal was gavaged for 7 days with 1 mL/200 g body weight (bw) of one of four treatments, depending on group assignment. The treatments were normal saline (control), 15 mg DAA/kg bw (low dose), 30 mg DAA/kg bw (mid dose), and 60 mg DAA/kg bw (high dose). Individual animal weight and feed intake were recorded on days 1, 4, and 7. On the 8th day, the rats were anesthetized and 0.5 mL blood was removed from the orbital sinus. Whole blood was centrifuged at 3,000 rpm for 10 min in a low speed centrifuge (model BFX5-320, Baiyang Centrifuge Factory, Liulizhuang, Hebei, China). The resulting serum was retained for assays.

2.3. Antioxidant Enzyme Activity Assays and Malondialdehyde Assay. Using a commercial bioassay kit (Jiancheng Bioengineering Institute, Nanjing, China), the SOD activity of serum was assayed. The superoxide dismutase activity assay utilized the production of a water soluble dye (WST-1 formazan) from a tetrazolium salt (WST-1) in the presence of SAR [25]. In a phosphate-buffered reaction mixture, xanthine and xanthine oxidase are incubated at 37°C in the presence of samples, blanks, SOD standards, and WST-1. During the reaction, SAR is generated from xanthine and oxygen. SOD catalyzes the dismutation of SAR, thereby reducing the amount available to oxidize WST-1 to WST-1 formazan. Sample results were compared against an SOD standard reference curve after the absorbance was read at 450 nm with a microplate reader (Epoch Microplate Spectrophotometer, BioTek, Winooski, VT, USA). The SOD activity is determined by calculating the WST-1 formazan inhibition rate and is expressed in U/mL.

GPx activities in serum samples were also determined with a commercially available bioassay kit (Jiancheng Bioengineering Institute, Nanjing, China). GPx activity was measured by determining reduced glutathione in the serum. Absorbance of sample, blanks, and standards were read at 412 nm with a microplate reader (Epoch Microplate Spectrophotometer, BioTek, Winooski, VT, USA). Enzyme activities were expressed as U/mL.

Malondialdehyde (MDA) concentrations were assayed with a commercial bioassay kit (Jiancheng Bioengineering Institute, Nanjing, China). MDA was detected according to the common colorimetric method involving the reaction of samples and 1,3,3,3 tetra-ethoxypropane standards with thiobarbituric acid in a 95°C water bath for 40 min. The absorbance of each of the samples and standards was measured at 532 nm (Epoch Microplate Spectrophotometer, BioTek, Winooski, VT, USA). Results were determined against the standard curve and expressed as nmol/mL.

2.4. Statistical Analysis. Basic summary statistics (mean, range, and standard deviation) were calculated. Intergroup differences were measured with Student's t-test, following Bartlett's test for homogeneity of variance.

Table 1: Mean (± standard deviation) weight (g) per animal.

DAA dose (mg/kg)	Day 1	Day 4	Day 7
0	189 ± 10.4	208 ± 21.2	220 ± 27.5
15	189 ± 8.26	207 ± 15.7	218 ± 22.2
30	189 ± 11.4	207 ± 20.7	217 ± 24.8
60	190 ± 8.97	207 ± 17.5	218 ± 24.0

3. Results and Discussion

Weights and feed intake rates among the different groups are compared in Tables 1 and 2. All groups experienced appropriate weight gain during the seven-day period [26], with no differences between any groups. There were no intragroup changes in mean feed intake. There were no feed intake differences between the groups on days 1 and 4. The low and mid dose groups had slightly lower feed intakes on day 7 than the control group, but these were within the expected

Table 2: Mean (± standard deviation) feed intake (g) per animal.

DAA dose (mg/kg)	Day 1	Day 4	Day 7
0	21.9 ± 5.49	20.6 ± 5.62	21.8 ± 4.18
15	19.1 ± 3.49	19.8 ± 2.64	18.3 ± 2.65*
30	21.8 ± 5.86	21.6 ± 5.12	18.3 ± 2.41*
60	20.0 ± 4.66	19.1 ± 2.27	18.7 ± 2.40

*$P < 0.05$ compared to control group on day 7 but within expected feed intake rates.

Table 3: Mean (± standard deviation) serum MDA concentration and activity of antioxidant enzymes.

DAA dose (mg/kg)	MDA (nmol/mL)	SOD (U/mL)	GPx (U/mL)
0	5.54 ± 0.77	115 ± 10.1	995 ± 148
15	4.96 ± 1.43	126 ± 17.3	1007 ± 169
30	4.45 ± 1.15*	128 ± 15.2*	983 ± 167
60	4.43 ± 0.79**	130 ± 8.83**	986 ± 101

*$P < 0.05$,**$P < 0.01$ compared to control group.

amounts for healthy Wistar rats [27]. There was no significant difference in feed intake between the control and high dose groups.

The effects of DAA intake on MDA concentration and antioxidant enzyme activities are summarized in Table 3. While mean serum MDA content in the low dose group is lower than that of the control group, the difference is not statistically significant. However, there is a trend of reduced serum MDA concentrations with increased DAA dose. Serum MDA of the mid and high dose groups was significantly lower than those observed in the controls. The approximate percent reductions in mean serum MDA in the mid and high dose groups were, respectively, 19.7 and 22.6% when compared to the control group.

Mean serum SOD activity tended to increase with DAA dose. While SOD activity in low dose group was almost 10% greater than that in the controls, the difference was only marginally significant ($P = 0.098$). On the other hand, SOD activities observed in the mid and high dose groups were significantly greater than that of the control group. Mid and high dose animals experienced, respectively, an average increase of 11.3 ($P < 0.05$) and 13.0% ($P < 0.01$) in serum SOD activity. Unlike SOD, GPx activities were not influenced by DAA intake at any of the doses evaluated.

DAA has apparent antioxidant activity when ingested. The effect of DAA on SOD activity helps to explain at least one mechanism whereby noni juice lowered plasma SAR in heavy smokers. SAR contributes to the eventual formation of MDA by means of reactive hydroxyl radicals formed either through the reduction of transition metal ions by SAR or from the degradation of peroxynitrite that is produced in reactions between SAR and nitric oxide [28]. Therefore, the increased dismutation of SAR to H_2O_2 and oxygen will lower the amount available for the formation of MDA. This suggests that one way in which DAA decreases lipid peroxidation, as measured by lower MDA levels, is by increasing SOD activity. This is further evidenced by the observed DNA protective effect of noni juice in heavy smokers, as MDA reacts readily with DNA bases to form lipid peroxidation-derived DNA adducts [11, 29].

One very interesting observation of this study is the inability of DAA to increase GPx activity. Increased SOD activity results in a decrease in SAR concentrations. But a consequence of SOD activity is the increased H_2O_2. H_2O_2, in turn, can cause oxidative damage, if not further metabolized into less reactive compounds. Elevated H_2O_2 has been found to increase MDA concentrations via lipid peroxidation [30]. But MDA decreased in our study, even though GPx activity was unaffected. Therefore, another pathway must have been involved in the control of H_2O_2 levels. Catalase is another antioxidant enzyme which promotes the degradation of H_2O_2 into water and oxygen [31]. Therefore, it may be that catalase activity is increased by DAA. This possibility is further supported by the fact that *Morinda citrifolia* leaves contain DAA [17] and that catalase activity was increased in lymphoma-bearing mice which had been fed crude *M. citrifolia* leaf extract [32]. Additionally, an aqueous extract of *M. citrifolia* leaves increased catalase activity in hyperlipidemic rats [33]. Other iridoids have also been reported to increase catalase activity [34], so this is a bioactivity associated with this class of compounds.

The results of this experiment demonstrate that DAA exerts an antioxidant effect by increasing SOD activity. This effect may be responsible, at least in part, for the antioxidant properties of noni juice as demonstrated in human trials and *in vivo*. The *in vitro* antioxidant activity of DAA against 4NQO may also be mediated through SOD activation, as the microorganism involved expresses this enzyme [35]. However, DAA does not appear to increase GPx activity by itself, at least under the conditions of this study. As discussed previously, noni juice increases GPx activity *in vivo*. Even though DAA is a major constituent of noni juice, the fruit also contains several other iridoids in minor concentrations [17, 36, 37]. Loganin, an iridoid similar in structure to epidihydrocornin found in noni fruit, increased GPx expression in rat mesangial cells that had been exposed to advanced glycation end products [38]. So, it is likely that another iridoid compound in noni, aside from DAA, is responsible for the increased GPx activity. It is also possible that interaction between several phytochemical constituents results in increased serum GPx.

4. Conclusion

The *in vivo* antioxidant activity of DAA has been demonstrated via oral administration to Wistar rats for 7 days. A dose-dependent trend was evident, with significant reduction in serum MDA and an accompanying increase in SOD activity at 30 and 60 mg/kg bw. DAA did not, however, increase serum GPx activity. Since serum MDA declined with increased dose, it is possible that DAA induces catalase activity. However, additional research is required to confirm this. Animal weights and feed intake, along with previous toxicity tests of DAA, do not provide any indication of toxicity. The results of the current study suggest that DAA is responsible,

at least in part, for the antioxidant activities observed in human trials. While it is possible that DAA's influence on SOD activity could explain the effect of noni juice on heavy smokers, the results also demonstrate that the effect of noni juice on GPx activity *in vivo* is not associated with DAA alone. Induction of GPx is likely due to another iridoid or a combination of phytochemical constituents.

Acknowledgment

This research was supported financially by Morinda Inc., a manufacturer of noni juice.

References

[1] J. F. Morton, "The ocean-going noni, or Indian Mulberry (*Morinda citrifolia*, Rubiaceae) and some of its "colorful" relatives," *Economic Botany*, vol. 46, no. 3, pp. 241–256, 1992.

[2] B. J. West, C. J. Jensen, J. Westendorf, and L. D. White, "A safety review of noni fruit juice," *Journal of Food Science*, vol. 71, no. 8, pp. R100–R106, 2006.

[3] M. Y. Wang, B. J. West, C. J. Jensen et al., "*Morinda citrifolia* (Noni): a literature review and recent advances in Noni research," *Acta Pharmacologica Sinica*, vol. 23, no. 12, pp. 1127–1141, 2002.

[4] A. Hirazumi and E. Furusawa, "An immunomodulatory polysaccharide-rich substance from the fruit juice of *Morinda citrifolia* (noni) with antitumour activity," *Phytotherapy Research*, vol. 13, no. 5, pp. 380–387, 1999.

[5] A. K. Palu, A. H. Kim, B. J. West, S. Deng, J. Jensen, and L. White, "The effects of *Morinda citrifolia* L. (noni) on the immune system: its molecular mechanisms of action," *Journal of Ethnopharmacology*, vol. 115, no. 3, pp. 502–506, 2007.

[6] Z. Mohd-Zin, A. Abdul-Hamid, and A. Osman, "Antioxidative activity of extracts from Mengkudu (*Morinda citrifolia* L.) root, fruit and leaf," *Food Chemistry*, vol. 78, no. 2, pp. 227–231, 2002.

[7] B. N. Su, A. D. Pawlus, H. Jung, W. J. Keller, J. L. McLaughlin, and A. D. Kinghorn, "Chemical constituents of the fruits of *Morinda citrifolia* (Noni) and their antioxidant activity," *Journal of Natural Products*, vol. 68, no. 4, pp. 592–595, 2005.

[8] M. Y. Wang and C. Su, "Cancer preventive effect of *Morinda citrifolia* (Noni)," *Annals of the New York Academy of Sciences*, vol. 952, pp. 161–168, 2001.

[9] A. K. Palu, R. D. Seifulla, and B. J. West, "*Morinda citrifolia* L., (noni) improves athlete endurance: its mechanisms of action," *Journal of Medicinal Plant Research*, vol. 2, no. 7, pp. 154–158, 2008.

[10] M. Y. Wang, L. Peng, M. N. Lutfiyya, E. Henley, V. Weidenbacher-Hoper, and G. Anderson, "*Morinda citrifolia* (noni) reduces cancer risk in current smokers by decreasing aromatic DNA adducts," *Nutrition and Cancer*, vol. 61, no. 5, pp. 634–639, 2009.

[11] M. Y. Wang, L. Peng, C. J. Jensen, S. Deng, and B. J. West, "Noni juice reduces lipid peroxidation-derived DNA adducts in heavy smokers," *Food Science & Nutrition*, vol. 1, no. 2, pp. 141–149, 2013.

[12] J. J. Zhang, L. Y. Wang, L. N. Ou et al., "Study on evaluation of antioxidant activity of Noni juice *in vivo*," *Science and Technology of Food Industry*, vol. 32, no. 7, pp. 392–393, 2011.

[13] A. Valavanidis, T. Vlachogianni, and K. Fiotakis, "Tobacco smoke: involvement of reactive oxygen species and stable free radicals in mechanisms of oxidative damage, carcinogenesis and synergistic effects with other respirable particles," *International Journal of Environmental Research and Public Health*, vol. 6, no. 2, pp. 445–462, 2009.

[14] I. Fridovich, "The biology of oxygen radicals," *Science*, vol. 201, no. 4359, pp. 875–880, 1978.

[15] G. C. Mills, "Hemoglobin catabolism. I. Glutathione peroxidase, an erythrocyte enzyme which protects hemoglobin from oxidative breakdown," *The Journal of Biological Chemistry*, vol. 229, no. 1, pp. 189–197, 1957.

[16] P. B. McCay, D. D. Gibson, K. L. Fong, and K. R. Hornbrook, "Effect of glutathione peroxidase activity on lipid peroxidation in biological membranes," *Biochimica et Biophysica Acta*, vol. 431, no. 3, pp. 459–468, 1976.

[17] O. Potterat, R. Von Felten, P. W. Dalsgaard, and M. Hamburger, "Identification of TLC markers and quantification by HPLC-MS of various constituents in noni fruit powder and commercial noni-derived products," *Journal of Agricultural and Food Chemistry*, vol. 55, no. 18, pp. 7489–7494, 2007.

[18] T. Nakamura, Y. Nakazawa, S. Onizuka et al., "Antimutagenicity of Tochu tea (an aqueous extract of *Eucommia ulmoides* leaves) : 1. The clastogen-suppressing effects of Tochu tea in CHO cells and mice," *Mutation Research*, vol. 388, no. 1, pp. 7–20, 1997.

[19] B. Li, D. Zhang, Y. Luo, and X. Chen, "Three new and antitumor anthraquinone glycosides from *Lasianthus acuminatissimus* MERR," *Chemical and Pharmaceutical Bulletin*, vol. 54, no. 3, pp. 297–300, 2006.

[20] D. H. Kim, H. J. Lee, Y. J. Oh et al., "Iridoid glycosides isolated from *Oldenlandia diffusa* inhibit LDL-oxidation," *Archives of Pharmacal Research*, vol. 28, no. 10, pp. 1156–1160, 2005.

[21] B. J. West, S. Deng, and C. J. Jensen, "Nutrient and phytochemical analyses of processed noni puree," *Food Research International*, vol. 44, no. 7, pp. 2295–2301, 2011.

[22] Y. Arima, C. Nishigori, T. Takeuchi et al., "4-Nitroquinoline 1-oxide forms 8-hydroxydeoxyguanosine in human fibroblasts through reactive oxygen species," *Toxicological Sciences*, vol. 91, no. 2, pp. 382–392, 2006.

[23] T. Nunoshiba and B. Demple, "Potent intracellular oxidative stress exerted by the carcinogen 4- nitroquinoline-N-oxide," *Cancer Research*, vol. 53, no. 14, pp. 3250–3252, 1993.

[24] S. Deng, B. J. West, A. K. Palu, and C. J. Jensen, "Determination and comparative analysis of major iridoids in different parts and cultivation sources of *Morinda citrifolia*," *Phytochemical Analysis*, vol. 22, no. 1, pp. 26–30, 2011.

[25] A. V. Peskin and C. C. Winterbourn, "A microtiter plate assay for superoxide dismutase using a water-soluble tetrazolium salt (WST-1)," *Clinica Chimica Acta*, vol. 293, no. 1-2, pp. 157–166, 2000.

[26] A. H. Pullen, "A parametric analysis of the growing CFHB (Wistar) rat," *Journal of Anatomy*, vol. 121, no. 2, pp. 371–383, 1976.

[27] F. Nistiar, O. Racz, A. Lukacinova et al., "Age dependency on some physiological and biochemical parameters of male Wistar rats in controlled environment," *Journal of Environmental Science and Health A*, vol. 47, no. 9, pp. 1224–1233, 2012.

[28] N. Hogg, V. M. Darley-Usmar, M. T. Wilson, and S. Moncada, "Production of hydroxyl radicals from the simultaneous generation of superoxide and nitric oxide," *Biochemical Journal*, vol. 281, no. 2, pp. 419–424, 1992.

[29] L. J. Marnett, "Lipid peroxidation—DNA damage by malondialdehyde," *Mutation Research*, vol. 424, no. 1-2, pp. 83–95, 1999.

[30] N. Kokita and A. Hara, "Propofol attenuates hydrogen peroxide-induced mechanical and metabolic derangements in the isolated rat heart," *Anesthesiology*, vol. 84, no. 1, pp. 117–127, 1996.

[31] P. Chelikani, I. Fita, and P. C. Loewen, "Diversity of structures and properties among catalases," *Cellular and Molecular Life Sciences*, vol. 61, no. 2, pp. 192–208, 2004.

[32] T. Anitha and S. Mohandass, "Anti-oxidant activity of *Morinda citrifolia* on lymphoma-bearing mice," *Ancient Science of Life*, vol. 26, no. 1-2, pp. 85–88, 2006.

[33] G. C. Chinta, V. Mullinti, K. Prashanthi, D. Sujata, B. Pushpakumari, and D. Ranganayakulu, "Anti-oxidant activity of the aqueous extract of the *Morinda citrifolia* leaves in triton WR-1339 induced hyperlipidemic rats," *Drug Invention Today*, vol. 2, no. 1, pp. 1–4, 2010.

[34] I. M. Villaseñor, "Bioactivities of iridoids," *Anti-Inflammatory and Anti-Allergy Agents in Medicinal Chemistry*, vol. 6, no. 4, pp. 307–314, 2007.

[35] S. Iuchi and L. Weiner, "Cellular and molecular physiology of Escherichia coli in the adaptation to aerobic environments," *Journal of Biochemistry*, vol. 120, no. 6, pp. 1055–1063, 1996.

[36] G. Liu, A. Bode, W.-Y. Ma, S. Sang, C.-T. Ho, and Z. Dong, "Two novel glycosides from the fruits of *Morinda citrifolia* (noni) inhibit AP-1 transactivation and cell transformation in the mouse epidermal JB6 cell line," *Cancer Research*, vol. 61, no. 15, pp. 5749–5756, 2001.

[37] B. N. Su, A. D. Pawlus, H. Jung, W. J. Keller, J. L. McLaughlin, and A. D. Kinghorn, "Chemical constituents of the fruits of *Morinda citrifolia* (Noni) and their antioxidant activity," *Journal of Natural Products*, vol. 68, no. 4, pp. 592–595, 2005.

[38] H. Xu, J. Shen, H. Liu, Y. Shi, H. Li, and M. Wei, "Morroniside and loganin extracted from Cornus officinalis have protective effects on rat mesangial cell proliferation exposed to advanced glycation end products by preventing oxidative stress," *Canadian Journal of Physiology and Pharmacology*, vol. 84, no. 12, pp. 1267–1273, 2006.

Hindawi Publishing Corporation
Journal of Analytical Methods in Chemistry
Volume 2013, Article ID 949830, 7 pages
http://dx.doi.org/10.1155/2013/949830

Research Article

Simultaneous Determination of Volatile Constituents from *Acorus tatarinowii* Schott in Rat Plasma by Gas Chromatography-Mass Spectrometry with Selective Ion Monitoring and Application in Pharmacokinetic Study

Xue Meng,[1] Xinfeng Zhao,[1] Shixiang Wang,[1] Pu Jia,[1] Yajun Bai,[1] Sha Liao,[1] and Xiaohui Zheng[1,2]

[1] *College of Life Sciences, Northwest University, P.O. Box 195, No. 229 Taibai North Road, Xi'an 710069, China*
[2] *Key Lab for New Drugs Research of TCM in Shenzhen, Shenzhen 518057, China*

Correspondence should be addressed to Xiaohui Zheng; zhengxh@nwu.edu.cn

Received 20 July 2013; Accepted 15 October 2013

Academic Editor: Shixin Deng

A sensitive and specific gas chromatographic-mass spectrometry with selected ion monitoring (GC-MS/SIM) method has been developed for simultaneous identification and quantification of α-asarone, β-asarone, and methyl eugenol of *Acorus tatarinowii* Schott in rat plasma. Chromatographic separation was performed on a Restek Rxi-5MS capillary column (30 m × 0.32 mm × 0.25 μm), using 1-naphthol as internal standard (IS). MS detection of these compounds and IS was performed at *m/z* 178, 208, 208, and 144. Intra- and interday precisions of all compounds of interest were less than 10%. The recoveries are situated in the range of 92.4–105.2%. Pharmacokinetics of methyl eugenol confirmed to be one-compartment open model, α-asarone and β-asarone was two-compartment open model, respectively. The method will probably be an alternative to simultaneous determination and pharmacokinetic study of volatile ingredients in *Acorus tatarinowii* Schott.

1. Introduction

Chinese medicines have played an important role in clinical therapy in China, Korea, and Japan attributed to high pharmacological activity and few complications. As a classic medicinal plant, the dry rhizome of *Acorus tatarinowii* Schott is officially listed in the Chinese Pharmacopoeia and widely used for fighting ailments such as epilepsy, digestive disorders, cerebrovascular disease, stroke, senile dementia, and diarrhea [1–5]. Recent studies have found that aqueous extract and volatile oil of *Acorus tatarinowii* Schott dose-dependently suppressed the intensity of APO-induced stereotypic behavior and locomotor activity and extended the duration of sleeping induced by pentobarbital [6, 7]. Inhalation of the volatile oil also has the properties of reversing decreased brain GABA levels induced by PTZ inhibition of GABA transaminase [8].

Low polar or nonpolar compounds including α-asarone, β-asarone, and methyl eugenol proved to be main bioactive ingredients in volatile oil of *Acorus tatarinowii* Schott in previous report [9]. β-Asarone has significant pharmacological effects on cardiovascular and central nervous system, while α-asarone possesses hypocholesterolemic, hypolipidemic, neuroprotective, and antiepileptic activities [10–16]. Methyl eugenol was also found to have antinociceptive, antibacterial, and antidepressive activities [17, 18]. These compounds were often used as reference standards for quality control of *Acorus tatarinowii* Schott due to outstanding pharmacological activities. The development of sensitive and rapid approach for simultaneous determination of these compounds was owing to increasing interest in the literature. High performance liquid chromatography (HPLC), gas chromatography (GC), and GC with mass spectrometric detection (MS) were the main assays for analyzing α- and β-asarone in the medicinal

plant and plasma in previous studies [19–23]. HPLC and MS method was also established for pharmacokinetics study of methyl eugenol in plasma [24, 25].

To our knowledge scope, few methods were found to be feasible for simultaneous determination of α-asarone, β-asarone, and methyl eugenol of *Acorus tatarinowii* Schott in biological samples, which produced issues of inaccurate evaluation of the medicinal plant and limitation of the pharmacokinetic study. This work was designed to develop a sensitive and valid method for determining α-asarone, β-asarone, and methyl eugenol of *Acorus tatarinowii* Schott in rat plasma. The work also aimed to apply the proposed assay in pharmacokinetic study of the three compounds after oral administration of volatile oil extracted from *Acorus tatarinowii* Schott.

2. Experimental

2.1. Chemicals and Reagents. α-Asarone (>98%) and 1-naphthol (>99%) were purchased from Sigma-Aldrich (St. Louis, MO, USA). Methyl eugenol (>99%) and β-asarone (>95%) were purchased from J&K Scientific Ltd (Guangdong, China). All other chemicals and reagents used in the experiment were of analytical grade unless stated specially. *Acorus tatarinowii* Schott was purchased from Xi'an Medical Company in China and identified by Professor Minfeng Fang in Northwest University.

The volatile oil of *Acorus tatarinowii* Schott was obtained by steam distillation of dry material of the plant. *Acorus tatarinowii* Schott (100.0 g) was put into 800 mL of distilled water and distilled for 8 h. The oil was collected from the condenser, dried by anhydrous sodium sulphate. The content of the oil in *Acorus tatarinowii* Schott was calculated to be 1.03% (v/w), with a determination of 0.50% methyl eugenol, 74.01% β-asarone, and 11.41% α-asarone by GC-MS analysis through area normalization method.

2.2. Preparation of Standard Solutions

2.2.1. Internal Standard. A stock solution of 1-naphthol (1.0 mg/mL) for IS was prepared in acetone and diluted to a concentration of 2.0 μg/mL with acetone.

2.2.2. Standard Solutions. Stock solution of α-asarone, β-asarone, and methyl eugenol was prepared by dissolving the appropriate amount of the standards in acetone. Mixed standard solution was prepared using the above solutions to give concentrations of 50.0 μg/mL for α-asarone, 50.0 μg/mL for β-asarone, and 50.0 μg/mL for methyl eugenol. All the solutions were stored at 4°C in amber glass tubes.

2.3. GC-MS/SIM Conditions. GC-MS analyses were performed with a Shimadzu GC-MS QP2010 (Kyoto, Japan). Chromatographic separation was achieved on a Restek Rxi-5MS capillary column (30 m × 0.32 mm I.D., 0.25 μm film thickness, Shimadzu, Japan) using nitrogen as carrier gas at 2 mL/min in a constant flow rate mode. The GC oven temperature was initially increased from 60°C to 120°C at a rate of 5°C/min, then elevated at a rate of at 2°C/min up to 150°C, and then raised to 240°C at a rate of 10°C/min, giving a total run time of 36 min. The temperatures of injector, interface, and ion source were 250, 280, and 230°C, respectively. Detection was operated by selected ionmonitoring (SIM) mode (70 eV, electron impact mode).

In the SIM mode, the peaks of α-asarone, β-asarone, methyl eugenol, and IS in plasma were identified by matching the retention time and the abundant ions of m/z 178 for methyl eugenol, m/z 208 for α-asarone, β-asarone, and m/z 144 for IS. The injection volume was 1.0 μL. Data were collected using the GC-MS solution (Kyoto, Japan).

2.4. Animals and Plasma Collection. Six healthy male Sprague-Dawley rats, weighing 250–280 g, were supplied by the Guangdong Laboratory Animals Monitoring Institute (Guangdong, China). The rats were housed in a standard animal holding room with normal access to food and water and 12 h light cycle. The animals were fasted overnight prior to dosing, with water allowance ad libitum. All animal experiments were carried out according to the Guidelines for the Care and Use of Laboratory Animals and were approved by the Animal Experimentation Ethics Committee.

Drug-free rat plasma samples were obtained from the postorbital venous plexus veins of anesthetized animals and collected into heparinized tubes. All the blood samples were centrifuged for 10 min at 8000 rpm to yield the supernatant stored at −20°C until analysis.

2.5. Sample Preparation. In a 1.5 mL Eppendorf tube, 100 μL of plasma was spiked with 10 μL of 2.0 μg/mL IS solution. An aliquot of 40 μL 10% (V : V) trichloracetic acid water solution and 600 μL acetonitrile was used to remove the proteins in the plasma through vortexed for 2 min followed by the centrifugation of 10 min at 8000 rpm. The supernatant was collected in a clean tube for next use, while the residue was extracted by 300 μL acetic ether for three times. The acetic ether layer and the above supernatant were collected together and evaporated to dryness under a stream of nitrogen. The residue was dissolved in 100 μL of acetone for further GC-MS analysis.

2.6. Method Validation

2.6.1. Calibration and Detection Limits. The linearity of α-asarone, β-asarone, and methyl eugenol was investigated by replicate analyses of calibration solutions with different concentration ranging from 5 to 5000 ng/mL and evaluated by linear regression. The limit of detection (LOD) was calculated by sequential diluting the analytes until the ratio of signal to noise equals 3 : 1. The limit of quantitation (LOQ) was considered as ten times of the signal to noise ratio.

2.6.2. Precision, Accuracy, and Stability. Quality control (QC) samples to determine the accuracy and precision of the method were independently prepared by dissolving the standard in plasma at low, medium, and high concentrations of 0.025, 0.25 and 2.5 μg/mL. The intraday precision and

Table 1: Analytical parameters for GC-MS of plasma analytes assayed by the present method.

Analytes	Calibration curve[a]	Correlation coefficient	LOD (ng/mL)	LOQ (ng/mL)
Methyl eugenol	$y = 5.874x + 0.014$	0.999	1.553	4.236
β-Asarone	$y = 6.469x - 0.027$	0.997	1.802	4.872
α-Asarone	$y = 6.326x - 0.020$	0.999	1.685	4.719

[a]In the linear regression equation, x is expressed as analytes concentration (μg/mL) and y is expressed as peak area of analytes/IS.

accuracy were determined within one day by analyzing the QC samples ($n = 6$). The interday precision and accuracy were determined on five separated days using the same QC samples. Precision was reported as the relative standard deviation (RSD). Accuracy was expressed as the relative error (RE).

The stability of analytes in the plasma was evaluated using the QC samples in triplicate. Test conditions included 4 freeze-thaw cycles and room temperature stability (0, 2, 4, 8, 12, and 24 h). The stabilities were assessed by analysis of the RSD of measured samples.

2.6.3. Recoveries and Matrix Effect. The extraction recovery of the three drugs was determined by calculating the peak areas obtained from blank plasma samples spiked with analyte before extraction with those from blank plasma samples, to which analytes were added after extraction. According to the guidance of USFDA, recovery experiments should be performed at three concentrations (low, medium, and high). This procedure was accordingly repeated for five replicates at three concentrations of 0.025, 0.25, and 2.5 μg/mL. In order to test the matrix effect on the ionization of the analyte, that is, the potential ion suppression or enhancement due to the matrix components, the drugs at three concentration levels were added to the extract of 0.1 mL of blank plasma, evaporated and reconstituted with 0.1 mL of acetone; the corresponding peak areas (A) were compared with those of the drugs standard solutions evaporated directly and reconstituted with the same solvent (B). The ratio (A/B × 100) % was used to evaluate the matrix effect. By the same method, the matrix effect of internal standard was also evaluated.

2.7. Pharmacokinetics Analysis. The GC-MS method was successfully applied in the pharmacokinetic studies of α-asarone, β-asarone, and methyl eugenol in rats. Volatile oil of *Acorus tatarinowii* Schott was administered orally to the rat in a single dose of 0.2 g/kg. Blood samples were collected in heparinized tube at 0, 5, 10, 20, 30, 60, 90, 120, 180, 300, 480, 720, 960, and 1200 min after dose. All the samples were extracted and analyzed under the proposed condition.

2.8. Data Analysis. The Microsoft Excel Program Drug and Statistics 2.0 (T.C.M. Shanghai, China) was employed to process and calculate the pharmacokinetic parameters. The parameters of the area under curve (AUC), the maximum plasma concentration (C_{max}) and the corresponding time (t_{max}), the half-life of absorption ($t_{1/2}$), and so forth were used to decrypt the pharmacokinetic properties of α-asarone, β-asarone, and methyl eugenol. Statistical analysis of the biological data was performed by the Student's t-test. All results were expressed as arithmetic mean ± standard deviation (SD).

3. Results and Discussion

3.1. Preparation of the Plasma Samples. In order to quantify drugs in a plasma sample, it is often necessary to disrupt the protein-drug binding for the production of the drugs-free form. Acetonitrile and trichloracetic acid were separately evaluated for extracting α-asarone, β-asarone, and methyl eugenol from plasma. When choosing the trichloracetic acid, the recoveries of α-asarone and β-asarone were less than 50%. When choosing the acetonitrile, the recoveries of α-asarone and β-asarone were near 80%. The recoveries of methyl eugenol and IS just have minor change. Interestingly, a mixture of acetonitrile and trichloracetic acid (10%) in ratios of 15 : 1 was found to be efficient to accomplish the extracting task. The recoveries of analytes were more than 90%. This solvent was accordingly used to prepare the plasma samples in the present work.

3.2. Calibration and Detection Limits. The linear regression analysis was constructed by plotting the peak area ratio of the three analytes to IS against the concentrations of α-asarone, β-asarone, and methyl eugenol in plasma samples, respectively, shown in Table 1. The regression equation of the curves and the correlation coefficients (r) was calculated to be $y = 6.326x - 0.020$ and $r = 0.999$ for α-asarone, $y = 6.469x - 0.027$ and $r = 0.997$ for β-asarone, and $y = 5.874x + 0.014$ and $r = 0.999$ for methyl eugenol, using weighted least squares linear regression (the weighing factor was $1/C$). For each drug, six calibration curves containing six concentrations (5, 25, 50, 250, 500, 2500, and 5000 ng/mL) were linear within the concentration range of 5–5000 ng/mL. The CV of the three drugs at each level varied from 2.0 to 12.3. And the relative bias of α-asarone, β-asarone, and methyl eugenol from the theoretical value varied from −3.0 to 4.6. As a result, the calibration curves of the three compounds exhibited good linearity within the experimental range. The LOD for α-asarone, β-asarone, and methyl eugenol was calculated to be 1.9, 1.8, and 1.5 ng/mL. The LOQ of the tested drugs was 4.7, 4.9, and 4.2 ng/mL.

3.3. Precision, Accuracy, and Stability. The data from QC samples were calculated to estimate the intraday and interday precision and accuracy of the method. The results are presented in Table 2. It was found that the intraday precision for

Table 2: Intraday ($n = 6$) and interday precision ($n = 5$) and accuracy of analytes from biological samples.

Analytes	Added (μg/mL)	Precision (RSD, %)		Accuracy (RE, %)	
		Intraday	Interday	Intraday	Interday
Methyl eugenol	0.025	5.18	8.10	5.15	3.65
	0.250	6.69	7.68	−7.62	−2.15
	2.500	4.11	4.74	−3.54	−4.34
β-Asarone	0.025	4.84	6.20	2.89	2.93
	0.250	6.34	3.75	−6.03	−3.22
	2.500	4.99	6.01	−4.88	−5.76
α-Asarone	0.025	7.08	4.80	−0.77	−4.53
	0.250	3.24	4.42	−4.74	4.04
	2.500	4.85	7.99	0.71	−4.01

Table 3: Matrix effects and extraction recovery of analytes in biological samples.

Analyte	Concentration (μg/mL)	Matrix effects (%, $n = 6$)	RSD (%)	Extraction recovery (%, $n = 5$)	RSD (%)
Methyl eugenol	0.025	93.8 ± 5.2	5.5	105.2 ± 5.4	5.1
	0.250	94.6 ± 5.8	6.1	92.4 ± 6.2	6.7
	2.500	105.2 ± 4.7	4.5	96.5 ± 4.0	4.1
β-Asarone	0.025	92.4 ± 6.6	6.5	102.9 ± 5.0	4.9
	0.250	98.6 ± 6.2	6.3	94.0 ± 6.0	6.4
	2.500	101.3 ± 3.8	3.8	95.1 ± 4.8	5.0
α-Asarone	0.025	96.9 ± 4.4	4.5	99.2 ± 7.0	7.1
	0.250	100.6 ± 7.8	7.8	95.3 ± 3.1	3.3
	2.500	103.8 ± 6.2	6.0	100.7 ± 4.9	4.9
I.S.	2.0	94.1 ± 4.0	4.3	93.6 ± 3.1	8.6

low, mid, and high QC levels of α-asarone was 7.08%, 3.24%, and 4.85%, respectively, and that of the interday analysis was 4.80%, 4.42%, and 7.99%, with an accuracy (RE) within −4.74 to 4.04%. The precision for β-asarone of the QCs was determined as 4.84%, 6.34% plus 4.99% for intraday and 6.20%, 3.75%, and 6.01% for interday. The accuracy was found ranging from −6.03 to 2.93%. For methyl eugenol, the intraday precisions were 5.18%, 6.69%, and 4.11%, while the interday precisions were 8.10%, 7.68%, and 4.74%. The accuracy of methyl eugenol ranged between −7.62 and 5.15% for the three levels of QC samples. The precision and accuracy of the present method conform to the criteria for the analysis of biological samples according to the guidance of USFDA, where the precision (RSD) determined at each concentration level is required not to exceed 15%.

The stabilities were demonstrated by analysis of the RSD of measured samples. The results indicated that analytes were stable at 2, 4, 8, 12, and 24 h at room temperature and during multiple freeze-thaw cycles (≥95.6%). The three compounds were believed to have good stability in 24 h at room temperature and during three freeze-thaw cycles.

3.4. Recoveries and Matrix Effect. The results are presented in Table 3. The recoveries of α-asarone from rat plasma were 99.2 ± 7.0, 95.3 ± 3.1, and 100.7 ± 4.9% at concentration levels of 0.025, 0.25, and 2.5 μg/mL, respectively, and the mean extraction recovery of IS was 93.6 ± 3.1%. The values for recoveries of β-asarone using the proposed method were 102.9 ± 5.0, 94.0 ± 6.0, and 95.1 ± 4.8%. For methyl eugenol, the extraction recoveries were calculated to be 105.2 ± 5.4, 92.4 ± 6.2, and 96.5 ± 4.0%. In terms of matrix effect, all the ratios (A/B × 100)% defined as in Section 2.6.3 were between 92.4 and 105.2%, which means no matrix effect for the three compounds and IS in using current method (Figure 1).

3.5. Pharmacokinetics Analysis. The present method was applied to the pharmacokinetic investigations of α-asarone, β-asarone, and methyl eugenol following single oral dose of 0.2 g/kg volatile oil of *Acorus tatarinowii* Schott. Mean plasma drug concentration-time curve of the three compounds in single dose study was shown in Figure 2, and the calculating parameters were in Table 4. The results indicated that the plasma profile of methyl eugenol was confirmed to be one-compartment open models, while the pharmacokinetic behavior of α-asarone and β-asarone was in line with two-compartment open model. Nevertheless, after oral administration of the volatile oil, the C_{max} of the three drugs were calculated to be 0.021, 0.53, and 2.47 μg/mL, with the t_{max} values of 10.00, 11.25, and 13.75 min. The AUC (0 ~ ∞) were determined as 2.49, 56.67, and 407.52 mg/L· min, while the values of AUC (0~t) were 2.13, 368.43, and 47.51 mg/L· min. The ratios of AUC (0 ~ ∞) versus AUC (0~t) for the three drugs were all less than 120%, which indicated that the proposed blood collecting time was feasible to evaluate the pharmacokinetic behaviors of the three compounds.

Table 4: Pharmacokinetic parameters of analytes in rats ($n = 6$).

Analytes	$T_{1/2\alpha}$ (min)	$T_{1/2\beta}$ (min)	$T_{1/2}$ (min)	$AUC_{(0\sim t)}$ (mg/L·min)	$AUC_{(0\sim\infty)}$ (mg/L·min)	CL (mL/min/kg)	Vd (L/kg)	T_{max} (min)	C_{max} (μg/mL)
Methyl Eugenol			67.66 ± 3.32	2.13 ± 0.27	2.49 ± 0.25	0.40 ± 0.04	39.35 ± 4.08	10.00 ± 0.00	0.021 ± 0.001
β-Asarone	54.39 ± 29.46	69.30 ± 0.21		368.43 ± 40.05	407.52 ± 55.78	0.38 ± 0.05	149.87 ± 90.78	13.75 ± 11.09	2.47 ± 0.58
α-Asarone	58.92 ± 20.80	69.28 ± 6.12		47.51 ± 28.49	56.67 ± 35.91	0.60 ± 0.44	22.93 ± 16.11	11.25 ± 6.29	0.53 ± 0.24

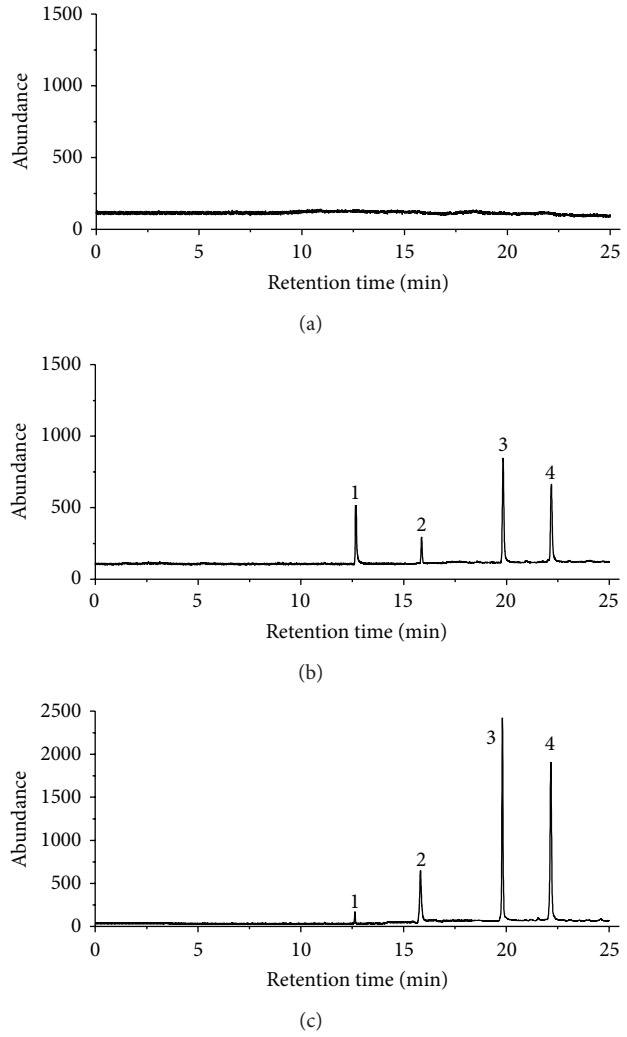

Figure 1: GC-MS/SIM chromatograms: (a) rat blank plasma sample; (b) standard solutions of methyl eugenol (0.2 μg/mL), β-asarone (0.2 μg/mL), α-asarone (0.2 μg/mL), and IS (0.1 μg/mL); (c) rat blood sample after a single oral administration of volatile oil of *Acorus tatarinowii* Schott. Peak 1: methyl eugenol; Peak 2: IS; Peak 3: β-asarone; Peak 4: α-asarone.

4. Conclusions

A novel GC-MS/SIM method for simultaneously qualitative and quantitative analysis of α-asarone, β-asarone, and methyl eugenolin rat plasma is described in this work. The method combines the excellent power of separation performed by GC to the high sensitivity of MS detection system operating in SIM mode and it has the properties of high specificity, precision, accuracy, and stability. The method has been confirmed to be successful in pharmacokinetics study of α-asarone, β-asarone and methyl eugenol in *Acorus tatarinowii* Schott, which probably provides an alternative to monitor the three drugs in preclinical study.

Conflict of Interests

The authors declare that there is no conflict of interests.

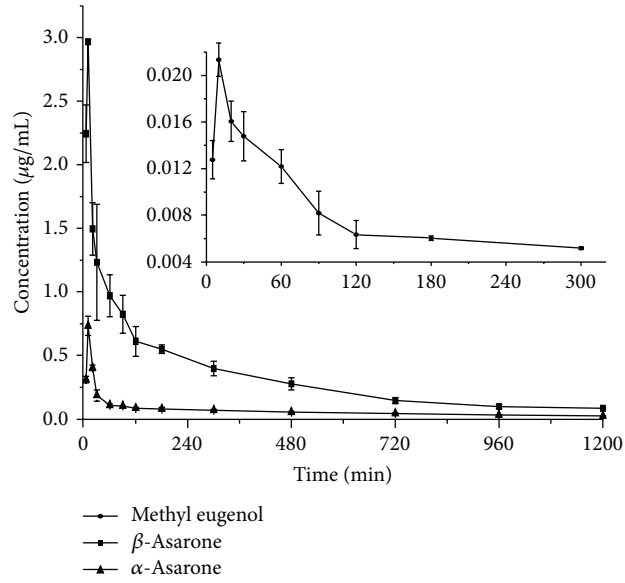

Figure 2: The mean plasma concentration-time profile of analytes in rats after oral administration volatile oil of *Acorus tatarinowii* Schott (0.2 g/kg).

Acknowledgments

This work was supported by grants from the Program for Changjiang Scholars and Innovative Research Team in Universities of China (IRT1174) and the Eleventh Five-Year National Science and Technology Support Program of China (no. 2008BAI51B01).

References

[1] Y. Irie and W. M. Keung, "Rhizoma acori graminei and its active principles protect PC-12 cells from the toxic effect of amyloid-β peptide," *Brain Research*, vol. 963, no. 1-2, pp. 282–289, 2003.

[2] B. Lee, Y. Choi, H. Kim et al., "Protective effects of methanol extract of Acori graminei rhizoma and Uncariae Ramulus et Uncus on ischemia-induced neuronal death and cognitive impairments in the rat," *Life Sciences*, vol. 74, no. 4, pp. 435–450, 2003.

[3] J. Cho, C. H. Yang, C. G. Park, H. Lee, and Y. H. Kim, "Inhibition of excitotoxic neuronal cell death by total extracts from oriental medicines used for stroke treatment," *Yakhak Hoeji*, vol. 44, no. 1, pp. 29–35, 2000.

[4] P. C. Dandiya and M. K. Menon, "Actions of asarone on behavior, stress, and hyperpyrexia, and its interactions with central stimulants," *Journal of Pharmacology and Experimental Therapeutics*, vol. 145, pp. 42–46, 1964.

[5] M. T. Hsieh, W. H. Peng, C. R. Wu, and W. H. Wang, "The ameliorating effects of the cognitive-enhancing Chinese herbs on scopolamine-induced amnesia in rats," *Phytotherapy Research*, vol. 14, no. 5, pp. 375–377, 2000.

[6] J.-F. Liao, S.-Y. Huang, Y.-M. Jan, L.-L. Yu, and C.-F. Chen, "Central inhibitory effects of water extract of Acori graminei rhizoma in mice," *Journal of Ethnopharmacology*, vol. 61, no. 3, pp. 185–193, 1998.

[7] S. B. Vohora, S. A. Shah, and P. C. Dandiya, "Central nervous system studies on an ethanol extract of Acorus calamus rhizomes," *Journal of Ethnopharmacology*, vol. 28, no. 1, pp. 53–62, 1990.

[8] B.-S. Koo, K.-S. Park, J.-H. Ha, J. H. Park, J.-C. Lim, and D.-U. Lee, "Inhibitory effects of the fragrance inhalation of essential oil from acorus gramineus on central nervous system," *Biological and Pharmaceutical Bulletin*, vol. 26, no. 7, pp. 978–982, 2003.

[9] G. Wei, Y.-Q. Fang, D.-H. Liu, and S.-F. Lin, "Study on GC-MS fingerprint analysis in rhizome of volatile oil of *Acorus tatarinowii*," *China Journal of Chinese Materia Medica*, vol. 29, no. 8, pp. 764–768, 2004.

[10] Q. D. Wu, Y. Q. Fang, Y. Z. Chen, Z. S. Kuan, S. Y. Wang, and Y. P. He, "Protective effects of volatile oil of *Acorus tatarinowii* schott and β-Asarone on cardiovascular system," *Traditional Chinese Drug Research and Clinical Pharmacology*, vol. 16, no. 4, pp. 244–247, 2005.

[11] J. Liu, C. Li, G. Xing et al., "Beta-asarone attenuates neuronal apoptosis induced by beta amyloid in rat hippocampus," *Yakugaku Zasshi*, vol. 130, no. 5, pp. 737–746, 2010.

[12] Y.-Q. Fang, C. Shi, L. Liu, and R.-M. Fang, "Pharmacokinetics of beta-asarone in rabbit blood, hippocampus, cortex, brain stem, thalamus and cerebellum," *Die Pharmazie*, vol. 67, no. 2, pp. 120–123, 2012.

[13] L. Rodríguez-Páez, M. Juárez-Sanchez, J. Antúnez-Solís, I. Baeza, and C. Wong, "α-asarone inhibits HMG-CoA reductase, lowers serum LDL-cholesterol levels and reduces biliary CSI in hypercholesterolemic rats," *Phytomedicine*, vol. 10, no. 5, pp. 397–404, 2003.

[14] L. Garduño, M. Salazar, S. Salazar et al., "Hypolipidaemic activity of α-asarone in mice," *Journal of Ethnopharmacology*, vol. 55, no. 2, pp. 161–163, 1997.

[15] J. Cho, Y. Ho Kim, J.-Y. Kong, C. Ha Yang, and C. Gook Park, "Protection of cultured rat cortical neurons from excitotoxicity by asarone, a major essential oil component in the rhizomes of Acorus gramineus," *Life Sciences*, vol. 71, no. 5, pp. 591–599, 2002.

[16] H. Chen, W. G. Li, X. B. Zhang et al., "Alpha-asarone from Acorus Gramineus alleviates epilepsy by modulating A-type gaba receptors," *Neuropharmacology*, vol. 65, no. 5, pp. 1–11, 2013.

[17] M. C. B. Norte, R. M. Cosentino, and C. A. Lazarini, "Effects of methyl-eugenol administration on behavioral models related to depression and anxiety, in rats," *Phytomedicine*, vol. 12, no. 4, pp. 294–298, 2005.

[18] S. Yano, Y. Suzuki, M. Yuzurihara et al., "Antinociceptive effect of methyleugenol on formalin-induced hyperalgesia in mice," *European Journal of Pharmacology*, vol. 553, no. 1–3, pp. 99–103, 2006.

[19] H. B. Wu and Y. Q. Fang, "Pharmacokinetics of β-asarone in rats," *Acta Pharmaceutica Sinica*, vol. 39, no. 10, pp. 836–8383, 2004.

[20] X. H. Ke, G. Wei, and Y. Q. Fang, "Assay of β-asarone and α-asarone in Rhizoma acori tatarinowii by HPLC," *Chinese Traditional Patent Medicine*, vol. 24, no. 10, pp. 791–792, 2002.

[21] L. P. Wei and M. H. Wu, "Pharmacokinetic study of β-asarone in volatile oil from *Acorus tatarinowii* in rabbits," *Chinese Traditional and Herbal Drugs*, vol. 36, no. 1, pp. 48–51, 2002.

[22] L. Liu and Y.-Q. Fang, "Analysis of the distribution of β-asarone in rat hippocampus, brainstem, cortex and cerebellum with gas chromatography-mass spectrometry (GC-MS)," *Journal of Medicinal Plant Research*, vol. 5, no. 9, pp. 1728–1734, 2011.

[23] C. Deng, S. Lin, T. Huang, G. Duan, and X. Zhang, "Development of gas chromatography/mass spectrometry following headspace solid-phase microextraction for fast determination of asarones in plasma," *Rapid Communications in Mass Spectrometry*, vol. 20, no. 14, pp. 2120–2126, 2006.

[24] S. W. Graves and S. Runyon, "Determination of methyleugenol in rodent plasma by high-performance liquid chromatography," *Journal of Chromatography B*, vol. 663, no. 2, pp. 255–262, 1995.

[25] D. B. Barr, J. R. Barr, S. L. Bailey et al., "Levels of methyleugenol in a subset of adults in the general U.S. population as determined by high resolution mass spectrometry," *Environmental Health Perspectives*, vol. 108, no. 4, pp. 323–328, 2000.

Hindawi Publishing Corporation
Journal of Analytical Methods in Chemistry
Volume 2013, Article ID 351671, 10 pages
http://dx.doi.org/10.1155/2013/351671

Research Article

In Vitro Antioxidative Evaluation of α- and β-Carotene, Isolated from Crude Palm Oil

Surashree Sen Gupta[1] and Mahua Ghosh[1,2]

[1] *Department of Chemical Technology, University of Calcutta, Kolkata, West Bengal 700 009, India*
[2] *Department of Chemical Technology, University College of Science & Technology, University of Calcutta, 92 A.P.C. Road, Kolkata 700009, India*

Correspondence should be addressed to Mahua Ghosh; mahuag@gmail.com

Received 22 May 2013; Revised 6 September 2013; Accepted 24 September 2013

Academic Editor: Jian Yang

The present work describes the isolation of α- and β-carotene from crude palm oil and their antioxidant potential in an *in vitro* model. Pure product was isolated by the method adopted. Antioxidant activities of the isolated α- and β-carotene were analyzed in five different concentrations of 0.001, 0.005, 0.01, 0.05, and 0.1% (w/v). From the several assays conducted, an observation was made that the antioxidant activity of the product shifted between antioxidant and prooxidant effects depending on the concentration and the system analyzed. The metal chelation, DPPH radical scavenging, and superoxide scavenging activities showed almost similar results in terms of high activity at lowest concentrations. ABTS-scavenging activity was displayed only by a particular antioxidant concentration of 0.1%. Lipid peroxidation assay pronounced the activity of 0.1% antioxidant in inhibiting oxidation of sensitive bioactive lipids. *In vitro* antidenaturation test again specified the efficacy of low concentrations in preventing protein denaturation. Through this study a definite dosage formulation for consumption of carotenoids is being proposed which will enhance health promotion and prevent chronic diseases when taken as fortified foods or dietary supplements.

1. Introduction

α- and β-carotene are important members of the carotenoid family. As a retinol precursor with a high conversion rate, α- and β-carotene provide a substantial proportion of the vitamin A in the human diet [1]. Recently some researchers have shown that α- and β-carotene, due to their antioxidant activities, possess important health-promoting activities which might be helpful in the prevention and protection against a number of serious health disorders such as cancer, cardiovascular disease, and colorectal adenomas [2]. For these reasons, there is a strong interest in using α- and β-carotene and other carotenoids as functional ingredients in food products.

Crude palm oil has a significant amount of carotene that can be extracted and, in recent years, various methods for extracting carotenes from palm oil have been developed. Of these, the method involving the combination of transesterification and molecular distillation processes is the most cost-effective one with ease of execution [3], and this was followed in this study.

A number of studies have shown that α- and β-carotene and other carotenoids have lipid-soluble antioxidant activity. In homogeneous lipid solutions, in membrane models, and also in intact cells, α- and β-carotene have been mostly studied [4, 5]. Recent findings suggest that the position and orientation of the carotenoids in the membrane are important factors in determining their relative effectiveness in protecting against free radicals [6]. α- and β-carotene partially or completely protect intact cells (e.g., human liver cell line HepG2) against oxidant-induced lipid peroxidation, and the protective effect is independent of provitamin A activity [4]. α- and β-carotene suppressed lipid peroxidation in mouse and rat tissues [5]. The consumption of food-based antioxidants like α- and β-carotene seems to be useful for the prevention of macular degeneration and cataracts [7]. A well-known fact is that α- and β-carotene quench singlet oxygen with higher efficiency than many other antioxidants [8].

In contrast to the physiologically relevant properties, the knowledge on antioxidant potential of α- and β-carotene, *in vitro*, is scarce as most studies conducted so far were *in vivo*. Hence, the aim of the present study was to isolate α- and β-carotene from crude palm oil, their characterization, and *in vitro* investigation of their antioxidative efficacy.

2. Experimental

2.1. Materials. Crude palm oil imported from Indonesia was collected from local Vanaspati manufacturer. All other reagents were of analytical grade and procured from Merck India Ltd., Mumbai. India.

2.2. Isolation of α- and β-Carotene from Crude Palm Oil. Crude palm oil was chemically transesterified with methanol and sodium hydroxide. Oil and alcohol were taken in different molar ratios and stirred while maintaining a high temperature for a definite time interval [3]. Syntheses of esters were monitored by thin layer chromatography. The effects of different reaction parameters for this particular reaction, such as temperature, substrate molar ratio, and concentration of alkali, were optimized with individual sets of reaction mixture. Oil : methanol ratio of 1 : 10 on weight basis, stirring rate of 200 rpm, temperature of 80°C for 3 hours, and a concentration of 0.2% NaOH were optimised for maximum yield of α- and β-carotene. A two-phase mixture comprising a glycerol phase and an ester phase consisting of fatty esters and the carotene was obtained. The ester phase was distilled at 300°C at 10^{-01} mbar pressure in a molecular distillation unit (SIBATA, Japan, serial no. N40394). The residue was diluted 5 times and saponified with ethanolic potassium hydroxide at 80°C. The carotene was extracted from the saponified residue with a mixture of hexane and water where the extract phase was rich in carotene. Pure carotene was obtained on solvent (hexane) removal which was crystallized and recrystallized with acetone.

2.3. Spectrophotometric Analysis. For spectrophotometric analysis 0.01 g measured amount of the crystallized carotene product was taken in a calibrated test tube and dissolved into 25 mL of petroleum ether. The solution was scanned under UV-visible spectrophotometer (UV-1700 PharmaSpec, UV-VIS Spectrophotometer, Shimadzu, Japan) between 300–600 nm. The λ_{max} value was noted and the molar extinction coefficient (ε_{max}) using 1 cm cell was calculated for definite concentration of the sample. Further spectral conformation was carried out by scanning the solid carotene crystals under the UV-visible range of 200–800 nm with UV spectrophotometer (U-3501, Hitachi, Japan).

2.4. Characterisation by Thin Layer Chromatography (TLC). Crystalline samples were dissolved in petroleum ether and spotted in glass TLC plates coated with silica gel stationary phase. The TLC plate was placed in a chamber saturated with solvent vapour. The solvent system consisted of 60% petroleum ether/20% acetone/20% dichloromethane [9]. After development of the plates, they were visualized by subjecting them to iodine vapour. The R_f values for the spot on the TLC plate were calculated:

$$R_f = \frac{\text{distance from baseline to sample front}}{\text{distance from baseline to solvent front}}. \quad (1)$$

2.5. Characterisation by High Performance Liquid Chromatography (HPLC). Analysis of the carotenoids was conducted using Waters HPLC (Milford, Massachusetts, US) with a Waters 1525 binary HPLC pump consisting of a vacuum degasser and a Waters 2487 dual λ absorbance detector. Reverse-phase HPLC equipped with Nova-pak C_{18} column, 3.9 × 150 mm, 4 μm was used for the analysis of the antioxidant. The UV detector was set at 450 nm. The mobile phase consisted of acetonitrile : methanol : tetrahydrofuran (50 : 45 : 5 by volume) [10]. The crystallized carotenoids were dissolved in 5 mL of the mobile phase. The mobile phase was isocratic solvent. Injection volume of 200 μL and the flow rate were set at 1 mL/min. Data acquisition was completed in 40 minutes.

2.6. Antioxidant Assay of Isolated Carotene Crystals. The antioxidant activity of the isolated carotenoids was examined by seven different *in vitro* assay systems. Different concentrations of the antioxidant were prepared in ethanol. The concentrations were 0.001, 0.005, 0.01, 0.05, and 0.1% (w/v). Their antioxidant activities were measured consecutively.

2.6.1. Assay of DPPH Radical-Scavenging Activity. Antioxidant activity of α- and β-carotene was determined by the scavenging activity of the stable DPPH free radical. The method was described by Katerere and Eloff [11]. Different concentrations of the test samples were placed into test tubes taking 0.2 mL from each of them with 4 mL of 0.2 mM of ethanolic solution of DPPH. Absorbance at 517 nm was determined after 40 minutes using a solution of ethanol and DPPH (3 : 1) as control. Radical scavenging activity was expressed as the inhibition percentage and was calculated using the following formulae:

$$\%\ \text{Radical scavenging activity} = \left[\frac{A_0 - A_1}{A_0}\right] \times 100, \quad (2)$$

where A_0 is the absorbance of the control and A_1 is the absorbance of the sample.

2.6.2. Assay of Reductive Potential. The reductive potential of the antioxidant was determined according to the method of Dorman and Hiltunen [12]. The reaction mixture containing different concentrations of the antioxidants (50–250 μg/mL) in 1 mL of ethanol, phosphate buffer (2.5 mL, 0.2 M, pH 6.6), and potassium ferricyanide (2.5 mL, 1% wt/vol) was incubated at 50°C for 20 minutes. A portion (2.5 mL) of trichloroacetic acid (10% wt/vol) was added to the mixture, which was then allowed to rest for 10 minutes. From the mixture 2.5 mL was taken and mixed with distilled water (2.5 mL) and $FeCl_3$ (0.5 mL, 0.1% wt/vol), and the absorbance was measured at 700 nm in a spectrophotometer. Higher absorbance of the reaction mixture indicated greater reductive potential.

2.6.3. Assay of Metal Chelating Activity. The Fe^{2+} chelating ability of antioxidants was estimated by the method of Dinis et al. [13]. Samples with concentrations of about 50–250 μg/mL were added to 0.08 mL of $FeCl_2$ (2.5 mmol/L) solution. To the system 0.3 mL of ferrozine (6 mmol/L) solution was added and the mixture was shaken vigorously and left to stand at room temperature for 10 minutes. Absorbance was thereby measured spectrophotometrically at 562 nm. Percentage of inhibition of ferrozine-Fe^{2+} complex formation was calculated as follows:

$$\% \text{ inhibition} = \left[\frac{A_0 - A_1}{A_0}\right] \times 100, \quad (3)$$

where A_0 is the absorbance of the control and A_1 is the absorbance of the sample.

2.6.4. ABTS Radical Scavenging Activity. ABTS radical cation scavenging activity of flaxseed lignan was assessed by the method of Re et al. [14] and Zhao et al. [15] with some minor modifications. Measured volume of 5 mL of 7 mM ABTS was mixed with 88 μL of 140 mM $K_2S_2O_8$ and kept overnight. Next day the solution was diluted with 50% ethanol and an initial absorbance of 0.7 was set at 734 nm. Then 1 mL of diluted ABTS was mixed with 20 μL of sample and absorbance was measured at 734 nm at 1-second intervals for 5 minutes.

2.6.5. Lipid Oxidation in a Linoleic Acid Emulsion Model System. The ammonium thiocyanate method was used to assess the antioxidant activity of flaxseed lignans with some minor modifications of the procedure of Gülçin [16]. A linoleic acid preemulsion was made by vortexing 0.28 g of linoleic acid with 0.28 g of Tween 20 in 50 mL of 0.05 μL phosphate buffer (pH 7.4). Working solutions of SDG (0.2 mL) were added and mixed with 2.5 mL linoleic acid emulsion and 2.3 mL phosphate buffer (0.2 μL), vortexed, and incubated at 37°C overnight. Aliquots (100 μL) from the incubated mixture were withdrawn at 1, 24, 48, 72, 96, and 120 hours of incubation and tested for lipid peroxidation by adding 5 mL of ethanol (75%), 0.1 mL of NH_4SCN (30% w/v), and 0.1 mL of $FeCl_2$ (0.1% w/v). The absorbance of the reaction mixture was measured at 500 nm against ethanol

$$\% \text{ inhibition} = \left[\frac{A_0 - A_1}{A_0}\right] \times 100, \quad (4)$$

where A_0 is the absorbance of the control and A_1 is the absorbance of the sample.

2.6.6. Superoxide Anion Scavenging Activity. Superoxide anion scavenging activity of flaxseed lignan was based on the method described by Yaping et al. [17] and Wang et al. [18] with some minor modifications. About 4.5 mL of Tris-HCl buffer (50 mmol/L, pH 8.2) and 1.0 mL tested samples with various concentrations were mixed in tubes with lids. Then the mixture was incubated for 20 min in the water bath at 25°C. Meanwhile, 0.4 mL of 25 mmol/L pyrogallol preheated at 25°C was added immediately. After 4 min, the reaction was terminated by 0.1 mL HCl solution (8 mol/L) and the mixture was centrifuged at 4000 rpm for 15 min. The absorbance of sample and control was determined by UV spectrophotometer at 325 nm. Scavenging activity was calculated using the following equation:

$$\text{Superoxide anion scavenging activity } (\%) = \frac{(A0 - As)}{A0} \times 100, \quad (5)$$

where $A0$ is the absorbance without sample and As is absorbance with sample.

2.6.7. Assay of In Vitro Anti-denaturation Effects. The assay helps to assess the anti-denaturation/anti-inflammatory effect of proteins. The method is based on the works of Williams [19]. An amount of 2.5 mL 1% BSA was mixed with 2.5 mL tris acetate buffer (0.05 M) and 2.5 mL of the test solutions. The mixtures were heated at 69°C for 4 minutes and cooled and then the absorbances of the turbidities were read at 660 nm

$$\% \text{ inhibition of denaturation} = \frac{(A0 - As)}{A0} \times 100, \quad (6)$$

where $A0$ is the absorbance of control and As is absorbance with sample.

2.7. Statistical Analysis. Statistical analysis was performed with one-way analysis of variance (ANOVA). When ANOVA detected significant differences between mean values, means were compared using Tukey's test. For statistical studies OriginLab software (Origin7, OriginLab Corporation, Northampton, UK) was used. Statistical significance was designated as $P < 0.05$. Three replications for each of the experiments and assays were conducted ($n = 3$). A mean of the three values was reported in each case. The values are expressed as Mean ± SEM.

3. Results and Discussions

3.1. Isolation, Spectroscopic Analysis, and TLC of β-Carotene. In the present work the palm oil was initially transesterified and then concentrated by distillation for isolating α- and β-carotene. Amount of the carotene crystals obtained was 1.2%. Spectroscopic studies showed maximum absorption at 440 nm (Figure 1(a)) and a minor absorbance peak at 466.6 nm (Figure 1(b)). The peak at 440 nm corresponds to the absorbance by β-carotene, as confirmed by calculation of the molar extinction coefficient (ε_{max})

$$\varepsilon_{max} = \frac{A}{CL}, \quad (7)$$

where A is absorbance of the specified molecule at maximum wavelength (λ_{max}), C is concentration of the active molecule, and L is distance (1 cm).

The extinction coefficient was calculated to be 1, 28, 300 L mol^{-1} cm^{-1} which is in correlation with established

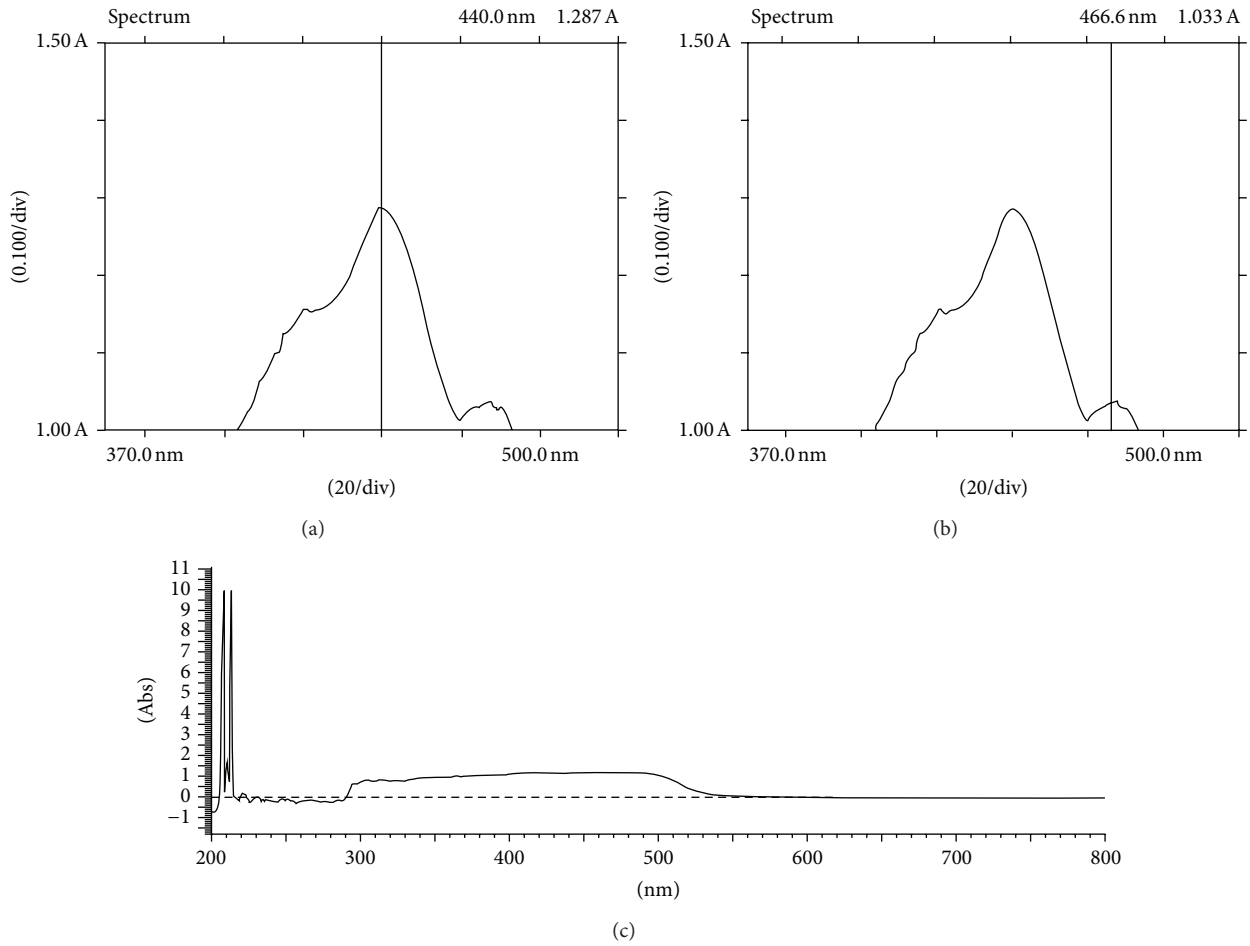

Figure 1: Absorbance spectrum of β-carotene/α-carotene pigments isolated from crude palm oil: (a) absorbance maxima of β-carotene at 440 nm; (b) absorbance of α-carotene at 466.6 nm; (c) absorbance profile of β-carotene/α-carotene mixture in a crystalline form.

values of extinction coefficient [20]. The minor peak at 466.6 nm is that of α-carotene which is in correlation with the extinction coefficient (1, 02, 979 L mol^{-1} cm^{-1}) of α-carotene [21].

The absorption at given wavelength range can be expressed as the sum of individual carotenoids as observed in Figure 1(c), where UV/visible spectrophotometric study of the crystalline carotenoid pigment displays a uniform plateau-shaped absorption range representing an assemblage of α- and β-carotene. The range was observed between 300 to 550 nm which is in harmony with previously derived results.

On thin layer chromatographic analysis R_f factor was calculated to be 0.95 which corresponds to previously reported values [22]. The single spot indicated that α- and β-carotene had overlapped over the specified area resulting in the incurrence of an intermediate value of retention factor.

3.2. Detection of β-Carotene Using High Performance Liquid Chromatography (HPLC). On HPLC two peaks were observed with retention times at 28.2 and 30.5 minutes. β-carotene eluted as a single peak at 30.5 minutes (Figure 2) and α-carotene at 28.2 minutes, as deciphered by comparison with authentic standards.

3.3. Antioxidant Assay of Isolated β-Carotene. The antioxidant activity of the isolated carotene crystals were examined by seven different *in vitro* assay systems. Different concentrations of the antioxidant was prepared in ethanol. The concentrations prepared were 0.001, 0.005, 0.01, 0.05, and 0.1% (w/v). Their antioxidant activities were measured in terms of DPPH radical scavenging activity, reducing activity, metal chelation, ABTS radical scavenging activity, lipid peroxidation, superoxide scavenging activity, and antidenaturation effect.

3.3.1. Assay of DPPH Radical-Scavenging Activity. The DPPH radical scavenging method was based on the reduction of methanolic DPPH solution in the presence of a hydrogen donating antioxidant, due to the formation of the nonradical form DPPH-H [23]. Monitoring the decrease of the radical in terms of decreasing absorbance values leads to the assessment of the antioxidant activity of the product. The carotene crystals were able to reduce and decolourise 1,1-diphenyl-2-picrylhydrazyl efficiently at low concentrations, via their hydrogen donating ability (Figure 3). This is an electron transfer-based assay which measures the capacity of an antioxidant in the reduction of an oxidant. Here the degree

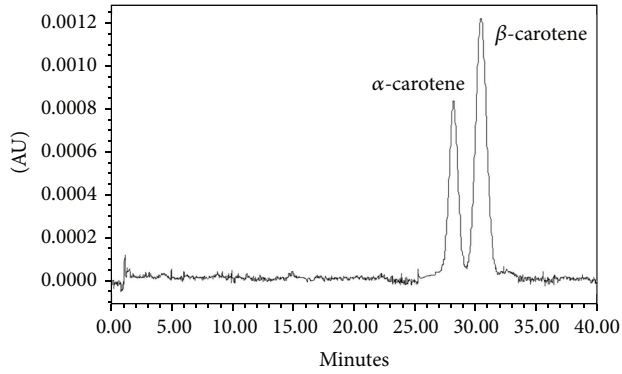

Figure 2: HPLC chromatogram of α- and β-carotene.

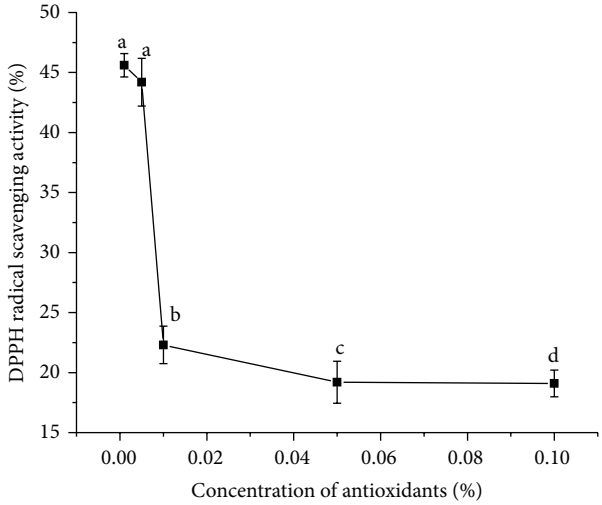

Figure 3: DPPH radical scavenging activity for α- and β-carotene crystals at different concentrations. Values are Mean ± SEM of 3 observations. At the 0.05 level, difference in superscripts (a, b, c, d) indicates significant difference in means.

of colour change is correlated with the sample's antioxidant activity.

The order of antioxidant potency by DPPH method is conclusive of the behavior of the antioxidant at different concentration gradients. Colour interference by α-carotene with DPPH chromogen and β-carotene may result in a lower measured DPPH activity at high concentrations [24]. Moreover the presence of higher concentrations of antioxidants results in prooxidant effects which induce oxidative stress, usually by inhibiting antioxidant systems. Hence the lowest concentration of the antioxidant (0.001%) that was analysed for DPPH radical scavenging activity was found to be the optimum concentration that showed efficacy in scavenging the free radicals. Furthermore, on comparing the mean values, all the concentration means varied significantly among themselves except for 0.001% and 0.005% concentrations at $P < 0.05$.

3.3.2. Assay of Reductive Potential. Again assay of reducing capacity is an effective means to understand the antioxidant

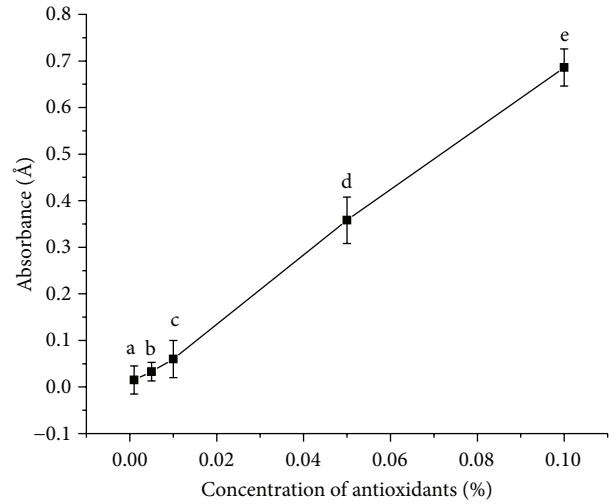

Figure 4: Reducing activity of α- and β-carotene crystals at different concentrations. Values are Mean ± SEM of 3 observations. At the 0.05 level, the difference in superscripts (a, b, c, d, e) indicates significant difference in means.

activity of various antioxidants. Reducing capacity serves as a significant indicator of the potential antioxidant activity of any bioactive species. Here reduction potential bears a proportional dependency on the absorbance measured (Figure 4). Here all the different concentration mean values were significantly different from each other at $P < 0.05$. The measured absorbance serves to indicate the change in reduction potential of the tested species. The reducing power (transformation of Fe^{3+} to Fe^{2+}) of the antioxidant makes it an efficient electron donor, which can react with free radicals to convert them to more stable products, thereby terminating radical chain reactions. The antioxidant exerts an antioxidant effect by reducing Fe^{3+} to Fe^{2+}. Such bioactive property of the antioxidant leads to the development of its chemoprotective potential too. From this assay it was deduced that in terms of reducing activity α- and β-carotene showed the expected tendency of concentration variation. With increasing carotenoid concentrations the absorbance increased indicating an increase in the reducing activity of the antioxidant. Hence higher amounts of the antioxidant will serve as an efficient reducing agent, though its radical scavenging activity showed a contrary behaviour.

3.3.3. Assay of Metal Chelating Activity. Again metal chelation activity is an example of a complexation reaction where Ferrozine [disodium salt of 3-(2-pyridyl)-5,6-bis(4-phenylsulfonic acid)-1,2,4-triazine] is a complex-forming agent of Fe(II) and will form a magenta complex Fe(II)-(Ferrozine)(III) with maximum absorbance at 562 nm. Hence in the presence of a reducing agent the complex formation is hampered resulting in decrease in the colour of the complex and hence a decrease in the absorbance. Measurement of absorbance therefore allows estimating the metal chelating activity of the coexisting chelator [25]. In this case α- and β-carotene interfered with the formation of ferrous-ferrozine

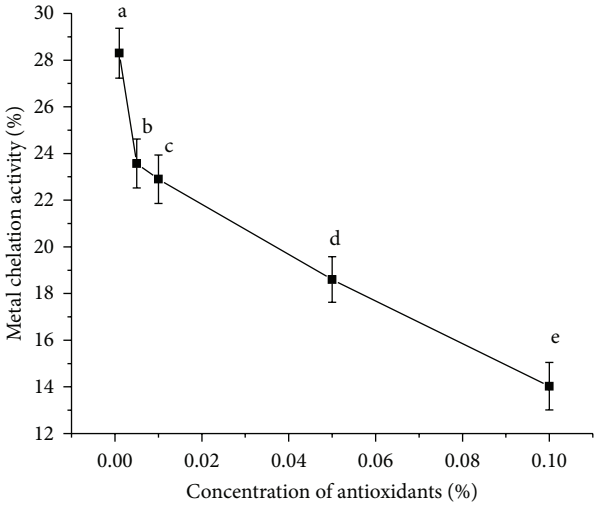

Figure 5: Metal chelation activity of α- and β-carotene crystals at different concentrations. Values are Mean ± SEM of 3 observations. At the 0.05 level, the difference in superscripts (a, b, c, d, e) indicates significant difference in means.

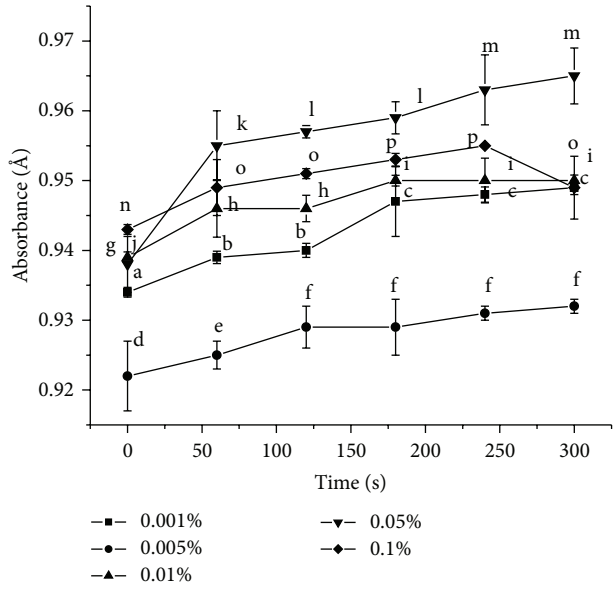

Figure 6: ABTS-radical scavenging activity of α- and β-carotene crystals at different concentrations. Values are Mean ± SEM of 3 observations. At the 0.05 level, at time intervals 0, 60, 120, 180, 240, and 300 seconds, the difference in superscripts indicates significant difference in means. Superscripts (1) (a, b, c) for 0.001%; (2) (d, e, f) for 0.005%; (3) (g, h, i) for 0.01%; (4) (j, k, l, m) for 0.05%; and (5) (n, o, p) for 0.1% are used.

complex. The steric hindrance generated by the bulky carbon chains of α- and β-carotene prevented the unsaturated groups from acting as chelating agents at higher concentrations. Moreover with increasing concentrations the prooxidant effect is active and α- and β-carotene become the source of complexation, resulting in higher absorbance values and hence reduced metal chelation activities (Figure 5). In fine, α- and β-carotene act as a better DPPH-radical scavenger than a metal chelator. The presence of unsaturated groups could be a contributing factor towards their effective reducing property. All the different concentration mean values were significantly different from each other at $P < 0.05$.

3.3.4. ABTS Radical Scavenging Activity. The ABTS assay is based on the ability of antioxidants to scavenge the long-life radical cation $ABTS^{+}$. The scavenging of radicals produces a decreased absorbance at 734 nm. Here absorbance was found to increase at 734 nm for all concentrations, except for 0.1% concentration (Figure 6). In case of 0.1% concentration, commencement of radical-scavenging activity was observed beyond 240 seconds, as indicated by lowering absorbance values.

Unlike DPPH radical scavenging activity, the ABTS-scavenging power was exhibited only at 0.1% antioxidant concentration. Apparently here the antioxidant activity of α- and β-carotene cannot be well differentiated based on their concentrations as can be established in the case of DPPH method or metal chelation. Generation of oxidative stress was evident from the increase in absorbance values at 0.05% concentration. The lowest concentration of 0.001% showed higher absorbance readings than the ones at 0.005% concentration. This could be due to the inability of the antioxidant to scavenge the long-life free radicals at the minimal concentration. At still higher value of 0.01% concentration, the absorbance value reaches an almost constant value beyond 4 minutes indicating a possibility of ABTS-scavenging capacity at higher time periods. At $P < 0.05$, for concentrations 0.001%, 0.005%, 0.01%, 0.05%, and 0.1% the population means were significantly different from each other throughout the time range tested except for: 60, 120 seconds and 180, 240, 300 seconds among themselves for 0.001% concentration; 120, 180, 240, 300 seconds among themselves for 0.005% concentration; 60, 120 seconds and 180, 240, 300 seconds among themselves for 0.01% concentration; 120, 180 seconds and 240, 300 seconds among themselves for 0.05% concentration; 60, 120, 300 seconds and 180, 240 seconds among themselves for 0.1% concentration.

3.3.5. Lipid Oxidation in a Linoleic Acid Emulsion Model System. The relative inhibitory effect of α- and β-carotene on lipid peroxidation using a model linoleic acid peroxidation assay is shown in Figure 7. The basis of lipid peroxidation method involves the use of heat as the free radical initiator which instigates the oxidation of Fe^{2+} to Fe^{3+} (8) and is consequently measured by assessing the amount of peroxyl radicals that is generated in the prepared linoleic acid emulsion, due to the lipid oxidation reaction of the linoleic acid [26]

$$Fe^{2+} + LOOH = Fe^{3+} + LO^{\bullet} + OH^{-}, \quad (8)$$

where LOOH denotes a lipid derived hydroperoxide and $LO^{\bullet}$ denotes a lipid peroxyl radical. The Fe^{3+} subsequently reacts with ammonium thiocyanate to form ferric thiocyanate. The absorbance at 500 nm measures the amount of ferric thiocyanate formed in the medium as a result of the above

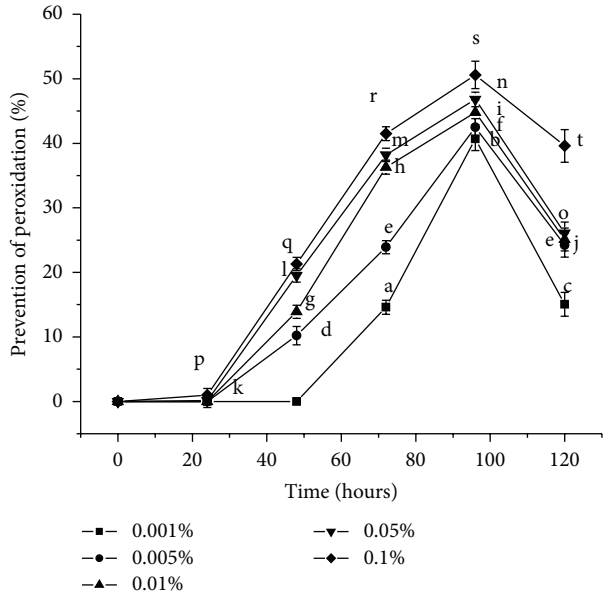

Figure 7: Prevention of lipid peroxidation by α- and β-carotene crystals at different concentrations. Values are Mean ± S.E.M of 3 observations. At the 0.05 level, for the time span 0 hours, 24 hours, 48 hours, 72 hours, 96 hours, and 120 hours, the difference in superscripts indicates significant difference in means. Superscripts (1) (a, b, c) for 0.001%; (2) (d, e, f) for 0.005%; (3) (g, h, i, j) for 0.01%; (4) (k, l, m, n, o) for 0.05%; and (5) (p, q, r, s, t) for 0.1% are used.

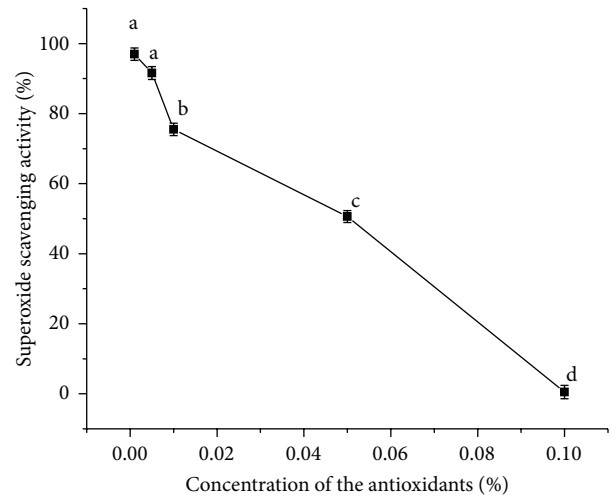

Figure 8: Superoxide scavenging activity by α- and β-carotene crystals at different concentrations. Values are Mean ± SEM of 3 observations. At the 0.05 level, the difference in superscripts (a, b, c, d) indicates significant difference in means.

reaction. Higher absorbance readings (i.e., lower prevention of lipid peroxidation) are associated with increased concentration of peroxyl radicals in the solution which occurs simultaneously with the formation of the colouring complex. α- and β-carotene served to scavenge the Fe^{2+} ion from the medium, where the scavenging efficacy increased with increasing concentration of the antioxidants. A variety of beta carotene isomers and metabolites were used to test for various *in vitro* assays like FRAP assay, lipid peroxidation, and so forth. No ferric reducing activity (FRAP assay) was observed for the isomers. Between the major isomers no significant differences in bleaching the $ABTS^{\bullet+}$ or in scavenging peroxyl radicals ($ROO^{\bullet}$) generated by thermal degradation of AAPH (using a chemiluminescence assay) were detected [27]. The carotenoids displayed lipophilic antioxidant activity by dissolving completely in the linoleic acid emulsion and serving as an efficient radical scavenger. A mixture of α- and β-carotene in association increased the activity of the product crystals against lipid peroxidation as indicated by high level of inhibition of lipid peroxidation and therefore sufficient antioxidant activity at higher concentrations.

In case of 0.001% concentration prevention of peroxidation was not detected before 72 hours unlike 0.1% concentration where 0.97% prevention was observed only after 24 hours. Beyond 4 days the inhibition of lipid peroxidation reduced for all concentrations. Thus antioxidant activity of the products showed potency maximum up to 4 days, beyond which the effectiveness diminished gradually and predominance of the peroxyl radicals was observed, as indicated by higher absorbance values. At $P < 0.05$, for the time span 0 hours, 24 hours, 48 hours, 72 hours, 96 hours, and 120 hours the population means are significantly different from each other for all the five different carotene concentrations except for: 72 from 120 hours for 0.005% concentration.

3.3.6. Superoxide Anion Scavenging Assay. Again α- and β-carotene crystals exhibited a concentration-dependent superoxide scavenging activity similar to DPPH radical scavenging activity. The losses of linearity in the dose response curve at low concentrations of α- and β-carotene were a reflection of not only their superoxide scavenging efficiency, but also the prooxidant effect of the products. As both α- and β-carotene can interchange between a reduced form and an oxidised form, they display antioxidant and pro-oxidant properties related to their dosage and half-life [28]. Necessary preponderance must be given to the antioxidant activity of carotenoids at low concentrations, especially while considering their scavenging activities (Figure 8). Here pyrogallol acted as the free radical initiator which absorbed oxygen from the air; turning purple from a colourless solution, by forming superoxide anions. Superoxide anion is an oxygen-centered reactive oxygen species (superoxide anion and hydrogen peroxide are the main reactive oxygen species causing the oxidation of cells and tissues). They react with protons in water solution to form hydrogen peroxide (9), which serve as a substrate for the generation of hydroxyl radicals and singlet oxygen [29]

$$2O_2^- + 2H^+ \longrightarrow H_2O_2 + O_2. \quad (9)$$

Superoxide radical is a very harmful species to cellular components as a precursor of more reactive oxygen species and is known to be produced *in vivo* and can result in the formation of H_2O_2 via dismutation reaction. H_2O_2 is a nonradical reactive oxygen species which acts as a strong

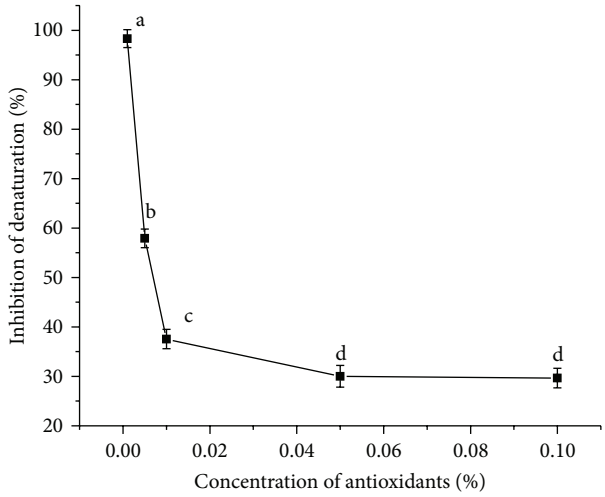

Figure 9: Inhibition of denaturation *in vitro* by α- and β-carotene crystals at different concentrations. Values are Mean ± SEM of 3 observations. At the 0.05 level, the difference in superscripts (a, b, c, d) indicates significant difference in means.

oxidant leading to harmful reactions. Here α- and β-carotene at a concentration of 0.001%, scavenged superoxide anions, with utmost efficiency, thereby reducing the probability of peroxide formation. Radical scavengers can be prooxidant unless linked to a radical sink, and superoxides are such radical sinks and hence efficiently scavenge radicals at low concentrations. Increasing concentrations of the antioxidants lead to the appearance of prooxidant activity resulting in the decrease in scavenging capacity. Here the antioxidant itself behaved as a radical that bigoted another radical with higher efficiency at lower concentrations and it promoted oxidation at higher concentrations. At $P < 0.05$, all the population means are significantly different from each other except for 0.001% and 0.005% concentrations.

3.3.7. Assay of In Vitro Antidenaturation Effects. The present study is the first of its kind to report the efficacy of β-carotene in protecting cells from denaturation/inflammatory effect *in vitro* (Figure 9).

When BSA is heated it undergoes denaturation and expresses antigens associated to Type III hypersensitive reaction which are related to diseases such as serum sickness, glomerulonephritis, rheumatoid arthritis, and systemic lupus erythematosus. An in-depth study of the antidenaturation effect of α- and β-carotene can be utilised for the treatment of such diseases by their specific dosage formulations. An efficient antioxidant is one which is able to compete with endogenous scavengers and interact with endogenous pathways by localizing themselves in the appropriate area. One of the features of several nonsteroidal anti-inflammatory drugs is their ability to stabilize (prevent denaturation) heat treated BSA at pathological pH [pH 6.2–6.5] [19]. The increased synthesis of heat shock results in a ubiquitous physiological response of cells to environmental stress and hence promotes degradation of proteins. In this study an attempt was made *in vitro* to study the course of action of α- and β-carotene in preventing thermal denaturation and aggregation of BSA protein at increased temperatures. A variety of cellular internal and external stress are generated due to environmental imbalance which leads to the formation of reactive oxygen species resulting in the origin of several disturbances in the normal redox conditions of the cells leading to their deterioration in the course of time. These stresses denature proteins enhancing the probability of the formation of reactive oxygen species in the medium, leading to inflammation and other physiological malfunctions. These aggregates, if not disposed of or their formation being prevented, can lead to cell death. In response to the appearance of damaged proteins, cells induce the expression of such harmful species. However as an effective antioxidant α- and β-carotene prevented such denaturation, which functioned as molecular chaperone and prevented protein aggregation or degradation. Carotenoids (including β-carotene) were found to promote health when taken at dietary levels, but showed adverse effects when consumed at a high dose by subjects who smoke or were exposed to asbestos [30]. The effectiveness was the greatest at low concentrations, which can be utilized in drug designing. The high apparent antioxidant capacity of α- and β-carotene at low concentrations also has an added advantage in terms of cost-effectiveness of the developed drug product. At $P < 0.05$, the concentration means are significantly different from each other except for the concentrations 0.05% and 0.1%.

4. Conclusion

From the results obtained, both α- and β-carotene were isolated effectively and their antioxidant study gave interesting observations. Table 1 summarizes the efficacy of the carotenoids in responding to the different antioxidant assays. While 0.001% concentration was effective DPPH/superoxide radical scavenger, metal chelator, and antidenaturant, 0.1% concentration showed effective reducing activity and lipid peroxidation. Moreover 0.1% was the only concentration which showed any ABTS radical scavenging activity. Compounds often enhance the antioxidant capacity of cells but are ineffective in test tube assays. The antioxidant activity of α- and β-carotene can shift into a prooxidant phase, depending on such factors as oxygen tension or carotenoid concentration. Good correlations observed among the different hydrophilic antioxidant assays, namely, metal chelation, DPPH radical, and superoxide scavenging activities, suggested that these methods have almost similar predictive capacity for antioxidant activities of various concentrations of α- and β-carotene. ABTS-scavenging activity was displayed at a particular antioxidant concentration of 0.1%. In case of lipophilic antioxidant assay it was observed that almost 51% inhibition of lipid peroxidation was displayed by 0.1% activity. The right dose essentially differentiates a potent remedy from a subsequent harmful intake. Hence in hydrophilic environment mostly lower concentrations of antioxidants were effective, whereas in lipophilic medium higher concentrations were effective. This could be due to the higher lipid affinity of the carotenoids, being nonpolar in nature.

Table 1: Relative efficacy of each antioxidant assay for individual antioxidant concentration.

Concentrations (%)	Antioxidant assay						
	DPPH radical scavenging activity (%)	Reducing activity (Å)	Metal chelation (%)	ABTS radical scavenging activity (%)	Lipid peroxidation (%)	Superoxide radical scavenging activity (%)	Anti-denaturation assay (%)
0.001	+++++	+	+++++	−	+	+++++	+++++
0.005	++++	++	++++	−	++	++++	++++
0.01	+++	+++	+++	−	+++	+++	+++
0.05	++	++++	++	−	++++	++	++
0.1	+	+++++	+	+	+++++	+	+

In consequence they can act as substantial chemoprotectants and prevent harmful physiological activities, if consumed in a proper dose.

Acknowledgment

The authors would like to acknowledge the "Council of Scientific and Industrial Research" (CSIR) for the financial support received.

References

[1] Y. Yuan, Y. Gao, L. Mao, and J. Zhao, "Optimisation of conditions for the preparation of β-carotene nanoemulsions using response surface methodology," *Food Chemistry*, vol. 107, no. 3, pp. 1300–1306, 2008.

[2] D. Albanes, "β-Carotene and lung cancer: a case study," *American Journal of Clinical Nutrition*, vol. 69, no. 6, pp. 1345S–1350S, 1999.

[3] M. Nitsche, W. Johannisbauer, and V. Jordan, "Process for Obtaining Carotene from Palm Oil," US Patent 5, 902, 890, 1999.

[4] A. A. Woodall, G. Britton, and M. J. Jackson, "Carotenoids and protection of phospholipids in solution or in liposomes against oxidation by peroxyl radicals: relationship between carotenoid structure and protective ability," *Biochimica et Biophysica Acta*, vol. 1336, no. 3, pp. 575–586, 1997.

[5] K. R. Martin, M. L. Failla, and J. C. Smith Jr., "β-Carotene and lutein protect HepG2 human liver cells against oxidant- induced damage," *Journal of Nutrition*, vol. 126, no. 9, pp. 2098–2106, 1996.

[6] T. Iyama, A. Takasuga, and M. Azuma, "β-carotene accumulation in mouse tissues and a protective role against lipid peroxidation," *International Journal for Vitamin and Nutrition Research*, vol. 66, no. 4, pp. 301–305, 1996.

[7] V. Agte and K. Tarwadi, "The importance of nutrition in the prevention of ocular disease with special reference to cataract," *Ophthalmic Research*, vol. 44, no. 3, pp. 166–172, 2010.

[8] P. Di Mascio, S. Kaiser, and H. Sies, "Lycopene as the most efficient biological carotenoid singlet oxygen quencher," *Archives of Biochemistry and Biophysics*, vol. 274, no. 2, pp. 532–538, 1989.

[9] P. F. Guo, *Preparation, antioxidant activity and stability of lycopene and β-carotene from Papaya [Ph.D. thesis]*, 2009.

[10] J. G. Jackson, E. L. Lien, S. J. White, N. J. Bruns, and C. F. Kuhlman, "Major carotenoids in mature human milk: longitudinal and diurnal patterns," *Journal of Nutritional Biochemistry*, vol. 9, no. 1, pp. 2–7, 1998.

[11] D. R. Katerere and J. N. Eloff, "Antibacterial and antioxidant activity of *Sutherlandia frutescens* (Fabaceae), a reputed anti-HIV/AIDS phytomedicine," *Phytotherapy Research*, vol. 19, no. 9, pp. 779–781, 2005.

[12] H. J. D. Dorman and R. Hiltunen, "Fe(III) reductive and free radical-scavenging properties of summer savory (*Satureja hortensis* L.) extract and subfractions," *Food Chemistry*, vol. 88, no. 2, pp. 193–199, 2004.

[13] T. C. P. Dinis, V. M. C. Madeira, and L. M. Almeida, "Action of phenolic derivatives (acetaminophen, salicylate, and 5-aminosalicylate) as inhibitors of membrane lipid peroxidation and as peroxyl radical scavengers," *Archives of Biochemistry and Biophysics*, vol. 315, no. 1, pp. 161–169, 1994.

[14] R. Re, N. Pellegrini, A. Proteggente, A. Pannala, M. Yang, and C. Rice-Evans, "Antioxidant activity applying an improved ABTS radical cation decolorization assay," *Free Radical Biology and Medicine*, vol. 26, no. 9-10, pp. 1231–1237, 1999.

[15] X. Zhao, H. Sun, A. Hou, Q. Zhao, T. Wei, and W. Xin, "Antioxidant properties of two gallotannins isolated from the leaves of Pistacia weinmannifolia," *Biochimica et Biophysica Acta*, vol. 1725, no. 1, pp. 103–110, 2005.

[16] İ. Gülçin, I. G. Şat, Ş. Beydemir, M. Elmastaş, and Ö. I. Küfrevioğlu, "Comparison of antioxidant activity of clove (Eugenia caryophylata Thunb) buds and lavender (*Lavandula stoechas L.*)," *Food Chemistry*, vol. 87, no. 3, pp. 393–400, 2004.

[17] Z. Yaping, Y. Wenli, W. Dapu, L. Xiaofeng, and H. Tianxi, "Chemiluminescence determination of free radical scavenging abilities of 'tea pigments' and comparison with 'tea polyphenols'," *Food Chemistry*, vol. 80, no. 1, pp. 115–118, 2003.

[18] J. Wang, Q. Zhang, Z. Zhang, and Z. Li, "Antioxidant activity of sulfated polysaccharide fractions extracted from Laminaria japonica," *International Journal of Biological Macromolecules*, vol. 42, no. 2, pp. 127–132, 2008.

[19] L. A. D. Williams, A. O'Connar, L. Latore et al., "The *in vitro* anti-denaturation effects induced by natural products and non-steroidal compounds in heat treated (Immunogenic) bovine serum albumin is proposed as a screening assay for the detection of anti-inflammatory compounds, without the use of animals, in the early stages of the drug discovery process," *West Indian Medical Journal*, vol. 57, no. 4, pp. 327–331, 2008.

[20] E. Biehler, F. Mayer, L. Hoffmann, E. Krause, and T. Bohn, "Comparison of 3 spectrophotometric methods for carotenoid

determination in frequently consumed fruits and vegetables," *Journal of Food Science*, vol. 75, no. 1, pp. C55–C61, 2010.

[21] R. J. Bushway, A. Yang, and A. M. Yamani, "Comparison of alpha- and beta-carotene content of supermarket vs. Roadside stand produced in Maine," *Technical Bulletin*, vol. 122, pp. 1–16, 1986.

[22] B. Fried, K. Beers, and J. Sherma, "Thin-layer chromatographic analysis of beta-carotene and lutein in Echinostoma trivolvis (Trematoda) rediae," *Journal of Parasitology*, vol. 79, no. 1, pp. 113–114, 1993.

[23] X. L. Li and A. G. Zhou, "Evaluation of the antioxidant effects of polysaccharides extracted from Lycium barbarum," *Medicinal Chemistry Research*, vol. 15, no. 9, pp. 471–482, 2007.

[24] T. Yamaguchi, H. Takamura, T. Matoba, and J. Terao, "HPLC method for evaluation of the free radical-scavenging activity of foods by using 1,1-diphenyl-2-picrylhydrazyl," *Bioscience, Biotechnology and Biochemistry*, vol. 62, no. 6, pp. 1201–1204, 1998.

[25] F. Yamaguchi, M. Saito, T. Ariga, Y. Yoshimura, and H. Nakazawa, "Free radical scavenging activity and antiulcer activity of garcinol from Garcinia indica fruit rind," *Journal of Agricultural and Food Chemistry*, vol. 48, no. 6, pp. 2320–2325, 2000.

[26] D. D. Kitts, Y. V. Yuan, A. N. Wijewickreme, and L. U. Thompson, "Antioxidant activity of the flaxseed lignan secoisolariciresinol diglycoside and its mammalian lignan metabolites enterodiol and enterolactone," *Molecular and Cellular Biochemistry*, vol. 202, no. 1-2, pp. 91–100, 1999.

[27] L. Mueller and V. Boehm, "Antioxidant activity of β-carotene compounds in different *in vitro* assays," *Molecules*, vol. 16, no. 2, pp. 1055–1069, 2011.

[28] C. C. Teow, V.-D. Truong, R. F. McFeeters, R. L. Thompson, K. V. Pecota, and G. C. Yencho, "Antioxidant activities, phenolic and β-carotene contents of sweet potato genotypes with varying flesh colours," *Food Chemistry*, vol. 103, no. 3, pp. 829–838, 2007.

[29] B. Halliwell, J. M. C. Gutteridge, and C. E. Cross, "Free radicals, antioxidants, and human disease: where are we now?" *Journal of Laboratory and Clinical Medicine*, vol. 119, no. 6, pp. 598–620, 1992.

[30] S. A. R. Paiva, R. M. Russell, and S. K. Dutta, "β-carotene and other carotenoids as antioxidants," *Journal of the American College of Nutrition*, vol. 18, no. 5, pp. 426–433, 1999.

Hindawi Publishing Corporation
Journal of Analytical Methods in Chemistry
Volume 2013, Article ID 246986, 9 pages
http://dx.doi.org/10.1155/2013/246986

Research Article

Comparative Analysis of the Volatile Components of *Agrimonia eupatoria* from Leaves and Roots by Gas Chromatography-Mass Spectrometry and Multivariate Curve Resolution

Xiao-Liang Feng,[1] Yun-biao He,[2] Yi-Zeng Liang,[3] Yu-Lin Wang,[1] Lan-Fang Huang,[1] and Jian-Wei Xie[1]

[1] *School of Chemical and Material Engineering, Quzhou College, Quzhou 324000, China*
[2] *Changde Institute for Food and Durg Control, Changde 415000, China*
[3] *College of Chemistry and Chemical Engineering, Central South University, Changsha 410083, China*

Correspondence should be addressed to Lan-Fang Huang; fq18guo@yahoo.com.cn

Received 10 June 2013; Revised 8 August 2013; Accepted 20 August 2013

Academic Editor: Shao-Nong Chen

Gas chromatography-mass spectrometry and multivariate curve resolution were applied to the differential analysis of the volatile components in *Agrimonia eupatoria* specimens from different plant parts. After extracted with water distillation method, the volatile components in *Agrimonia eupatoria* from leaves and roots were detected by GC-MS. Then the qualitative and quantitative analysis of the volatile components in the main root of *Agrimonia eupatoria* was completed with the help of subwindow factor analysis resolving two-dimensional original data into mass spectra and chromatograms. 68 of 87 separated constituents in the total ion chromatogram of the volatile components were identified and quantified, accounting for about 87.03% of the total content. Then, the common peaks in leaf were extracted with orthogonal projection resolution method. Among the components determined, there were 52 components coexisting in the studied samples although the relative content of each component showed difference to some extent. The results showed a fair consistency in their GC-MS fingerprint. It was the first time to apply orthogonal projection method to compare different plant parts of *Agrimonia eupatoria*, and it reduced the burden of qualitative analysis as well as the subjectivity. The obtained results proved the combined approach powerful for the analysis of complex *Agrimonia eupatoria* samples. The developed method can be used to further study and quality control of *Agrimonia eupatoria*.

1. Introduction

Agrimonia eupatoria, one of Rosaceae plant family, mainly locates in Zhejiang, Yunnan, Guangdong, Guangxi, and other places of China [1]. As a traditional Chinese medicine (TCM) listed in the Chinese Pharmacopoeia, *Agrimonia eupatoria* has long been used to cure many diseases, such as tumors, Meniere's syndrome, and trichomonas vaginitis [2, 3]. It also has the function of antitumor antidiabetic, hemostatic, and antibacterial [4–6]. Although *Agrimonia eupatoria* contains up to tens or even hundreds of compounds, only a limited number of compounds, such as agrimony, agrimony lactone, tannin, flavonoids, glycosides, and the volatile components, might be the main active components, which are responsible for pharmaceutical or toxic effects [7, 8]. To ensure the reliability and repeatability of pharmacological and clinical research and understand their bioactivities and possible side effects of active compounds, it is necessary to study all of the phytochemical constituents of botanical extracts and develop a method for quality control of *Agrimonia eupatoria*. For example, the volatile constituents are known to exhibit pharmacological and biological activity, and it is used for sterilization and antibacterial active role [8]. Thus the analysis

of the volatile ingredients in *Agrimonia eupatoria* is very important.

As for the analysis of the volatile compounds in *Agrimonia eupatoria*, only a few reports have been seen in the literature [9, 10]. They are usually performed with gas chromatography (GC) and gas chromatography-mass spectrometry (GC-MS), which are based on gas chromatographic retention indices or MS for qualitative and quantitative analysis. However, because the composition of *Agrimonia eupatoria* is very complicated and the contents of many important volatile components in *Agrimonia eupatoria* are very low, suitable sample-preparing methods are necessary before detection by GC-MS, such as steam distillation [9]. Although preparing methods are used for the analysis process of the complicated *Agrimonia eupatoria* samples, it is still impossible to obtain complete separation of all the volatile chemical constituents of *Agrimonia eupatoria*. In these general GC or GC-MS reports, it is difficult to assess the purity of chromatographic peaks and the peak inspected as one component may be a mixture of several components. The results obtained by these methods which have been mentioned above would be questionable. Fortunately, with the development of hyphenated instruments, multidimensional data revealing the compositions of samples can be obtained from GC-MS, HPLC-DAD, and so on. Then, many associated chemometric methods [11–18], which can be used to resolve multidimensional data, have been developed. Thus, more information for chemical analysis both in chromatographic separation and in spectral identification can be obtained, which makes it possible to interpret these complex systems.

On the other hand, there may be some sameness and differences to exist in *Agrimonia eupatoria* from different plant parts. To find the pharmacological active components that exist in essential oils exactly, it is important that the method for the detailed study of the components in *Agrimonia eupatoria* from different plant parts, such as the root and leaf, was established.

In this paper, two chemometrics methods, subwindow factor analysis [13] and orthogonal projection resolution (OPR) [14], were used to analyze the volatile constituents of *Agrimonia eupatoria* from different plant parts for the first time. The volatile components of *Agrimonia eupatoria* from two different plant parts were extracted with water distillation and subjected to GC-MS analysis. Firstly, the qualitative and quantitative analysis of volatile components in the main root of *Agrimonia eupatoria* was completed with the help of subwindow factor analysis. Secondly, the common peaks in leaf of *Agrimonia eupatoria* were extracted with orthogonal projection method. At last, to those constituents in leaf, which were not identified with OPR method, the qualitative analysis was also performed with subwindow factor analysis. Then, a simple and reliable combined approach for the systematic study of the volatile constituents in the main root and leaf *Agrimonia eupatoria* was developed. Not only more information was obtained, but also the reliability of components was improved. The obtained results can provide foundation for further development of fingerprint and quality control of *Agrimonia eupatoria*.

2. Theory and Method

2.1. Subwindow Factor Analysis (SFA). The detailed process of SFA has been described in the literature [13]; here only a brief depiction of the method is given.

According to the Lambert-Beer Law, a two-dimensional data $\mathbf{X}_{m\times n}$ produced by hyphenated instruments can be expressed as the product of two matrices as follows:

$$\mathbf{X}_{m\times n} = \mathbf{C}_{m\times p}\ \mathbf{S}^{T}_{n\times p} + \mathbf{E}, \tag{1}$$

where $\mathbf{X}_{m\times n}$ denotes response matrix representing p components of m spectra measured at regular time intervals and at n different wavelengths or mass-to-charge ratios. Matrix $\mathbf{C}$ is the pure composed of p columns, each one describing the chromatographic concentration profile of a pure chemical species. Similarly, the matrix $\mathbf{S}^{T}$ consists of p rows corresponding to pure spectra of the chemical species. Matrix $\mathbf{E}$ denotes measurement noise. The superscript T represents the transpose of matrix.

It is crucial to identify left and right subwindows of SFA. In the former an interfering compound starts to elute before the analyte appears in a chromatogram to the left of the analyte, and in the latter another interference continues to elute after the analyte has stopped eluting. The rank analysis can provide the number of chemical components of the left and right ones, say m_1 and m_2, respectively. And the number of components in the combination of left and right ones is $m_1 + m_2 - 1$, since the analyte is common to both. One may then find an orthogonal basis $\{\mathbf{g}_1, \mathbf{g}_2, \ldots \mathbf{g}_{m1}\}$ spanning the spectral subspace of the left subwindow and a similar basis $\{\mathbf{f}_1, \mathbf{f}_2, \ldots \mathbf{f}_{m2}\}$ spanning that of the right subwindow, corresponding to matrices $\mathbf{G}$ and $\mathbf{F}$, by means of singular-value decomposition. The common spectral vector $\mathbf{v}$ to both subspaces can be written as linear combinations of both sets of basis for an ideal case:

$$\begin{aligned} \mathbf{v} &= \mathbf{G}\mathbf{a}, \\ \mathbf{v} &= \mathbf{F}\mathbf{b}. \end{aligned} \tag{2}$$

Under the conditions, $\mathbf{a}^{T}\mathbf{a} = \mathbf{b}^{T}\mathbf{b} = 1$. In reality, $\mathbf{G}\mathbf{a}$ and $\mathbf{F}\mathbf{b}$ are not identical on account of interference from noise and background and so forth. And we search for vectors $\mathbf{a}$ and $\mathbf{b}$ which minimize the squared norm:

$$N = \|\mathbf{G}\mathbf{a} - \mathbf{F}\mathbf{b}\|^{2} = \mathbf{a}^{T}\mathbf{G}^{T}\mathbf{G}\mathbf{a} + \mathbf{b}^{T}\mathbf{F}^{T}\mathbf{F}\mathbf{b} - 2\mathbf{a}^{T}\mathbf{G}^{T}\mathbf{F}\mathbf{b}. \tag{3}$$

Since $\mathbf{G}^{T}\mathbf{G} = \mathbf{I}m_1$ and $\mathbf{F}^{T}\mathbf{F} = \mathbf{I}m_2$ (unit matrices of dimension $m_1 \times m_1$, and $m_2 \times m_2$, resp.), we obtain

$$N = 2 - 2\mathbf{a}^{T}\mathbf{G}^{T}\mathbf{F}\mathbf{b}. \tag{4}$$

Here, if $\mathbf{a}$ and $\mathbf{b}$ are the left and right singular vectors, respectively, associated with the first largest singular value d_1 of the matrix $\mathbf{G}^{T}\mathbf{F}$ inserting this result in (3), we again obtain

$$N = 2\left(1 - d_1\right). \tag{5}$$

The singular values d_i of the matrix $\mathbf{G}^{T}\mathbf{F}$ are in the range $0 \le d_i \le 1$, and the larger the value of d_1 is, the closer

the agreement between **Ga** and **Fb** is. Thus, it makes a spectrum control possible that only vector **v** is common for the left and right two windows. Therefore, one can directly obtain component spectra. If all the pure spectra are available, the concentration profiles could be achieved by using prior information of spectra and linear regression:

$$\mathbf{C} = \mathbf{XS}\left(\mathbf{S}^T\mathbf{S}\right)^{-1}. \quad (6)$$

It is worth noting that if there is no common vector the largest singular value d_1 will be significantly less than 1. On the other hand, if there are two or more common vectors, the second singular value d_2, even the third one, or more will also be close to 1. In both cases, one lacks information for the unique identification of the spectral vector **v**.

2.2. Orthogonal Projection Resolution (OPR). Because it has been described in detail in the literature [14], a brief depiction of orthogonal projection resolution was given as follows.

The orthogonal projection matrix $\mathbf{P}_i$ on to the complementary subspace X_i^T is defined as:

$$\mathbf{P}_i = I - \mathbf{X}_i^T\left(\mathrm{X}_i^T\right)^+, \quad (7)$$

where the superscript + denotes the Moore-Penrose pseudoinverse and **I** designates the identity matrix. X_i^T represents different submatrices, which are a series of fixed size window matrices moving along the chromatographic direction.

Assume that the subspace spanned by the mixture spectra in X_i^T is **M**. The residue vector $\mathbf{r}_i$ is given by

$$\mathbf{r}_i = \mathbf{P}_i\mathbf{v}_a, \quad (8)$$

where $\mathbf{v}_a$ denotes the spectrum of certain component that is resolved by the SFA and $\mathbf{r}_i$ is the projection of $\mathbf{v}_a$ on the orthogonal complementary subspace of **M**. Therefore, one has the length of the residue vector:

$$\mathrm{re}_i = \left\|\mathbf{r}_i\right\|^2 \quad (i = 1, 2, \ldots, m - w + 1), \quad (9)$$

where $\|\mathbf{r}_i\|$ designates the Euclidean norm of the vector, m is the number of measured chromatographic points, and w is the size of window.

Plotting the valve of re_i versus the index i, one can obtain a graph. Here we call it spectrum projection graph, which can tell us whether the component is present or absent and where the component elutes. Suppose that the submatrix $\mathbf{X}_i$ contains component a. Then the spectrum of component a is in the subspace **M** spanned by the mixture spectra in X_i^T; hence the length of the residue vector will be close to zero. Otherwise, if the component a is not in the submatrix X_i^T, then re_i will have a relatively large valve.

3. Experimental

3.1. Instruments. GC-MS was performed with Shimadzu GCMS-QP2010 instrument. The volatile constituents in both the main root and leaf of *Agrimonia eupatoria* were separated on a 30 m × 0.25 mm I.D. fused silica capillary column coated with 0.25 μm film OV-1.

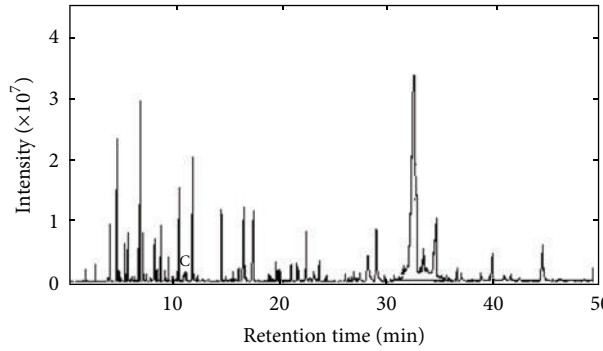

Figure 1: The chromatograms of the volatile components in main root of *Agrimonia eupatoria*.

3.2. Materials and Regents. The main root and leaf of *Agrimonia eupatoria* were obtained from a Zhejiang herbs nursery and were identified by a researcher from Institute of Materia Medica, Hunan Academy of Traditional Chinese Medicine and Materia Medica. Ether and anhydrous sodium sulfate were of analytical grade.

3.3. Extraction of the Volatile Components. The main root and leaf of *Agrimonia eupatoria* were dried at 40°C for about 40 min. Some 400 g dried *Agrimonia eupatoria* and 1200 mL distilled water were premixed, then placing them into a standard extractor. The mixture was allowed to stand for 30 min at room temperature before extracting the essential oil. Essential oil was obtained by the standard extracting method for essential oil in TCMs according to the Chinese Pharmacopoeia [19]. Effluent was extracted with ether, and the ether was removed by blowing with nitrogen under low temperature. The obtained essential oils were dried with anhydrous sodium sulfate and stored in the refrigerator at 4°C prior to analysis.

3.4. Detection of Essential Oil. GC-MS was used to obtain chromatograms of essential oils. The oven was held at 70°C for 1 min during injection, then temperature programmed at 3°C min^{-1} to a final temperature of 210°C, and held for 5 min. Inlet temperature was kept at 270°C all the time. 1.0 μL volume of essential oil was injected into the GC. Helium carrier gas at a constant flow-rate of 1.0 mL·min^{-1} and a 5 : 1 split ratio were used simultaneously. Mass spectrometer was operated in full scan and electron impact (EI+) modes with an electron energy of 70 eV; interface temperature: 270°C; MS source temperature: 230°C; MS quadrupole temperature: 160°C. In the range of m/z 30 to 500, mass spectra were recorded with 3.12 s·scan^{-1} velocity.

3.5. Data Analysis. Data analysis was performed on a Pentium based IBM compatible personal computer. All programs of the chemometrical resolution methods were coded in MATLAB 6.5 for windows. The library searches and spectral matching of the resolved pure components were conducted on the National Institute of Standards and Technology (NIST) MS database containing about 107000 compounds.

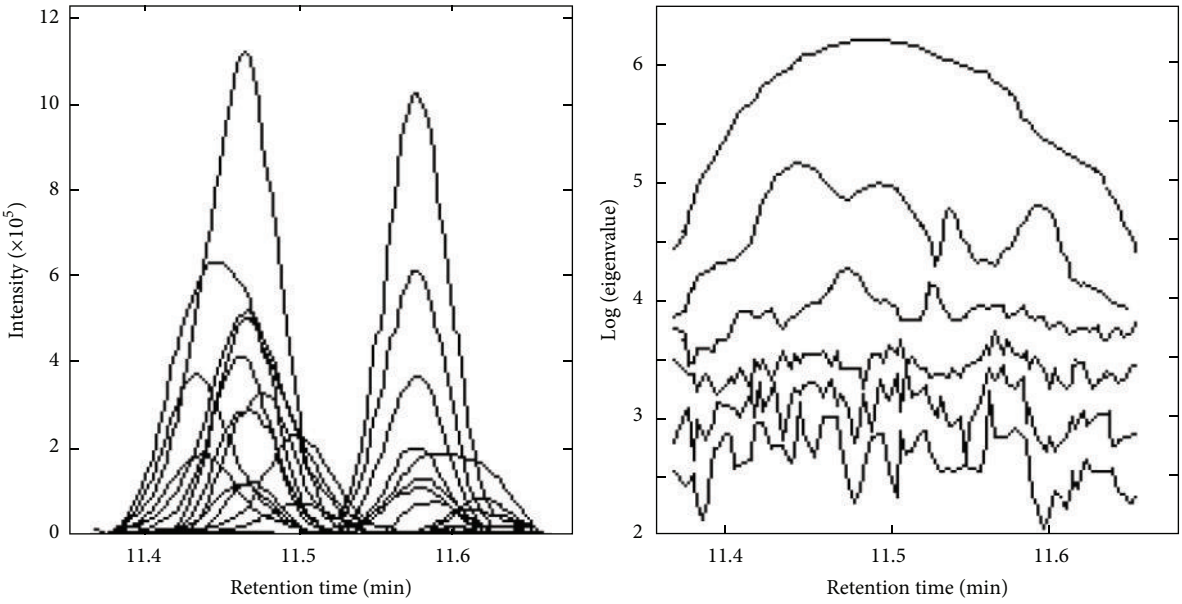

Figure 2: The total ion chromatogram (TIC) of the peak cluster C (a) and its rank map.

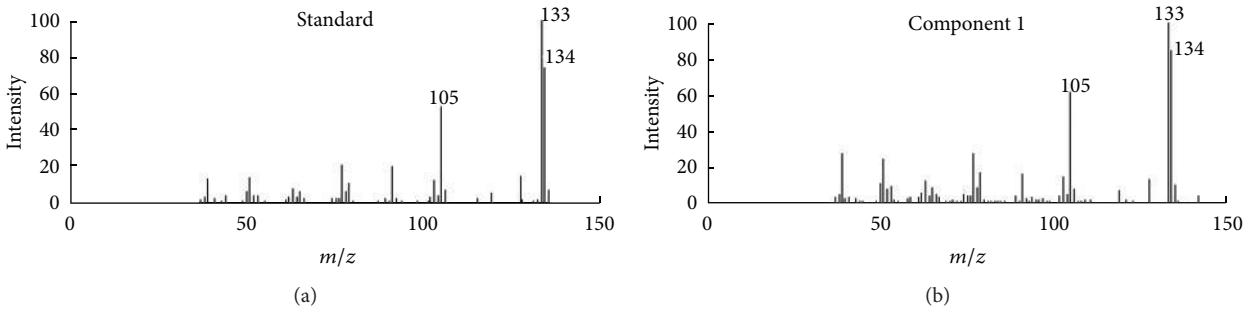

Figure 3: Resolved mass spectrum of component 1 by SFA and standard mass spectrum of 3,4-dimethylbenzaldehyde.

4. Results and Discussion

4.1. Resolution of the Overlapping Peaks. The total ionic current (TIC) chromatogram of the volatile components in main root of *Agrimonia eupatoria* was shown in Figure 1 (its data matrix was denoted as $\mathbf{X}_1$). The intensities of the peaks recorded vary greatly. Although many chromatographic peaks are separated, here still some of eluted components overlapped, and the concentrations of some volatile components were very low. If directly searched in the NIST mass database, incorrect identification of compounds may be obtained. There were two reasons for this. First, if the chromatographic peaks were directly searched with the NIST MS database, the similarity indices (SIs) for many of these compounds were quite low. Sometimes the same component was searched at different retention time. Another reason, since peaks associated with column background and residual gases existed unavoidably in two-dimensional data obtained by mass spectral measurement, the component with low concentration was very difficult to be identified directly with the NIST mass database. However, if these overlapped peaks and the components with low content were resolved into pure spectra and chromatograms, the identification of components can be improved to a reliable extent.

The matrix ($\mathbf{X}_1$) was divided into many submatrix. The chromatographic segment $\mathbf{X}$ within 11.36–11.70 min, named peak cluster C, was taken as an example. The whole procedure of this approach was demonstrated as follows.

Figure 2(a) was an original chromatogram from 11.36 min to 11.70 min (peak cluster C). Intuitively there were two chemical components in this overlapping peak. However, it was impossible to get the correct qualitative and accurate quantitative results if this overlapping peak was identified directly with automatic integration and mass similarity matching provided by GC-MS workstation. The quantitative analysis of this peak cluster was also impossible, because the area of each component cannot be obtained. Here, SFA [13] was used to resolve this overlapped peak with high efficiency and accepted accuracy.

First, fix-sized moving window evolving factor analysis (FSMWEFA) was used to obtain the rank map after background correction with PCA [11]. The eluting sequences of

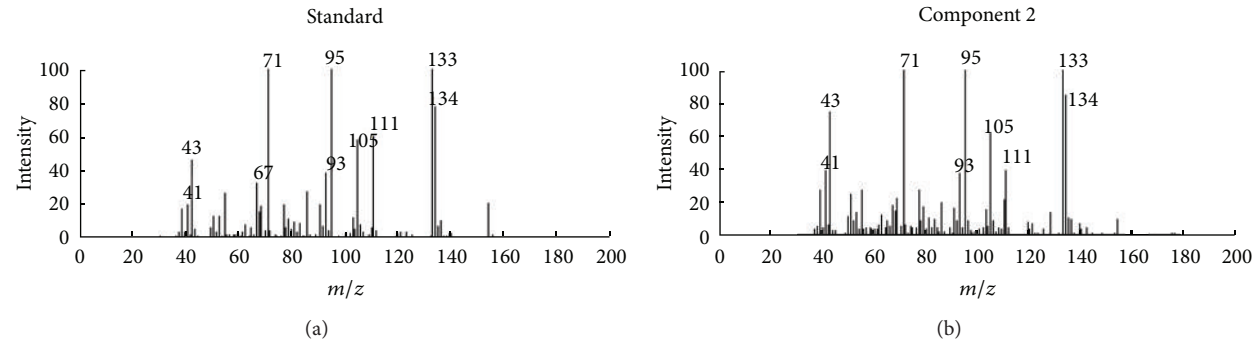

Figure 4: Resolved mass spectrum of component 2 by SFA and standard mass spectrum of 2,4-dimethylbenzaldehyde.

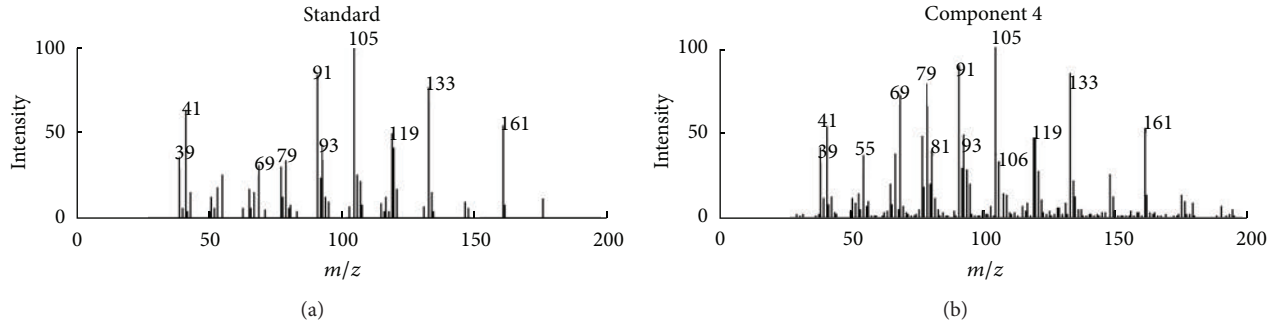

Figure 5: Resolved mass spectrum of component 4 by SFA and standard mass spectrum of 2-cyclopropylidene-1,7,7-trimethyl-bicyolo[2,2,1] heptane.

individual components can be seen from the rank map, which was shown in Figure 2(b). A clear insight into peak cluster C was shown in the rank map. Then, the number of pure components hidden in the peak cluster and the eluting information of each component can be obtained. Determination of both left and right subwindows of each component for the use of SFA also became clear with the information mentioned above. Then, the pure spectrum of each component can be extracted by SFA directly by analyzing the correlation of two subwindows without previous resolution of their concentration profiles. The corresponding extracted mass spectrum of components 1, 2, and 4 was shown in Figures 3, 4, and 5, respectively. After all the pure spectra had been obtained, the concentration profiles could be generated by using prior information of spectra and linear regression: $\mathbf{C} = \mathbf{XS}\ (\mathbf{S}^T\mathbf{S})^{-1}$ (see (6) in Section 2.1), which were shown in Figure 6.

4.2. Qualitative Analysis. Identification of the components in cluster C can be conducted by similarity searches in the NIST mass database and verified with retention indices, when each pure spectrum in cluster C was extracted and the resolved chromatographic profiles of these five components were obtained with SFA. Components 1, 2, and 4 may be 3,4-dimethylbenzaldehyde, 2,4-dimethylbenzaldehyde, and 2-cyclopropylidene-1,7,7-trimethyl-bicyolo[2,2,1] heptane, with the respective match values of 0.947, 0.967, and 0.954 (see Figures 3, 4, and 5, resp.). The match values of 0.73 and 0.68

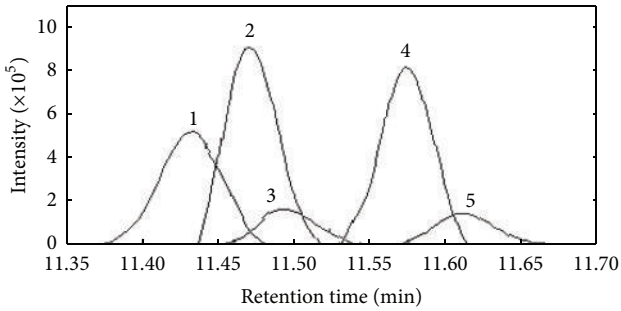

Figure 6: The resolved chromatogram of cluster C.

for components 3 and 5, respectively, were too low for reliable identification of their chemical nature.

In the same way, the spectrum of each component in other segments can be obtained. Then, the corresponding identification of all the volatile components in main root of *Agrimonia eupatoria* was acquired. The qualitative results were listed in Table 1. 68 of 87 separated constituents in the total ion chromatogram of the volatile components in main root of *Agrimonia eupatoria* were identified. Comparing the obtained result with those of the literature [9, 10], this combined approach was more reliable and more components were identified satisfactorily.

4.3. Quantitative Analysis. Quantitative analysis was performed with the overall volume of two-way response of each

Table 1: Identification and quantification of the volatile chemical constituents in main root and leaf of *Agrimonia eupatoria*.

Series no.	Retention time (min)		Compound name	Molecule structure	Relative content (%)
	$\mathbf{X}_1$ [a]	$\mathbf{X}_2$ [b]			
1	4.639	4.612	α-Pinene	$C_{10}H_{16}$	8.31
2	4.853	—	Hexanal	$C_6H_{12}O$	0.05
3	5.172	5.123	β-Pinene	$C_{10}H_{16}$	1.27
4	5.368	5.322	Camphene	$C_{10}H_{16}$	3.21
5	5.714	5.692	3-Octanol	$C_{10}H_{18}O$	0.27
6	6.032	5.971	Cymene	$C_{10}H_{14}$	0.18
7	6.354	6.289	D-Limonene	$C_{10}H_{16}$	1.29
8	6.632	6.617	Eucalyptol	$C_{10}H_{18}O$	3.26
9	7.290	7.195	α-trans-Ocimene	$C_{10}H_{16}$	0.51
10	7.572	7.547	Linalool	$C_{10}H_{18}O$	5.72
11	8.157	8.093	α-Campholenal	$C_{10}H_{16}O$	0.72
12	8.682	8.631	L-Camphor	$C_{10}H_{16}O$	2.11
13	9.104	—	Borneol	$C_{10}H_{18}O$	0.07
14	10.241	10.196	4-Terpineol	$C_{10}H_{18}O$	1.47
15	10.473	10.432	α-Terpineol	$C_{10}H_{18}O$	4.21
16	10.761	—	p-Menth-1-en-4-ol	$C_{10}H_{18}O$	0.06
17	10.941	10.906	Pulegone	$C_{10}H_{16}O$	0.17
18	11.417	—	3,4-Dimethylbenzaldehyde	$C_9H_{10}O$	0.41
19	11.472	11.427	2,4-Dimethylbenzaldehyde	$C_9H_{10}O$	0.72
20	11.576	11.512	2-Cyclopropylidene-1,7,7-trimethyl-bicyolo [2,2,1]heptane	$C_{13}H_{20}$	0.52
21	11.712	11.621	1-(2-Furyl)-1-hexanone	$C_{10}H_{14}O_2$	4.87
22	11.801	11.762	Bergamot oil	$C_{12}H_{20}O_2$	1.42
23	12.129	—	Nonanoic acid	$C_9H_{18}O_2$	0.06
24	12.374	12.327	2-Methyl-4-hydroxyacetophenone	$C_9H_{20}O_2$	0.10
25	12.871	12.821	Thymol	$C_{10}H_{14}O$	0.82
26	12.902	—	Carvacrol	$C_{10}H_{14}O$	0.44
27	13.914	13.865	Anethole	$C_{10}H_{12}O$	0.07
28	14.265	14.211	Bornyl acetate	$C_{12}H_{20}O_2$	3.72
29	14.794	14.738	Neryl acetate	$C_{12}H_{20}O_2$	0.47
30	14.917	14.872	Geraniol acetate	$C_{12}H_{20}O_2$	0.61
31	15.504	—	Furan,2,5-dibutyl-	$C_{12}H_{20}O$	0.04
32	15.765	15.718	Decanoic acid	$C_{10}H_{20}O_2$	0.06
33	16.020	15.951	Eugenol methyl ether	$C_{11}H_{14}O_2$	0.52
34	16.812	16.762	α-Cedrene	$C_{15}H_{24}$	2.87
35	17.059	17.012	α-Longipinene	$C_{15}H_{24}$	1.42
36	17.215	17.153	Caryophyllene	$C_{15}H_{24}$	0.81
37	17.475	—	β-Cedrene	$C_{15}H_{24}$	0.14
38	18.176	18.093	Geranyl acetone	$C_{13}H_{22}O$	0.84
39	19.721	—	Copaene	$C_{15}H_{24}$	0.05
40	20.305	20.242	Longofolene	$C_{15}H_{24}$	0.11
41	20.437	20.381	Aromadendrene	$C_{15}H_{24}$	0.42
42	21.530	21.477	Curcumene	$C_{15}H_{22}$	0.72
43	21.875	21.813	β-Selinene	$C_{15}H_{24}$	0.92
44	22.041	21.872	α-Selinene	$C_{15}H_{24}$	0.47
45	23.057	22.971	δ-Guaiene	$C_{15}H_{24}$	0.61
46	23.285	—	α-Himachalene	$C_{15}H_{24}$	0.13
47	24.561	24.510	α-Bisabolene	$C_{15}H_{24}$	0.42
48	25.527	—	Acoradiene	$C_{15}H_{24}$	0.23
49	25.673	25.615	τ-Cadinene	$C_{15}H_{24}$	0.43
50	25.858	25.792	Cuparene	$C_{15}H_{24}$	0.37

Table 1: Continued.

Series no.	Retention time (min)		Compound name	Molecule structure	Relative content (%)
	$\mathbf{X}_1$ [a]	$\mathbf{X}_2$ [b]			
51	26.006	25.921	Myristicin	$C_{11}H_{12}O_3$	0.45
52	26.821	—	α-Guaiene	$C_{15}H_{24}$	0.09
53	27.210	27.115	trans-Nerolidol	$C_{15}H_{26}O$	0.22
54	27.708	27.647	e-Cadinene	$C_{15}H_{24}$	0.92
55	28.419	—	Caryophyllene oxide	$C_{15}H_{24}O$	0.58
56	29.275	17.292	δ-Cadinene	$C_{15}H_{24}$	1.53
57	31.510	31.432	Cedrol	$C_{15}H_{26}O$	14.37
58	31.576	31.425	epi-Cedrol	$C_{15}H_{26}O$	1.15
59	32.470	—	Muurolol	$C_{15}H_{26}O$	0.46
60	33.132	33.040	α-Cadinol	$C_{15}H_{26}O$	1.43
61	33.674	33.592	Patchoulol	$C_{15}H_{26}O$	2.17
62	34.342	—	Epiglobulol	$C_{15}H_{26}O$	0.08
63	35.027	34.631	Cubenol	$C_{15}H_{26}O$	0.72
64	37.167	37.102	Cedryl acetate	$C_{17}H_{28}O_2$	0.76
65	39.492	39.422	Torreyol	$C_{15}H_{26}O$	0.38
66	39.861	39.784	Farnesyl acetate	$C_{17}H_{28}O_2$	1.73
67	41.216	—	α-Eudesmol	$C_{15}H_{26}O$	0.06
68	44.875	44.793	6,10,14-Trimethyl-2-pentadecanone	$C_{18}H_{36}O$	1.24

[a]Representing the main root of *Agrimonia eupatoria.*
[b]Representing the leaf of *Agrimonia eupatoria.*
—: correlative component is not found in $\mathbf{X}_2$.

component and normalization method. After all the pure chromatographic profile and mass spectrum of each component in main root of *Agrimonia eupatoria* were resolved, the total two-way response of each component can be obtained from the outer product of the concentration vector and the spectrum vector for each component, namely, $\mathbf{C}_i\mathbf{S}_i^T$. Similar to the general chromatographic quantitative method with peak area or height, the concentration of each component is proportional to the overall volume of its two-way response ($\mathbf{C}_i\mathbf{S}_i^T$). The identified components amounted quantitatively to 87.03% of the total content. The final relative quantitative results were also listed in Table 1.

4.4. Analysis of Correlative Components. Traditional Chinese medicines (TCM) usually are very complex system. Differences maybe exist in the same Chinese herb from different areas, or different growing seasons, different plant parts of the same herb. Thus, it is very important to develop a reliable approach to analyze them. The volatile components in leaf of *Agrimonia eupatoria* have also been investigated under the same experimental conditions. Curve 1 and curve 2 in Figure 7 were the TIC chromatograms of response $\mathbf{X}_1$ from main root and $\mathbf{X}_2$ from leaf obtained from GC-MS, respectively. It was shown from Figure 7 that $\mathbf{X}_2$ was consistent in eluting components with $\mathbf{X}_1$, but the concentration distribution of some individuals was a little different. Generally, one may analyze each component in leaf of *Agrimonia eupatoria* one by one with relevant resolution method and similarity search in MS library mentioned above. However it was time-consuming to do this. The obtained information of $\mathbf{X}_1$ may help to reduce some arduous and unnecessary work when we compare the quality of main root and leaf of *Agrimonia eupatoria*.

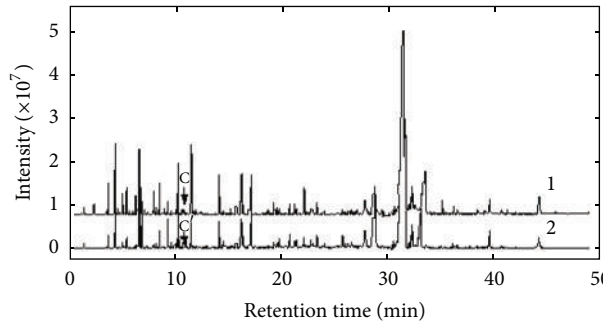

Figure 7: The chromatograms of the volatile components in the main root (curve 1) and leaf (curve 2) of *Agrimonia eupatoria*.

Here, orthogonal projection resolution (OPR) [14] was adopted to identify each correlative component directly instead of resolving each sample data one by one with the pure component spectra in $\mathbf{X}_1$ resolved by SFA projecting onto sample $\mathbf{X}_2$.

The chromatographic segment submatrix $\mathbf{X}$ from $\mathbf{X}_1$ within 11.36–11.70 min, named peak cluster C, was also used to show the procedure. As showed in Section 4.1, five components existed in it, and the pure spectrum of each component in it has been extracted with SFA. Because the retention time drift was not severe, the submatrix $\mathbf{X}'$ of $\mathbf{X}_2$, named peak cluster C′, can be selected from 11.00 to 12.20 min. Then the pure spectrum v_1 and v_4 of components

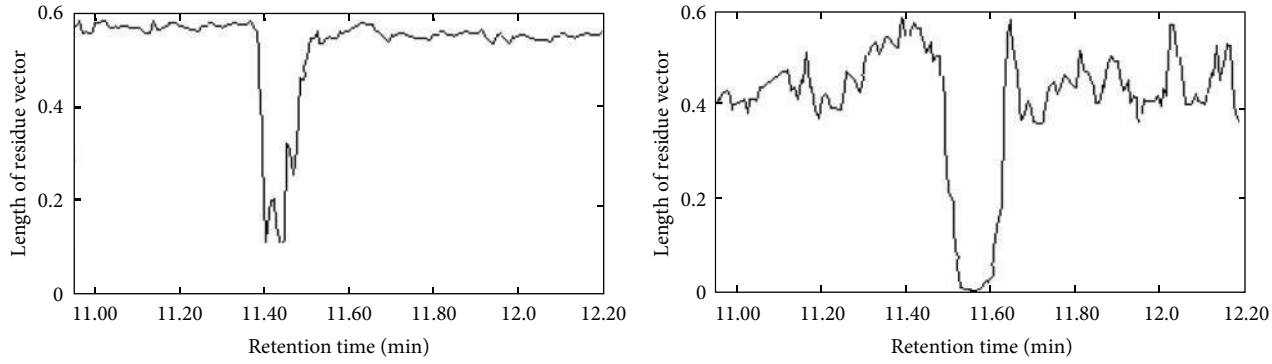

Figure 8: Spectrum projection graphs of component 1 (a) and 4 (b).

Table 2: Qualitative results of some other volatile chemical constituents in leaf of *Agrimonia eupatoria*.

Series no.	Retention time (min)	Compound name	Molecule structure
1	4.812	Prenal	C_5H_8O
2	6.359	1-Hexanol	$C_6H_{14}O$
3	10.717	Isomenthone	$C_{10}H_{18}O$
4	11.397	Carvone	$C_{10}H_{14}O$
5	12.105	Phenmethyl acetate	$C_9H_{10}O_2$
6	12.912	4-Hydroxy-3-methylacetophenon	$C_9H_{10}O_2$
7	14.493	4,4-Dimethyladamantan-2-ol	$C_{12}H_{20}O$
8	17.421	Germacrene D	$C_{15}H_{24}$
9	19.172	β-Damascone	$C_{13}H_{18}O$
10	25.310	Cadala-1(10),3,8-triene	$C_{15}H_{22}$
11	28.312	Longipinocarvone	$C_{15}H_{28}O$
12	32.413	Costunolide	$C_{15}H_{20}O_2$
13	34.172	cis-7-Tetradecen-1-ol	$C_{14}H_{28}O$
14	34.247	Hexahydrofarnesyl acetone	$C_{18}H_{36}O$

1 (3,4-dimethylbenzaldehyde) and 4 (2-cyclopropylidene-1,7,7-trimethyl-bicylo[2,2,1] heptane) were orthogonal projected to $\mathbf{X}'$. The spectrum projection graph was shown in Figure 8. It can be seen from Figure 8 that there was a range in which the length of the residue vector was close to zero to component 4. Considering the value of re_i was quite close to 0 and due to errors and interference from noise and background and so forth, in actual systems, component 2-cyclopropylidene-1,7,7-trimethyl-bicyolo[2,2,1] heptane was determined to also exist in the studied leaf of *Agrimonia eupatoria*. However, to component 1 there was not a range in which the length of the residue vector was close to zero and one can determine that component 3,4-dimethylbenzaldehyde did not exist in the studied leaf sample. Similar to this way, other correlative components, which coexisted in main root and leaf of *Agrimonia eupatoria*, could be obtained. The results were also listed in Table 1. In total, there were 52 components common to two different plant parts of *Agrimonia eupatoria*. However, because of the very low signal-to-noise ratio, some of the components may have gone undetected.

To those constituents not to be common components in the studied leaf of *Agrimonia eupatoria*, the performed procedure for main root of *Agrimonia eupatoria* was also used to extract pure spectrum of each component as described in Section 4.1. Accordingly, identification of these components were performed as in Section 4.2. Thirty components in essential oil of the studied leaf sample, which were not found in main root of *Agrimonia eupatoria* sample, were identified with SFA. The results were listed in Table 2.

4.5. Comparison of Samples. As shown in Tables 1 and 2, 68 and 65 volatile constituents in the main root and leaf of *Agrimonia eupatoria* were identified, respectively. Among the identified components, there were 52 common components existing in the two studied samples, but the content of each component in leaf is lower than that in main root. The main components in both main root and leaf of *Agrimonia eupatoria* were cedrol, α-pinene, linalool, α-terpineol, α-eudesmol, eucalyptol, and so on. The results indicated that both main root and leaf of *Agrimonia eupatoria* were consistent to some extent. By the use of similarity assessment soft, a pattern recognition program recommend by the Chinese Pharmacopoeial committee [20], the common pattern of two specimens can be constructed. The similarity of $\mathbf{X}_1$ and

$\mathbf{X}_2$ to their common chromatogram was 0.9462 and 0.9417, respectively. Obviously the similarity was relatively high, but some differences also existed between them. However, components not common to both parts were generally low in abundance. The difference reflects the discrepancy between the main root and leaf of *Agrimonia eupatoria*.

5. Conclusions

Combined chemometric methods were first used to analyze the volatile components in main root and leaf of *Agrimonia eupatoria*. After extraction with water distillation method, the volatile components in *Agrimonia eupatoria* were detected by GC-MS. The pure spectrum of each volatile component in main root of *Agrimonia eupatoria* was extracted with SFA. Then, OPR was used to obtain the correlative components from leaf sample. This study shows that the application of combined approach is a powerful tool, which does aim at comprehensivly revealing the quality and quantity of chemical constituents of *Agrimonia eupatoria* samples from different plant parts. The obtained information can be used for effective evaluation of similarity or differences of analytical samples. This developed method can also be used for quality control of *Agrimonia eupatoria* samples.

Acknowledgments

This research work was financially supported by Province Natural Science Foundation of Zhejiang of P.R China (Grant no. Y4110075) and Zhejiang Qianjiang Talent Project (Grant no. 2010R10054). The research work was also financially supported by Welfare Technology Research Project of Zhejiang of P.R China (Grant no. 2013C31124) and Quzhou Technology Projects (Grant no. 2013Y003).

References

[1] F. Lu, X. Y. Ba, and Y. Z. He, "Chemical constituents of Agrimoniae Herba," *Chinese Traditional and Herbal Drugs*, vol. 43, no. 5, pp. 851–855, 2012.

[2] J. J. Kim, J. Jiang, D. W. Shim et al., "Anti-inflammatory and anti-allergic effects of *Agrimonia pilosa* Ledeb extract on murine cell lines and OVA-induced airway inflammation," *Journal of Ethnopharmacology*, vol. 140, no. 2, pp. 213–221, 2012.

[3] H. A. Ali, N. H. A. Orooba, and W. A. S. Khulood, "Cytotoxic effects of *Agrimonia eupatoria* L. against cancer cell lines *in vitro*," *Journal of the Association of Arab Universities for Basic and Applied Sciences*, 2013.

[4] W. L. Li, H. C. Zheng, J. Bukuru, and N. De Kimpe, "Natural medicines used in the traditional Chinese medical system for therapy of diabetes mellitus," *Journal of Ethnopharmacology*, vol. 92, no. 1, pp. 1–21, 2004.

[5] K. Zhang, L. Dai, and Z. R. Zheng, "Isolation and characterization of an acidic polysaccharide from *Agrimonia Pilosa* Ledeb," *Chinese Journal of Biochemical Pharmaceutics*, vol. 29, no. 3, pp. 171–174, 2008.

[6] Z. J. Jin, "The chemical composition and clinical research progress of *Agrimonia eupatoria*," *West China Journal of Pharmaceutical Sciences*, vol. 21, no. 5, pp. 468–472, 2006.

[7] Y. Pan, H. Liu, Y. Zhuang, L. Ding, L. Chen, and F. Qiu, "Studies on isolation and identification of flavonoids in herbs of *Agrimonia Pilosa*," *Zhongguo Zhongyao Zazhi*, vol. 33, no. 24, pp. 2925–2928, 2008.

[8] X. Y. Ba, Y. Z. He, F. Lu, and L. L. Shi, "Research progress of *Agrimonia Pilosa* Ledeb," *Journal of Liaoning University of Traditional Chinese Medicine*, vol. 13, no. 5, pp. 258–260, 2011.

[9] Y. Zhao, P.-Y. Li, and J.-P. Liu, "Studies on chemical constituents of essential oil from Hainyvein *Agrimonia Pilosa*," *Chinese Pharmaceutical Journal*, vol. 36, no. 10, pp. 672–673, 2001.

[10] Y. H. Pei, X. Li, and T. R. Zhu, "Studies on the chemical constituents from the root-sprouts of *Agrimonia Pilosa* Ledeb," *Acta Pharmaceutica Sinica*, vol. 24, no. 6, pp. 431–437, 1989.

[11] H. L. Shen, R. Manne, Q. S. Xu, D. Chen, and Y. Liang, "Local resolution of hyphenated chromatographic data," *Chemometrics and Intelligent Laboratory Systems*, vol. 45, no. 1-2, pp. 323–328, 1999.

[12] C. J. Xu, J. H. Jiang, and Y. Z. Liang, "Evolving window orthogonal projections method for two-way data resolution," *Analyst*, vol. 124, no. 10, pp. 1471–1476, 1999.

[13] R. Manne, H. L. Shen, and Y. Z. Liang, "Subwindow factor analysis," *Chemometrics and Intelligent Laboratory Systems*, vol. 45, no. 1-2, pp. 171–176, 1999.

[14] F. C. Sánchez, S. C. Rutan, M. D. G. García, and D. L. Massart, "Resolution of multicomponent overlapped peaks by the orthogonal projection approach, evolving factor analysis and window factor analysis," *Chemometrics and Intelligent Laboratory Systems*, vol. 36, no. 2, pp. 153–164, 1997.

[15] B. Y. Li, Y. Hu, Y. Z. Liang, L. F. Huang, C. Xu, and P. Xie, "Spectral correlative chromatography and its application to analysis of chromatographic fingerprints of herbal medicines," *Journal of Separation Science*, vol. 27, no. 7-8, pp. 581–588, 2004.

[16] Y. Z. Liang, *White, Grey and Black Multicomponent Systems and Their Chemometric Algorithms*, Hunan Publishing House of Science and Technology, Changsha, China, 1996.

[17] F. Q. Guo, Y. Z. Liang, C. J. Xu, and L. F. Huang, "Determination of the volatile chemical constituents of Notoptergium incium by gas chromatography-mass spectrometry and iterative or non-iterative chemometrics resolution methods," *Journal of Chromatography A*, vol. 1016, no. 1, pp. 99–110, 2003.

[18] Y. M. Wang, L. Z. Yi, Y. Z. Liang et al., "Comparative analysis of essential oil components in Pericarpium Citri Reticulatae Viride and Pericarpium Citri Reticulatae by GC-MS combined with chemometric resolution method," *Journal of Pharmaceutical and Biomedical Analysis*, vol. 46, no. 1, pp. 66–74, 2008.

[19] Chinese Pharmacopoeia Committee, *Chinese Pharmacopoeia*, Appendix 62, Publishing House of People's Health, Beijing, China, 2000.

[20] P. Xie, S. Chen, Y. Liang, X. Wang, R. Tian, and R. Upton, "Chromatographic fingerprint analysis-a rational approach for quality assessment of traditional Chinese herbal medicine," *Journal of Chromatography A*, vol. 1112, no. 1-2, pp. 171–180, 2006.

Hindawi Publishing Corporation
Journal of Analytical Methods in Chemistry
Volume 2013, Article ID 710972, 7 pages
http://dx.doi.org/10.1155/2013/710972

Research Article

UPLC-TOF-MS Characterization and Identification of Bioactive Iridoids in *Cornus mas* Fruit

Shixin Deng, Brett J. West, and C. Jarakae Jensen

Research and Development Department, Morinda Inc., 737 East, 1180 South, American Fork, UT 84003, USA

Correspondence should be addressed to Shixin Deng; shixin_deng@morinda.com

Received 14 August 2013; Accepted 20 August 2013

Academic Editor: Shao-Nong Chen

Cornus mas L. is indigenous to Europe and parts of Asia. Although *Cornus* is widely considered to be an iridoid rich genera, only two iridoids have been previously found in this plant. The lack of information on taxonomically and biologically active iridoids prompted us to develop and optimize an analytical method for characterization of additional phytochemicals in *C. mas* fruit. An ultra performance liquid chromatography (UPLC) coupled with photodiode array spectrophotometry (PDA) and electrospray time-of-flight mass spectrometry (ESI-TOF-MS) was employed and mass parameters were optimized. Identification was made by elucidating the mass spectral data and further confirmed by comparing retention times and UV spectra of target peaks with those of reference compounds. Primary DNA damage and antigenotoxicity tests in *E. coli* PQ37 were used to screen the iridoids for biological activity. As a result, ten phytochemicals were identified, including iridoids loganic acid, loganin, sweroside, and cornuside. Nine of these were reported for the first time from *C. mas* fruit. The iridoids did not induce SOS repair of DNA, indicating a lack of genotoxic activity in *E. coli* PQ37. However, loganin, sweroside, and cornuside did reduce the amount of DNA damage caused by 4-nitroquinoline 1-oxide, suggesting potential antigenotoxic activity.

1. Introduction

Cornus mas L. is commonly known as European cornelian cherry and belongs to the Cornaceae family. It is a tall deciduous shrub or small tree (3–6 m in height) that is indigenous to Europe and parts of Asia [1, 2]. The fruit is edible but is astringent when unripe. Traditionally, *C. mas* has been used for improving health conditions, such as bowel complaints, fever, and diarrhea [3–6]. Fresh European cornelian cherry fruits are often processed to produce drinks, syrups, and jams [7, 8].

Some investigations of the nutritional and phytochemical properties of European cornelian cherry fruit have been reported previously. The fruit is reported to contain 0.1–0.3% fat, 0.4% protein, 21.7% carbohydrate, 0.8% ash, 0.5% dietary fiber, 6.6–15.1% total sugar (fructose 33.1–43.1%, glucose 53.6–63.1%), and 4.22–9.96% reducing sugars [3, 9]. The fruit has pH 2.7–3.2 and contains at least 15 amino acids, including aspartic acid, glutamic acid, serine, histidine, glycine, threonine, arginine, alanine, tyrosine, valine, phenylalanine, isoleucine, leucine, lysine, and proline [9]. Minerals in *C. mas* fruit include copper (1.2 to 8.1 mg/kg dry weight), iron, zinc, phosphorus, potassium, calcium, magnesium, and sulphur [9]. The vitamin C content of the fruit is reported to be 16.4 to 38.5 mg/100 g [9].

C. mas fruit has been found to contain a wide range of phytochemicals, including tannins (131.51–601.2 mg/L), phenolics (29.76–74.83 mg/g dry), organic acids (4.6–7.4%), anthocyanin, fatty acids, and flavonoids [3, 4, 10–16]. Anthocyanins seem to have been a popular subject of previous *C. mas* research. Anthocyanins have been found in the range of 1.12 to 2.92 mg/g in different *C. mas* fruit sources [14, 16, 17]. Two studies from Du and Francis reported the presence of five anthocyanins in the fruit, namely, delphinidin 3-galactoside, cyanidin 3-galactoside, cyanidin 3-rhamnosyl-galactoside, pelargonidin 3-galactoside, and pelargonidin 3-rhamnosylgalactoside [18, 19]. Cyanidin 3-glucoside, cyanidin 3-rutinoside, and pelargonidin 3-glucoside were identified by Tural and Koca [15], with pelargonidin 3-*O*-glucoside being the most abundant followed by cyanidin 3-*O*-β-D-galactoside. Pelargonidin 3-*O*-rutinoside was present only in trace amounts [17]. Delphinidin 3-*O*-β-galactopyranoside,

cyanidin 3-*O*-β-galactopyranoside, and pelargonidin 3-*O*-β-galactopyranoside were also identified in *C. mas* fruit [3].

Eight flavonoids have been previously isolated from the methanolic extract of *C. mas* fruit. These include aromadendrin 7-*O*-β-D-glucoside, quercetin 3-*O*-β-D-xyloside, quercetin 3-*O*-α-L-rhamnoside, quercetin 3-*O*-rutinoside, quercetin 3-*O*-β-D galactoside, quercetin 3-*O*-β-D-glucose, quercetin 3-*O*-β-D-glucoside, and kaempferol 3-*O*-galactoside [17]. Fatty acids identified in the fruit include lauric acid, myristic acid, pentadecenoic acid, palmitic acid, palmitoleic acid, stearic acid, oleic acid, vaccenic acid, linoleic acid, linolenic acid, and *cis*-10,12-octadecadienoic acid [9].

Cornus is widely considered to be an iridoid rich genera. However, there is very little information regarding the occurrence of iridoids in *C. mas*. Only two iridoids, secologanin and loganic acid, have been previously reported to occur in *C. mas*, with only one being reported for the fruit [20–22]. The current investigation was prompted by a lack of information on taxonomically critical and biologically active iridoids in *C. mas* fruit. The aim of this study is to identify more phytochemical compounds in the *C. mas* fruit, particularly bioactive iridoids, by using ultra performance liquid chromatography (UPLC) coupled with photodiode array spectrophotometry (PDA) and electrospray time-of-flight mass spectrometry (ESI-TOF-MS).

2. Materials and Methods

2.1. Chemicals and Standards. Optima acetonitrile (MeCN, lot no. 125783), methanol (MeOH, lot no. 124876), and formic acid of LC-MS grade were purchased from Fisher Scientific Co. (Fair Lawn, NJ, USA). Chromasolv® Water (H_2O, lot no. SHBB9224V) of LC-MS grade was purchased from Sigma-Aldrich (St. Louis, MO, USA). Tartaric acid, malic acid, chlorogenic acid, gallic acid, and rutin standards were purchased from Sigma-Aldrich (St. Louis, MO, USA). Citric acid was purchased from Fisher Scientific Co. Loganic acid was obtained from ChromaDex (Irvine, CA, USA). Loganin, sweroside, and cornuside were purchased from Chengdu Biopurify Phytochemicals Ltd (Sichuan, China). The purities of all standards were higher than 98%. The standards were accurately weighed and then dissolved in an appropriate volume of MeOH to produce corresponding stock standard solutions. Working standard solutions were prepared by diluting the stock solutions with MeOH at different concentrations. All stock and working solutions were maintained at 0°C in a freezer.

2.2. Sample Collection and Preparation. *C. mas* fruit samples were collected from wild trees in the mountains near Kastamonu, Turkey, in 2012. A voucher specimen is deposited in Research and Development Department laboratory of Morinda Inc. (American Fork, Utah, USA). The raw fruits were mashed into puree and the seeds were removed. One gram of mashed fruit puree was weighed accurately and 9 mL of 50% MeOH in H_2O was added. The mixture was sonicated for 30 minutes and then centrifuged. The supernatant was transferred into a volumetric flask and volume brought to 10 mL with 50% MeOH in H_2O. All samples were filtered through a nylon microfilter (0.45 μm pore size) before UPLC analysis.

2.3. Instrumentation and Chromatographic Conditions. Analyses were performed with an Agilent 1260 Infinity LC System coupled to an Agilent 6230 time-of-flight (TOF) LC/MS System (Agilent Technologies, Santa Clara, CA). The Agilent 1260 LC module was coupled with a photodiode array (PDA) detector and a 6230 time-of-flight MS detector, along with a binary solvent pump and an autosampler. Chromatographic separations were performed with an Atlantis reverse phase C18 column (4.6 mm × 250 mm; 5 μm, Waters Corporation, Milford, MA, USA). The pump was connected to a gradient binary solvent system: A, 0.1% formic acid in H_2O (v/v) and B, 0.1% formic acid in MeCN. The mobile phase was programmed consecutively in linear gradients as follows: 0–5 min, 98% A and 2% B; 40 min, 70% A and 30% B; 46–52 min, 2% A and 98% B; and 53–55 min, 98% A and 2% B. The ionization source was Agilent Jet Stream, with electrospray ionization (ESI) negative mode employed for acquisition of mass spectra. The elution was run at a flow rate of 0.8 mL/min. UV spectra were monitored in the range of 200 nm and 400 nm. Injection volume was 2 μL for each of the sample solutions, followed by needle wash. The column temperature was maintained at 40°C. Nitrogen, supplied by a nitrogen generator (model no. NM32LA, Peak Scientific Instruments Ltd, Scotland, UK), was used as the drying and nebulizer gas. Other MS instrumental conditions are summarized as follows: drying gas temperature and flow rate were 350°C and 11.0 L/min, respectively; nebulizer pressure was 50 psi; sheath gas temperature and flow rate were 350°C and 12.0 L/min, respectively; capillary, nozzle, and fragmentor voltages were 3500, 500, and 100 V, respectively; skimmer was 65.0; Oct 1 RF V_{pp} was 750. The instrument state was set to high resolution mode (4 GHz). Tuning and calibration were performed before sample runs. Data collection and integration were performed using MassHunter workstation software (version B.05.00). The data was collected in the range of 100 and 1700 m/z.

2.4. Accurate Mass Measurement. Data were stored in both centroid and profile formats during acquisition. Two independent reference lock-mass ions, purine (m/z 119.03632) and HP-0921 (m/z 966.000725), were employed to ensure mass accuracy and reproducibility.

2.5. Characterization of Phytochemicals. Identification of phytochemical compounds **1–10** was accomplished by elucidating mass spectral data. Compound identities were then confirmed by comparing the UPLC retention times and UV spectra of target peaks with those of reference compounds.

2.6. Primary DNA Damage Test in E. coli PQ37. The SOS chromotest in *E. coli* PQ37 was used to determine the potential for loganic acid, loganin, sweroside, and cornuside to induce primary DNA damage. This test was carried out according to a previously developed method [23]. *E. coli* PQ37

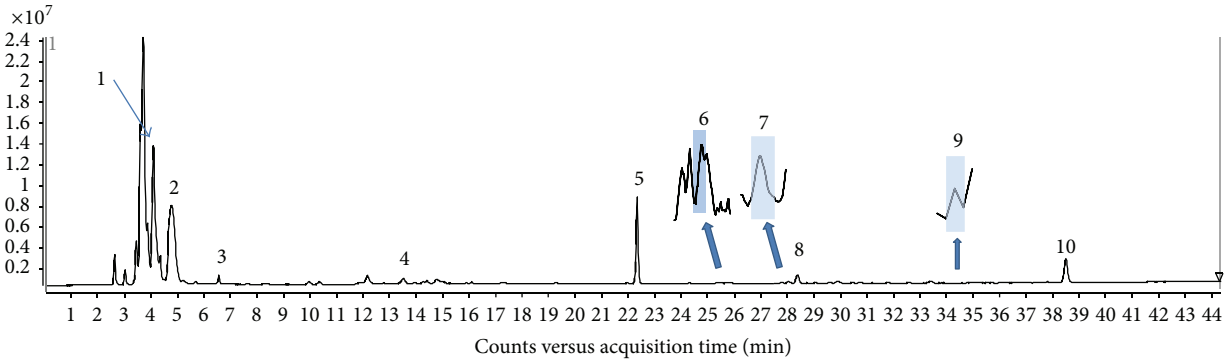

Figure 1: The typical total ion chromatogram (TIC) of *C. mas* fruit puree. Ionization source performed on Agilent Jet Stream TOF-MS with electrospray ionization (ESI) negative mode. (1) x-axis represents retention time and y-axis is intensity of m/z peaks. (2) Peaks 1–10 were identified as tartaric acid (**1**), malic acid (**2**), citric acid (**3**), gallic acid (**4**), chlorogenic acid (**6**), rutin (**9**), and four iridoids, loganic acid (**5**), loganin (**7**), sweroside (**8**), and cornuside (**10**). (3) Peaks 6, 7, and 9 were enlarged by zooming in.

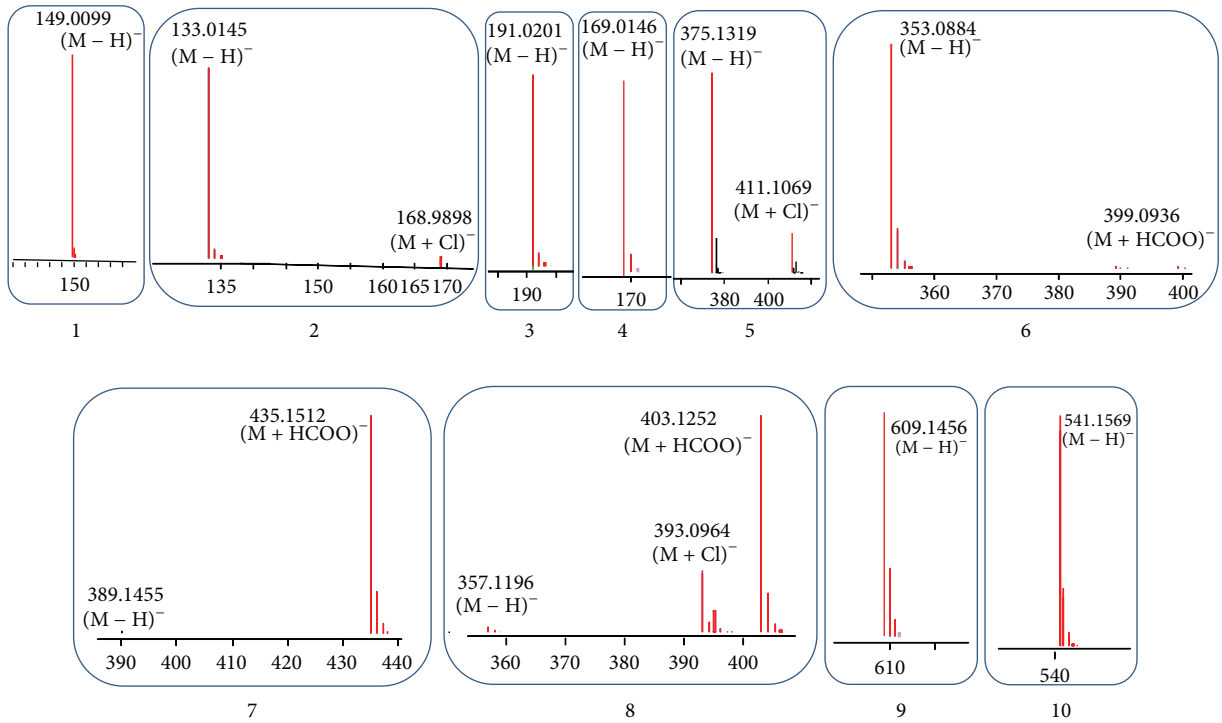

Figure 2: Accurate mass spectra (mass-to-charge, m/z), in ESI negative mode, of phytochemical peaks identified in *C. mas* fruit by Agilent TOF detector. (1) Numbers 1–10 represent peaks to be characterized, that is, tartaric acid (**1**), malic aicd (**2**), citric acid (**3**), gallic acid (**4**), chlorogenic acid (**6**), a flavonoid glycoside rutin (**9**), and four iridoids, loganic acid (**5**), loganin (**7**), sweroside (**8**), and cornuside (**10**). (2) Accurate mass-to-charge (m/z) is labeled on the top of each peak.

was incubated in LB medium in a 96-well plate at 37°C in the presence of the iridoids for 2 hours. The concentrations tested were 7.81, 15.6, 31.2, 62.5, 125, 250, 500, and 1000 μg mL^{-1}. Following incubation with replicate samples, 5-bromo-4-chloro-3-indolyl-β-D-galactopyranoside was added to the wells to detect β-galactosidase enzyme activity, which is induced during SOS repair of damaged DNA. Nitrophenyl phosphate is also added to the wells to measure alkaline phosphatase activity, an indicator of cell viability. The samples were again incubated and the absorbance of each sample, blanks, and controls was measured at 410 and 620 nm with a microplate reader. Vehicle blanks and positive controls, 1.25 μg mL^{-1} 4-nitroquinoline 1-oxide (4NQO), were included in this test. The induction factor of each material was calculated by dividing the absorbance of the sample at 620 nm by that of the blank, while also correcting for cell viability. Induction factors less than two indicate an absence of genotoxic activity.

2.7. Antigenotoxicity Test in E. coli PQ37. The primary DNA damage test was performed again, similar to the method

Table 1: Chromatographic and mass spectral data of phytochemical compounds identified in *C. mas* fruits.

Number	Name	Formula	RT	*m/z*	Mass		Score	Area
1	Tartaric acid	$C_4H_6O_6$	4.084	149.0099	150.0171	$[M-H]^-$	96.91	26316227
2	Malic acid	$C_4H_6O_5$	4.863	133.0145, 168.9898	134.0218	$[M-H]^-$ $[M+Cl]^-$	99.32	28327606
3	Citric acid	$C_6H_8O_7$	6.57	191.0201	192.0273	$[M-H]^-$	98.81	4041717
4	Gallic acid	$C_7H_6O_5$	13.529	169.0146	170.0219	$[M-H]^-$	85.94	4663081
5	Loganic acid	$C_{16}H_{24}O_{10}$	22.345	375.1319, 411.1069	376.1372	$[M-H]^-$ $[M+Cl]^-$	98.79	3904847
6	Chlorogenic acid	$C_{16}H_{18}O_9$	25.725	353.0884	354.0956	$[M-H]^-$	98.43	575436
7	Loganin	$C_{17}H_{26}O_{10}$	28.028	389.1455, 435.1512	390.153	$[M-H]^-$ $[M+HCOO]^-$	98.79	954718
8	Sweroside	$C_{16}H_{22}O_9$	28.393	357.1196, 393.0964, 403.1252	358.127	$[M-H]^-$ $[M+Cl]^-$ $[M+HCOO]^-$	98.84	3613261
9	Rutin	$C_{27}H_{30}O_{16}$	34.772	609.1456	610.1532	$[M-H]^-$	98.25	28498
10	Cornuside	$C_{24}H_{30}O_{14}$	38.501	541.1569	542.1641	$[M-H]^-$	93.36	17943814

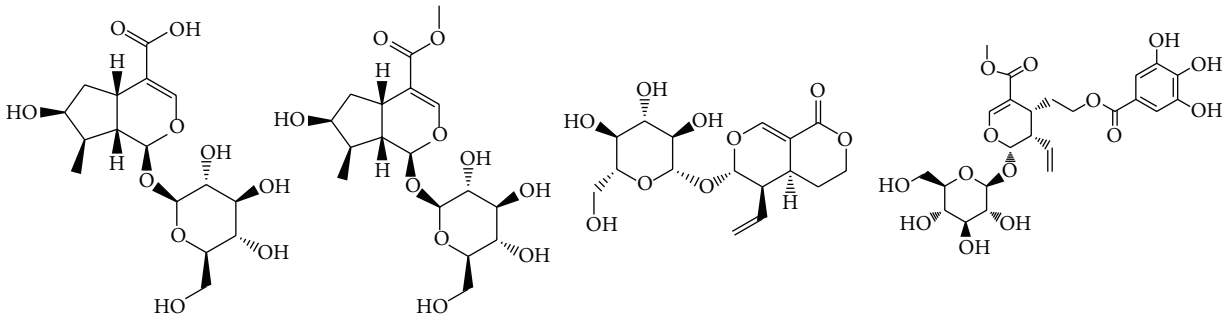

Loganic acid (**5**): $C_{16}H_{24}O_{10}$ Loganin (**7**): $C_{17}H_{26}O_{10}$ Sweroside (**8**): $C_{16}H_{22}O_9$ Cornuside (**10**): $C_{24}H_{30}O_{14}$

Figure 3: Chemical structures of iridoids identified in *C. mas* fruit by UPLC-TOF-MS.

described above. However, the method was modified to include incubation of *E. coli* PQ37 in the presence of 1.25 μg mL^{-1} 4NQO with 250 μg mL^{-1} loganic acid, loganin, sweroside, or cornuside. Induction factors were calculated in the same manner as described above. The percent reduction in genotoxicity was determined by dividing the difference between the induction factor of 4NQO and the blank (induction factor of 1) by the difference between the induction factor of 4NQO plus iridoid sample and the blank. Experiments were performed in triplicate.

3. Results and Discussion

Although the application of LC-MS may minimize the need for chromatographic separation, a good LC separation may prevent ion suppression and isobaric interferences in the MS analysis. The UPLC system delivered a more rapid and effective separation than HPLC, especially for the wide range of phytochemicals identified. UPLC also facilitated the simultaneous determination of the phytochemical matrix of our samples. The flow rate, solvent system, and column were optimized for the UPLC system relative to the analysis of phytochemicals in *C. mas* fruit samples. A moderate flow rate of 0.8 mL/min accommodated electrospray source, column separation and optimized sensitivity and resolution. Better peak shape and resolution for each target peaks, as well as optimal sensitivity for ion detection, were obtained by adding 0.1% formic acid. The column temperature was kept at 40°C to minimize column pressure due to flow rate. A gradient solvent system of MeCN-H_2O ensured complete separation of target peaks within a limited time frame. The UPLC system delivered good separation and eliminated the overlap of targeted phytochemical peaks.

The time-of-flight mass spectral detector is known for providing accurate and precise mass information. It can accurately measure mass values with a mass error less than 5 ppm. The generation of empirical formulae results in possible identification of phytochemicals by means of elemental composition analysis. Our experiments used electrospray ionization and were operated in negative mode as the interface since it generated higher signal information for the compounds with less interruption compared to positive mode. All other mass spectral parameters, including drying gas flow and temperature, nebulizer pressure, and sheath gas

Table 2: Primary DNA damage assay in *E. coli* PQ37.

Compound	Concentration (μg mL^{-1})	Induction factor (mean ± standard deviation)
Loganic acid	1000	1.095 ± 0.004
	500	1.080 ± 0.038
	250	0.994 ± 0.003
	125	1.058 ± 0.025
	62.5	1.006 ± 0.024
	31.2	1.027 ± 0.003
	15.6	1.012 ± 0.003
	7.81	0.965 ± 0.031
Loganin	1000	0.995 ± 0.044
	500	1.013 ± 0.029
	250	1.036 ± 0.018
	125	1.051 ± 0.038
	62.5	1.029 ± 0.001
	31.2	1.041 ± 0.001
	15.6	1.033 ± 0.006
	7.81	1.016 ± 0.036
Sweroside	1000	1.028 ± 0.008
	500	1.021 ± 0.005
	250	1.032 ± 0.008
	125	1.043 ± 0.013
	62.5	1.009 ± 0.042
	31.2	1.001 ± 0.010
	15.6	1.029 ± 0.017
	7.81	0.939 ± 0.022
Cornuside	1000	1.068 ± 0.015
	500	1.030 ± 0.018
	250	1.012 ± 0.000
	125	1.074 ± 0.040
	62.5	1.023 ± 0.030
	31.2	1.026 ± 0.016
	15.6	1.019 ± 0.029
	7.81	0.959 ± 0.019
4NQO	1.25	3.365 ± 0.516

Table 3: Antigenotoxicity test in *E. coli* PQ37.

Compound	Concentration (μg mL^{-1})	Induction factor (mean ± standard deviation)
4NQO	1.25	3.365 ± 0.516
4NQO + loganic acid	250*	3.278 ± 0.260
4NQO + loganin	250*	2.497 ± 0.821
4NQO + sweroside	250*	2.259 ± 0.325
4NQO + cornuside	250*	2.587 ± 0.199

*Iridoid concentration; 4NQO concentration is 1.25 μg mL^{-1}.

flow and temperature, were also optimized in order to achieve good sensitivity and resolution.

The total ion chromatogram (TIC) of *C. mas* fruit is shown in Figure 1. Negative ion electrospray LC-MS chromatograms of the fruit puree resulted in the identification of 10 peaks. Deprotonated molecular ions $[M-H]^-$, chlorinated ions $[M + Cl]^-$, and/or formic acid adducts $[M + HCOO]^-$ of the compounds were identified with the TOF detector. As a result, accurate molecular weights were determined. Since peaks 6, 7, and 9 were not clearly visible on the TIC chromatogram due to their low concentration, zoomed-in peaks are provided accordingly.

Accurate mass spectra (mass-to-charge, m/z) of the phytochemical peaks identified are shown in Figure 2. Peaks 1–4 were compounds that eluted early from the column. Peaks 1, 3, and 4 had deprotonated molecular ions $[M - H]^-$ with m/z values of 149.0099, 191.0201, and 169.0146, respectively, corresponding to the molecular formula of $C_4H_6O_6$, $C_6H_8O_7$, and $C_7H_6O_5$. Peak 2 had $[M - H]^-$ and $[M + Cl]^-$ with m/z values of 133.0145 and 168.9898, respectively, matching the molecular formula $C_4H_6O_5$. Compound 6 had $[M - H]^-$ and $[M + HCOO]^-$ at m/z 353.0884 and 399.0936, corresponding to $C_{16}H_{24}O_{10}$. Comparisons against reference compound retention revealed that peaks 1–4 and 6 were organic acids, namely, tartaric acid (**1**), malic acid (**2**), citric acid (**3**), gallic acid (**4**), and chlorogenic acid (**6**). By the same methods, peak 9 was determined to be rutin (**9**), a flavonoid glycoside.

Peak 5 is a major peak on the chromatogram, eluting at 22.345 min and displaying both $[M - H]^-$ and $[M + Cl]^-$ at m/z 375.1319 and 411.1069. Its molecular formula was determined to be $C_{16}H_{24}O_{10}$. Peak 7 showed $[M - H]^-$ and $[M + HCOO]^-$ at m/z 389.1455 and 435.1512. Peak 8 exhibited a deprotonated m/z, a chlorinated m/z, and a formic acid adduct of 357.1196, 393.0964, and 403.1252, respectively. Peak 10 had deprotonated ions with m/z value of 541.1569. By comparing these pieces of information with UV and mass spectra, as well as retention times of reference compounds, peaks 5, 7, 8, and 10 were identified as the iridoids loganic acid (**5**), loganin (**7**), sweroside (**8**), and cornuside (**10**). A summary of the chromatographic and mass spectral data of the phytochemical compounds identified in *C. mas* fruit is given in Table 1. Chemical structures of the iridoids in *C. mas* fruit are provided in Figure 3.

These iridoids have displayed many potential biological activities. Loganic acid has potent anti-inflammatory activity [24]. Loganin and sweroside were observed to have strong antibacterial, antifungal, and antispasmodic activities [25]. Loganin was also found to have neuroprotective effects [26]. Cornuside has remarkable antioxidant activity and may provide protection against acute myocardial ischemia and reperfusion injury [27].

In the primary DNA damage test in *E. coli* PQ37 (Table 2), the mean induction factors for loganic acid, loganin, sweroside, and cornuside, at 1000 μg mL^{-1}, were 1.095, 0.995, 1.028, and 1.068, respectively. At all concentrations tested, these iridoids did not induce any SOS repair at a frequency significantly above that of the blank. Statistically, induction factors were not different from that of the blank, and all results remained well below the twofold criteria for genotoxicity.

SOS chromotest results have a high level of agreement (86%) with those from the reverse mutation assay [28]. Therefore, the SOS chromotest has some utility in predicting potential mutagenicity, in addition to primary DNA damage. These results are consistent with previously published genotoxicity tests of other food derived iridoids [29].

In the antigenotoxicity test, 4NQO exhibited obvious genotoxicity, inducing SOS repair more than 3-fold above that of the vehicle blank. Incubation with loganic acid did not significantly reduce 4NQO induction factors. However, loganin, sweroside, and cornuside apparently reduced the amount of 4NQO that caused DNA damage, as mean induction factors were lowered to below 3 in cells incubated in the presence of these iridoids (Table 3).

4. Conclusions

The UPLC-TOF-MS method reported has been shown to be useful for secondary metabolite profiling of *Cornus mas* fruit. With this method, a total of ten phytochemicals were identified, including five organic acids and four iridoids. To our knowledge, this is the first time that **1–4** and **6–10** have been identified in *C. mas* fruit. Loganin, sweroside, cornuside, and loganic acid will provide valuable information for chemical taxonomy. Iridoids, together with other characteristic components, can be used for identification, authentication, and standardization of *C. mas* fruit raw materials and commercial products. The iridoids in the fruit did not display any toxicity. On the other hand, these iridoids exhibited potential anti-genotoxic activity. Our findings also warrant future research on the safety and efficacy of *C. mas*.

References

[1] O. Rop, J. Mlcek, D. Kramarova, and T. Jurikova, "Selected cultivars of cornelian cherry (*Cornus mas* L.) as a new food source for human nutrition," *African Journal of Biotechnology*, vol. 9, no. 8, pp. 1205–1210, 2010.

[2] H. Hassanpour, Y. Hamidoghli, and H. Samizadeh, "Some fruit characteristics of Iranian cornelian cherries (*Cornus mas* L.)," *Notulae Botanicae Horti Agrobotanici Cluj-Napoca*, vol. 40, no. 1, pp. 247–252, 2012.

[3] N. P. Seeram, R. Schutzki, A. Chandra, and M. G. Nair, "Characterization, quantification, and bioactivities of anthocyanins in *Cornus* species," *Journal of Agricultural and Food Chemistry*, vol. 50, no. 9, pp. 2519–2523, 2002.

[4] F. Demir and I. H. Kalyoncu, "Some nutritional, pomological and physical properties of cornelian cherry (*Cornus mas* L.)," *Journal of Food Engineering*, vol. 60, no. 3, pp. 335–341, 2003.

[5] S. Ercisli, "A short review of the fruit germplasm resources of Turkey," *Genetic Resources and Crop Evolution*, vol. 51, no. 4, pp. 419–435, 2004.

[6] S. Ercisli, "Cornelian Cherry germplasm resources of Turkey," *Journal of Fruit and Ornamental Plant Research*, vol. 12, pp. 87–92, 2004.

[7] S. Celik, I. Bakrc, and I. G. Şat, "Physicochemical and organoleptic properties of yogurt with cornelian cherry paste," *International Journal of Food Properties*, vol. 9, no. 3, pp. 401–408, 2006.

[8] P. Brindza, J. Brindza, D. Tóth, S. V. Klimenko, and O. Grigorieva, "Slovakian cornelian cherry (*Cornus mas* L.): potential for cultivation," *Acta Horticulturae*, vol. 760, pp. 433–438, 2007.

[9] P. Brindza, J. Brindza, D. Tóth, S. V. Klimenko, and O. Grigorieva, "Biological and commercial characteristics of cornelian cherry (*Cornus mas* L.) population in the gemer region of Slovakia," *Acta Horticulturae*, vol. 818, pp. 85–94, 2009.

[10] M. Güleryüz, I. Bolat, and L. Pirlak, "Selection of table cornelian cherry (*Cornus mas* L.) types in çoruh valley," *Turkish Journal of Agriculture and Forestry*, vol. 22, no. 4, pp. 357–364, 1998.

[11] M. Didin, A. Kızılaslan, and H. Fenercioglu, "Suitability of some cornelian cherry cultivars for fruit juice," *Gida*, vol. 25, no. 6, pp. 435–441, 2000.

[12] S. Klimenko, "The Cornelian cherry (*Cornus mas* L.): collection, preservation, and utilization of genetic resources," in *Protection of Genetic Resources of Pomological Plants and Selection of Genitors with Traits Valuable For Sustainable Fruit Production*, vol. 12 of *Journal of Fruit and Ornamental Plant Research*, pp. 93–98, 2004.

[13] D. Marinova, F. Ribarova, and M. Atanassova, "Total phenolics and total flavonoids in bulgarian fruits and vegetables," *Journal of the University of Chemical Technology and Metallurgy*, vol. 40, no. 3, pp. 255–260, 2005.

[14] G. E. Pantelidis, M. Vasilakakis, G. A. Manganaris, and G. Diamantidis, "Antioxidant capacity, phenol, anthocyanin and ascorbic acid contents in raspberries, blackberries, red currants, gooseberries and Cornelian cherries," *Food Chemistry*, vol. 102, no. 3, pp. 777–783, 2007.

[15] S. Tural and I. Koca, "Physico-chemical and antioxidant properties of cornelian cherry fruits (*Cornus mas* L.) grown in Turkey," *Scientia Horticulturae*, vol. 116, no. 4, pp. 362–366, 2008.

[16] K. U. Yilmaz, S. Ercisli, Y. Zengin, M. Sengul, and E. Y. Kafkas, "Preliminary characterisation of cornelian cherry (*Cornus mas* L.) genotypes for their physico-chemical properties," *Food Chemistry*, vol. 114, no. 2, pp. 408–412, 2009.

[17] A. M. Pawlowska, F. F. Camangi, and A. Braca, "Quali-quantitative analysis of flavonoids of *Cornus mas* L. (Cornaceae) fruits," *Food Chemistry*, vol. 119, no. 3, pp. 1257–1261, 2010.

[18] C.-T. Du and F. J. Francis, "Anthocyanins from *Cornus mas*," *Phytochemistry*, vol. 12, no. 10, pp. 2487–2489, 1973.

[19] C. T. Du and F. J. Francis, "A new anthocyanin from *Cornus mas* L.," *Hortscience*, vol. 8, no. 1, pp. 29–30, 1973.

[20] S. R. Jensen, A. Kjaer, and B. J. Nielsen, "The genus M*Comus*: non-flavonoid glucosides as taxonomic markers," *Biochemical Systematics and Ecology*, vol. 3, no. 2, pp. 75–78, 1975.

[21] K. Alicja, S. Antoni, S. Anna, and O. Jan, "Sposob otrzymywania kwasu loganowego, Biuletyn Urzedu Patentowego (Bulletin of the Patent Office)," no. 2, p. 4, 2010, http://ipu.uprp.pl/portal/web/guest/wydawnictwawupbup.

[22] B. J. West, S. Deng, C. J. Jensen, A. K. Palu, and L. F. Berrio, "Antioxidant, toxicity, and iridoid tests of processed Cornelian cherry fruits," *International Journal of Food Science and Technology*, vol. 47, no. 7, pp. 1392–1397, 2012.

[23] F. Fish, I. Lampert, A. Halachmi, G. Riesenfeld, and M. Herzberg, "The SOS chromotest kit: a rapid method for the detection of genotoxicity," *Toxicity Assessment*, vol. 2, no. 2, pp. 135–147, 1987.

[24] S. Wei, H. Chi, H. Kodama, and G. Chen, "Anti-inflammatory effect of three iridoids in human neutrophils," *Natural Product Research*, vol. 27, no. 10, pp. 911–915, 2013.

[25] B. Dinda, S. Debnath, and Y. Harigaya, "Naturally occurring secoiridoids and bioactivity of naturally occurring iridoids and secoiridoids. A review, part 2," *Chemical and Pharmaceutical Bulletin*, vol. 55, no. 5, pp. 689–728, 2007.

[26] J. Shi, C. J. Li, J. Z. Yang, Y. H. Yuan, N. H. Chen, and D. M. Zhang, "Coumarin glycosides and iridoid glucosides with neuroprotective effects from *Hydrangea paniculata*," *Planta Medica*, vol. 78, no. 17, pp. 1844–1850, 2012.

[27] W.-L. Jiang, S.-M. Zhang, X.-X. Tang, and H.-Z. Liu, "Protective roles of cornuside in acute myocardial ischemia and reperfusion injury in rats," *Phytomedicine*, vol. 18, no. 4, pp. 266–271, 2011.

[28] R. Legault, C. Blaise, D. Rokosh, and R. Chong-Kit, "Comparative assessment of the SOS chromotest kit and the mutatox test with the Salmonella plate incorporation (Ames test) and fluctuation tests for screening genotoxic agents," *Environmental Toxicology and Water Quality*, vol. 9, no. 1, pp. 45–57, 1994.

[29] B. J. West, S. Deng, and C. J. Jensen, "Nutrient and phytochemical analyses of processed noni puree," *Food Research International*, vol. 44, no. 7, pp. 2295–2301, 2011.

Hindawi Publishing Corporation
Journal of Analytical Methods in Chemistry
Volume 2013, Article ID 536490, 6 pages
http://dx.doi.org/10.1155/2013/536490

Research Article

Antioxidant Activity and Volatile and Phenolic Profiles of Essential Oil and Different Extracts of Wild Mint (*Mentha longifolia*) from the Pakistani Flora

Tahseen Iqbal, Abdullah Ijaz Hussain, Shahzad Ali Shahid Chatha, Syed Ali Raza Naqvi, and Tanveer Hussain Bokhari

Institute of Chemistry, Government College University Faisalabad, Faisalabad 38000, Pakistan

Correspondence should be addressed to Abdullah Ijaz Hussain; abdullahijaz@gcuf.edu.pk

Received 29 May 2013; Revised 13 August 2013; Accepted 28 August 2013

Academic Editor: Shao-Nong Chen

The antioxidant activity and free radical scavenging capacity of the essential oil and three different extracts of wildly grown *Mentha longifolia* (*M. longifolia*) were studied. The essential oil from *M. longifolia* aerial parts was isolated by hydrodistillation technique using Clevenger-type apparatus. The extracts were prepared with three solvents of different polarity (*n*-hexane, dichloromethane, and methanol) using Soxhlet extractor. Maximum extract yield was obtained with methanol (12.6 g/100 g) while the minimum with dichloromethane (3.50 g/100 g). The essential oil content was found to be 1.07 g/100 g. A total of 19 constituents were identified in the *M. longifolia* oil using GC/MS. The main components detected were piperitenone oxide, piperitenone, germacrene D, borneol, and β-caryophyllene. The total phenolics (TP) and total flavonoids (TF) contents of the methanol extract of *M. longifolia* were found to be significantly higher than dichloromethane and hexane extracts. The dichloromethane and methanol extracts exhibited excellent antioxidant activity as assessed by 2,2′-diphenyl-1-picrylhydrazyl (DPPH) free radical scavenging ability, bleaching β-carotene, and inhibition of linoleic acid peroxidation assays. The essential oil and hexane extract showed comparatively weaker antioxidant and free radical scavenging activities. The results of the study have validated the medicinal and antioxidant potential of *M. longifolia* essential oil and extracts.

1. Introduction

Free radicals are considered to initiate oxidation that leads to aging and causes diseases in human beings [1, 2]. Moreover, activated oxygen incorporates reactive oxygen species (ROS) which consists of free radicals ($^1O_2$, $O_2^{\bullet-}$, $^{\bullet}OH$, $ONOO^-$) and nonfree radicals (H_2O_2, NO, and R–OOH) [3]. ROS are liberated by virtue of stress, and thus, an imbalance is developed in the body that damages cells in it and causes health problems [2, 4]. Moreover, oxidation in processed foods, enriched with fats and oils, during storage leads to spoilage and quality deterioration [5].

The use of synthetic antioxidants such as butylated hydroxyanisole (BHA), and butylated hydroxytoluene (BHT) and tertiary butylhydroquinone (TBHQ) have been restricted because of their carcinogenicity and other toxic properties [3, 6]. Thus, the interest in natural antioxidants has increased considerably. Natural antioxidants can be phenolic compounds (tocopherols, flavonoids, and phenolic acids) and carotenoids (lutein, lycopene, and carotene). Growing evidence has shown an inverse correlation between the intake of dietary antioxidants and the risk of chronic diseases such as coronary heart disease, cancer, and several other aging-related health concerns [1, 7].

Natural antioxidant compounds exhibit their antioxidant activity by various mechanisms including chain breaking by donation of hydrogen atoms or electrons that convert free radicals into more stable species and decomposing lipid peroxides into stable final products [1]. Different *in vitro* assays simply provide an idea of the protective efficacy of the test model. Thus it is necessary to use at least two methods depending on the expected antioxidant potential and/or on the origin of the substance. Most commonly used methods for the determination of antioxidant activity of plant

essential oils and extracts are 2,2-di(4-*tert*-octaphenyl)-1-picrylhydrazyl (DPPH$^{\bullet}$) radical scavenging assay, inhibition of linoleic acid peroxidation, and bleaching of β-carotene in linoleic acid system assays. DPPH radical scavenging assay is the most popular and frequently used for the determination of antioxidant activity of essential oils and plant extracts [1, 7, 8]. Bleachability of β-carotene in linoleic acid system is another simple, reproducible, and time efficient method for rapid evaluation of antioxidant properties [1, 7, 8]. Measurement of inhibition of linoleic acid peroxidation is also an effective method for the assessment of antioxidant activity of the plant samples.

Mentha longifolia (wild mint) belongs to genus *Mentha* (family Lamiaceae) and grows widely throughout the temperate regions of the world [8]. The different herbal and food products from *Mentha* species have been in use since ancient times for the treatment of heart burns, indigestion, colic, flatulence, coughs and flu, nausea, irritable bowel syndrome, gall-bladder and bile ducts, herpes, and certain skin infections including acne and pigmentation [7–9]. Research work on plants from different regions resulted in the innovation of biologically active substances [8, 10]. Therefore the study was conducted to investigate the chemical composition and antioxidant and antimicrobial activities of essential oil and three different extracts from *M. longifolia* native to dry region of Pakistan.

2. Materials and Methods

2.1. Collection and Pretreatment of Plant Material. Aerial parts of wild mint (*M. longifolia* L.) were collected during May-June from South Punjab, Pakistan. The specimens were further identified and authenticated by a taxonomist, Dr. Qasim Ali (Assistant Professor), Department of Botany, Government College University Faisalabad. Collected specimens were dried at 35°C in a hot air oven (IM-30 Irmec, Germany) and grinded to 80 mesh and stored in polyethylene bags at −4°C.

2.2. Chemicals and Reagents. Linoleic acid, 2,2′-diphenyl-1-picrylhydrazyl, gallic acid, Folin-Ciocalteu reagent, ascorbic acid, trichloroacetic acid, sodium nitrite, aluminum chloride, ammonium thiocyanate, ferrous chloride, ferric chloride, potassium ferricyanide, butylated hydroxytoluene (99.0%), and homologous series of C_9–C_{24} *n*-alkanes and various reference chemicals used to identify the constituents were obtained from Sigma Chemical Co. (St. Louis, MO, USA). All other chemicals (analytical grade), that is, anhydrous sodium carbonate ferrous chloride, ammonium thiocyanate, chloroform, and methanol, used in this study were purchased from Merck (Darmstadt, Germany), unless stated otherwise. All culture media and standard antibiotic discs were purchased from Oxoid Ltd. (Hampshire, UK).

2.3. Isolation of Essential Oil. The oven-dried and ground fennel seeds (80 mesh) were subjected to hydrodistillation for 4 h, using a Clevenger-type apparatus. The obtained essential oil was dried over anhydrous sodium sulfate, filtered, and stored at −4°C until analyzed.

2.4. Preparation of Extracts. Ground (80 mesh) *M. longifolia* sample (100 g) was subjected to extraction for 4 h using Soxhlet unit. The plant materials were extracted in sequence with three solvents of different polarity, that is, *n*-hexane, dichloromethane and methanol. The extracts were concentrated under vacuum at 45°C, using a vacuum rotary evaporator (N–N Series, Eyela, Rikakikai Co. Ltd., Tokyo, Japan), and stored at −4°C until used for further analyses.

2.5. Analysis of the Essential Oil

2.5.1. Gas Chromatography/Mass Spectrometry Analysis. The *M. longifolia* essential oil composition was determined on Agilent-Technologies (Little Falls, CA, USA) 6890N Network gas chromatographic (GC) system, equipped with an Agilent-Technologies 5975 inert XL Mass selective detector and Agilent-Technologies 7683B series autoinjector. Compounds were separated on HP-5 MS capillary column (30 m × 0.25 mm, film thickness 0.25 μm; Little Falls, CA, USA). A sample of 1.0 μL was injected in the split mode with split ratio 1 : 100. Helium was used as a carrier gas at a flow rate of 1.5 mL/min. For GC/MS detection, an electron ionization system, with ionization energy of 70 eV, was used. The column oven temperature was programmed from 80°C to 220°C at the rate of 4°C/min; initial and final temperatures were held for 3 and 10 min, respectively. Mass scanning range was 50–550 *m/z* while the injector and MS transfer line temperatures were set at 220 and 290°C, respectively. All quantifications were done by a built-in data-handling program of the equipment used (Perkin-Elmer, Norwalk, CT, USA). The composition was reported as a relative percentage of the total peak area.

2.5.2. Compounds Identification. The components of the *M. longifolia* essential oil were identified by comparison of their retention indices relative to (C_9–C_{24}) *n*-alkanes either with those of published data or with authentic compounds [11, 12]. Compounds were further identified and authenticated using their complete mass fragmentation data compared to the NIST02.L and WILEY7n.L mass spectral libraries and published mass spectra and, wherever possible, by coinjection with authentic standards (α-pinene, β-pinene, limonene, cis-β-ocimene, δ-terpinene, 1,8-cineol, linalool, borneol, α-terpineol, thymol, piperitenone, piperitenone oxide, β-caryophyllene, germacrene D, calamenene, cis-jasmone, and caryophyllene oxide) [1, 13, 14].

2.6. Antioxidant Activity

2.6.1. Determination of Total Phenolics (TP) and Total Flavonoids (TF) Contents. Amounts of total phenolics (TP) and total flavonoids (TF) in the *M. longifolia* extracts were determined using Folin-Ciocalteu reagent method and aluminum chloride colorimetric assay, respectively, as reported previously [15].

2.6.2. DPPH Radical Scavenging Assay. 2,2′-Diphenyl-1-picrylhydrazyl (DPPH) free radical assay was carried out to measure the free radical scavenging activity as reported

previously [9]. Briefly, *M. longifolia* essential oil, extracts, piperitenone compound, and BHT concentrations in methanol (1–100 μg/mL) were mixed with 2 mL of 90 μM methanol solution of DPPH. After 30 min incubation period at room temperature, the absorbance was read at 517 nm. The scavenging (%) was calculated by the following formula:

$$\text{Scavenging}\,(\%) = 100 \times \left\{ \frac{\left(A_{\text{blank}} - A_{\text{sample}}\right)}{A_{\text{blank}}} \right\}, \quad (1)$$

where A_{blank} is the absorbance of the DPPH solution and A_{sample} is the absorbance of the extract solution. Extract concentration providing 50% scavenging (IC_{50}) was calculated from the graph plotted between scavenging percentage and extract concentration.

2.6.3. Antioxidant Activity Determination in Linoleic Acid System. The antioxidant activity of *M. longifolia* essential oil and extracts weas determined in terms of measurement of % inhibition of peroxidation in linoleic acid system following the reported method with some modification [16]. Essential oil and extracts (5 mg) were added to a solution mixture of linoleic acid (0.13 mL), 99.8% ethanol (10 mL), and 10 mL of 0.2 M sodium phosphate buffer (pH 7). Total mixture was diluted to 25 mL with distilled water. The solution was incubated at 40°C for 175 h. The extent of oxidation was measured by peroxide value using the colorimetric method as reported previously [15].

2.6.4. Bleaching of β-Carotene in Linoleic Acid System. Antioxidant activity of *M. longifolia* essential oil and extracts was also assessed by bleaching of β-carotene/linoleic acid emulsion system as reported previously [1]. Briefly, a stock solution of β-carotene-linoleic acid mixture was prepared by dissolving 0.1 mg β-carotene, 20 mg linoleic acid, and 100 mg Tween 40 in 1.0 mL of chloroform (HPLC grade). The chloroform was removed under vacuum in rotary evaporator at 50°C. Then, 50 mL of distilled water saturated with oxygen (30 min, 100 mL min^{-1}) was added with vigorous shaking. A 5.0 mL of this reaction mixture was dispensed to test tubes with 200 μL of the essential oil or trans-anethole solution, prepared at 4.0 g L^{-1} concentrations, and the absorbance was immediately ($t = 0$) measured at 490 nm against a blank, consisting of an emulsion without β-carotene. Then emulsion was incubated for 50 h at room temperature, and the absorbance was recorded at different time intervals. The same procedure was repeated with BHT and blank. Antioxidant capacities of the fennel essential oils were compared with BHT and blank.

2.7. Statistical Analysis. All the experiments were conducted in triplicate unless stated otherwise, and data are presented as mean ± standard deviation (SD). Statistical analysis of the data was performed by Analysis of Variance (ANOVA) using STATISTICA 5.5 (Stat Soft Inc, Tulsa, OK, USA) software, and probability value $P \leq 0.05$ was considered to denote a statistically significant difference.

Table 1: Yield of *M. longifolia* essential oil and hexane, dichloromethane, and methanol extracts.

Samples	Yield (g/100 g)*
Essential oil	1.07 ± 0.10^{a}
n-Hexane extract	7.30 ± 0.32^{c}
Dichloromethane extract	3.50 ± 0.21^{b}
Methanol extract	12.60 ± 0.70^{d}

*Values are mean ± SD of three samples of *M. longifolia* analyzed individually in triplicate.
Different letters in superscript represent significant ($P < 0.05$) difference within solvents.

3. Results and Discussion

3.1. Percentage Yield of Essential Oil and Different Extracts. Yield (g/100 g of dry plant material) of *Mentha longifolia* essential oil and *n*-hexane, dichloromethane, and methanol extracts is given in Table 1. Maximum yield was obtained with methanol (12.60 g/100 g). The minimum yield was obtained with dichloromethane (3.50 g/100 g). The essential oil yield from the aerial parts of *M. longifolia* was found to be 1.07 g/100 g. Nonpolar extract yield (*n*-hexane) was found to be 7.30 g/100 g. Tukey's range test revealed the significant ($P < 0.05$) difference among the extract yield with solvents of different polarities. Differences in yield of extracts from different solvents might be attributed to the availability of extractable component of different polarities.

3.2. Essential Oil Composition. The retention indices, percentage composition, and identification methods for the essential oil of *M. longifolia* are given in Table 2. Nineteen compounds, 96.79% of the total oil, were identified from the oil (Figure 1). The most abundant constituents (>5%) in the essential oil of *M. longifolia* were found to be piperitenone oxide (28.3%), piperitenone (24.9%), germacrene D (8.16%), borneol (5.96%), and β-caryophyllene (5.94%). Analyzed essential oil mainly consisted of oxygenated monoterpenes (67.24%) followed by sesquiterpene hydrocarbons (17.19%), monoterpene hydrocarbons (7.31%), and oxygenated sesquiterpenes (5.05%).

The variation in the essential oil composition of *M. longifolia* is reported in the literature from different part of the world [8, 17, 18]. Our results reported the essential oil composition of *M. longifolia* essential oil from South Punjab, Pakistan, where the weather conditions are very hot and dry. Variations in the chemical compositions of essential oil across countries might be attributed to the varied agroclimatic (climatical, seasonal, and geographical) conditions of the regions, isolation regimes, and adaptive metabolism of plants.

3.3. Antioxidant Activity

3.3.1. Total Phenolics (TP) and Total Flavonoids (TF) Contents. Amount of total phenolics and total flavonoids is given in Figure 2. The highest TP was found in methanol extract (71.43 mg/g acid of dry plant material, measured as gallic equivalent) and the lowest in hexane extract (1.7 mg/g acid of dry plant material, measured as gallic equivalent). Similarly,

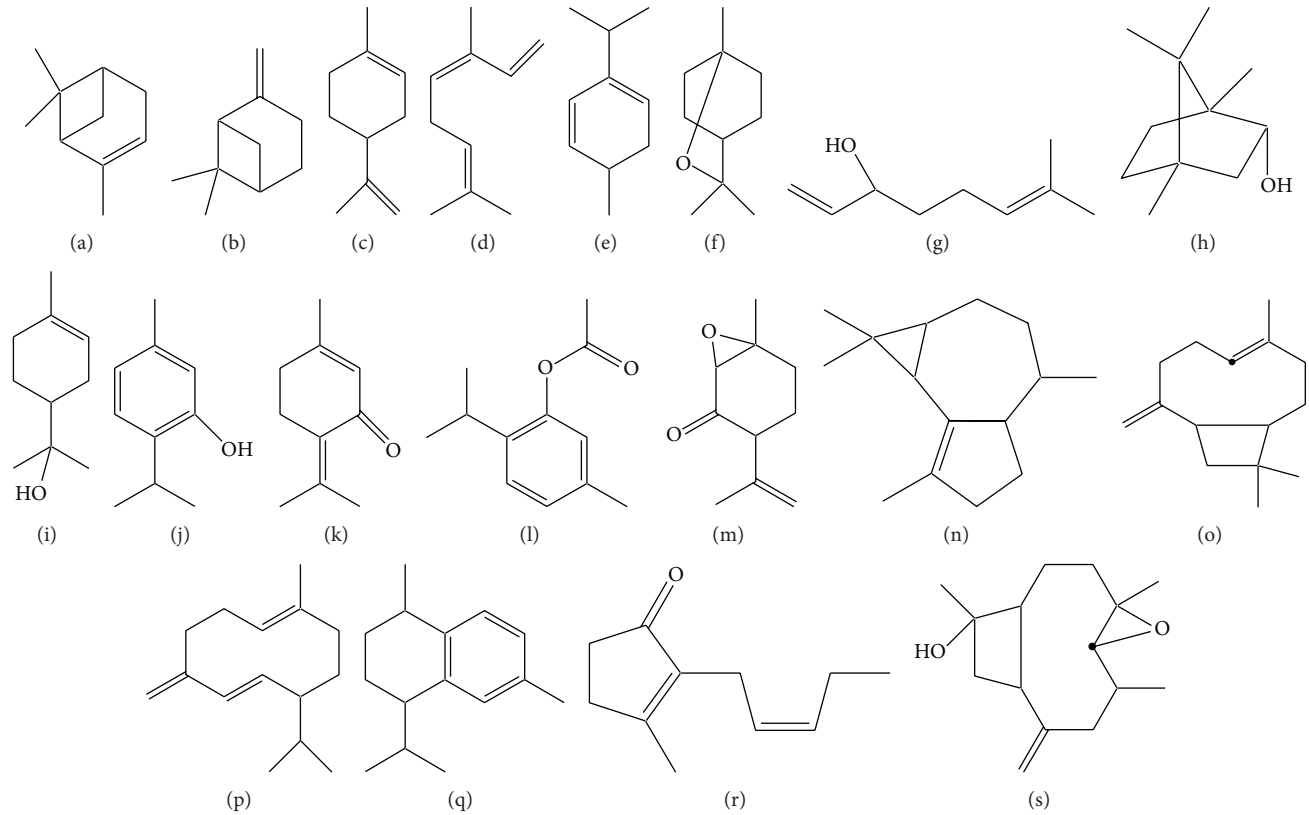

Figure 1: Structure of major compounds detected from *M. longifolia* essential oil. (a) α-Pinene; (b) β-pinene; (c) limonene; (d) *cis*-β-ocimene; (e) δ-terpinene; (f) 1,8-cineole; (g) linalool; (h) borneol; (i) α-terpineol; (j) thymol; (k) piperitenone; (l) thymol acetate; (m) piperitenone oxide; (n) α-gurjunene; (o) β-caryophyllene; (p) germacrene D; (q) calamenene; (r) *cis*-jasmone; (s) caryophyllene oxide.

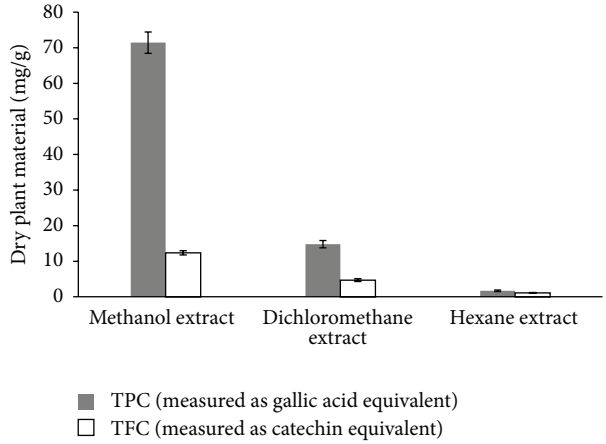

Figure 2: Total phenolics (TP) and total flavonoids (TF) contents of *n*-hexane, dichloromethane, and methanol extracts of *M. longifolia*.

the amount of TF in methanol, dichloromethane, and hexane extracts was found to be 12.35, 4.7, and 1.1 mg/g acid of dry plant material, measured as catechin equivalent. The effect of different solvent systems on the amount of TP and TF was significant ($P < 0.05$). Methanol has been proven as effective solvent to extract phenolic compounds [6].

3.3.2. DPPH Radical Scavenging Assay. The ability of *M. longifolia* essential oil and different extract to donate proton to DPPH free radical and change its color from violet to yellow is accessed in this assay. Concentration of extracts and essential oil scavenging 50% of DPPH radical is shown in Table 3. IC_{50} value ranged from 6.70 to 33.3 μg/mL. Greater IC_{50} value (maximum radical scavenging activity) was observed with methanol extract of *M. longifolia,* and lesser IC_{50} value was recorded with *n*-hexane extract. IC_{50} values of *M. longifolia* essential oil and dichloromethane extracts were found to be comparable with IC_{50} value of the piperitenone, a major compound of *M. longifolia* essential oil. IC_{50} value of methanol extract is significantly ($P < 0.05$) better than hexane and dichloromethane extracts and essential oil and comparable with synthetic antioxidant, BHT.

3.3.3. Antioxidant Activity Determination in Terms of Inhibition of Linoleic Acid Peroxidation. The antioxidants activity has also been assessed as ability to prevent the oxidation of linoleic acid. Therefore, inhibition of linoleic acid oxidation was also used to assess the antioxidant activity of *M. longifolia* extracts and essential oil. All extracts and essential oil exhibited appreciable inhibition of linoleic acid peroxidation (Table 3) ranging from 9.9 to 91.6%. Methanol extract showed maximum antioxidant activity (91.6%) followed by dichloromethane extract (89.3%) which is comparable with

Table 2: Chemical composition of *M. longifolia* essential oil.

Components[b]	RI[c]	Molecular mass	% Composition[a]	Mode of identification[d]	Quality (%)[e]
Monoterpene hydrocarbons			**(7.31)**		
α-Pinene	939	136	0.76 ± 0.06	RT, RI, MS	97
β-Pinene	979	136	2.14 ± 0.19	RT, RI, MS	96
Limonene	1029	136	1.80 ± 0.19	RT, RI, MS	94
cis-β-Ocimene	1037	136	1.98 ± 0.11	RT, RI, MS	97
δ-Terpinene	1089	136	0.63 ± 0.04	RI, MS	96
Oxygenated monoterpenes			**(67.24)**		
1,8-Cineol	1031	154	2.00 ± 0.17	RT, RI, MS	98
Linalool	1097	154	0.98 ± 0.10	RT, RI, MS	98
Borneol	1169	154	5.96 ± 0.44	RT, RI, MS	96
α-Terpineol	1189	154	1.17 ± 0.09	RT, RI, MS	98
Thymol	1290	150	2.85 ± 0.20	RT, RI, MS	99
Piperitenone	1343	150	24.9 ± 1.34	RT, RI, MS	97
Thymol acetate	1352	192	1.08 ± 0.08	RI, MS	94
Piperitenone oxide	1370	166	28.3 ± 1.6	RT, RI, MS	96
Sesquiterpene hydrocarbons			**(17.19)**		
α-Gurjunene	1410	204	1.11 ± 0.18	RI, MS	96
β-Caryophyllene	1421	204	5.94 ± 0.32	RT, RI, MS	99
Germacrene D	1485	204	8.16 ± 1.01	RT, RI, MS	99
Calamenene	1540	202	1.98 ± 0.17[d]	RT, RI, MS	98
Oxygenated sesquiterpenes			**(5.05)**		
cis-Jasmone	1393	164	1.13 ± 0.11[a]	RT, RI, MS	96
Caryophyllene oxide	1583	220	3.92 ± 0[b]	RT, RI, MS	97
Total			**96.79**		

[a]Values are mean ± standard deviation of three samples of *M. longifolia* essential oil, analyzed individually in triplicate.
[b]Compounds are listed in order of elution from a HP-5MS column; [c]retention indices relative to C_9–C_{24} *n*-alkanes on the HP-5MS column; [d]mode of identifications; RT: identification based on retention time; RI: identification based on retention index; MS: identification based on comparison of MS data compared with those from the NIST02.L and WILEY7n.L mass spectral libraries; [e]matching percentage with the NIST02.L and WILEY7n.L mass spectral libraries.

Table 3: Antioxidant activity of *M. longifolia* essential oil and *n*-hexane, dichloromethane, and methanol extracts.

Samples	Antioxidant activity*	
	DPPH, IC_{50}, (μg mL^{-1})	Inhibition of linoleic acid peroxidation (%)
Essential oil	21.8 ± 1.2[c]	37.3 ± 1.3[c]
n-Hexane extract	33.3 ± 1.7[d]	9.9 ± 0.7[a]
DCM extract	21.2 ± 1.7[c]	89.3 ± 2.9[d]
Methanol extract	6.70 ± 0.3[a]	91.6 ± 2.3[d]
Piperitenone	22.7 ± 1.5[c]	31.3 ± 2.1[b]
BHT	9.90 ± 0.2[b]	90.9 ± 2.7[d]

*Values are mean ± standard deviation of three samples of each *Thymus* species, analyzed individually in triplicate. Mean followed by different superscript letters in the same column represents significant difference ($P < 0.05$).
NT: not tested.

the activity of BHT standard (90.6%). *M. longifolia* essential oil and hexane extract showed weaker antioxidant activity. Polar extract exhibited significantly ($P \leq 0.05$) higher antioxidant activity than nonpolar extracts which might be due to the higher concentration of TP and TF contents [15].

3.3.4. Antioxidant Activity Determination in Terms of Bleaching of β-Carotene in Linoleic Acid System. Bleaching β-carotene with linoleic acid system as antioxidant activity of the *M. longifolia* essential oil and extracts is presented in Figure 3. The greater is the effectiveness of an antioxidant, the slower will be the colour depletion. In Figure 3 smaller decline in absorbance of β-carotene indicates a lower rate of oxidation of linoleic acid and higher antioxidant activity in the presence of *M. longifolia* methanol and dichloromethane extracts and BHT. Hexane extract and essential oil showed poor antioxidant activity.

4. Conclusion

Methanol extracts of *Mentha longifolia* exhibited excellent antioxidant activity and free radical scavenging capacity followed by dichloromethane extract, essential oil, and hexane

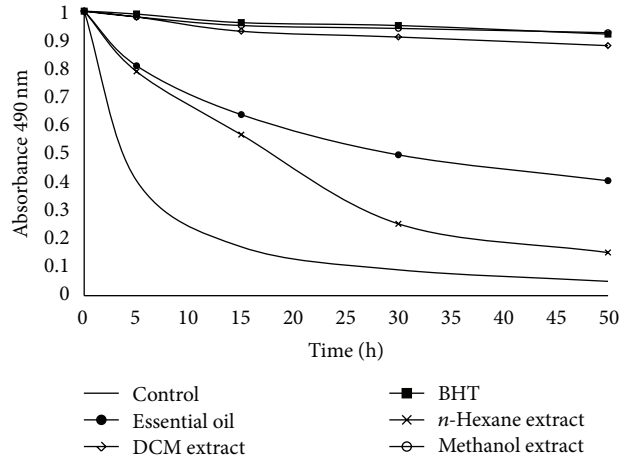

Figure 3: Antioxidant activity of *M. longifolia* essential oil and *n*-hexane, dichloromethane, and methanol extracts in terms of bleaching of β-carotene-linoleic acid emulsion.

extract. High TP and TF contents and antioxidant potential of *M. longifolia* extracts lead to its possible use as a food preservative. Moreover, they may be used in pharmaceutical and natural therapies for treatment of oxidative stress.

Acknowledgment

Grants supports by the Higher Education Commission (HEC), Islamabad, Pakistan, under the National Research Program for University (NRPU) scheme are highly acknowledged.

References

[1] A. I. Hussain, F. Anwar, S. T. H. Sherazi, and R. Przybylski, "Chemical composition, antioxidant and antimicrobial activities of basil (*Ocimum basilicum*) essential oils depends on seasonal variations," *Food Chemistry*, vol. 108, no. 3, pp. 986–995, 2008.

[2] F. Shahidi and P. K. Wanasundara, "Phenolic antioxidants," *Critical Reviews in Food Science abd Nutrition*, vol. 32, no. 1, pp. 67–103, 1992.

[3] B. Sultana, F. Anwar, and R. Przybylski, "Antioxidant activity of phenolic components present in barks of *Azadirachta indica, Terminalia arjuna, Acacia nilotica*, and *Eugenia jambolana* Lam. trees," *Food Chemistry*, vol. 104, no. 3, pp. 1106–1114, 2007.

[4] D. Huang, O. U. Boxin, and R. L. Prior, "The chemistry behind antioxidant capacity assays," *Journal of Agricultural and Food Chemistry*, vol. 53, no. 6, pp. 1841–1856, 2005.

[5] S. A. S. Chatha, A. I. Hussain, J. Bajwa, and M. Sagir, "Antioxidant activity of different solvent extracts of rice bran at accelerated storage of sunflower oil," *Journal of Food Lipids*, vol. 13, no. 4, pp. 424–433, 2006.

[6] P. Siddhuraju and K. Becker, "Antioxidant properties of various solvent extracts of total phenolic constituents from three different agroclimatic origins of drumstick tree (*Moringa oleifera* Lam.) leaves," *Journal of Agricultural and Food Chemistry*, vol. 51, no. 8, pp. 2144–2155, 2003.

[7] A. I. Hussain, F. Anwar, S. A. S. Chatha, A. Jabbar, S. Mahboob, and P. S. Nigam, "*Rosmarinus officinalis* essential oil: antiproliferative, antioxidant and antibacterial activities," *Brazilian Journal of Microbiology*, vol. 41, no. 4, pp. 1070–1078, 2010.

[8] A. I. Hussain, F. Anwar, P. S. Nigam, M. Ashraf, and A. H. Gilani, "Seasonal variation in content, chemical composition and antimicrobial and cytotoxic activities of essential oils from four *Mentha* species," *Journal of the Science of Food and Agriculture*, vol. 90, no. 11, pp. 1827–1836, 2010.

[9] A. I. Hussain, F. Anwar, S. Rasheed, P. S. Nigam, O. Janneh, and S. D. Sarker, "Composition, antioxidant and chemotherapeutic properties of the essential oils from two *Origanum* species growing in Pakistan," *Revista Brasileira de Farmacognosia*, vol. 21, no. 6, pp. 943–952, 2011.

[10] F. Anwar, A. I. Hussain, S. T. H. Sherazi, and M. I. Bhanger, "Changes in composition and antioxidant and antimicrobial activities of essential oil of fennel (*Foeniculum vulgare* Mill.) fruit at different stages of maturity," *Journal of Herbs, Spices and Medicinal Plants*, vol. 15, no. 2, pp. 187–202, 2009.

[11] Y. Massada, *Analysis of Essential Oils by Gas Chromatography and Mass Spectrometry*, John Wiley & Sons, New York, NY, USA, 1976.

[12] R. P. Adam, *Identification of Essential Oils Components by Gas Chromatography/Quadrupole Mass Spectroscopy*, Allured Publishing, Carol Stream, Ill, USA, 2001.

[13] F. Anwar, M. Ali, A. I. Hussain, and M. Shahid, "Antioxidant and antimicrobial activities of essential oil and extracts of fennel (*Foeniculum vulgare* Mill.) seeds from Pakistan," *Flavour and Fragrance Journal*, vol. 24, no. 4, pp. 170–176, 2009.

[14] K. Vagionas, K. Graikou, O. Ngassapa, D. Runyoro, and I. Chinou, "Composition and antimicrobial activity of the essential oils of three *Satureja* species growing in Tanzania," *Food Chemistry*, vol. 103, no. 2, pp. 319–324, 2007.

[15] A. I. Hussain, S. A. S. Chatha, S. Noor et al., "Effect of extraction techniques and solvent systems for the extraction of antioxidant components from peanut (*Arachis hypogaea* L.) Hulls," *Food Analytical Methods*, vol. 5, no. 4, pp. 890–896, 2012.

[16] S. Iqbal, M. I. Bhanger, and F. Anwar, "Antioxidant properties and components of some commercially available varieties of rice bran in Pakistan," *Food Chemistry*, vol. 93, no. 2, pp. 265–272, 2005.

[17] A. M. Viljoen, S. Petkar, S. F. van Vuuren, A. C. Figueiredo, L. G. Pedro, and J. G. Barroso, "The chemo-geographical variation in essential oil composition and the antimicrobial properties of "wild mint"—*Mentha longifolia* subsp. *polyadena* (Lamiaceae) in Southern Africa," *Journal of Essential Oil Research*, vol. 18, pp. 60–65, 2006.

[18] M. Gulluce, F. Sahin, M. Sokmen, H. Ozer, D. Daferera, and A. Sokmen, "Antimicrobial and antioxidant properties of the essential oils and methanol extract from *Mentha longifolia* L. ssp. *longifolia*," *Food Chemistry*, vol. 103, no. 4, pp. 1449–1456, 2007.

Hindawi Publishing Corporation
Journal of Analytical Methods in Chemistry
Volume 2013, Article ID 432465, 6 pages
http://dx.doi.org/10.1155/2013/432465

Research Article

A Sensitive and Selective Method for Determination of Aesculin in Cortex Fraxini by Liquid Chromatography Quadrupole Time-of-Flight Tandem Mass Spectrometry and Application in Pharmacokinetic Study

Yi Li, Hui Guo, Yinying Wu, Qianqian Geng, Danfeng Dong, Huili Wu, and Enxiao Li

Department of Medical Oncology, First Affiliated Hospital of Medical College, Xi'an Jiaotong University, No. 277, Yanta Western Road, Xi'an, Shaanxi 710061, China

Correspondence should be addressed to Yi Li; liyi_0712@163.com

Received 6 July 2013; Accepted 22 August 2013

Academic Editor: Shao-Nong Chen

A rapid and sensitive method for determining aesculin of Cortex fraxini in rat was developed using high-performance liquid chromatography (HPLC) quadrupole time-of-flight (QTOF) tandem mass (MS/MS). Rat plasma was pretreated by fourfold methanol to remove plasma proteins. Chromatographic separation was performed on a reverse phase column. A tandem mass spectrometric detection with an electrospray ionization (ESI) interface was achieved using collision-induced dissociation (CID) under positive ionization mode. The MS/MS patterns monitored were m/z 341.2716 → m/z 179.1043 for aesculin and m/z 248.3025 → m/z 120.9130 for tinidazole (internal standard). The linear range was calculated to be 10.0–1500.0 ng/mL with a detection limit of 2.0 ng/mL. The inter- and intraday accuracy and precision were within ±7.0%. Pharmacokinetic study showed that aesculin was confirmed to be a one-compartment open model. The method is believed to have good linear range, high sensitivity and recoveries, and superior analytical efficiency. It will probably be an alternative for pharmacokinetic study of aesculin.

1. Introduction

Cortex fraxini, named "Qin Pi" in China, is the dry barks of Oleaceae plant *Fraxinus rhynchophylla* Hance, *F. rhynchophylla* Hance, or *Fraxinus paxiana* [1]. Cortex fraxini is confirmed to inhibit the growth of dysentery bacillus and staphylococcus [2] as well as have diuretic, anticoagulant, antiallergic, and antioxidant effects [3–5]. As a favorite and largely used medicinal plant in traditional Chinese practice, it is the main herb in a formula frequently prescribed for fighting diseases including bacterial enteritis, acute or chronic enteritis, acute nephritis, and ulcerous coloitis [6].

Aesculin is described as a marker for estimating quality of Cortex fraxini in Chinese pharmacopeia due to inhibiting xanthine oxidase and having antioxidant activity and antitumor activity [7, 8]. The methodologies on the basis of the tandem of HPLC-DAD-MS [9, 10] and capillary electrophoresis [11–14] have been widely used to quantify the amount of aesculin in this plant and its preparations. Ultraviolet absorption spectrum has also been used in the measuring of aesculin in Cortex fraxini through artificial neural network [15]. In addition, a high-performance liquid chromatographic method was established for pharmacokinetic study of aesculin in a previous report [16]. Recently, a method using high performance liquid chromatography with fluorescent detection has been developed for monitoring aesculin in rabbit plasma [17]. These assays have a potential to be officially applied in the quality control of Cortex fraxini and pharmacokinetic study of aesculin.

High performance liquid chromatography (HPLC) using tandem mass (MS/MS) spectrometric detection is an authorized approach for pharmacokinetic study of a drug ascribed to high sensitivity, specificity, and speed. A reliable method by HPLC-MS/MS for pharmacokinetic study on aesculin plays a crucial role in guiding the clinic use and ensuring the quality control of Cortex fraxini as well as providing an

alternative for monitoring aesculin in other matrices. This work is designed to develop a sensitive method for the determination of aesculin in rat plasma. Moreover, the aims of this work also included the application of the proposed method in the pharmacokinetic study on aesculin in Cortex fraxini.

2. Material and Methods

2.1. Materials and Reagents. Standards of aesculin (bath no. 111731-200501, purity > 99.5%) and tinidazole (bath no. 100336-0001, purity > 99.5%, internal standard) were acquired thanks to the help of the National Institute for the Control of Pharmaceutical and Biological Products (Beijing, China). Ammonium formate and formic acid were from Sigma-Aldrich Company (St. Louis, MO, USA). HPLC grade methanol was purchased from Fisher Scientific (Springfield, NJ, USA). Cortex fraxini was purchased from Xi'an Medical Material Company (Xi'an, China). Other reagents were analytical grade unless specified.

2.2. Instruments and Conditions. Target compounds were determined using a high performance liquid chromatography (HPLC) electrospray (ESI) quadrupole time-of-flight (QTOF)—tandem mass spectrometric system acquired from Agilent (Wilmington, DE, USA). The LC instrument was an Agilent 1200 series, consisting of vacuum degasser unit, autosampler, a binary high-pressure pump, and a thermostatted column compartment. The QTOF mass spectrometer was an Agilent 6520 model, furnished with a dual-spray ESI source.

Chromatographic separation was performed on a Zorbax-C_{18} column (2.1 × 150 mm, 5 μm; Littleforts, Philadelphia, PA, USA) at 25°C. The mobile phase consisted of water (containing 5×10^{-3} M ammonium formate and 0.1% formic acid) and methanol (60 : 40, v/v) at a flow rate of 0.2 mL/min. Under these conditions, the total run time was less than 5.0 min.

Liquid nitrogen was used as nebulizing (35 psi) and drying gas (350°C, 7.5 L/min) in the dual ESI source. The QTOF experiment was performed in the 4 GHz high-resolution mode, and compounds were ionized in positive ESI, applying a capillary voltage of 3000 V. A reference calibration solution (Agilent calibration solution B) was continuously sprayed in the source of the QTOF system, employing the ions with *m/z* 121.0509 and *m/z* 922.0098 for recalibrating the mass axis ensuring the accuracy of mass assignments throughout the whole run. The MassHunter Workstation software was used to control all the acquisition parameters of the LC-ESI-QTOF system and also to process the obtained data.

The precursor ions for aesculin and IS were obtained using a common fragmented voltage of 175 V. Collision energy was optimized with the aim of obtaining a minimum of two product ions for each precursor. Mass patterns of aesculin and IS were generated regarding maximum signal intensity of molecular ions and fragment ions, by consecutively infusing standard solutions of aesculin (2.0 ng/mL) and IS (1.0 ng/mL), aided by a model 22 syringe pump (Harvard Apparatus, MA, USA) at a flow rate of 500 μL/h. The optimal transitions were *m/z* 341.2716 $[M + H]^+$ of parent ion to *m/z* 179.1043 of daughter ion for aesculin and *m/z* 248.2035 $[M + H]^+$ of parent ion to *m/z* 120.9130 of daughter ion for IS.

2.3. Extraction of the Herb. The extract of Cortex fraxini was prepared by the following method. 50.0 g of Cortex fraxini was grinded to pieces of 40 bore size and extracted two times with 150 mL ethanol/water (50 : 50 V : V) for 20 min endurance each time to exact most of aesculin in the herb. The suspension was filtered and the resulting solution was concentrated to 50 mL. The concentration of aesculin in the extraction was determined to be 40 mg/mL by HPLC method.

2.4. Preparation of the Plasma Samples. An aliquot of 0.2 mL rat plasma was transferred into a 1.5 mL eppendorf tube in the presence of 1.0 μL of IS working solution (1.0 μg/mL). 0.8 mL methanol was added to the plasma to remove protein and extract aesculin by vortex mixing for 1.0 min. The sample was further centrifuged at 8000 rpm for 3.0 min. The supernatant was aspirated into a 1.5 mL tube and evaporated to dryness under an N_2 stream. Finally, the residue was reconstituted with 0.1 mL mobile phase to be analyzed by LC-MS/MS. The injection volume was 20.0 μL.

2.5. Preparations of Standards Curves and Quality Control (QC) Samples. Stock solution of aesculin was prepared in methanol at 5.0 mg/mL. The stock solution was then diluted with methanol to produce a series of standard or QC working solutions at the desired concentrations. Stock solutions for IS were prepared at 0.1 mg/mL in methanol and diluted with methanol to yield an IS working solution at the concentration of 10.0 ng/mL.

The calibration standards were freshly prepared by adding 20 μL of the appropriate standard working solutions to 200 μL blank plasma and prepared using the proposed method to obtain concentrations of aesculin at 5.0, 10.0, 50.0, 100.0, 200.0, 400.0, 800.0, 1000.0, and 1500.0 ng/mL. Low, medium, and high levels of QC samples were prepared at the concentrations of 40.0, 500.0, and 1200.0 ng/mL. All solutions described above were stored at 4.0°C.

2.6. Matrix Effect and Extraction Recovery. Absolute matrix effect was employed to test the extent of MS signal suppression or enhancement. It was defined by comparing the peak areas of analytes added in six different lots of plasma (A) with mean peak areas of the standards at the same concentrations in the reconstitution solvent (B) and expressed as ($A/B \times 100\%$). Relative matrix effect was used to evaluate the variations of different lots of plasma resulting from the matrix effect and was calculated by the coefficients of variation [CV %] of peak area of analytes added after extraction from six different lots of blank plasma.

Extraction recovery was calculated by comparing peak areas of QC samples (C) with the mean peak areas of analytes added after extraction in six different lots of plasma (A) and expressed as ($C/A \times 100\%$).

2.7. Method Validation. Validation of the proposed HPLC-QTOF-MS/MS method was assessed according to the results of specificity, linearity, accuracy, intraday and interday precision, recovery, and stability. The specificity was confirmed by

analyzing six different lots of blank rat plasma. Five validation batches were assayed to assess the linearity, accuracy, and precision of the method. Each batch included a set of calibration standards and five replicates of QC samples at low, medium, and high concentration level, and was processed on five separate days. The linearity of each curve was assessed by plotting the peak area ratio of the analyte to IS versus the corresponding concentration of the analytes in the freshly prepared plasma calibrators. The accuracy of the assay was expressed by [(calculated concentration by the regression equations)/(spiked concentration)] × 100%, and the precision was evaluated by relative standard deviation (RSD). The stability of aesculin in spiked samples was measured under desired conditions that could reflect situations to be encountered during actual sample handling and analysis, including thawed plasma at room temperature for 8.0 h, frozen plasma at −20°C for 30 days, plasma samples after three cycles of freeze and thaw, and the processed samples kept at 4.0°C for 48 h. The stability of the analyte in stock solution was also evaluated.

2.8. Pharmacokinetic Application. Sprague-Dawley rats, weighing 265 ± 15 g, were supplied by the Experimental Animal Center of Xi'an Jiaotong University. The rats were kept in standard animal holding room at a temperature of 23 ± 2°C and relative humidity of 60 ± 10%. The animals were acclimatized to the facilities for 7 days and then fasted with free access to water for 12 h prior to each experiment. The ethics of animal experiments were in accordance with the approval of the Department of Health Guidelines in Care and Use of Animals.

Twelve rats were divided into three groups randomly ($n = 6$). The rats of one group were administered with 0.5% carboxymethylcellulose sodium salt (CMC-Na) with the dose of 5.0 mL/kg aqueous solution to form control group. For the rats of the other group, single oral dose of 5.0 mL/kg Cortex fraxini extract was administered. Blood samples were collected in heparinized eppendorf tube via the ear edge vein before dosing and subsequently at 0.0, 0.083, 0.17, 0.33, 0.50, 0.75, 1.00, 1.5, 2.0, 3.0, 4.0, 5.0, and 6.0 h after oral administration. The blood samples were centrifuged at 8000 rpm for 3.0 min to separate the plasma.

3. Results and Discussion

3.1. Optimization of Chromatographic Separation and MS/MS Conditions. The separation and ionization of aesculin and IS were affected by the composition of mobile phase. Accordingly, different ratios (80 : 20, 60 : 40, and 50 : 50) of water/methanol were used as mobile phase. The ratio of 20 : 80 of water/methanol (v : v) was used as the mobile phase regarding retention time and peak shape of aesculin and IS. Ammonium formate was applied to provide the ionic strength, and formic acid was used to guarantee an acidic environment of aesculin and IS. It was found that a mixture of water containing 5.0×10^{-3} M ammonium formate and 0.1% formic acid and methanol could obviously improve peak shape and clear the increased mass spectral intensity. This solution was finally adopted as the mobile phase because the intensities of aesculin and IS were decreased substantially when the concentrations of ammonium formate increased (10, 20, and 30 mM were investigated).

Selection of tandem mass transitions and related acquisition parameters were evaluated for the best response under positive and negative ESI mode by infusing a standard solution, via a syringe pump. It was found that the analytes mainly generated positive product ions. The transitions for analysis of aesculin and IS were accordingly produced at m/z 341.2716 → m/z 179.1043 for aesculin and m/z 248.2035 → m/z 120.9130 for IS because these two transitions were specific and had the strongest intensities. Under the optimized conditions, good chromatographic separation and mass spectral signals were achieved in the assay of the plasma sample.

3.2. Matrix Effect and Extraction Recovery. Endogenous substances could interfere with aesculin determination due to the extreme low concentration of the compound in plasma. Using an appropriate internal standard is an important approach to reduce the matrix effects. In this study, tinidazole was used as internal standard. In Table 1, all the values $(A/B \times 100)\%$ were between 94.2% and 106.4%, which means little matrix effect for aesculin and IS using the proposed method. The extraction recoveries of usnic acid from rat plasma were 97.6 ± 7.4, 95.8 ± 6.6, and 105.3 ± 4.1% at concentration levels of 40.0, 500.0.0, and 1200.0 ng/mL, respectively.

3.3. Method Validation

3.3.1. Specificity. The base peak of each mass spectrum for aesculin and IS was observed from Q1 scans during the infusion of the neat solution in positive mode. Two precursor ions, m/z 341.2716 $[M + H]^+$ for aesculin and m/z 248.3025 $[M + H]^+$ for IS, were subjected to collision-induced dissociation (CID). The product ions were recorded as m/z 179.1043 $[M\text{-glu}]^+$ and m/z 120.9130 $[M\text{-}C_4H_9SO_2]^+$, respectively. Mass transition patterns, m/z 341.2716 → 179.1043, and m/z 248.3025 → 120.9130, were selected to monitor aesculin and IS. Representative MS/MS extracted chromatograms of blank sample, low, medium, and high levels of QC samples plus plasma sample collected at 0.17 h after administration are shown in Figure 1. No endogenous peaks were found to be coeluted with the analytes, ensuring high specificity of the method.

3.3.2. Linearity and Sensitivity. Nine-point calibration curves were prepared ranging from 10.0 to 1500.0 ng/mL for aesculin. The regression parameters of slope, intercept, and correlation coefficient were calculated by $1/x$ weighted linear regression. Linearity was achieved with correlation coefficients greater than 0.9902 for all validation batches, shown in Table 2. The proposed method offered a limit of detection (LOD) of 2.0 ng/mL ($S/N = 3$) and a limit of quantitation (LOQ) of 8.0 ng/mL ($S/N = 10$), which is sensitive enough to investigate our pharmacokinetic behaviors of the compound.

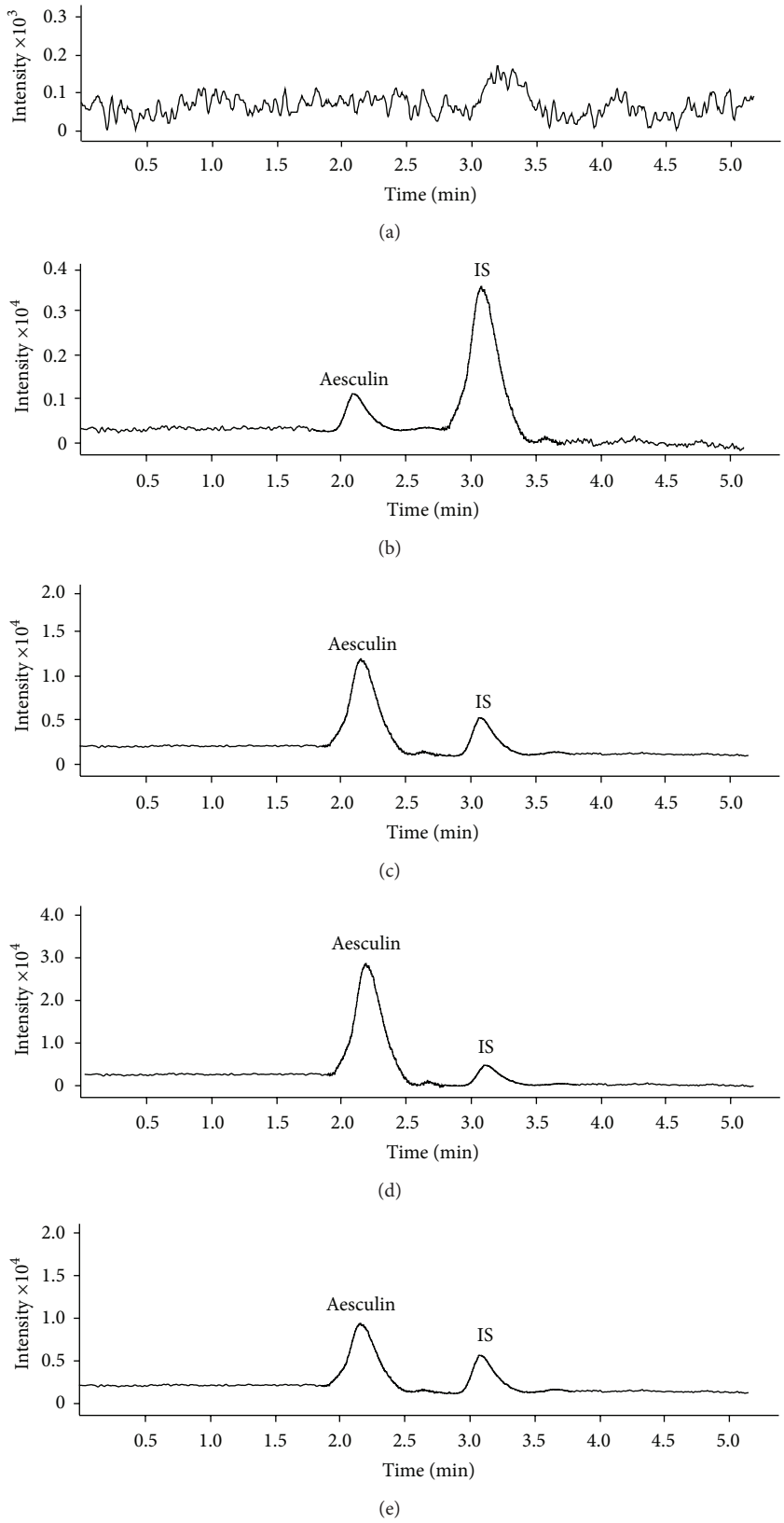

Figure 1: Representative extracted chromatograms for (a) blank plasma, (b) blank plasma containing 40.0 ng/mL aesculin and 10.0 ng/mL IS, (c) blank plasma containing 500.0 ng/mL aesculin and 10.0 ng/mL IS, (d) blank plasma containing 1200.0 ng/mL aesculin and 10.0 ng/mL IS, and (e) plasma sample collected at 0.17 after single oral dose of Cortex fraxini extract (5.0 mL/kg).

Table 1: Matrix effects and extraction recovery of aesculin and the internal standard in rat plasma.

Analytes	Concentration (ng/mL)	Matrix effects (%, $n = 6$)	CV (%)	Extraction recovery (%, $n = 5$)	CV (%)
Aesculin	40.0	98.1 ± 5.6	5.7	97.6 ± 7.4	7.6
	500.0	106.4 ± 3.8	3.6	95.8 ± 6.6	6.9
	1200.0	94.2 ± 6.9	7.3	105.3 ± 4.1	3.9
IS	10.0	96.2 ± 3.3	3.4	97.5 ± 5.8	5.9
	10.0	100.6 ± 5.2	5.2	104.7 ± 4.8	4.6
	10.0	104.2 ± 4.1	3.9	98.2 ± 3.9	4.0

Table 2: Linearity for assay of aesculin in rat plasma.

Analytical batch	Slope	Intercept	Regression equation	Correlation coefficient
1	0.0365	0.0332	$y = 0.0365x + 0.0332$	$r = 0.9902$
2	0.0384	0.0341	$y = 0.0384x + 0.0341$	$r = 0.9915$
3	0.0352	0.0337	$y = 0.0352x + 0.0337$	$r = 0.9946$
4	0.0379	0.0354	$y = 0.0379x + 0.0354$	$r = 0.9952$
5	0.0369	0.0327	$y = 0.0369x + 0.0327$	$r = 0.9929$

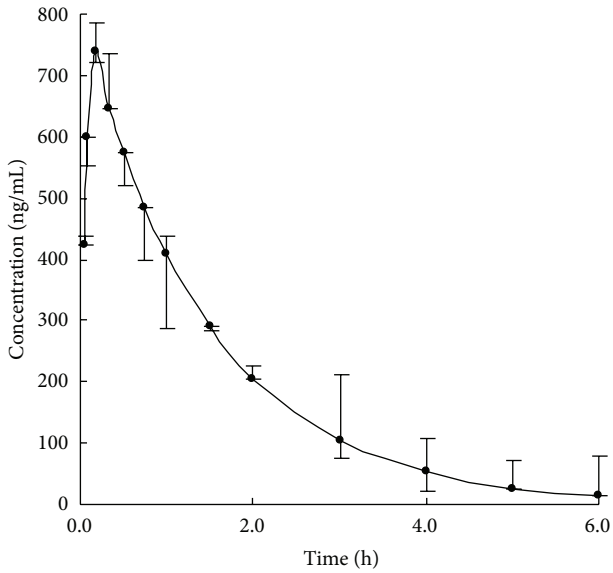

Figure 2: Mean plasma concentration-time profile of aesculin after administration of Cortex fraxini extract in rats ($n = 6$).

3.3.3. Accuracy and Precision. The accuracy and the precision were analyzed by the QC samples at three concentrations. The assay accuracy and precision results are summarized in Table 3. The data obtained was within the acceptable limits to meet the guideline for bioanalytical methods (http://www.fda.gov).

3.3.4. Stability. The stability of aesculin in plasma tested in this work implied that no significant degradation occurred at room temperature for 7.0 h and at −20°C for 20 days. The plasma samples after three freeze and thaw cycles and the processed samples kept in the autosampler (4.0°C) for 48 h were stable. The stock solutions of aesculin and IS in methanol gave a good stability at 4°C for 15 days.

3.4. Comparison with Previous Methods. Chen et al. [16] have developed a high performance liquid chromatography method for determination of aesculin in rat plasma. In the report, the limit of detection was 24.0 ng/mL and the limit of quantification was evaluated to be 57.4 ng/mL. The method in this work is believed to be more sensitive than the previous method due to lower limits of detection and quantification. Another research by the same group [17] has developed a method using high performance liquid chromatography coupled to fluorescent detection for quantification of aesculin in rabbit plasma. The method gave a total run time of near 15 min, even using complicated sample preparation. Compared with the method, the assay in this work has high analyzing speed, simple sample preparation, and high selectivity from the selective ion patterns. All the above properties enable the application of the present method in pharmacokinetic study of aesculin. than the previous method due to lower limits of detection and quantification. Another research by the same group [17] has developed a method using high performance liquid chromatography coupled to fluorescent detection for quantification of aesculin in rabbit plasma. The method gave a total run time of near 15 min, even using complicated sample preparation. Compared with the method, the assay in this work has high analyzing speed, simple sample preparation, and high selectivity from the selective ion patterns. All the above properties enable the application of the present method in pharmacokinetic study of aesculin.

3.5. Pharmacokinetics. The method was successfully applied to the pharmacokinetic study of aesculin in rats. The mean plasma concentration-time profile of aesculin after administration is shown in Figure 2. The pharmacokinetic parameters

Table 3: Intraday ($n = 5$) and interday ($n = 5$) precision and accuracy for assay of aesculin in rat plasma.

Concentration (ng/mL)	Intraday ($n = 5$)			Interday ($n = 5$)		
	Mean ± SD (ng/mL)	RSD (%)	Accuracy (%)	Mean ± SD (ng/mL)	RSD (%)	Accuracy (%)
40.0	40.2 ± 1.4	3.5	100.5	38.5 ± 1.2	3.1	96.3
500.0	487.5 ± 15.2	3.1	97.5	490.7 ± 11.6	2.4	98.1
1200.0	1226.0 ± 86.3	7.0	102.2	1217.0 ± 75.8	6.2	101.4

of aesculin were calculated by the second version of an Excel software named Drug and Statistics (Shanghai, China). The pharmacokinetic process of aesculin was confirmed to be a one-compartment open model. The maximum plasma concentration (C_{max}) was calculated to be 739.5 ± 32.4 ng/mL with a value of 0.17 ± 0.02 h for the time to reach maximum plasma concentration (t_{max}). The half-life for absorption ($t_{1/2}$) was 1.21 ± 0.03 h, providing the evidence that aesculin can exert its therapeutic effect quickly. The total exposures measured as $AUC_{(0-\infty)}$ (area under concentration-time curve) and $AUC_{(0-t)}$ were calculated to be 2120 ± 152 and 1850 ± 167 ng/mL·h. The time points for plasma collection are accordingly believed to be acceptable due to the fact that ratio of $AUC_{(0-\infty)}$ versus $AUC_{(0-t)}$ is lower than 120%. Accordingly, the proposed method is believed to be suitable to the determining aesculin in biological fluids and will probably be an alternative for pharmacokinetic study on aesculin.

4. Conclusion

A sensitive, selective, and rapid HPLC-QTOF-MS/MS assay for monitoring aesculin in rat plasma was developed. The method proves to be capable of reducing ion suppression and offering superior sensitivity with an LOQ of 10.0 ng/mL, satisfactory selectivity, and short run time less than 4.0 min. The method has been successfully applied in a pharmacokinetic study of aesculin in rat, providing an alternative for clinical determination of the compound.

References

[1] China Pharmacopoeia Committee, *Pharmacopoeia of the People'S Republic of China*, Peoples Medicinal Publishing House, Beijing, China, 2010.

[2] G. J. Xiu, *Raw Pharmacognosy*, The People Health Press, Beijing, China, 1995.

[3] C.-R. Wu, M.-Y. Huang, Y.-T. Lin, H.-Y. Ju, and H. Ching, "Antioxidant properties of Cortex fraxini and its simple coumarins," *Food Chemistry*, vol. 104, no. 4, pp. 1464–1471, 2007.

[4] W.-S. Chang, C.-C. Lin, S.-C. Chuang, and H.-C. Chiang, "Superoxide anion scavenging effect of coumarins," *American Journal of Chinese Medicine*, vol. 24, no. 1, pp. 11–17, 1996.

[5] Y. Pan, J. Zhu, H. Wang et al., "Antioxidant activity of ethanolic extract of Cortex fraxini and use in peanut oil," *Food Chemistry*, vol. 103, no. 3, pp. 913–918, 2007.

[6] J.-M. Li, X. Zhang, X. Wang, Y.-C. Xie, and L.-D. Kong, "Protective effects of cortex fraxini coumarines against oxonate-induced hyperuricemia and renal dysfunction in mice," *European Journal of Pharmacology*, vol. 666, no. 1–3, pp. 196–204, 2011.

[7] C.-J. Wang, Y.-J. Hsieh, C.-Y. Chu, Y.-L. Lin, and T.-H. Tseng, "Inhibition of cell cycle progression in human leukemia HL-60 cells by esculetin," *Cancer Letters*, vol. 183, no. 2, pp. 163–168, 2002.

[8] S. H. Duncan, H. J. Flint, and C. S. Stewart, "Inhibitory activity of gut bacteria against Escherichia coli O157 mediated by dietary plant metabolites," *FEMS Microbiology Letters*, vol. 164, no. 2, pp. 283–288, 1998.

[9] Z. Shi, X. Zhu, and H. Zhang, "Micelle-mediated extraction and cloud point preconcentration for the analysis of aesculin and aesculetin in Cortex fraxini by HPLC," *Journal of Pharmaceutical and Biomedical Analysis*, vol. 44, no. 4, pp. 867–873, 2007.

[10] L. Zhou, J. Kang, L. Fan et al., "Simultaneous analysis of coumarins and secoiridoids in Cortex Fraxini by high-performance liquid chromatography-diode array detection-electrospray ionization tandem mass spectrometry," *Journal of Pharmaceutical and Biomedical Analysis*, vol. 47, no. 1, pp. 39–46, 2008.

[11] T. You, X. Yang, and E. Wang, "End-column amperometric detection of aesculin and aesculetin by capillary electrophoresis," *Analytica Chimica Acta*, vol. 401, no. 1-2, pp. 29–34, 1999.

[12] Z. Zhang, Z. Hu, and G. Yang, "Identification and determination of aesculin and aesculetin in ash barks by capillary zone electrophoresis," *Chromatographia*, vol. 44, no. 3-4, pp. 162–168, 1997.

[13] C. Li, A. Chen, X. Chen, X. Ma, X. Chen, and Z. Hu, "Non-aqueous capillary electrophoresis for separation and simultaneous determination of fraxin, esculin and esculetin in Cortex fraxini and its medicinal preparations," *Biomedical Chromatography*, vol. 19, no. 9, pp. 696–702, 2005.

[14] T. Bo, H. Liu, and K. A. Li, "High-speed determination of aesculin and aesculetin in Cortex fraxini by micellar electrokinetic chromatography," *Chromatographia*, vol. 55, no. 9-10, pp. 621–624, 2002.

[15] L. F. Bai, H. T. Zhang, H. X. Wang et al., "Analysis of ultraviolet absorption spectrum of Chinese herbal medicine—Cortex Fraxini by double ANN," *Spectrochimica Acta Part A*, vol. 65, no. 3-4, pp. 863–868, 2006.

[16] Q. H. Chen, S. X. Hou, J. Zheng et al., "Determination of aesculin in rat plasma by high performance liquid chromatography method and its application to pharmacokinetics studies," *Journal of Chromatography B*, vol. 858, no. 1-2, pp. 199–204, 2007.

[17] Q. H. Chen, Y. Zeng, J. C. Kuang et al., "Quantification of aesculin in rabbit plasma and ocular tissues by high performance liquid chromatography using fluorescent detection: application to a pharmacokinetic study," *Journal of Pharmaceutical and Biomedical Analysis*, vol. 55, no. 1, pp. 161–167, 2011.

Hindawi Publishing Corporation
Journal of Analytical Methods in Chemistry
Volume 2013, Article ID 572896, 9 pages
http://dx.doi.org/10.1155/2013/572896

Research Article

Evaluating the Polyphenol Profile in Three Segregating Grape (*Vitis vinifera* L.) Populations

Alberto Hernández-Jiménez,[1] Rocío Gil-Muñoz,[2] Yolanda Ruiz-García,[1] Jose María López-Roca,[1] Adrián Martinez-Cutillas,[2] and Encarna Gómez-Plaza[1]

[1] *Food Science and Technology Department, Faculty of Veterinary Science, University of Murcia, Campus de Espinardo, 30071 Murcia, Spain*
[2] *Instituto Murciano de Investigación y Desarrollo Agroalimentario, Carretera La Alberca s/n, 30150 Murcia, Spain*

Correspondence should be addressed to Encarna Gómez-Plaza; encarna.gomez@um.es

Received 20 May 2013; Accepted 17 July 2013

Academic Editor: Shixin Deng

This paper explores the characteristics of the anthocyanin and flavonol composition and content in grapes from plants resulting from intraspecific crosses of *Vitis vinifera* varieties Monastrell × Cabernet Sauvignon, Monastrell × Syrah, and Monastrell × Barbera, in order to acquire information for future breeding programs. The anthocyanin and flavonol compositions of twenty-seven hybrids bearing red grapes and 15 hybrids bearing white grapes from Monastrell × Syrah, 32 red and 6 white from Monastrell × Cabernet Sauvignon, and 13 red from Monastrell × Barbera have been studied. Among the intraspecific crosses, plants with grapes presenting very high concentrations of anthocyanins and flavonols were found, indicating a transgressive segregation for this character, and this could lead to highly colored wines with an increased benefits for human health. As regards the qualitative composition of anthocyanins and flavonols, the hydroxylation pattern of the hybrids that also may influence wine color hue and stability presented intermediate values to those of the parentals, indicating that values higher than that showed by the best parental in this respect will be difficult to obtain. The results presented here can be helpful to acquire information for future breeding efforts, aimed at improving fruit quality through the effects of flavonoids.

1. Introduction

Anthocyanins are responsible for the color of red grape varieties and the wines produced from them. Flavonols are also important because they participate both in stabilizing anthocyanins in young red wines through copigmentation and in increasing the health-related properties of wine [1, 2]. Grape anthocyanins and flavonols are final products arising from the flavonoid biosynthetic pathway (Figure 1). *Vitis vinifera* varieties are characterized by the presence of 3-O-glucosides of delphinidin, peonidin, petunidin, cyanidin, and malvidin, together with their acylated derivatives [3]. The 3-O-glucosides of kaempferol, quercetin, and myricetin are the major flavonols in grapes as first reported by Cheynier and Rigaud [4] and recently confirmed by Castillo-Muñoz et al. [5], with quercetin glycosides usually being dominant [5], although a high presence of quercetin-3-O-glucuronide has also been observed in some varieties such as Petit Verdot [5, 6].

When studying grapes for winemaking, it is not only the quantity of anthocyanins that is important. The hydroxylation pattern of the B-ring of anthocyanins is one of the main structural features of flavonoids and is an important determinant of their coloration, stability, and antioxidant capacity. Trihydroxylated anthocyanins (delphinidin, petunidin, and malvidin-3-glucosides) are more stable in wines than dihydroxylated ones (cyanidin and peonidin-3-glucosides) [7]. Those with orthodiphenolic groups (cyanidin, delphinidin, and petunidin) have an enhanced susceptibility to oxidation. The methoxylated anthocyanins are also more stable. The same applies to acylated anthocyanins, since their esterification of anthocyanins promotes intramolecular aggregation or stacking, which protects the oxonium ion from decomposition [8].

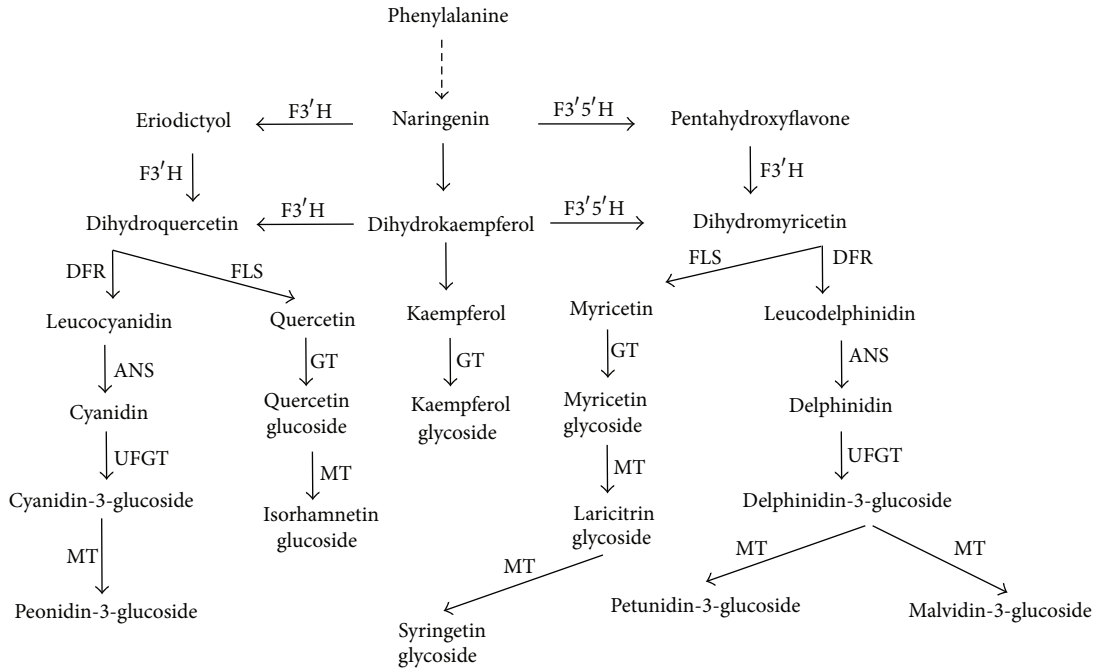

Figure 1: Flavonoid biosynthetic pathway. PAL: phenyl ammonia lyase, F3′H: flavonoid-3′-hydroxylase, F3′5′H: flavonoid-3′,5′-hydroxylase, UFGT: UDP-glucose: flavonoid 3-O-glucosyltransferase, MT: methyl transferase, DFR: dihydroxyflavanol-4-reductase, ANS: anthocyanin synthase, and FLS: flavonol synthase.

As hydroxylation of the B-ring is carried out by flavonoid-3′-hydroxylase (F3′H) and flavonoid-3′,5′-hydroxylase (F3′5′H) enzymes, the composition of anthocyanins in grape skins will be determined by the relative activities of these enzymes. At the same time, methyl transferase (MT) activity will determine the different methoxylation patterns of B ring and acyl transferase the presence of acyl derivatives. Most of these enzymes also control the synthesis of flavonols.

Plant adaptation to different environments and centuries of selection by humans has produced numerous genotypes in which the intensity of the red coloration varies extensively. A mixture of variation in anthocyanin content and the relative proportion of different anthocyanins can produce different phenotypes for skin pigmentation with consequent technological and nutritional differences [9]. Also, these differences could be a very useful chemotaxonomical tool [3].

At present, cross-breeding and bud mutation are still the most common way for developing new wine grape cultivars [10]. The determination of the mechanisms of the inheritance of the flavonoid composition could help in the election of the parentals in the breeding programs. The objective of this study therefore was to explore the characteristics of the anthocyanin and flavonol composition and content in intraspecific hybrids of Monastrell × Syrah, Monastrell × Cabernet Sauvignon, and Monastrell × Barbera, in order to acquire information for future breeding efforts aimed at improving fruit quality through the effects of flavonoids and to provide an insight into the mechanisms that control the inheritance of flavonoid characteristics among hybrids.

2. Material and Methods

A collection of plants arising from crosses from Monastrell × Syrah, Monastrell × Cabernet Sauvignon, and Monastrell × Barbera was used in this study. The study was conducted in an experimental vineyard of 1 ha located in Bullas (Murcia, SE Spain). The parentals (Monastrell, Syrah, Cabernet Sauvignon, and Barbera) were planted in 1997, whereas the seeds for the interspecific hybrids were planted in 2000. The training system was a bilateral cordon trellised to a three-wire vertical system, and drip irrigation was applied. Planting density was 2.5 m between rows and 1.25 m between vines. Two two-bud spurs (4 nodes) were left at pruning time. Grapes were sampled in 2007.

The plants derived from Monastrell self-pollination and from pollen donors other than Syrah, Cabernet Sauvignon, or Barbera were identified genetically and discarded using the microsatellite (SSR, Simple Sequence Repeat) loci segregating 1 : 1 : 1 : 1 according to Bayo-Canha et al. [11]. Total DNA was extracted from approximately 20 mg of young frozen leaves using a DNeasy Plant Mini Kit (Qiagen, Valencia, CA, USA) following the manufacturer's protocol. Genotyping was carried out as described in Adam-Blondon et al. [12]. PCR products were separated by capillary electrophoresis performed on an ABI Prism 3100 genetic analyzer (Applied Biosystems, Carlsbad, CA, USA), and the fragments were sized using GeneMapper software (Applied Biosystems, Carlsbad, CA, USA).

Grapes were harvested at a total of soluble solids content between 23 and 27°Brix. The sampling was randomly made by picking berries from the top, central, and bottom parts of

several clusters of each hybrid vine. The size of the sample was around 300 berries, which were bulked and separated in 3 subsamples of approximately 100 berries to run triplicate analyses. Grape samples were kept frozen (−20°C) until extraction and analysis.

2.1. Anthocyanin Monoglycosides and Flavonols in Berry Skins. Grapes were peeled with the help of a scalpel. Samples (2 g) were immersed in methanol (40 mL) in hermetically closed tubes and placed on a stirring plate at 150 rpm and 25°C. After 2 hours, the methanolic extracts were acidified with 5% formic acid (1 : 2 v/v), filtered through 0.2 μm PTFE filters, and analysed by HPLC.

2.2. Identification and Quantification of Anthocyanins. The HPLC analyses were performed on a Waters 2695 liquid chromatograph (Waters, PA, USA), equipped with a Waters 2996 diode array detector and a Primesep B2 column (Sielc, Illinois, USA), 25 × 0.4 cm, 5 μm particle size, using as solvents water plus 5% formic acid (solvent A) and HPLC grade acetonitrile (solvent B) at a flow rate of 0.8 mL min^{-1}. Elution was performed with a gradient starting with 5% B to reach 9% B at 28 min, 13% B at 30 min, 21% B at 52 min, 24% B at 65 min, and 70% B at 75 min, maintaining this gradient for 5 minutes. Chromatograms were recorded at 520 nm (anthocyanins) and 360 nm (flavonols).

Identification of the compounds was carried out by comparing their UV spectra recorded with the diode array detector and those reported in the literature. Also, an HPLC-MS analysis was made to confirm the identity of each peak. An LC-MSD-Trap VL-01036 liquid chromatograph-ion trap mass detector (Agilent Technologies, Waldbronn, Germany) equipped with an electrospray ionization (ESI) system was used. Elution was performed in the HPLC analysis conditions described previously, with a flow rate of 0.8 mL min^{-1}. The heated capillary and voltage were maintained at 350°C and 4 kV, respectively. Mass scans (MS) were measured from m/z 100 up to m/z 800.

Anthocyanins were quantified at 520 nm as malvidin-3-glucoside, using malvidin-3-glucoside chloride as external standard (Extrasynthèse, Genay, France). Flavonols were quantified at 360 nm as quercetin-3-glucoside, using this compound as external standard (Sigma, Missouri, USA).

2.3. Statistical Data Treatment. All the analyses were performed with the statistical package Statgraphics 5.1.

3. Results and Discussion

For this study, 27 hybrids bearing red grapes and 15 hybrids bearing white grapes from Monastrell × Syrah, 32 red and 6 white from Monastrell × Cabernet Sauvignon, and 13 red from Monastrell × Barbera were studied. The presence of white hybrids in Monastrell × Cabernet Sauvignon and Monastrell × Syrah indicates the heterozygous nature of the parentals in regard to genes controlling anthocyanin synthesis, whereas Barbera, being homozygous [13], does not produce hybrids bearing white grapes. Boss et al. [14] and Kobayashi et al. [15] showed that expression of the UDP-glucose: flavonoid 3-O-glucosyltransferase (UFGT) gene is critical for anthocyanin biosynthesis in grape. Experiments with the berry skins of white and red cultivars revealed that the UFGT gene was expressed in all the red cultivars but not in the white ones whereas the other genes involved in anthocyanin biosynthesis (Figure 1) are expressed in both white and red cultivars. The presence or absence of the enzyme UFGT is controlled by Myb-related regulatory genes, and the insertion of the retroelement *Gret1* in the promoter region of *VvmybA1* gene appears to be associated with white-fruited cultivars when present in a homozygous state. Pigmented cultivars possess at least one allele at the *VvmybA1* locus not containing this large retroelement [13, 16], as is the case of parentals of this study.

Table 1 shows the results of the anthocyanin analysis for the studied grapes and Figure 2 the range of concentrations among the hybrids. Syrah grapes contained higher concentration of anthocyanins than Monastrell grapes. The mean concentration in their hybrid grapes (16.31 mg/g fresh skin) was slightly higher than in Syrah (15.06 mg/g fresh skin), and the maximum value reached by the grapes of one seedling (39.49 mg/g fresh skin) was twice the value found in Syrah. Cabernet Sauvignon and Barbera grapes also showed higher concentration, of anthocyanins than Monastrell and were similar to that of Syrah grapes. The mean values of anthocyanin content in the grapes of their seedlings were slightly lower than in Cabernet Sauvignon and Barbera (14.42 and 12.08 mg/g fresh skin respectively) and higher than that shown by Monastrell grapes (7.40 mg/g fresh skin), and, again, the maximum value found in their seedlings was double that of Cabernet Sauvignon and Barbera grapes. Many hybrids presented grapes with much higher concentration than their parentals as can be seen in Figure 2. The appearance of a large number of hybrids in which the anthocyanin concentration is not within the range of concentration of their parental phenotypes is called transgressive segregation, frequent in intraspecific crosses and in domesticated populations. The occurrence of the segregation of a given trait manifested mainly in one direction (as happens in our case, most of the hybrids showing higher values of anthocyanin concentration than the parentals) may imply that the trait has undergone fairly constant directional selection or a certain overdominance of the genes controlling phenolic synthesis [17, 18]. Similar results were found by Liang et al. [10] in grapes, but our findings differ from those of Ju et al. [19] in apples that found that crossing between two red-fruited apple cultivars produced less colored progeny. A previous work exploring the proanthocyanidin content of Monastrell × Syrah hybrid grapes also reported this type of segregation for this character [20].

As stated previously, the presence of the enzyme UFGT is necessary for anthocyanin biosynthesis. However, the biosynthesis of the different anthocyanin precursors is driven upstream of the enzyme UFGT by the activity of F3′H and F3′5′H enzymes, which add either a single hydroxyl group or two to dihydrokaempferol (Figure 1). Once converted to dihydroquercetin or dihydromyricetin, these intermediates flow through common downstream enzymes to form

Table 1: Mean values ($n = 3$) of the anthocyanin profile and total anthocyanin content (mg/g fresh skin) in Monastrell, Syrah and Cabernet, Sauvignon grapes and their hybrids.

	% del.	% cyan.	% pet.	% peon.	% malv.	% nonacylated	% acylated	% dihydrox.	% trihydrox.	Total (mg/g)
Monastrell										
Mean	12.5	13.7	10.0	20.0	39.7	55.2	44.8	37.7	62.3	7.40
Syrah										
Mean	7.2	3.6	8.1	10.9	68.1	49.6	50.3	16.7	83.3	15.06
CS										
Mean	9.6	5.2	10.1	7.4	67.7	45.9	54.1	12.6	87.4	15.07
Barbera										
Mean	9.8	3.1	13.9	4.7	68.6	65.6	34.3	7.7	92.3	14.02
Mon. × Sy. (27)[a]										
Mean	10.0	7.1	8.6	15.4	54.8	43.2	56.8	26.5	73.4	16.31
Minimum	5.7	3.2	6.4	6.5	29.5	46.2	29.7	13.2	46.2	3.86
Maximum	24.3	15.4	13.9	37.5	72.7	70.2	71.3	53.7	86.8	39.49
Mon. × CS. (32)[b]										
Mean	12.4	6.0	13.3	10.5	57.8	52.5	47.2	16.5	83.5	14.44
Minimum	7.5	3.5	9.4	5.6	44.4	35.2	31.3	9.5	68.9	4.87
Maximum	23.4	12.1	20.3	21.5	68.5	68.6	64.7	31.1	90.5	28.67
Mon. × Bar. (13)[c]										
Mean	10.9	7.7	13.3	16.2	51.9	72.0	28.0	23.9	76.1	12.08
Minimum	4.1	1.1	9.0	4.4	31.7	41.5	10.1	6.7	55.2	1.61
Maximum	17.0	14.6	19.7	36.4	77.9	89.8	58.5	44.7	93.3	27.88

[a,b,c]The number in parenthesis represents the number of hybrids for each crossing.
% del.: percentage of delphinidin derivatives, % cyan.: percentage of cyanidin derivatives, % pet.: percentage of petunidin derivatives, % peon.: percentage of peonidin derivatives, % malv.: percentage of malvidin derivatives, % nonacylated: percentage of nonacylated anthocyanins, % acylated.: percentage of acylated anthocyanins, % dihydrox.: percentage of dihydroxylated anthocyanins, % trihydrox.: percentage of trihydroxylated anthocyanins, and Total (mg/g): total anthocyanin content (mg per g of skin).

disubstituted and trisubstituted anthocyanins, when UFGT is expressed, and to form other polyphenols (flavanols, flavonols) at different developmental stages. All the studied hybrids bearing red grapes synthesised all five anthocyanins (the dihydroxylated cyaniding, peonidin-3-glucosides, the trihydroxylated delphinidin, petunidin, and malvidin-3-glucosides), together with their acylated derivatives. This means that all the parentals and the hybrids expressed functional F3′H and F3′5′H genes for the synthesis of 3′4′-OH and 3′4′5′-OH anthocyanins, as well as methyltransferases (*MT*) for the methylation of primary anthocyanins. As regards the percentage of the different anthocyanins in the different parentals, Monastrell grapes were characterized by a high percentage of cyanidin, suggesting a lower F3′5′H activity than in the other varieties. A low expression of F3′5′H has been associated with cyanidin-based anthocyanins in grape leafs [21]. The percentages of malvidin-based anthocyanins in Monastrell did not exceed 40%, so the total percentage of trihydroxylated anthocyanins was low. The percentage of trihydroxylated anthocyanins reached 83% in Syrah grapes, 87.4% in Cabernet Sauvignon grapes, and 92.3% in Barbera grapes. The percentage of trihydroxylated anthocyanins was even higher in some Monastrell × Cabernet Sauvignon and Monastrell × Barbera hybrids, reaching values as high as 90.5% and 93%, respectively. The mean value of the percentage of trihydroxylated anthocyanins in the hybrid grapes is close to the mean value between both parentals. The segregation can be fitted to a normal distribution, and a very low number of hybrids presented higher or lower values than in the parentals, as can be seen in Figure 3. These results were similar to those obtained during the first screening of the anthocyanin profile in Monastrell × Cabernet Sauvignon grapes [22]. In spite of the presence of all anthocyanin biosynthetic enzymes in all the investigated hybrids (since all the possible structures were found), a genotype-specific regulation of the structural genes along the core pathway and at the main branching points is presumed to underlie the observed methoxylation and hydroxylation variations among the grapes from the parentals and those of their hybrid plants.

With regard to the percentage of anthocyanin acylation, Barbera grapes showed the lowest percentage of acylation (34.3%), followed by Monastrell (44.8%), and Cabernet Sauvignon showed the highest percentages (54%). The mean values of the percentage of acylated anthocyanins for Monastrell × Cabernet Sauvignon hybrids were 47%, 56.8% for Monastrell × Syrah (higher than the percentage found in Syrah) while the hybrid grapes from Monastrell × Barbera showed the lowest percentages of acylation (28%). As in the case of the anthocyanin concentration data, there was a tendency towards higher values of acylation in the hybrids, and no hybrid contained only nonacylated anthocyanins.

As regards flavonols (Table 2), these flavonoids were present in both white and red grapes. We could identify mono- (kaempferol), di- (quercetin and isorhamnetin),

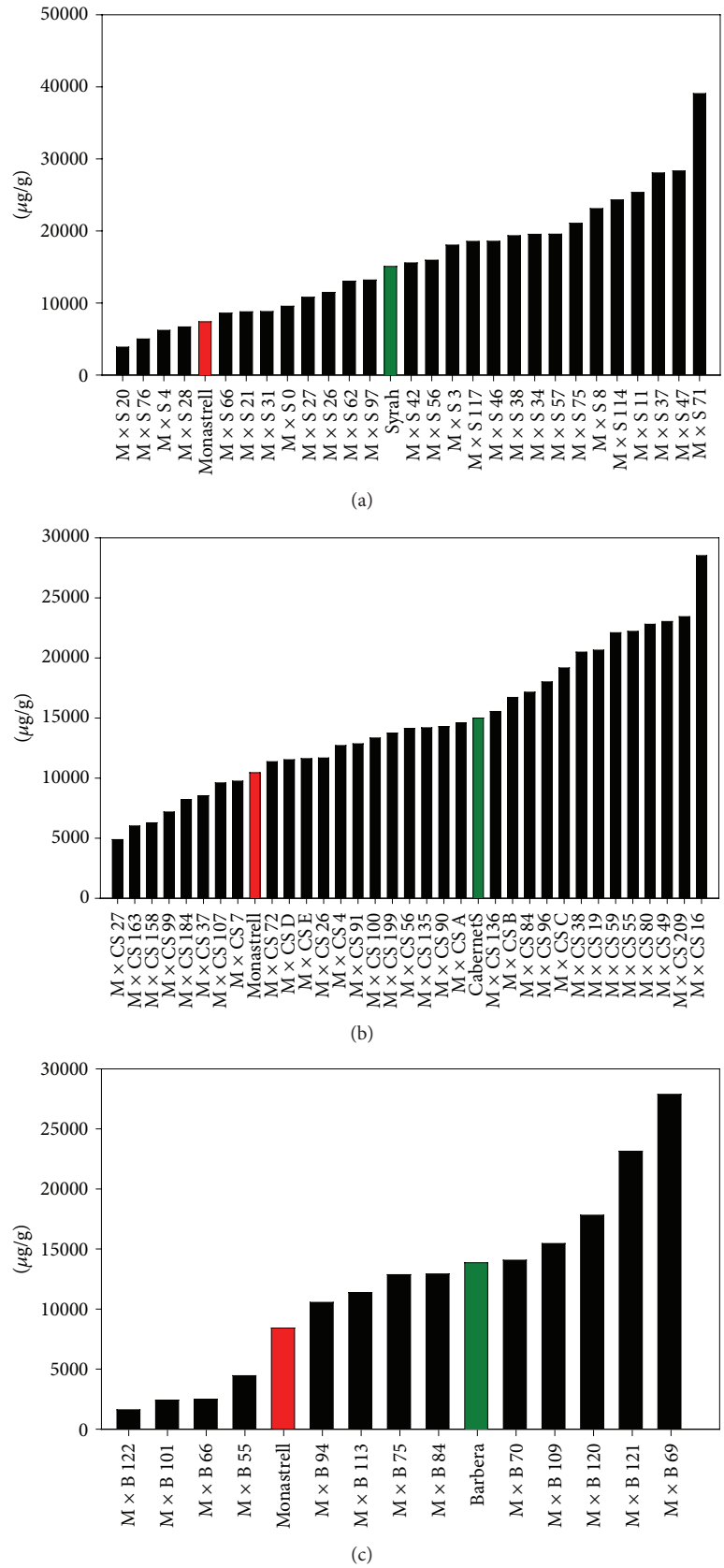

Figure 2: Concentration of anthocyanins in Monastrell × Syrah (a), Monastrell × Cabernet Sauvignon (b), and Monastrell × Barbera (c) hybrid grapes (each bar represents the mean value of three samples).

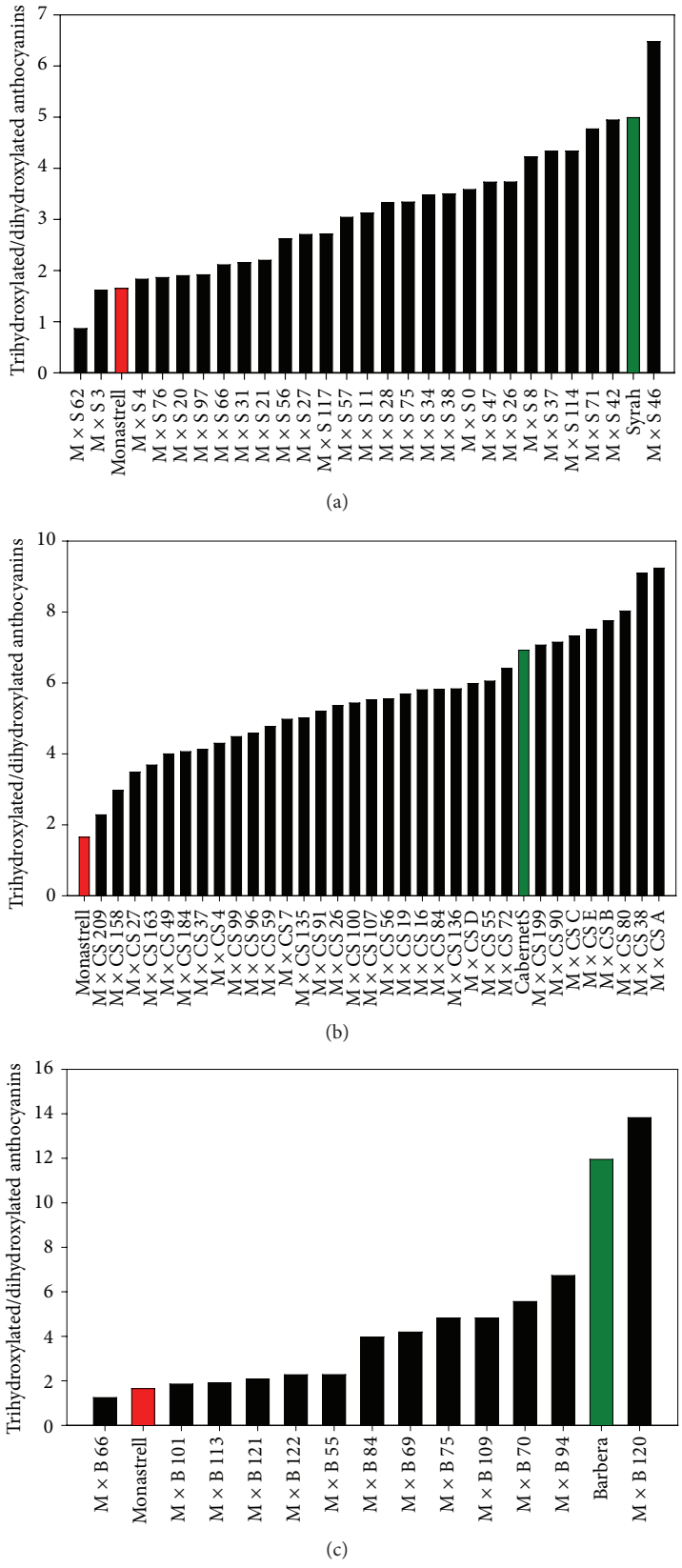

Figure 3: Trihydroxylated/dihydroxylated anthocyanins ratios in Monastrell × Syrah (a), Monastrell × Cabernet Sauvignon (b), and Monastrell × Barbera (c) hybrid grapes.

Table 2: Mean values of the flavonol profile and total flavonol content (mg/g fresh skin) in Monastrell, Syrah, and Cabernet Sauvignon grapes and their hybrids ($n = 3$).

	% monohydr.	% dihydr.	% trihydrox.	Total
Monastrell				
Mean	10.9	70.7	18.4	0.56
Syrah				
Mean	13.4	44.2	42.4	0.73
CS.				
Mean	14.7	44.6	40.7	0.19
Barbera				
Mean	4.3	53.3	42.4	0.49
Red hybrids				
Mon. × Sy.				
Mean	10.4	52.4	37.2	0.73
Minimum	5.3	36.3	16.5	0.18
Maximum	16.0	72.6	55.0	1.83
Mon. × CS.				
Mean	11.3	51.1	37.6	0.37
Minimum	5.0	35.2	20.3	0.11
Maximum	20.9	65.0	58.3	0.78
Mon. × Bar.				
Mean	9.4	61.9	28.7	0.42
Minimum	4.7	42.9	8.7	0.12
Maximum	13.6	83.9	43.4	1.39
White hybrids				
Mon. × Sy.				
Mean	13.4	84.1	2.4	0.35
Minimum	4.1	74.6	0.6	0.08
Maximum	23.7	94.7	7.2	1.28
Mon. × CS.				
Mean	20.0	74.8	5.1	0.08
Minimum	16.8	68.9	0.9	0.02
Maximum	25.9	78.4	12.7	0.18

% monohydrox.: percentage of monohydroxylated flavonols, % dihydrox: percentage of dihydroxylated flavonols, % trihydrox.: percentage of trihydroxylated flavonols, Total: total flavonol content (mg per g of skin).

and trihydroxylated (myricetin, laricitrin, and syringetin) flavonol glycosides (glucosides, glucoronides, and small quantities of galactosides). In red grapes, the monohydroxylated flavonols represented the lowest percentage, especially in Barbera grapes (4.3%). Monastrell grapes presented a very high percentage of dihydroxylated flavonols (70.7%), much higher than in the other varieties and, therefore, a lower percentage of trihydroxylated flavonols whereas Barbera, Syrah, and Cabernet Sauvignon grapes reached a percentage of trihydroxylated flavonols of around 45–50%. This fact indicates lower F3′5′H activity in Monastrell grapes, as also observed for the anthocyanins.

As regards the flavonol content, Cabernet Sauvignon grapes showed low concentrations of flavonols and Monastrell and Syrah much higher concentrations while the highest value was found in red grapes from a hybrid plant from Monastrell × Syrah (Table 2, Figure 4), reaching values as high as 1.83 mg/g of skin. In the hybrids bearing white grapes, a lower concentration of flavonols was measured compared with that of the hybrids bearing red grapes. Azuma et al. [23, 24] stated that Myb genes, besides the regulation of the UFGT expression, appear to enhance the expression of all the genes involved in the anthocyanin biosynthesis pathway because the transcription of all anthocyanin biosynthesis genes appears to be slightly activated, which would explain the higher concentration of flavonols in red grapes. Also, in these white skinned grapes, trihydroxylated flavonols were barely present. Mattivi et al. [25], studying the flavonol profile of several grape varieties, did not detect trihydroxylated flavonols in white grapes. Bogs et al. [26] did not find significant expression of F3′5′H and UFGT in white grape varieties, which suggests a related regulation of F3′5′H and UFGT during berry ripening and justifies the almost null presence of trihydroxylated flavonols in white grapes. F3′5′H was detected in white grapes var. Chardonnay but prior to veraison [26] since it is needed for flavanol biosynthesis, which seems to be controlled differently; indeed, no differences in the percentage of trihydroxylated flavanols were observed between the red and white grapes arising from the cross of Monastrell × Syrah [20]. However, other studies stated that flavonol synthase (FLS) was not upregulated when UFGT was expressed and that the increase in flavonols in red grapes was a consequence of an increase flux through the flavonoid pathway [27].

4. Conclusions

The study of the anthocyanin and flavonol profiles of the grapes from the hybrid plants can be useful for a targeted informative metabolomic analysis [28], a tool for selecting promising grapes according to their profile and/or content.

Seedlings with grapes presenting very high concentrations of anthocyanins and flavonols can be expected from intraspecific crosses, and these resulting grapes could lead to highly colored wines, with increased health-related properties. In this way, three plants arising from Monastrell × Syrah (hybrids 8, 37, and 71) presented anthocyanin and flavonol concentrations higher than 20 and 1 mg/g fresh skin, respectively (Figures 2 and 4). Also, four plants arising from Monastrell × Cabernet Sauvignon (hybrids 38, 59, 55, and 80) and two from Monastrell × Barbera (hybrid plants 120, 121) showed anthocyanin values higher than 20 mg/g fresh skin accompanied with high concentration of flavonols (Figures 2 and 4). The hydroxylation pattern, which also influences wine color and its stability, will be strongly influenced by the parentals pattern since values higher than that shown by the best parental in this respect will be difficult to obtain. Also, in the case of the crosses between heterozygous parentals (Monastrell, Cabernet Sauvignon, and Syrah) hybrids bearing white grapes can be obtained, some of them with a high concentration of flavonols, that could be of importance in the health properties of this fruit and its derived products, such as the wine. The information obtained in this study should be helpful for selecting parentals for breeding programs.

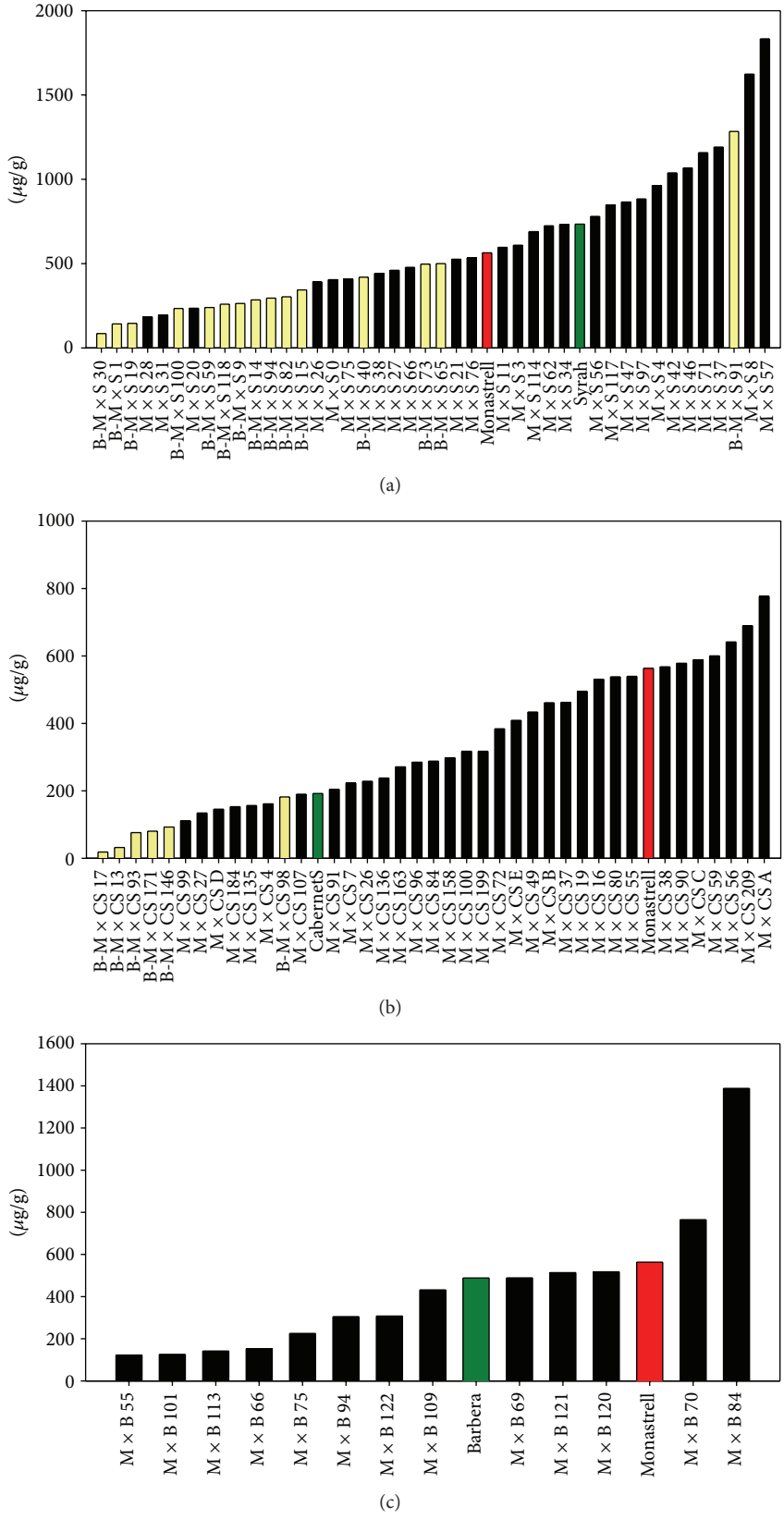

Figure 4: Concentration of flavonols in Monastrell × Syrah (a), Monastrell × Cabernet Sauvignon (b), and Monastrell × Barbera (c) hybrid grapes (yellow bars indicate white grape bearing hybrids).

Acknowledgment

This work was made possible by financial assistance of the Ministerio de Ciencia e Innovación, Project AGL2006-11019.

References

[1] F. Alén-Ruiz, M. S. García-Falcón, M. C. Pérez-Lamela, E. Martínez-Carballo, and J. Simal-Gándara, "Influence of major polyphenols on antioxidant activity in Mencia and Brancellao red grapes," *Food Chem*, vol. 113, pp. 53–60, 2008.

[2] S. C. Forester and A. L. Waterhouse, "Metabolites are key to understanding health effects of wine polyphenolics," *Journal of Nutrition*, vol. 139, no. 9, pp. 1324S–1831S, 2009.

[3] A. Ortega-Regules, I. Romero-Cascales, J. M. López-Roca, J. M. Ros-García, and E. Gómez-Plaza, "Anthocyanin fingerprint of grapes: environmental and genetic variations," *Journal of the Science of Food and Agriculture*, vol. 86, no. 10, pp. 1460–1467, 2006.

[4] V. Cheynier and J. Rigaud, "HPLC separation and characterization of flavonols in the skins of *Vitis vinifera* var Cinsault," *American Journal of Enology and Viticulture*, vol. 37, pp. 248–252, 1986.

[5] N. Castillo-Muñoz, S. Gómez-Alonso, E. García-Romero, and I. Hermosín-Gutiérrez, "Flavonol profiles of *Vitis vinifera* red grapes and their single-cultivar wines," *Journal of Agricultural and Food Chemistry*, vol. 55, no. 3, pp. 992–1002, 2007.

[6] N. Castillo-Muñoz, S. Gómez-Alonso, E. García-Romero, M. V. Gómez, A. H. Velders, and I. Hermosín-Gutiérrez, "Flavonol 3-O-glycosides series of *Vitis vinifera* Cv. Petit Verdot red wine grapes," *Journal of Agricultural and Food Chemistry*, vol. 57, no. 1, pp. 209–219, 2009.

[7] P. Sarni, H. Fulcrand, V. Souillol, J. M. Souquet, and V. Cheynier, "Mechanisms of anthocyanin degradation in grape must like model solutions," *Journal of the Science of Food and Agriculture*, vol. 69, no. 3, pp. 385–391, 1995.

[8] C. Malien-Aubert, O. Dangles, and M. J. Amiot, "Color stability of commercial anthocyanin-based extracts in relation to the phenolic composition. Protective effects by intra- and intermolecular copigmentation," *Journal of Agricultural and Food Chemistry*, vol. 49, no. 1, pp. 170–176, 2001.

[9] H. Chang, H. C. Eun, and S. C. Hyang, "Quantitative Structure-Activity Relationship (QSAR) of antioxidative anthocyanidins and their glycosides," *Food Science and Biotechnology*, vol. 17, no. 3, pp. 501–507, 2008.

[10] Z. Liang, C. Yang, J. Yang et al., "Inheritance of anthocyanins in berries of *Vitis vinifera* grapes," *Euphytica*, vol. 167, no. 1, pp. 113–125, 2009.

[11] A. Bayo-Canha, J. I. Fernández-Fernández, A. Martínez-Cutillas, and L. Ruiz-García, "Phenotypic segregation and relationships of agronomic traits in Monastrell × Syrah wine grape progeny," *Euphytica*, vol. 186, pp. 393–407, 2012.

[12] A. F. Adam-Blondon, C. Roux, D. Claux, G. Butterlin, D. Merdinoglu, and P. This, "Mapping 245 SSR markers on the *Vitis vinifera* genome: a tool for grape genetics," *Theoretical and Applied Genetics*, vol. 109, no. 5, pp. 1017–1027, 2004.

[13] A. R. Walker, E. Lee, J. Bogs, D. A. J. McDavid, M. R. Thomas, and S. P. Robinson, "White grapes arose through the mutation of two similar and adjacent regulatory genes," *Plant Journal*, vol. 49, no. 5, pp. 772–785, 2007.

[14] P. K. Boss, C. Davies, and S. P. Robinson, "Analysis of the expression of anthocyanin pathway genes in developing *Vitis vinifera* L. cv Shiraz grape berries and the implications for pathway regulation," *Plant Physiology*, vol. 111, no. 4, pp. 1059–1066, 1996.

[15] S. Kobayashi, M. Ishimaru, K. Hiraoka, and C. Honda, "Myb-related genes of the Kyoho grape (Vitis labruscana) regulate anthocyanin biosynthesis," *Planta*, vol. 215, no. 6, pp. 924–933, 2002.

[16] D. Lijavetzky, L. Ruiz-García, J. A. Cabezas et al., "Molecular genetics of berry colour variation in table grape," *Molecular Genetics and Genomics*, vol. 276, no. 5, pp. 427–435, 2006.

[17] M. C. de Vicente and S. D. Tanksley, "QTL analysis of transgressive segregation in an interspecific tomato cross," *Genetics*, vol. 134, no. 2, pp. 585–596, 1993.

[18] L. H. Rieseberg, M. A. Archer, and R. K. Wayne, "Transgressive segregation, adaptation and speciation," *Heredity*, vol. 83, no. 4, pp. 363–372, 1999.

[19] Z. Ju, C. Liu, Y. Yuan, Y. Wang, and G. Liu, "Coloration potential, anthocyanin accumulation, and enzyme activity in fruit of commercial apple cultivars and their F1 progeny," *Scientia Horticulturae*, vol. 79, no. 1-2, pp. 39–50, 1999.

[20] A. Hernández-Jiménez, E. Gómez-Plaza, A. Martínez-Cutillas, and J. A. Kennedy, "Grape skin and seed proanthocyanidins from Monastrell × Syrah grapes," *Journal of Agricultural and Food Chemistry*, vol. 57, no. 22, pp. 10798–10803, 2009.

[21] H. Kobayashi, S. Suzuki, F. Tanzawa, and T. Takayanagispi, "Low expression of flavonoid 3',5'-hydroxylase (F3',5'H) associated with cyanidin-based anthocyanins in grape leaf," *American Journal of Enology and Viticulture*, vol. 60, no. 3, pp. 362–367, 2009.

[22] E. Gómez-Plaza, R. Gil-Muñoz, A. Hernández-Jiménez, J. M. López-Roca, A. Ortega-Regules, and A. Martínez-Cutillas, "Studies on the anthocyanin profile of *Vitis vinifera* intraspecific hybrids (Monastrell × Cabernet Sauvignon)," *European Food Research and Technology*, vol. 227, no. 2, pp. 479–484, 2008.

[23] A. Azuma, S. Kobayashi, N. Mitani et al., "Genomic and genetic analysis of Myb-related genes that regulate anthocyanin biosynthesis in grape berry skin," *Theoretical and Applied Genetics*, vol. 117, no. 6, pp. 1009–1019, 2008.

[24] A. Azuma, S. Kobayashi, H. Yakushiji, M. Yamada, N. Mitani, and A. Sato, "VvmybA1 genotype determines grape skin color," *Vitis*, vol. 46, no. 3, pp. 154–155, 2007.

[25] F. Mattivi, R. Guzzon, U. Vrhovsek, M. Stefanini, and R. Velasco, "Metabolite profiling of grape: flavonols and anthocyanins," *Journal of Agricultural and Food Chemistry*, vol. 54, no. 20, pp. 7692–7702, 2006.

[26] J. Bogs, A. Ebadi, D. McDavid, and S. P. Robinson, "Identification of the flavonoid hydroxylases from grapevine and their regulation dining fruit development," *Plant Physiology*, vol. 140, no. 1, pp. 279–291, 2006.

[27] F. Quattrocchio, A. Baudry, L. Lepiniec, and E. Grotewold, "The regulation of flavonoid biosynthesis," in *The Science of Flavonoids*, E. Grotewold, Ed., pp. 97–122, Springer, New York, NY, USA, 2008.

[28] J. M. Cevallos-Cevallos, J. I. Reyes-De-Corcuera, E. Etxeberria, M. D. Danyluk, and G. E. Rodrick, "Metabolomic analysis in food science: a review," *Trends in Food Science and Technology*, vol. 20, no. 11-12, pp. 557–566, 2009.

Hindawi Publishing Corporation
Journal of Analytical Methods in Chemistry
Volume 2013, Article ID 817091, 5 pages
http://dx.doi.org/10.1155/2013/817091

Research Article

Reliable HPLC Determination of Aflatoxin M1 in Eggs

Mostafa M. H. Khalil,[1] Ahmed M. Gomaa,[2] and Ahmed Salem Sebaei[2]

[1] *Chemistry Department, Faculty of Science, Ain Shams University, Cairo 11566, Egypt*
[2] *QCAP Laboratory, Agriculture Research Center, Ministry of Agriculture, Giza 12311, Egypt*

Correspondence should be addressed to Ahmed Salem Sebaei; ahsebaei@gmail.com

Received 29 May 2013; Revised 20 June 2013; Accepted 9 July 2013

Academic Editor: Jian Yang

Aflatoxin M1 is the foremost metabolite of aflatoxin B1 in humans and animals, which may be present in animal products from animals fed with aflatoxin B1 contaminated feed. In this study a high performance liquid chromatography method for determination of aflatoxin M1 in eggs was described. The egg samples were diluted with warmed water and the toxin was immunoextracted followed by fluorescence detection. The average recovery of aflatoxin M1 at the three different levels 0.05, 0.1, and 0.5 μg/kg varied between 87% and 98%. The method is linear from the limit of quantification 0.05 μg/kg up to 3 μg/kg levels. This method is intended for aflatoxin M1 analyses in eggs simply with minimum toxin lose, excellent recovery, and accurate results with the limit of detection 0.01 μg/kg.

1. Introduction

Mycotoxins are toxins produced by molds that cause diseases called mycotoxicosis [1]. Aflatoxins, the most common mycotoxins, are toxic metabolites produced by certain fungi that can occur in foods and feeds. Aflatoxin M1 (AFM1) is usually considered to be a detoxication byproduct of aflatoxin B1 and it is also the hydroxylated metabolite present in animal products that eat foods containing the aflatoxin B1 toxin. Aflatoxin M1 is cytotoxic and its acute toxicity is similar to that of aflatoxin B1 [2] and was classified in Group 2B as possibly carcinogenic to humans [3]. AFM1 is very slightly soluble in water, freely soluble in moderately polar organic solvents and insoluble in non-polar solvents. AFM1 is unstable to ultraviolet light in the presence of oxygen, pH (<3, >10) and oxidizing agents. On the other hand AFM1 has an intensely fluorescent in ultraviolet light [4]; its structural formula is given in Figure 1. Processing and storage cause a little effect on AFM1 content in milk and milk products [2, 5, 6].

AFM1 has been found worldwide in a range of animal products, including milk and milk products types, eggs, meat, and meat products [7–14].

Several chromatographic methods for AFM1 determination in various commodities include ELISA and flow-injection immunoassay system [15–17], HPLC methods with solid phase and immunoaffinity separations [18, 19], and other chromatographic post column, mass, and tandem mass spectrometry detection [20–22]. This study develops an HPLC method using immunoaffinity column with rapid and reasonable high test recovery comparable with other intended methods of analyses.

2. Materials and Methods

2.1. Chemicals and Materials. All chemicals and reagents were of HPLC and analytical grade. Deionized water that was used throughout the experiments was generated by Milli-Q A10 FOCN53824k. Methanol and acetonitrile were (Labscan) (HPLC), with assay >99%. Standard of aflatoxin M1 (>98%) solution and Visiprep SPE vacuum manifold were purchased from Sigma Aldrich. Afla M1 immunoaffinity column was purchased from VICAM for HPLC aflatoxin M1 analysis (G1007). All performance parameters and statistical experiments were applied on chicken eggs samples.

2.2. Standard and Calibration Preparation. 1 mL of 10 μg/mL of AFM1 in acetonitrile was diluted in 10 mL volumetric flask with acetonitrile to obtain 1 μg/mL as a working solution. Stock and working solution were kept in freezer at −20°C,

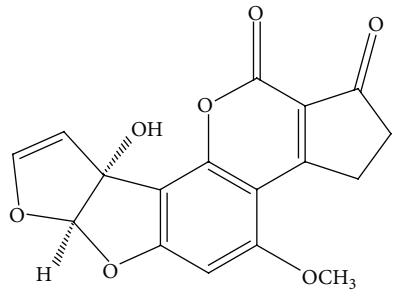

M1: $C_{17}H_{12}O_7$ Mol.wt: 328.3

Figure 1: Structural formula for aflatoxin M1.

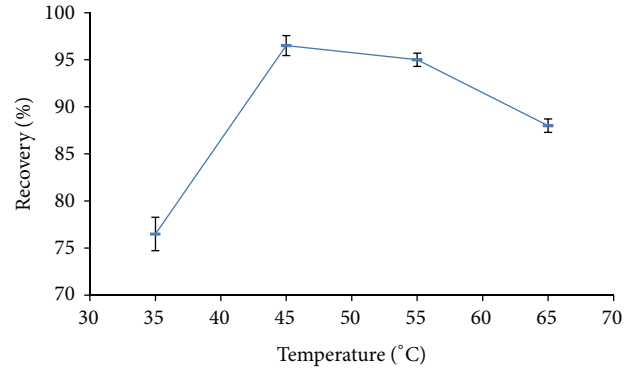

Figure 2: Effect of various extraction temperatures on AFM1 recovery (mean ± SD, $n = 2$).

the expiry date of the standard as indicated in the certificate of analysis. 0.05, 0.1, 0.5, 1.0 and 10 μg/L are prepared by diluting the working standard in acetonitrile : water (30 : 70 v/v), 100 μL of the solution was subjected to HPLC analysis and the correlation coefficient must be greater than 0.99.

2.3. Sample Preparation. 5 grams of well-homogenized egg was added into 250 mL plastic bottle and 80 mL water added to the plastic bottle and the mixture warmed before analysis to 45°C for 30 min and centrifugated at 4000 rpm for 10 min. After filtration of the aliquot over small piece of cotton to separate fat (upper) layer from defatted phase, defatted solution passed completely through Afla M1 affinity column at a rate of about 1-2 drops/second until air comes through column. It should take 20 min for egg to flow through the column. The flow slowed down using the stopcock. Column was removed from plastic syringe barrel then 10 mL of purified water added through the column for washing with a rate of about 1-2 drops/second. Affinity column was eluted by passing 1.5 mL acetonitrile: methanol (60 : 40 v/v) through column at a rate of about 2-3 drops/second and collecting all of the sample elution (1.5 mL) in glass cuvette then 0.5 mL purified water through column at the same rate and collecting all of the sample eluation (1.5 + 0.5 mL) in the same glass cuvette (2 mL total volume). Vortex used to homogenize the eluation and 100 μL of it were injected onto HPLC.

2.4. HPLC Analysis. High performance liquid chromatography instrument model HP Agilent 1200 series from Germany equipped with quaternary pump (G1311A), vacuum degasser (G1379B), autosampler (G1313A), and fluorescence detector Agilent 1260 infinity/1200 series (G1321A), analytical column: Agilent Eclipse plus C18 5 μm 4.6 × 250 mm. Software: Chemistation for LC, Rev. B. 04.03 [16]. HPLC-pump flow rate: 0.8 mL min^{-1}. AFM1 mobile phase : acetonitrile 30 : water 60 : methanol 10 (v/v/v). Detector parameters: fluorescence detector at (360 nm excitation, 440 nm emission).

2.5. Statistical Analysis. The method described was developed and optimized for all procedure steps with statistical treatments that enhance and optimize the test recovery, minimize time and reagents, and reduce matrix interferences as possible. Firstly AFM1 statistically optimized to be extracted in one rapid and efficient step. Regarding that eggs considered to be one of the most important food and very heavy and difficult matrix for analytical chemistry separation techniques, we secondly minimize the matrix as possible using the most prober immunoaffinity separation criteria. Finally AFM1 peak was chromatographically separated well.

3. Results and Discussion

3.1. Optimization of the HPLC Determination

3.1.1. Extraction. AFM1 contamination been reported in egg samples [23, 24], so a rapid and simple HPLC method was developed in this study for AFM1 determination in eggs. Relatively polar solvents are the most efficient solvents that have been used for extracting mycotoxins and water offers higher extraction efficiencies in mixtures, by increasing penetration of the organic solvent [25, 26]. Since AFM1 is very slightly soluble in water [2, 27], a suitable amount of water (80 mL) was added for extraction from egg tissues and it is the lowest amount facilitating the flow over the manifold system without blocking the immunoaffinity column taking into account the heavy density and viscosity of egg samples.

3.1.2. Effect of Temperature and Time. In order to optimize the best extraction conditions the effect of temperature and time were checked for highest recovery yield which was expressed by mean recovery from two replicates for each experiment result. Figure 2 exhibits that the extraction of AFM1 from eggs increased generally as the extraction temperature increased (where the time is fixed to 40 min. for the four results) till it reached the maximum at 45°C and the recovery decreased insignificantly till 65°C. Figure 3 exhibits a significant recovery trend relative to the time of extraction (where the temperature fixed at 40°C). Recovery reached a maximum value at 30 min. and decreased significantly till the incubation time 120 min. This study suggested that an efficient extraction could be with the application of 45°C and 30 min. for best enhanced recovery.

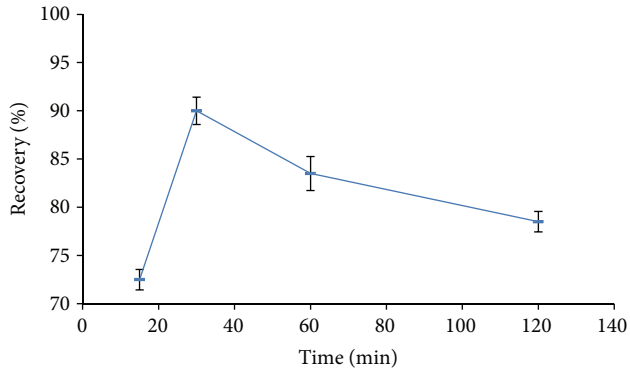

Figure 3: Effect of various times of incubation on AFM1 recovery (mean ± SD, $n = 2$).

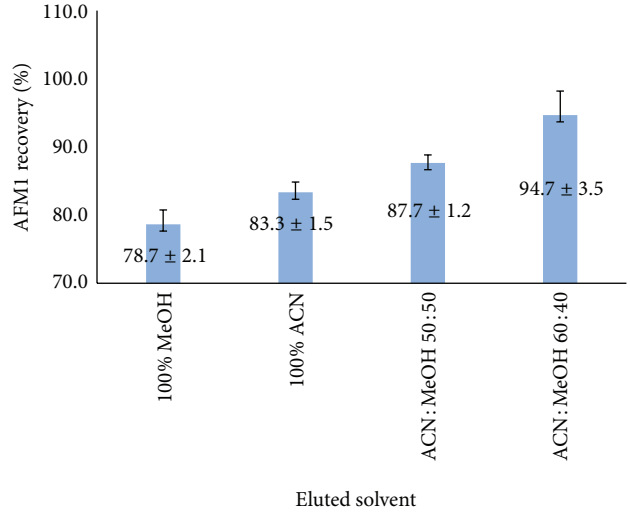

Figure 4: Selection of eluted solvent of methanol- (MeOH-) acetonitrile (ACN) for spiked egg samples (mean ± SD, $n = 3$, and SD expressed by error bars) at a level of 0.05 μg/kg.

3.1.3. Elution. Various amounts from relatively polar solvents (acetonitrile and methanol) were tested and tried out for highest AFM1 test recovery in elution step and the recovery expressed as average recovery from 3 replicates for each solvent (Figure 4). All solvents offer test recovery in agreement with the European Union Commission Directive no. 401/2006 [28] from 70% to 110% for the range above 0.05 μg/kg but the best recoveries were obtained from the mixture acetonitrile : methanol (60 : 40 v/v) as reported.

3.1.4. HPLC Analysis. AFM1 was separated sufficiently without matrix interferences with the optimum mobile phase acetonitrile : water : methanol (30 : 60 : 10 v/v/v) which delivers fast AFM1 peak release where the method takes only 10 minutes and good symmetry (S > 0.85) for peak shape (Figure 5) with Agilent Eclipse plus C18. Chromatographic separation was performed with 0.8 mL/min so the method used minimal reagent quantities. The method shows excellent linearity with correlation coefficient 0.99995 with minimum

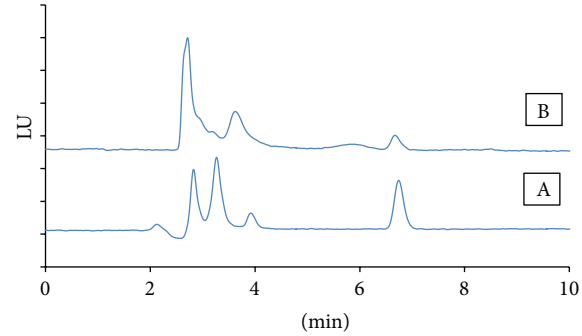

Figure 5: AFM1 HPLC-FLD chromatograms for 0.5 μg/kg standard (A) and 0.05 μg/kg egg spiked sample (B).

variation in the calibration curve obtained from five levels 0.05, 0.1, 0.5, 1.0, and 10 μg/L.

3.2. Method Validation (Fit for Purpose Approach). Includes all of the procedures that demonstrate that a particular method used for quantitative measurement of analytes is reliable and reproducible for the intended use. EURACHEM [29, 30] and FDA [31] guidelines were followed for checking the method validation performance parameters which are summarized in Table 1.

3.2.1. LOQ and LOD. Limit of quantification (LOQ) is the lowest amount of an analyte in a sample that can be quantitatively determined with suitable precision. The accuracy analyte peak (response) was identifiable, discrete, and reproducible with a precision of 9%. Limit of detection (LOD) is the minimum concentration of analyte that can be detected with acceptable certainty, though not quantifiable with acceptable precision and statistically determined as a trice of the standard deviation of sample blanks spiked at lowest acceptable concentration measured (Table 1). The method LOQ (0.05 μg/kg) was represented at the lowest European Union MRL's [28] for AFM1 in milk and milk products and it is worth to mention that there is no regulations for AFM1 in eggs. The method was sensitive, with a detection limit 0.01 μg/kg better than that reported by [32, 33].

3.2.2. Precision and Trueness. Trueness is the degree of agreement of the mean value from a series of measurements with the true value or accepted reference value related to systematic error (bias). The method trueness was checked by certified reference material, proficiency test for milk powder matrix instead of egg by the same method because of unavailability and statistical trueness calculation which was estimated by spiked samples at different levels on eggs samples and bias expressed as absolute relative difference percent (RD%) must not exceed 20% (Table 1). Precision is degree of agreement of replicate measurements under specified conditions. The precision is described by statistical methods such as a standard deviation or confidence limit and less precision is reflected by a larger standard deviation and was classified as repeatability and reproducibility which

Table 1: Trueness calculations and recoveries (mean ± SD, $n = 6$) for 3 spiking levels in eggs, LOD, LOQ, CRM[1], and PT[2] for AFM1.

Mycotoxin	Commodity	Spiking level (μg/kg)	Recovery (%)	$X - T^*$	Bias (RD %)[#]	LOD (μg/kg)	LOQ (μg/kg)	FAPAS CRM T04120 Accepted range (0.33–0.84) μg/kg	FAPAS PT T04124 Assign value (0.505 μg/kg)
AFM1	Eggs	0.05	95.3 ± 9.3	2.3	4.7	0.012	0.05	0.64	0.29, Z-score = −1.9
		0.10	98.0 ± 6.0	2.0	2.0				
		0.50	87.1 ± 6.7	64.3	12.9				

[1] Certified reference materials.
[2] Proficiency test.
[*] X: expected value, T: mean value.
[#] Relative difference.

was shown to be 9% and 13%, respectively, less than 20% in agreement with EU guideline 96/23/EC [34] and less than 15% in agreement with FDA guideline [31].

3.2.3. Method Linearity and Test Recovery. Method linearity was checked by making recovery tests at three different levels of 0.05, 0.1, and 0.5 μg/kg on eggs samples. Method was found to be linear from the limit of quantitation, 0.05, up to 0.5 μg/kg with a strong correlation coefficient 0.99984. The check for method linearity performed with test recoveries for six replicates at the three different levels on eggs samples. As reported in Table 1, the method has excellent recoveries which varied between 87% and 98% at levels of 0.1 and 0.5 μg/kg, respectively, which is in agreement with [28] between 70% and 110% and better than that reported by [11, 35].

3.2.4. Uncertainty Measurement. The parameter associated with the result of a measurement that characterizes the dispersion of the values that could reasonably be attributed to the measured value. Uncertainty was estimated (at 95% confidence level and coverage factor of $k = 2$) to be in the range of ±33. Bias reported from uncertainty using t-test statistical calculations shows that the method recovery is significantly different from 100%, so the analytical result must be reported correctly for recovery for controlling compliance according to EURACHEM Guide for Quantifying Uncertainty [36].

4. Conclusion

Mycotoxins have serious effects on humans and animals. Thus, for ensuring food safety and monitoring the AFM1 hazards in animal products like eggs, a quick and accurate method was presented. This study aimed to optimize HPLC method with less interference, lowest reagent quantities, being safer for technicians, and being more easy to use. Several method validation parameters including LOQ, LOD, linearity, precision, trueness, test recoveries, and uncertainty measurement were checked for method performance. Characteristics of performance parameters indicate that the method is capable of determination of AFM1 in eggs with excellent analytical results and is recommended for food safety monitoring programs.

Acknowledgments

QCAP laboratory and Professor Dr. Ashraf Elmarsafy are gratefully acknowledged for all supports for this study.

References

[1] M. Friend, J. C. Franson, and E. A. Ciganovich, *Field Manual of Wildlife Diseases*, USGS, Washington, DC, USA, 1999.

[2] JECFA, "World Health Organization, safety evaluation of certain mycotoxins in food," in *Proceedings of the 56th Meeting of the Joint FAO/WHO Expert Committee on Food Additives (JECFA)*, WHO Food Additives Series No. 47, International Programme on Chemical Safety, Geneva, Switzerland, 2001.

[3] IARC, *Some Naturally Occurring Substances: Food Items and Constituents, Heterocyclic Aromatic Amines and Mycotoxins*, vol. 56 of *Monographs on the Evaluation of Carcinogenic Risk to Humans*, IARC, Lyon, France, 1993.

[4] IARC, *Some Traditional Herbal Medicines, Some Mycotoxins, Naphthalene and Styrene*, vol. 82 of *Monographs on the Evaluation of Carcinogenic Risk to Humans*, IARC, Lyon, France, 2002.

[5] M. H. Iha, C. B. Barbosa, I. A. Okada, and M. W. Trucksess, "Aflatoxin M_1 in milk and distribution and stability of aflatoxin M_1 during production and storage of yoghurt and cheese," *Food Control*, vol. 29, no. 1, pp. 1–6, 2013.

[6] R. D. Josephs, F. Ulberth, H. P. van Egmond, and H. Emons, "Aflatoxin M_1 in milk powders: processing, homogeneity and stability testing of certified reference materials," *Food Additives and Contaminants*, vol. 22, no. 9, pp. 864–874, 2005.

[7] S. Z. Iqbal and M. R. Asi, "Assessment of aflatoxin M_1 in milk and milk products from Punjab, Pakistan," *Food Control*, vol. 30, no. 1, pp. 235–239, 2013.

[8] A. Sadia, M. A. Jabbar, Y. Deng et al., "A survey of aflatoxin M_1 in milk and sweets of Punjab, Pakistan," *Food Control*, vol. 26, no. 2, pp. 235–240, 2012.

[9] C. A. F. Oliveira and J. C. O. Ferraz, "Occurrence of aflatoxin M_1 in pasteurised, UHT milk and milk powder from goat origin," *Food Control*, vol. 18, no. 4, pp. 375–378, 2007.

[10] S. Rawal and R. A. Coulombe, "Metabolism of aflatoxin B1 in Turkey liver microsomes: the relative roles of cytochromes P450 1A5 and 3A37," *Toxicology and Applied Pharmacology*, vol. 254, no. 3, pp. 349–354, 2011.

[11] A. Zaghini, G. Martelli, P. Roncada, M. Simioli, and L. Rizzi, "Mannanoligosaccharides and aflatoxin B1 in feed for laying hens: effects on egg quality, aflatoxins B1 and M_1 residues in eggs, and aflatoxin B1 levels in liver," *Poultry Science*, vol. 84, no. 6, pp. 825–832, 2005.

[12] S. M. Herzallah, "Determination of aflatoxins in eggs, milk, meat and meat products using HPLC fluorescent and UV detectors," *Food Chemistry*, vol. 114, no. 3, pp. 1141–1146, 2009.

[13] G. L. Neff and G. T. Edds, "Aflatoxins B1 and M_1: tissue residues and feed withdrawal profiles in young growing pigs," *Food and Cosmetics Toxicology*, vol. 19, no. 6, pp. 739–742, 1981.

[14] M. A. Qureshi, J. Brake, P. B. Hamilton, W. M. Hagler Jr., and S. Nesheim, "Dietary exposure of broiler breeders to aflatoxin results in immune dysfunction in progeny chicks," *Poultry Science*, vol. 77, no. 6, pp. 812–819, 1998.

[15] B. Sarimehmetoglu, O. Kuplulu, and T. H. Celik, "Detection of aflatoxin M_1 in cheese samples by ELISA," *Food Control*, vol. 15, no. 1, pp. 45–49, 2004.

[16] S. C. Pei, Y. Y. Zhang, S. A. Eremin, and W. J. Lee, "Detection of aflatoxin M_1 in milk products from China by ELISA using monoclonal antibodies," *Food Control*, vol. 20, no. 12, pp. 1080–1085, 2009.

[17] M. Badea, L. Micheli, M. C. Messia et al., "Aflatoxin M_1 determination in raw milk using a flow-injection immunoassay system," *Analytica Chimica Acta*, vol. 520, no. 1-2, pp. 141–148, 2004.

[18] J. E. Lee, B. M. Kwak, J. H. Ahn, and T. H. Jeon, "Occurrence of aflatoxin M_1 in raw milk in South Korea using an immunoaffinity column and liquid chromatography," *Food Control*, vol. 20, no. 2, pp. 136–138, 2009.

[19] Y. Wang, X. Liu, C. Xiao et al., "HPLC determination of aflatoxin M_1 in liquid milk and milk powder using solid phase extraction on OASIS HLB," *Food Control*, vol. 28, no. 1, pp. 131–134, 2012.

[20] A. C. Manetta, L. Di Giuseppe, M. Giammarco et al., "High-performance liquid chromatography with post-column derivatisation and fluorescence detection for sensitive determination of aflatoxin M_1 in milk and cheese," *Journal of Chromatography A*, vol. 1083, no. 1-2, pp. 219–222, 2005.

[21] Y. Nonaka, K. Saito, N. Hanioka, S. Narimatsu, and H. Kataoka, "Determination of aflatoxins in food samples by automated on-line in-tube solid-phase microextraction coupled with liquid chromatography-mass spectrometry," *Journal of Chromatography A*, vol. 1216, no. 20, pp. 4416–4422, 2009.

[22] E. Beltrán, M. Ibáñez, J. V. Sancho, M. A. Cortés, V. Yus, and F. Hernández, "UHPLC-MS/MS highly sensitive determination of aflatoxins, the aflatoxin metabolite M_1 and ochratoxin A in baby food and milk," *Food Chemistry*, vol. 126, no. 2, pp. 737–744, 2011.

[23] A. N. Tchana, P. F. Moundipa, and F. M. Tchouanguep, "Aflatoxin contamination in food and body fluids in relation to malnutrition and cancer status in Cameroon," *International Journal of Environmental Research and Public Health*, vol. 7, no. 1, pp. 178–188, 2010.

[24] A. W. Yunus, E. Razzazi-Fazeli, and J. Bohm, "Aflatoxin B1 in affecting broiler's performance, immunity, and gastrointestinal tract: a review of history and contemporary issues," *Toxins*, vol. 3, no. 6, pp. 566–590, 2011.

[25] A. S. Sebaei, A. M. Gomaa, G. G. Mohamed, and F. A. Nour El-Dien, "Simple validated method for determination of deoxynivalenol and zearalenone in some cereals using high performance liquid chromatography," *The American Journal of Food Technology*, vol. 7, pp. 668–678, 2012.

[26] M. J. Hinojo, A. Medina, F. M. Valle-Algarra, J. V. Gimeno-Adelantado, M. Jiménez, and R. Mateo, "Fumonisin production in rice cultures of *Fusarium verticillioides* under different incubation conditions using an optimized analytical method," *Food Microbiology*, vol. 23, no. 2, pp. 119–127, 2006.

[27] H. Mohammadi, "A review of aflatoxin M_1, milk, and milk products," in *Aflatoxins—Biochemistry and Molecular Biology*, chapter 19, InTech, Rijeka, Croatia, 2011, http://www.intechopen.com/books/aflatoxins-biochemistry-and-molecular-biology/a-review-of-aflatoxin-m1-milk-and-milk-products.

[28] European Commission (EC) REGULATION No 401/2006, "Laying down the methods of sampling and analysis for the official control of the levels of mycotoxins in foodstuffs," *Official Journal of the European Union L*, vol. 70, pp. 12–34, 2006.

[29] EURACHEM, *The Fitness for Purpose of Analytical Methods, a Laboratory Guide to Method Validation and Related Topics*, LGC, Teddington, UK, 1998, http://www.eurachem.org/images/stories/Guides/pdf/valid.pdf.

[30] EURACHEM, *Guide to Quality in Analytical Chemistry, an Aid to Accreditation*, CITAC, 2002, http://www.eurachem.org/images/stories/Guides/pdf/CITAC_EURACHEM_GUIDE.pdf.

[31] FDA, *Guidelines for the Validation of Chemical Methods for the FDA Foods Program*, 2012, http://www.fda.gov/downloads/ScienceResearch/FieldScience/UCM298730.pdf.

[32] A. Zaghini, L. Sardi, A. Altafini, and L. Rizzi, "Residues of aflatoxins B1 and M_1 in different biological matrices of swine orally administered aflatoxin B1 and *Saccharomyces cerevisiae*," *Italian Journal of Animal Science*, vol. 4, no. 2, pp. 488–490, 2005.

[33] J. F. Gregory and D. Manley, "High performance liquid chromatographic determination of aflatoxins in animal tissues and products," *Journal of the Association of Official Analytical Chemists*, vol. 64, no. 1, pp. 144–151, 1981.

[34] European Commission (EC) REGULATION No 657/EC, "Implementing Council Directive 96/23/EC concerning the performance of analytical methods and the interpretation of results," *Official Journal of the European Union L*, vol. 221, pp. 8–36, 2002.

[35] M. W. Trucksess and L. Stoloff, "Determination of aflatoxicol and aflatoxins B1 and M_1 in eggs," *Journal of the Association of Official Analytical Chemists*, vol. 67, no. 2, pp. 317–320, 1984.

[36] EURACHEM/CITAC Guide CG 4, *Quantifying Uncertainty in Analytical Measurement*, 2012, http://www.eurachem.org/images/stories/Guides/pdf/QUAM2012_P1.pdf.

Hindawi Publishing Corporation
Journal of Analytical Methods in Chemistry
Volume 2013, Article ID 385473, 4 pages
http://dx.doi.org/10.1155/2013/385473

Research Article

Quantitative Determination of Flavonoids and Chlorogenic Acid in the Leaves of *Arbutus unedo* L. Using Thin Layer Chromatography

Željan Maleš,[1] Darija Šarić,[2] and Mirza Bojić[1]

[1] *University of Zagreb, Faculty of Pharmacy and Biochemistry, A. Kovačića 1, 10000 Zagreb, Croatia*
[2] *Agency for Medicinal Products and Medical Devices of Croatia, Ksaverska cesta 4, 10000 Zagreb, Croatia*

Correspondence should be addressed to Mirza Bojić; mirza.bojic@gmail.com

Received 26 May 2013; Accepted 11 July 2013

Academic Editor: Shixin Deng

The plant species *Arbutus unedo* shows numerous beneficial pharmacological effects (antiseptic, antidiabetic, antidiarrheal, astringent, depurative, antioxidant, antihypertensive, antithrombotic, and anti-inflammatory). For the medicinal use, standardization of extracts is a necessity, as different compounds are responsible for different biological activities. In this paper, we analyze monthly changes in the content of quercitrin, isoquercitrin, hyperoside, and chlorogenic acid. Methanolic extracts of the leaves are analyzed by HPTLC for the identification and quantification of individual polyphenol, and DPPH test is used to determine antioxidant activity. Based on the results obtained, the leaves should be collected in January to obtain the highest concentrations of hyperoside and quercitrin (0.35 mg/g and 1.94 mg/g, resp.), in June, July, and October for chlorogenic acid (1.45–1.46 mg/g), and for the fraction of quercitrin and isoquercitrin in November (1.98 mg/g and 0.33 mg/g, resp.). Optimal months for the collection of leaves with the maximum recovery of individual polyphenol suggested in this work could direct the pharmacological usage of the polyvalent herbal drugs.

1. Introduction

Arbutus unedo L. (Ericaceae, English strawberry tree) is an evergreen shrub or a small tree reaching up to 12 m in height. It is found mainly in European Mediterranean region growing in maquis, evergreen scrub, woodland margins, and on rocky slopes. The leaves of *A. unedo* are alternate, simple, oblanceolate, dark green, leathery, short-stalked, and toothed. The flowers are bell shaped, with recurved lobes, 8-9 mm long, white, often tinged with pink or green, and honey scented. The fruits are globose berries about 15–20 mm in diameter, ripening through yellow to scarlet and deep crimson. Since the fruits take about 12 months to ripen, a tree carries mature fruits and flowers at the same time, and the appearance of both during winter months also makes this plant very popular for specimen plantings [1, 2].

The leaves of *A. unedo* are used as a urinary antiseptic, antidiabetic, antidiarrheal, astringent, depurative, antioxidant, antihypertensive, antithrombotic, anti-inflammatory agent [3–8]. Chemical investigations of leaves and fruits show the presence of essential oil, flavonoids, proanthocyanidins, iridoid glucosides, sugars, nonvolatile and phenolic acids, vitamins C and E and carotenoids [9–13].

As a pharmacological activity can rarely be attributed to a group of compounds as it is the case with polyphenols and antioxidant activity, the identification and quantification of individual compounds responsible for a biological activity are of interest. The objective of this paper was the identification and quantification of chlorogenic acid and flavonoids: quercitrin, isoquercitrin, and hyperoside using a simple thin layer chromatography technique.

2. Experimental

2.1. Plant Materials, Reagents, Chemicals, and Solutions. Each month in the year of 2003 the leaves of ten *A. unedo* plants were collected on five different locations on the island of Dugi

otok, Božava municipality (44° 8′ 30″ N, 14° 54′ 30″ E). Voucher specimens (no. 99450-99461) were deposited at the Department of Pharmaceutical Botany, Faculty of Pharmacy and Biochemistry, University of Zagreb. Solvents of the analytical grade were obtained from Kemika (Croatia) and standards (quercitrin, isoquercitrin, hyperoside, and chlorogenic acid) were purchased from C. Roth (Germany). 2,2-Diphenyl-1-picrylhydrazyl was supplied by Sigma-Aldrich (USA) and HPTLC silica gel 60 F254 by Merck (Germany).

2.2. Sample and Standard Preparation. Extracts of *A. unedo* were prepared by the reflux extraction of leaves powder in methanol for 5 minutes; final concentration being 0.1 g/mL. The standards of polyphenols were prepared as 1 mg/mL solutions in methanol.

2.3. Thin Layer Chromatography. Thin layer chromatography was performed on 10 × 20 cm HPTLC silica gel 60 F254 plates (Merck, Germany). Ethyl acetate-formic acid-acetic acid-water in volume ratio 100 : 11 : 11 : 26 was used as mobile phase [14]. After development plates were air dried and recorded at 254 and 366 nm, identification and quantification were performed by TLC densitometry using CAMAG TLC Scanner 3 and WinCATS software version 1.3.4 (Switzerland). Quantification was performed using calibration curves (peak area of chromatogram versus mass of standard applied in the form of band) for individual standard in triplicate.

2.4. DPPH Test. Antioxidant activity was assessed using stable free radical 2,2-diphenyl-1-picrylhydrazyl (DPPH). DPPH solution was prepared by dissolving DPPH in ethanol to obtain the final concentration of 0.3 mM. Decolorization of DPPH in the presence of extract (100 : 1 volume ration) was measured on Varian Cary 50 Bio spectrophotometer (USA). Antioxidant activity (AA) was expressed as a percentage of quenching of the stable free radical at $\lambda = 518$ nm as follows:

$$\mathrm{AA} = \frac{(A_0 - A)}{A_0} \times 100, \quad (1)$$

where A_0 represents the absorbance of blank (methanol) and A absorbance of the extract measured 1 minute after mixing.

3. Results and Discussion

Qualitative analysis of polyphenols in leaves and fruits of *A. unedo* [14] showed presence of nine bands in the methanol extracts. Seven polyphenol standards were used and four flavonoids and chlorogenic acid were identified, out of which we were able to determine the content (quantify) of chlorogenic acid, quercitrin, isoquercitrin, and hyperoside.

Identification of each polyphenol was based on the color of the band observed under $\lambda = 366$ nm, R_F value, and matching UV-Vis spectra *in situ* with the standard used (Table 1).

Volumes of extracts applied to the plate were adjusted to correspond to ranges of linearity for individual polyphenol that were 0.2–1.6 μg per band for chlorogenic acid, 1.0–5.0 μg per band for quercitrin, 2.5–12.5 μg per band for isoquercitrin, and 0.2–0.6 μg per band for hyperoside. The results of HPTLC quantification of an individual polyphenol are presented in Table 2.

Table 1: Parameters of identification of the polyphenols analyzed.

Polyphenol	R_F	Color under $\lambda = 366$ nm
Quercitrin	0.80	Yellow-green
Isoquercitrin	0.64	Yellow-green
Hyperoside	0.57	Yellow-green
Chlorogenic acid	0.49	Blue

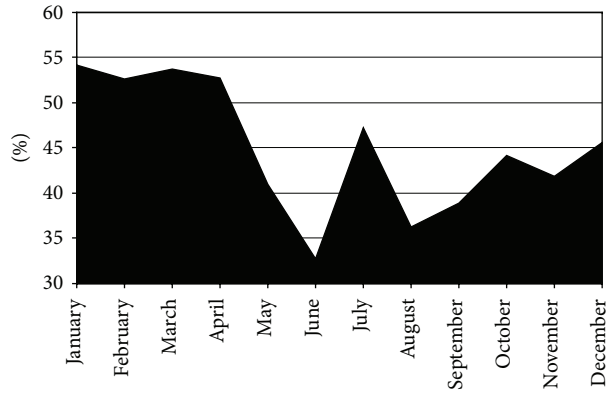

Figure 1: Variation of antioxidant activity expressed in percentages during the year.

Compared to the results of the total flavonoids of 1.30–2.00 g per 100 g of dried leaves from our previous study [14], quercitrin, isoquercitrin, and hyperoside (2.38 mg/g—sum of individual flavonoids for June, Table 2) can be accounted for up to 12% of dry powder. However, it should be noticed that methods for determination of total flavonoids usually use hydrolyzed extracts, meaning that aglycones are analyzed, whereas all the analyzed polyphenols in this work present flavonoid glycosides.

As suggested by Oliveira et al. [15], methanolic extracts have greater antioxidant activity compared to ethanolic and water based. The antioxidant activity values of methanolic extracts of *A. unedo* were determined during a period of 12 months (Figure 1).

The results of the antioxidant activity vary with the month observed and cannot be attributed to any of the analyzed polyphenols individually ($r^2 < 0.25$); rather it presents the overall activity of the total extracted polyphenols including phenolic acids and flavonoids other than analyzed chlorogenic acid, quercitrin, isoquercitrin and hyperoside. These flavonoids are attributed up to only 12% of total flavonoids.

Specific pharmacological activity is usually the result of a specific substance; for example, the inhibition of 3-hydroxy-3-methylglutaryl coenzyme A reductase can be attributed to quercetin, hyperoside, rutin, and chlorogenic acid fractions of *Crataegus pinnatifida* Bge. [16]. Thus, to achieve a specific action of the extracts of *A. unedo,* leaves should be collected during the months when the concentration of individual substance responsible for specific action is the highest. This means, based on the results obtained, that the leaves

Table 2: Content of individual polyphenol during the year in the leaves of *A. unedo* expressed in mg per g of dry sample.

	Quercitrin	Isoquercitrin	Hyperoside	Chlorogenic acid
January	1.94 ± 0.08	nd	0.35 ± 0.03	0.70 ± 0.09
February	1.34 ± 0.22	nd	0.12 ± 0.03	0.76 ± 0.09
March	1.38 ± 0.21	nd	nd	1.06 ± 0.19
April	1.38 ± 0.17	nd	0.11 ± 0.03	1.13 ± 0.07
May	1.21 ± 0.05	nd	0.11 ± 0.02	1.06 ± 0.12
June	2.20 ± 0.17	0.07 ± 0.01	0.11 ± 0.04	1.45 ± 0.34
July	1.56 ± 0.09	nd	nd	1.46 ± 0.13
August	1.78 ± 0.30	0.09 ± 0.05	0.21 ± 0.01	1.11 ± 0.14
September	1.74 ± 0.14	nd	nd	0.79 ± 0.16
October	1.78 ± 0.04	nd	nd	1.45 ± 0.59
November	1.98 ± 0.21	0.33 ± 0.08	0.16 ± 0.01	0.76 ± 0.11
December	1.46 ± 0.26	0.13 ± 0.09	0.24 ± 0.01	0.61 ± 0.05

Results expressed as mean ± standard deviation.
nd: not detected.

should be collected in January to obtain the highest concentrations of hyperoside and quercitrin (0.35 mg/g and 1.94 mg/g, resp.), in June, July, and October for chlorogenic acid (1.45–1.46 mg/g), and for the fraction of quercitrin and isoquercitrin in November (1.98 mg/g and 0.33 mg/g, resp.).

4. Conclusion

Different studies have shown beneficial effects of *A. unedo* for human health and suggested the usage of standardized extracts in medicinal products. Although antioxidant activity well correlates with the total content of polyphenols, phenolic acids, and flavonoids [15], a specific action, for example, an antiaggregatory [6] or an anti-inflammatory action [7], is probably the consequence of specific compound(s) to which extracts should be standardized. For this purposes the thin layer chromatography presents simple and readily available technique.

Conflict of Interest

The authors declare no conflict of interests.

Acknowledgments

This work was supported by the Ministry of Science, Education and Sports of the Republic of Croatia, Grant nos. 006-0061117-1237 and 006-0061117-1239.

References

[1] R. Domac, *Flora of Croatia: Manual For Determination of Plants*, Školska knjiga, Zagreb, Croatia, 2002.

[2] Č. Šilić, *Atlas of Trees and Shrubs*, Svjetlost, Sarajevo, Bosnia, 3rd edition, 1988.

[3] S. Afkir, T. B. Nguelefack, M. Aziz et al., "*Arbutus unedo* prevents cardiovascular and morphological alterations in L-NAME-induced hypertensive rats. Part I: cardiovascular and renal hemodynamic effects of *Arbutus unedo* in L-NAME-induced hypertensive rats," *Journal of Ethnopharmacology*, vol. 116, no. 2, pp. 288–295, 2008.

[4] D. Andrade, C. Gil, L. Breitenfeld, F. Domingues, and A. P. Duarte, "Bioactive extracts from *Cistus ladanifer* and *Arbutus unedo* L," *Industrial Crops and Products*, vol. 30, no. 1, pp. 165–167, 2009.

[5] M. Bnouham, F. Z. Merhfour, A. Legssyer, H. Mekhfi, S. Maâllem, and A. Ziyyat, "Antihyperglycemic activity of *Arbutus unedo*, *Ammoides pusilla* and *Thymelaea hirsuta*," *Pharmazie*, vol. 62, no. 8, pp. 630–632, 2007.

[6] M. El Haouari, J. J. López, H. Mekhfi, J. A. Rosado, and G. M. Salido, "Antiaggregant effects of *Arbutus unedo* extracts in human platelets," *Journal of Ethnopharmacology*, vol. 113, no. 2, pp. 325–331, 2007.

[7] S. Mariotto, E. Esposito, R. Di Paola et al., "Protective effect of *Arbutus unedo* aqueous extract in carrageenan-induced lung inflammation in mice," *Pharmacological Research*, vol. 57, no. 2, pp. 110–124, 2008.

[8] A. Pabuçcuoğlu, B. Kivçak, M. Baş, and T. Mert, "Antioxidant activity of Arbutus unedo leaves," *Fitoterapia*, vol. 74, no. 6, pp. 597–599, 2003.

[9] L. Barros, A. M. Carvalho, J. S. Morais, and I. C. F. R. Ferreira, "Strawberry-tree, blackthorn and rose fruits: detailed characterisation in nutrients and phytochemicals with antioxidant properties," *Food Chemistry*, vol. 120, no. 1, pp. 247–254, 2010.

[10] B. Kivcak, T. Mert, B. Demirci, and K. H. C. Baser, "Composition of the essential oil of *Arbutus unedo*," *Chemistry of Natural Compounds*, vol. 37, no. 5, pp. 445–446, 2001.

[11] P. Lebreton and C. Bayet, "The physiological and biochemical variability of the strawberry tree *Arbutus unedo* L. (Ericaceae)," *Acta Pharmaceutica*, vol. 52, no. 2, pp. 83–90, 2002.

[12] M. M. Özcan and H. Haciseferogullan, "The strawberry (*Arbutus unedo* L.) fruits: chemical composition, physical properties and mineral contents," *Journal of Food Engineering*, vol. 78, no. 3, pp. 1022–1028, 2007.

[13] K. Pallauf, J. C. Rivas-Gonzalo, M. D. del Castillo, M. P. Cano, and S. de Pascual-Teresa, "Characterization of the antioxidant composition of strawberry tree (*Arbutus unedo* L.) fruits," *Journal of Food Composition and Analysis*, vol. 21, no. 4, pp. 273–281, 2008.

[14] Ž. Maleš, M. Plazibat, V. B. Vundać, and I. Žuntar, "Qualitative and quantitative analysis of flavonoids of the strawberry tree—*Arbutus unedo* L. (Ericaceae)," *Acta Pharmaceutica*, vol. 56, no. 2, pp. 245–250, 2006.

[15] I. Oliveira, V. Coelho, R. Baltasar, J. A. Pereira, and P. Baptista, "Scavenging capacity of strawberry tree (*Arbutus unedo* L.) leaves on free radicals," *Food and Chemical Toxicology*, vol. 47, no. 7, pp. 1507–1511, 2009.

[16] X.-L. I. Ye, W.-W. Huang, Z. Chen et al., "Synergetic effect and structure-activity relationship of 3-hydroxy-3-methylglutaryl coenzyme a reductase inhibitors from crataegus pinnatifida bge," *Journal of Agricultural and Food Chemistry*, vol. 58, no. 5, pp. 3132–3138, 2010.

Hindawi Publishing Corporation
Journal of Analytical Methods in Chemistry
Volume 2013, Article ID 350801, 5 pages
http://dx.doi.org/10.1155/2013/350801

Research Article

Combining Electronic Tongue Array and Chemometrics for Discriminating the Specific Geographical Origins of Green Tea

Lu Xu, Si-Min Yan, Zi-Hong Ye, Xian-Shu Fu, and Xiao-Ping Yu

Zhejiang Provincial Key Laboratory of Biometrology and Inspection & Quarantine, College of Life Sciences, China Jiliang University, Hangzhou 310018, China

Correspondence should be addressed to Zi-Hong Ye; zhye@cjlu.edu.cn and Xiao-Ping Yu; yxp@cjlu.edu.cn

Received 14 May 2013; Accepted 30 June 2013

Academic Editor: Shao-Nong Chen

The feasibility of electronic tongue and multivariate analysis was investigated for discriminating the specific geographical origins of a Chinese green tea with Protected Designation of Origin (PDO). 155 Longjing tea samples from three subareas were collected and analyzed by an electronic tongue array of 7 sensors. To remove the influence of abnormal measurements and samples, robust principal component analysis (ROBPCA) was used to detect outliers in each class. Partial least squares discriminant analysis (PLSDA) was then used to develop a classification model. The prediction sensitivity/specificity of PLSDA was 1.000/1.000, 1.000/0.967, and 0.950/1.000 for longjing from Xihu, Qiantang, and Yuezhou, respectively. Electronic tongue and chemometrics can provide a rapid and reliable tool for discriminating the specific producing areas of Longjing.

1. Introduction

Green tea, unfermented and made from the leaves of the *Camellia sinensis* plant, is one of the most popular beverages consumed across the world [1–3]. The property and chemical components of green teas are influenced by many factors, such as tea species, harvest season, climate, geographical locations, and processing. In China, among various factors, the geographical origin is recognized as an important aspect of tea. Because of the similar tea species, cultivation and processing conditions in a specific tea-producing area, many teas are named after their geographical origins.

Longjing tea is a green tea produced in Xihu and its surrounding areas (Hangzhou, China). As a famous green tea with Protected Designation of Origin (PDO), Longjing is recognized as one of the top green teas for its special appearance (flat and straight leaves), flavor, and taste. Various methods for distinguishing Longjing from other teas have been reported [4–6]. However, little information has been available on the feasibility of discriminating Longjing from its three specific subproducing areas, namely, Xihu, Qiantang, and Yuezhou. As the quality and prices of Longjing tea from the above three producing areas are different, it is necessary to develop effective analysis methods for discrimination of Longjing from different subproducing areas.

Because of the similarity (processing, appearance, and taste) among different subproducing areas, the specific geographical origins of Longjing are usually distinguished by sensory analysis. However, because it is very expensive and may take years to train a tea taster, it would be more efficient to use some nonhuman techniques. Recent years have witnessed increased applications of electronic tongue technology to analysis of wines, milk, tea, beer, juice, and so on [7–10]. In these applications, a very good time stability and sensitivity are obtained using electronic tongue sensors. Moreover, a good correlation between human and electronic tongue judgment has been observed, which makes it a promising alternative to human sensory analysis of teas.

This paper was focused on developing a rapid analysis method for discriminating specific subproducing areas of Longjing tea by electronic tongue and chemometrics. Robust principal component analysis (ROBPCA) [11, 12] was used to detect outliers in each class. Partial least squares discriminant analysis (PLSDA) [13] was used to develop the classification model.

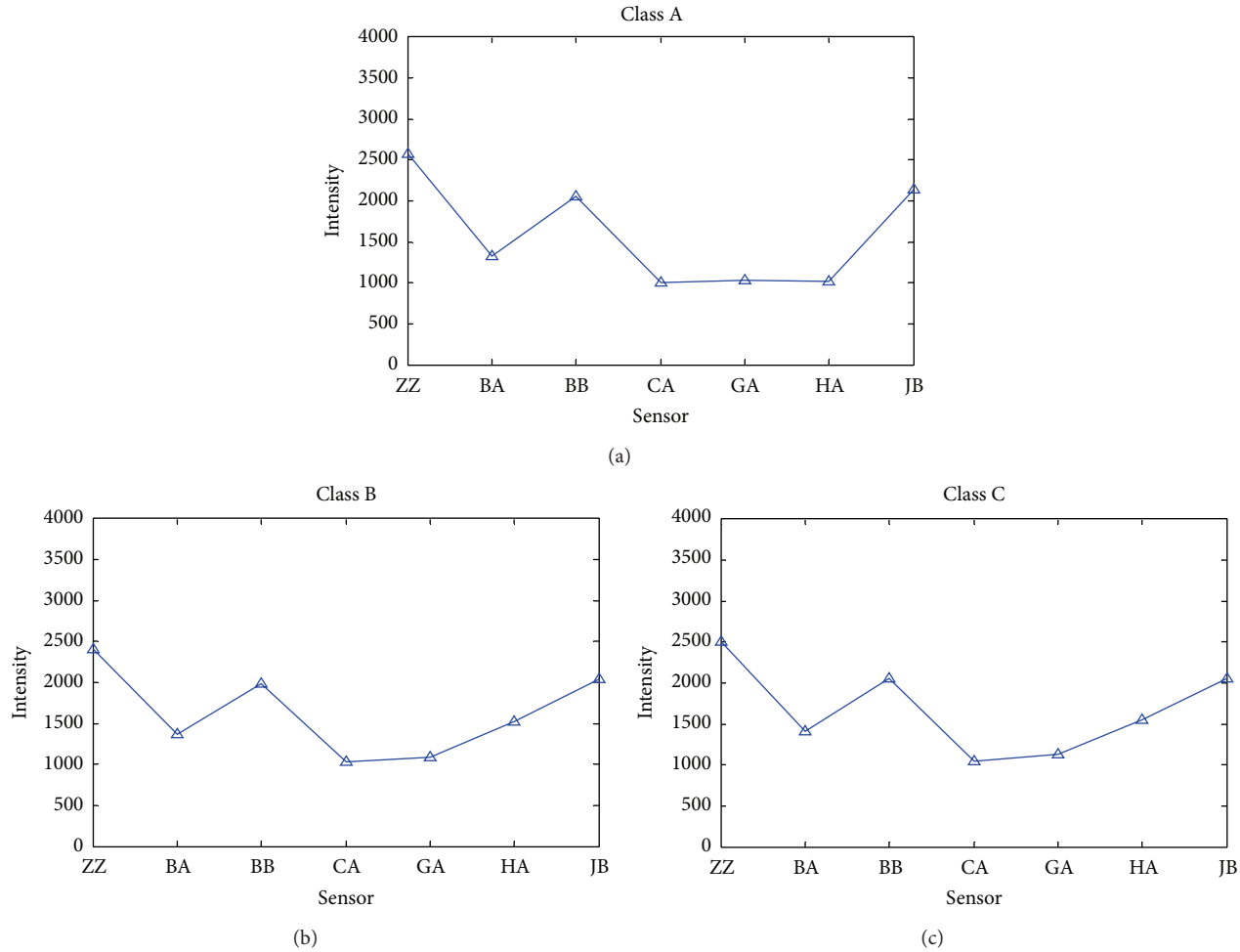

Figure 1: The average feature spectrum of Longjing tea of class A, class B, and class C.

Table 1: Sensor sensitivity (pC) of ASTREE electronic tongue system.

Basic tastes	Substances	ZZ	BA	BB	CA	GA	HA	JB
Sour	Citric acid	7	6	7	7	7	6	6
Salty	KCL	7	4	4	5	4	4	4
Sweet	Glucose	7	4	7	7	4	4	4
Bitter	Caffeine	5	4	4	5	4	4	4
Savory	L-arginine	6	4	6	5	5	4	5

2. Experimental and Methods

2.1. Tea Samples and Electronic Tongue Analysis. 155 Longjing samples were collected from the local tea plantations in Xihu (32 samples, class A), Qiantang (59 samples, class B), and Yuezhou (64 samples, class C). All the samples were preserved in a cool (about 4°C), dark, and dry place with integral packaging before preparation of tea extract. Six gram of each sample was added with 250 mL boiling deionized water and infused for 10 min. The infusion was then filtered into a beaker and cooled to the room temperature (25°C) by water bath for electronic tongue analysis.

The tea infusion was analyzed by an ASTREE Electronic Tongue system (Alpha M.O.S., Toulouse, France). The detection system consists of one reference electrode (Ag/AgCl) and 7 liquid cross selective sensors (ZZ, BA, BB, CA, GA, HA, and JB). The cross-sensitivity and selectivity of the sensor array are listed in Table 1. The sensors array analyzed the solutions of tea samples with sampling interval of 1 s. Each sample was measured for 150 s, which can ensure a stable response.

2.2. Data Preprocessing, Outlier Detection, and Data Splitting. All the data analysis was performed on MATLAB 7.0.1 (Mathworks, Sherborn, MA, USA). The responses of the 7 sensors reported at 150 s were used for the subsequent data analysis. Outliers in the data would degrade the classification models and prediction performance, so robust principal component analysis (ROBPCA) was used to detect outliers in each class of samples. ROBPCA can obtain robust projections of the original data points and avoid the masking effects caused by multiple outliers. With the computed robust score distance (SD) and orthogonal distance (OD), ROBPCA can classify an object into one of the four groups: regular points (with small SD and small OD), good PCA-leverage points (with large

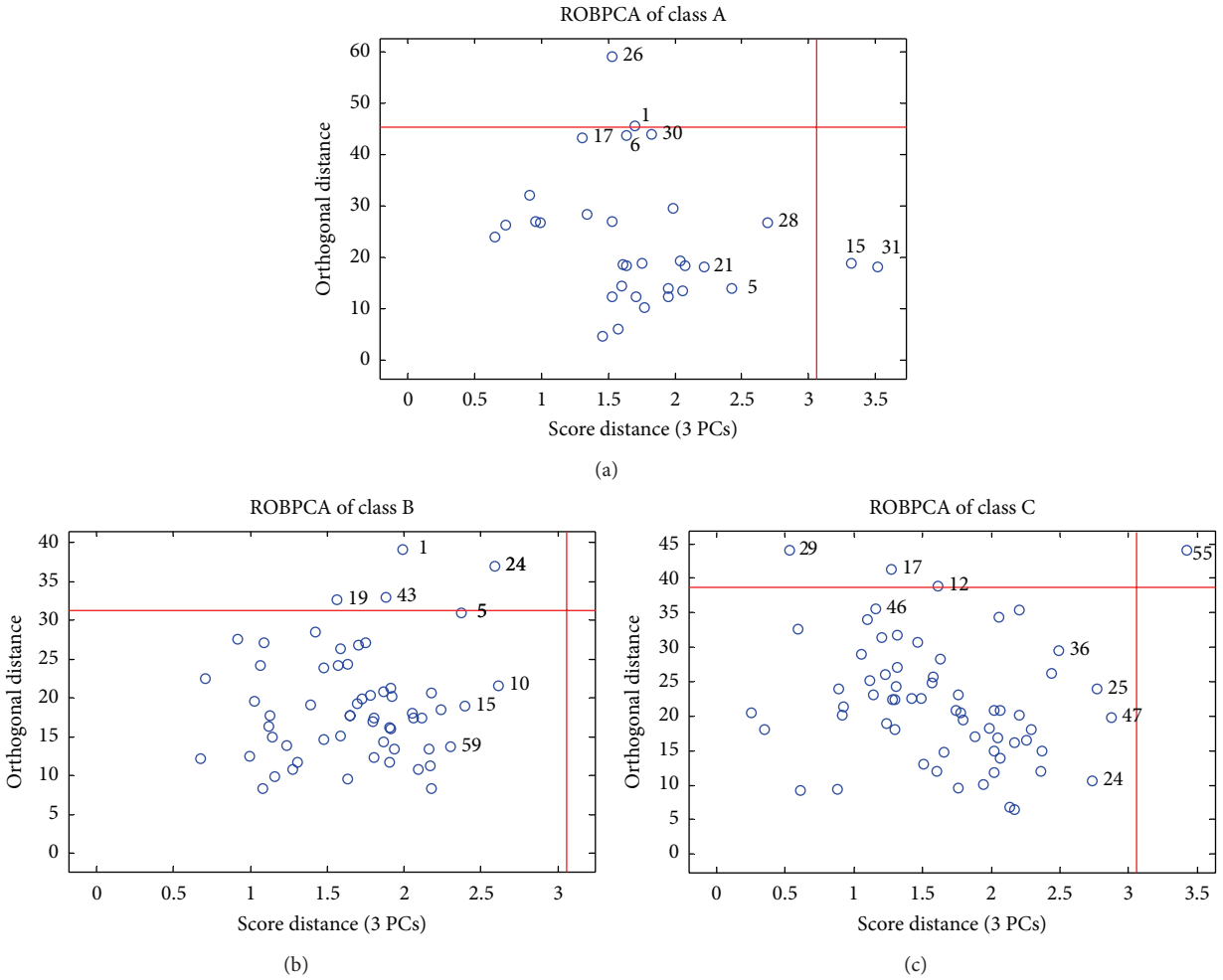

Figure 2: ROBPCA of the electronic tongue data: the outlier plots for Longjing samples from Xihu (class A), Qiantang (class B), and Yuezhou (class C).

SD and small OD), orthogonal outliers (with small SD and large OD), and bad PCA-leverage points (with large SD and large OD). With outliers deleted, the DUPLEX algorithm [14] was used to divide the measured data into a training set and test set. DUPLEX algorithm can obtain a test set of samples distributed uniformly in the range of training samples.

2.3. PLSDA. For multiclass classification, PLSDA can be performed by regressing each column of a dummy response matrix $\mathbf{Y}$ on the measured data $\mathbf{X}$ by PLS. For the ith (i = 1, 2, and 3) column in $\mathbf{Y}$, an element is set a value of 1 if the corresponding object is from class i; otherwise, it is assigned a value of 0. For prediction, a new sample is classified into class i when the ith element of its predicted response vector is nearest to 1. Monte Carlo cross validation (MCCV) [15] was used to estimate the number of components in PLSDA by minimizing the mean percentage error of MCCV (MPEMCCV):

$$\text{MPEMCCV} = \frac{\sum_{i=1}^{B} N_i}{\sum_{i=1}^{B} M_i}, \tag{1}$$

where B is the numbers of MCCV data splitting, M_i is the number of prediction objects, and N_i is the number of wrongly predicted for the ith MCCV data splitting. Model sensitivity and specificity of prediction for each class were used to evaluate the performance of classification models:

$$\text{Sensitivity} = \frac{\text{TP}}{\text{TP} + \text{FN}},$$
$$\text{Specificity} = \frac{\text{TN}}{\text{TN} + \text{FP}}, \tag{2}$$

where TP, FN, TN, and FP represent the numbers of true positives, false negatives, true negatives, and false positives, respectively. For classification, objects in each class were denoted as positives and the other two classes were denoted as negatives.

3. Results and Discussion

The average electronic tongue features for each class of Longjing tea are shown in Figure 1. Seen from Figure 1, the features of the three classes have very similar response

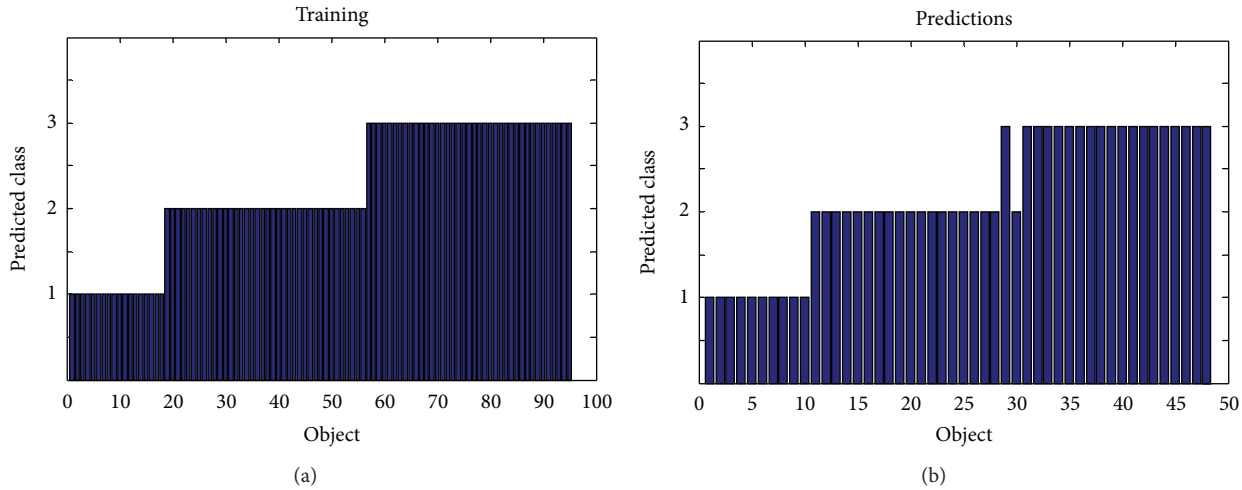

Figure 3: PLSDA training (objects 1–18, class A; objects 19–55, class B; objects and 56–95, class C) and prediction (objects 1–10, class A; objects 11–28, class B; and objects 29–48, class C) of the specific Longjing geographical origins. The height of a bar indicates to which class an object is assigned by PLSDA.

patterns. The features of class B and C are very similar and different from those of class A, especially in the responses of GA and HA. ROBPCA was used for outlier detection with a significance level of 0.05. Because each class of tea has a different probability distribution, ROBPCA models were performed separately on each class. Figure 2 demonstrates the ROBPCA plots for the three classes. For each class, a ROBPCA model with three principal components (PCs) was selected because including more PCs would not reduce the residuals significantly. Three PCs explained 89.7, 91.5 and 92.1 percents of the total variances of each class, respectively. For outlier diagnosis, bad PCA-leverage points, good PCA-leverage points and orthogonal outliers were excluded to obtain a representative data set distributed in the entire range of measured samples. The numbers of objects with large SD and OD were denoted. As a result, for class A, two orthogonal outliers (objects 1 and 26) and two good PCA-leverage points (objects 15 and 31) were deleted; for class B, four orthogonal outliers (objects 1, 19, 24, and 43) were deleted; for class C, three orthogonal outliers (objects 12, 17, and 29) and one bad PCA-leverage point (object 55) were deleted.

The DUPLEX algorithm was then performed to divide the remaining 143 tea samples into training and test objects. Finally, 95 samples (class A, 18; class B, 37; and class C, 40) were used for training and 48 samples (class A, 10; class B, 18; and class C, 20) for prediction. PLSDA model was developed and MCCV was used to select the number of latent variables (LVs). For MCCV, the original 95 training samples were randomly split into training (50%) and test objects (50%) for 100 times. The lowest MPEMCCV value was obtained with a three-component PLSDA model.

The training and prediction results of a three-component PLSDA are demonstrated in Figure 3. The sensitivity/specificity of PLSDA for classes A, B, and C was 1.000(10/10)/1.000(38/38), 1.000(18/18)/0.967(29/30), and 0.950(19/20)/1.000(28/28), respectively. The training accuracy was 1 and for prediction only one object from class C was wrongly assigned to class B, indicating the effectiveness of electronic tongue for classification of Longjing tea samples.

4. Conclusions

Rapid and effective discrimination of Longjing green tea from different subproducing areas was performed using electronic tongue and chemometrics. The sensitivity/specificity of PLSDA for classes A, B, and C was 1.000/1.000, 1.000/0.967, and 0.950/1.000, respectively. Electronic tongue and chemometrics can provide a rapid and reliable tool for discriminating the specific producing areas of Longjing. Compared with human sensory analysis, this method is easier to perform and the more attractive economically. In the future studies, the comparison of chemical methods, for example, LC/UV/MS, to the electronic tongue analysis will be performed to investigate the statistical correlation between the chemistry and the tastes of Longjing tea.

Authors' Contribution

Lu Xu and Si-Min Yan equally contributed to this study.

Acknowledgments

This work was financially supported by the National Public Welfare Industry Projects of China (no. 201210010, 201210092, and 2012104019), the National Natural Science Foundation of China (no. 31000357), Hangzhou Programs for Agricultural Science and Technology Development (no. 20101032B28), and the Key Scientific and Technological Innovation Team Program of Zhejiang Province (no. 2010R50028).

References

[1] L. Xu, D.-H. Deng, and C.-B. Cai, "Predicting the age and type of tuocha tea by fourier transform infrared spectroscopy and chemometric data analysis," *Journal of Agricultural and Food Chemistry*, vol. 59, no. 19, pp. 10461–10469, 2011.

[2] Y.-L. Lin, I.-M. Juan, Y.-L. Chen, Y.-C. Liang, and J.-K. Lin, "Composition of polyphenols in fresh tea leaves and associations of their oxygen-radical-absorbing capacity with antiproliferative actions in fibroblast cells," *Journal of Agricultural and Food Chemistry*, vol. 44, no. 6, pp. 1387–1394, 1996.

[3] T. Karak and R. M. Bhagat, "Trace elements in tea leaves, made tea and tea infusion: a review," *Food Research International*, vol. 43, no. 9, pp. 2234–2252, 2010.

[4] H. Yu, J. Wang, H. Xiao, and M. Liu, "Quality grade identification of green tea using the eigenvalues of PCA based on the E-nose signals," *Sensors and Actuators B*, vol. 140, no. 2, pp. 378–382, 2009.

[5] H. Yu and J. Wang, "Discrimination of LongJing green-tea grade by electronic nose," *Sensors and Actuators B*, vol. 122, no. 1, pp. 134–140, 2007.

[6] K. Wei, L.-Y. Wang, J. Zhou et al., "Comparison of catechins and purine alkaloids in albino and normal green tea cultivars (*Camellia sinensis* L.) by HPLC," *Food Chemistry*, vol. 130, no. 3, pp. 720–724, 2012.

[7] L. Escuder-Gilabert and M. Peris, "Review: highlights in recent applications of electronic tongues in food analysis," *Analytica Chimica Acta*, vol. 665, no. 1, pp. 15–25, 2010.

[8] L. Sipos, Z. Kovács, V. Sági-Kiss, T. Csiki, Z. Kókai, and A. Fekete, "Discrimination of mineral waters by electronic tongue, sensory evaluation and chemical analysis," *Food Chemistry*, vol. 135, no. 4, pp. 2947–2953, 2012.

[9] L. Gil-Sánchez, J. Soto, R. Martínez-Máñez, E. Garcia-Breijo, J. Ibáñez, and E. Llobet, "A novel humid electronic nose combined with an electronic tongue for assessing deterioration of wine," *Sensors and Actuators A*, vol. 171, no. 2, pp. 152–158, 2011.

[10] R. N. Bleibaum, H. Stone, T. Tan, S. Labreche, E. Saint-Martin, and S. Isz, "Comparison of sensory and consumer results with electronic nose and tongue sensors for apple juices," *Food Quality and Preference*, vol. 13, no. 6, pp. 409–422, 2002.

[11] M. Hubert, P. J. Rousseeuw, and S. Verboven, "A fast method for robust principal components with applications to chemometrics," *Chemometrics and Intelligent Laboratory Systems*, vol. 60, no. 1-2, pp. 101–111, 2002.

[12] H.-F. Cui, Z.-H. Ye, L. Xu, X.-S. Fu, C.-W. Fan, and X.-P. Yu, "Automatic and rapid discrimination of cotton genotypes by near infrared spectroscopy and chemometrics," *Journal of Analytical Methods in Chemistry*, vol. 2012, Article ID 793468, 7 pages, 2012.

[13] M. Barker and W. Rayens, "Partial least squares for discrimination," *Journal of Chemometrics*, vol. 17, no. 3, pp. 166–173, 2003.

[14] R. D. Snee, "Validation of regression models: methods and examples," *Technometrics*, vol. 19, pp. 415–428, 1977.

[15] Q.-S. Xu and Y.-Z. Liang, "Monte Carlo cross validation," *Chemometrics and Intelligent Laboratory Systems*, vol. 56, no. 1, pp. 1–11, 2001.